

Interaction of *Listeria monocytogenes* and *Streptococcus pneumoniae* with ciliated epithelium

Thesis submitted for the degree of  
Doctor of Philosophy  
at the University of Leicester

by

Mina Fadaee-Shohada B.Sc. (Hons)  
Department of Infection, Immunity and Inflammation  
University of Leicester

12<sup>th</sup> April 2010

**For my family**

## Statement of Originality

This accompanying thesis submitted for the degree of PhD entitled “Interaction of *Listeria monocytogenes* and *Streptococcus pneumoniae* with ciliated epithelium” is based on work conducted by the author in the Department of Infection, Immunity and Inflammation of the University of Leicester during the period between October 2005 and April 2010.

All the work recorded in this thesis is original unless otherwise acknowledged in the text or by references.

None of this work has been submitted for another degree in this or any other University.

Signed: \_\_\_\_\_

Date: \_\_\_\_\_

## Abstract

### **Title: Interaction of *Listeria monocytogenes* and *Streptococcus pneumoniae* with ciliated epithelium**

**by  
Mina Fadaee-Shohada**

Cilia are hair-like structures that extend from the surface of cells, including the lining of the respiratory tract and the ependymal surface of brain ventricles. Cilia have a role in host defence as the coordinated beating of cilia keeps the epithelium layer clear of debris and pathogens. Defects in the ciliary structure are associated with a wide range of human diseases, including meningitis and primary ciliary dyskinesia (PCD).

This thesis describes the effect of *Listeria monocytogenes*, a model pathogen that causes meningitis and encephalitis, on rat brain ependymal cilia. This interaction resulted in an altered behaviour of both ependymal cilia and listeria, but was dependent on the listeria strain used. Commonly, listeria attached to cilia and formed aggregates which reduced the ciliary beat amplitude (the distance between the maximum forward position of the cilia tip and the maximum backward position of the ciliary tip). Cilia outside the aggregates also displayed reduced ciliary beat amplitude but this was not as low as those cilia associated with aggregates. Ciliary beat frequency within the aggregates was unchanged. The formation of listerial aggregates appeared to be dependent on a transcription factor that regulates virulence (PrfA), since mutants with a PrfA deletion did not form aggregates.

Secondly, this thesis investigated the effect of *Streptococcus pneumoniae* on respiratory epithelium from PCD and healthy individuals. PCD is a chronic respiratory disease where cellular output of nitric oxide is very low. Pneumococcal challenge of healthy ciliated epithelium resulted in an increase in nitric oxide, which was not observed in ciliated epithelium from PCD patients. Conversely, ciliated epithelium from PCD patients displayed significantly higher levels of some cytokine and chemokines both before and after pneumococcal infection, compared to healthy ciliated epithelium. Interestingly, ciliated epithelium from PCD patients with a ciliary static phenotype displayed the highest levels of cytokine and chemokines, both at basal level and following pneumococcal infection. As with listeria, pneumococci were also shown to bind to cilia and form aggregates. This phenomenon appeared to be initiated by pneumococcal binding to the tip of the cilium. The formation of aggregates was dependent on neuraminidase A (NanA), a key virulence factor that aids adherence, since NanA mutants did not form any aggregates.

## **Acknowledgments**

This thesis would not have been possible without the kind support, guidance, and the remarkable patience of my thesis supervisors – Prof Peter Andrew and Prof Chris O’Callaghan. I cannot thank you both enough for giving me this opportunity.

In addition I would like to thank those people who spent their time and shared their knowledge, to help me complete this thesis. Dr Robert Hirst and Dr Claire Smith thank you so much for all your help and guidance over the years. Not forgetting the help from Andrew Rutman, Norman Baker, Gwyneth Williams and Sarah Glenn. I am also grateful to all my friends at the University of Leicester, for their continued moral support.

My deepest gratitude goes to my father, Mohsen, and my grandmother, Angela, whose continued support and love has shown itself in so many practical ways. I owe you both so much. Furthermore, a very important thank you to my other Grandmother Farah and my Aunt Hoori, whose support, encouragement and help with my school work, whilst I was living in Iran, was crucial to my later success in science. Their help was compounded by Nahid who cared for me and Mr Salehi who saw the potential in my coming to England to study, so a big thank you to them both.

Finally, I am forever indebted to my partner James for his understanding, endless patience and encouragement when it was most required. I must not forget my poodles Daisy and Alfie, whose antics, love and affection, have been vital to my sanity and kept a smile on my face when I most needed it.

## Abbreviations

|                |  |
|----------------|--|
| ALI            | air liquid interface   |
| ATP            | adenosine triphosphate   |
| BA             | blood agar   |
| BAB            | blood agar base  |
| Bap            | biofilm associated protein   |
| BEBM           | bronchial epithelial cell base medium                                  |
| BEGM           | bronchial epithelial growth medium                                     |
| BHI            | brain heart infusion broth   |
| BSA            | bovine serum albumin   |
| cAMP           | cyclic adenosine monophosphate   |
| CBA            | ciliary beat amplitude   |
| CBF            | ciliary beat frequency   |
| CFSE           | 5-and-6-carboxy-2',7'-dichlorofluorescein diacetate succinimidyl ester |
| Cfu            | colony forming units   |
| cGMP           | cyclic guanosine monophosphate   |
| CPS            | capsular polysaccharide  |
| CSF            | cerebrospinal fluid  |
| EDTA           | ethylenediaminetetraacetic acid  |
| eNOS           | endothelial nitric oxide synthase                                      |
| FITC           | fluorescein isothiocyanate   |
| GTP            | guanosine triphosphate   |
| IFT            | intraflagella transport  |
| Ig             | Immunoglobulin   |
| iNOS           | inducible NOS  |
| LDH            | lactate dehydrogenase  |
| LLO            | listeriolysin O  |
| LPS            | lipopolysaccharide   |
| MEM            | minimal essential medium   |
| NanA           | neuraminidase A  |
| NF- $\kappa$ B | nuclear factor-kappaB  |
| NHBE           | normal human bronchial epithelial                                      |
| nNOS           | neuronal nitric oxide synthase   |
| NO             | nitric oxide   |

|      |  |
|------|--|
| NOS  | nitric oxide synthase                                    |
| OD   | optical density  |
| PAC1 | adenylate cyclase-activating polypeptide type 1 receptor |
| PBS  | phosphate buffered saline                                |
| PCD  | primary ciliary dyskinesia                               |
| prfA | positive regulatory factor A                             |
| SEM  | scanning electron microscopy                             |
| TEER | transepithelial electrical resistance                    |
| WT   | wild-type  |

### **Symbols**

|   |         |
|---|---------|
| § | section |
|---|---------|

## List of contents

|  |           |
|--|-----------|
| <i>Abstract</i> .....  | <i>iv</i> |
| <i>Acknowledgements</i> .....  | <i>v</i>  |
| <i>Abbreviations</i> .....   | <i>vi</i> |
| <i>CHAPTER ONE: Introduction</i> .....   | <i>1</i>  |
| <i>Part A: Cilia</i>   |           |
| <i>1.1 Cilia</i> .....   | <i>2</i>  |
| <i>1.2 Classification of cilia</i> .....   | <i>2</i>  |
| <i>1.2.1 Primary cilia</i> .....   | <i>3</i>  |
| <i>1.2.2 Motile cilia</i> .....  | <i>4</i>  |
| <i>1.3 Ciliary ultrastructure</i> .....  | <i>4</i>  |
| <i>1.3.1 Ciliary membrane</i> .....  | <i>6</i>  |
| <i>1.3.2 Microtubular structures</i> .....   | <i>9</i>  |
| <i>1.3.3 Microtubule associated proteins</i> .....   | <i>11</i> |
| <i>1.3.3.1 Dynein arms</i> .....   | <i>11</i> |
| <i>1.3.3.2 Radial spokes</i> .....   | <i>11</i> |
| <i>1.3.3.3 Nexin links</i> .....   | <i>13</i> |
| <i>1.3.3.4 Dynein regulatory complex</i> .....   | <i>13</i> |
| <i>1.3.3.5 Other microtubule associated proteins</i> .....                                 | <i>13</i> |
| <i>1.3.3.6 Basal body</i> .....  | <i>14</i> |
| <i>1.4 Mechanism of motion</i> .....   | <i>14</i> |
| <i>1.5 Ciliogenesis</i> .....  | <i>17</i> |
| <i>1.6 Ependymal cilia</i> .....   | <i>20</i> |
| <i>1.6.1 Cerebral spinal fluid (CSF)</i> .....   | <i>22</i> |
| <i>1.6.2 Regulation of ciliary beat frequency (CBF) and CSF flow in the ependyma</i> ..... | <i>25</i> |

|  |   |    |
|--|---|----|
| 1.6.3  | <i>Ependymal ciliary defects and disease</i> .....        | 27 |
| 1.7  | <i>Lung/ Respiratory cilia</i> .....                      | 28 |
| 1.7.1  | <i>Respiratory mucus and mucociliary clearance</i> .....  | 30 |
| 1.7.2  | <i>Regulation of CBF in the airways</i> .....             | 31 |
| 1.7.2.1  | <i>Regulation of CBF by cyclic nucleotides</i> .....      | 33 |
| 1.7.2.2  | <i>Role of protein kinase C</i> .....                     | 34 |
| 1.7.2.3  | <i>Role of calcium in ciliary beat regulation</i> .....   | 34 |
| 1.7.2.4  | <i>Regulation of CBF by intracellular pH</i> .....        | 35 |
| 1.7.3  | <i>Nitric Oxide in the respiratory tract</i> .....        | 35 |
| 1.7.4  | <i>Respiratory ciliary defects and disease</i> .....      | 35 |
| <br><i><u>Part B: Primary Ciliary Dyskinesia (PCD)</u></i> |   |    |
| 1.8  | <i>History</i> .....                                      | 40 |
| 1.9  | <i>Pathophysiology</i> .....                              | 40 |
| 1.10   | <i>Genetics and inheritance</i> .....                     | 47 |
| 1.11   | <i>Associations with primary ciliary dyskinesia</i> ..... | 53 |
| 1.12   | <i>Diagnosis of primary ciliary dyskinesia</i> .....      | 56 |
| <br><i><u>Part C: Pathogenic bacteria</u></i>              |   |    |
| 1.13   | <i>Streptococcus pneumoniae: The pneumococcus</i> .....   | 58 |
| 1.13.1   | <i>Pneumococcal carriage and colonisation</i> .....       | 59 |
| 1.14   | <i>S. pneumoniae virulence factors</i> .....              | 60 |
| 1.14.1   | <i>Pneumolysin</i> .....                                  | 60 |
| 1.14.2   | <i>Neuraminidases</i> .....                               | 64 |
| 1.14.3   | <i>Other pneumococcal virulence factors</i> .....         | 65 |

|  |   |    |
|--|---|----|
| 1.15   | <i>Listeria monocytogenes</i> .....   | 69 |
|  | 1.15.1 Intracellular infectious cycle and associated virulence factors..... | 69 |
|  | 1.15.2 PrfA: the regulatory switch for virulence.....                       | 73 |
| 1.16   | Outline of the thesis.....  | 77 |
| <br><i>CHAPTER TWO: Material and Methods</i> ..... |   | 79 |
| 2.1  | Chemicals.....  | 80 |
| 2.2  | Bacterial growth media.....   | 80 |
| 2.3  | Preparation of tryptone soya agar and blood agar plates.....                | 81 |
| 2.4  | Bacterial strains and growth conditions.....                                | 81 |
| 2.5  | Antibiotics and media supplements.....                                      | 84 |
| 2.6  | Serotyping pneumococci.....   | 84 |
| 2.7  | Viable counts.....  | 85 |
| 2.8  | Ependymal cell culture.....   | 85 |
| 2.9  | Infection of ependymal cells.....   | 86 |
| 2.10   | Nasal respiratory cell culture.....   | 86 |
|  | 2.10.1 Subjects.....  | 87 |
|  | 2.10.2 Collagen coating.....  | 87 |
|  | 2.10.3 Brush biopsy.....  | 89 |
|  | 2.10.4 Basal cells.....   | 89 |
|  | 2.10.5 Air liquid interface (ALI) cultures.....                             | 91 |
|  | 2.10.6 Transepithelial electrical resistance measurements.....              | 91 |
| 2.11   | Infection of basal and ciliated respiratory cells.....                      | 92 |
| 2.12   | Interaction between microspheres and cilia.....                             | 92 |
| 2.13   | Measurement of ciliary beat frequency (CBF).....                            | 93 |
| 2.14   | Measurement of ciliary beat amplitude.....                                  | 94 |

|      |   |     |
|------|---|-----|
| 2.15 | <i>Measurement of bacterial aggregation.....</i>  | 95  |
| 2.16 | <i>Scanning electron microscopy.....</i>  | 95  |
| 2.17 | <i>Immunohistochemical characterisation of basal cells.....</i>                             | 96  |
| 2.18 | <i>Fluorescent labelling of basal and ciliated cells infected with<br/>Pneumococci.....</i> | 97  |
| 2.19 | <i>Image analysis software.....</i>   | 101 |
| 2.20 | <i>Assay of nitric oxide in culture.....</i>  | 101 |
|      | 2.20.1 <i>Preparation of glass vessel.....</i>  | 102 |
|      | 2.20.2 <i>Preparation of the standards and unknown samples.....</i>                         | 103 |
| 2.21 | <i>Trypan blue assay.....</i>   | 105 |
| 2.22 | <i>Measurement of cell viability.....</i>   | 105 |
| 2.23 | <i>Adherence assay.....</i>   | 106 |
| 2.24 | <i>Invasion assay.....</i>  | 107 |
| 2.25 | <i>Chemokine and cytokine analysis.....</i>   | 107 |
| 2.26 | <i>Statistical analysis.....</i>  | 110 |
|      | <i>CHAPTER THREE: Results (ependymal cilia and Listeria).....</i>                           | 111 |
| 3.1  | <i>Overview.....</i>  | 112 |
| 3.2  | <i>Interaction of wild-type L. monocytogenes and ciliated ependymal cells.....</i>          | 113 |
| 3.3  | <i>Role for PrfA?.....</i>  | 122 |
| 3.4  | <i>Role for biofilms associated protein?.....</i>   | 122 |
|      | <i>CHAPTER FOUR: Results (respiratory cilia and pneumococci).....</i>                       | 124 |
| 4.1  | <i>Overview.....</i>  | 125 |
| 4.1  | <i>Establishment of air-liquid interface epithelial cell cultures.....</i>                  | 126 |
| 4.2  | <i>Interaction of wild- type S. pneumoniae with ciliated respiratory cells.....</i>         | 131 |
|      | 4.2.1 <i>Studying the surface charge of cilia.....</i>                                      | 135 |
| 4.3  | <i>Cytotoxicity of ciliated respiratory cells induced by pneumococci.....</i>               | 137 |
| 4.4  | <i>Nitric oxide release from ciliated respiratory cells.....</i>                            | 138 |

|   |   |     |
|---|---|-----|
| 4.5   | <i>Number of recovered pneumococci following two hour exposure to PCD and healthy ciliated respiratory cells.....</i>   | 140 |
| 4.6   | <i>Pneumococcal induced chemokine release from ciliated cells.....</i>  | 141 |
| 4.7   | <i>Pneumococcal induced cytokine release from ciliated cells.....</i>   | 144 |
| <i>CHAPTER FIVE: Results (respiratory basal cells and pneumococci).....</i> |   | 147 |
| 5.1   | <i>Overview.....</i>  | 148 |
| 5.2   | <i>Basal cell culture.....</i>  | 149 |
| 5.3   | <i>Characterisation of basal cells.....</i>   | 150 |
| 5.4   | <i>Cytotoxicity of basal cells induced by pneumococci.....</i>  | 151 |
| 5.5   | <i>Pneumococcal adhesion and invasion of respiratory basal cells.....</i>   | 152 |
| 5.6   | <i>Nitric oxide release from basal cells.....</i>   | 157 |
| 5.7   | <i>Pneumococcal induced chemokines and cytokine release from basal cells... </i>  | 159 |
| <i>CHAPTER SIX: Discussion.....</i>   |   | 161 |
| 6.1   | <i>The behavior of L. monocytogenes and ciliated rat ependymal cells is altered during their co-culture.....</i>  | 162 |
| 6.2   | <i>The behavior of S. pneumoniae and ciliated respiratory cells is altered during their co-culture.....</i>   | 166 |
|   | 6.2.1 <i>The effect of respiratory ciliated cells on S. pneumoniae.....</i>   | 166 |
|   | 6.2.2 <i>The effect of S. pneumoniae on respiratory ciliated cells.....</i>   | 172 |
| 6.3   | <i>Comparisons between healthy normal and PCD respiratory cells in their response to pneumococci.....</i>   | 174 |
|   | 6.3.1 <i>Respiratory cells from PCD patients show no increase in nitric oxide production following infection with pneumococci.....</i>                        | 174 |
|   | 6.3.2 <i>Respiratory cells from PCD patients have increased levels of cytokine and chemokines compared to respiratory cells from healthy individuals.....</i> | 176 |
|   | 6.3.3 <i>Pneumococcal adhesion and invasion of respiratory basal cells; a comparison between basal cells from healthy normal and PCD patients.....</i>        | 180 |

|                             |     |
|-----------------------------|-----|
| <i>APPENDIX A</i> .....     | 185 |
| <i>APPENDIX B</i> .....     | 189 |
| <i>REFERENCE LIST</i> ..... | 200 |
| <i>PUBLICATIONS</i> .....   | 266 |

**CHAPTER ONE - INTRODUCTION**

This chapter is divided into three main sections; in part A the ciliary structure, function and their relation to disease will be described. Part B is dedicated to the genetic disorder, primary ciliary dyskinesia and in part C *Streptococcus pneumoniae* and *Listeria monocytogenes* as model organisms that infect the respiratory and ependymal cilia respectively will be described.

## **Part A: Cilia**

### ***1.1 Cilia***

Cilia are hair-like structures that protrude from the surface of cells. Cilia are found throughout the body in, for example, the upper and lower respiratory tract, Eustachian tube and sinuses, the middle ear, the lining of the ependymal surface of the brain ventricles, and in the reproductive tracts in both male and females (Schidlow 1994). Most of our knowledge regarding cilia comes from the study of model organisms such as *Chlamydomonas* (a biflagellated, unicellular algae) or *Caenorhabditis elegans* (a free-living, transparent nematode) (Witman *et al.* 1978, Barr 2005, Wang *et al.* 2006). Defects in the ciliary structure are associated with a wide range of human diseases, including hydrocephalus, primary ciliary dyskinesia (PCD), some forms of retinal degeneration, and polycystic liver and kidney disease (see reviews: (Afzelius 2004, Badano *et al.* 2006, Fliegauf *et al.* 2007)).

### ***1.2 Classification of cilia***

Cilia are classified as either motile or primary cilia. Over the last decade cilia have regained the attention of the scientific community, mainly due to the recognition of the importance of primary cilia (see reviews: (Vogel 2005, Benzing and Walz 2006)).

However, mammalian motile cilia remain an important cellular component with multiple functions. This thesis focuses on motile cilia particularly ependymal and respiratory cilia. However, before discussing motile cilia in detail, a brief description of primary cilia is given below.

### **1.2.1 Primary cilia**

Primary cilia are single nonmotile cilia (except motile nodal cilia in vertebrates) and have a similar structure to that of motile cilia (see §1.3), except they lack inner and outer dynein arms and the central pair; hence they are termed “nine+zero” cilia. Primary cilia were first described by Zimmerman more than 100 years ago (Zimmermann 1898) and for a long time they remained an organelle of obscure function. Over the past few years this outlook has dramatically changed and primary cilia are now recognised as sensory organelles for transmission and detection of chemical and mechanical information from the cell’s extracellular environment. For example, the primary cilia in the kidney-tubule epithelial cells have been shown to detect flow of urine by bending, resulting in the transmission of a calcium-mediated signal to the cell (Praetorius and Spring 2001, Nauli *et al.* 2003). In a similar manner, motile cilia in the embryonic node are thought to detect fluid flow, to signal the establishment of left-right asymmetry during early development (Nonaka *et al.* 1998, McGrath and Brueckner 2003, Okada *et al.* 2005). For a more detailed view on the function of sensory cilia see the recent review by Badano and colleagues (Badano *et al.* 2006).

Various diseases have been associated with primary non motile cilia. Abnormal monocilia may be responsible for diseases such as, Bardet Biedl syndrome, nephronophthisis and Alstrom syndrome (Badano *et al.* 2006). Dysfunction of sensory

primary cilia has been demonstrated in polycystic kidney disease (Nauli *et al.* 2003, Yokoyama 2004).

### **1.2.2 Motile cilia**

Motile cilia in humans are located on the apical surface of ependymal cells within, the central nervous system, on ependymal cells of the ventricles and the spinal canal; the upper and lower respiratory tract, reproductive organs, including the oviduct, testes and as sperm flagellae (Ferkol and Leigh 2006). Many diseases are associated with defective motile cilia. Primary ciliary dyskinesia is one of the most prominent genetic abnormality involving cilia in the respiratory tract and is discussed in detail in part B of the introduction. A detailed description of the structure of cilia is given below.

### **1.3 Ciliary ultrastructure**

Cilia are composed of ~250 polypeptides organised into specific multiprotein structures (Satir 1989, Afzelius 2000, Ostrowski *et al.* 2002). The axonemes of motile cilia are constructed from nine doublet microtubules, dynein arms and radial spokes surrounding a central pair of singlet microtubules (Figure 1.1). This forms the 9+2 arrangement which extends from the basal body (see §1.3.3.6). The axoneme is a uniform structure that repeats exactly every 96nm along the ciliary axoneme. The repetitive unit consists of four outer dynein arms, three inner dynein arms, three radial spokes, and one pair of interdoubtlet links (Satir and Sleight 1990). Each component of the ciliary axoneme will be discussed in detail below.

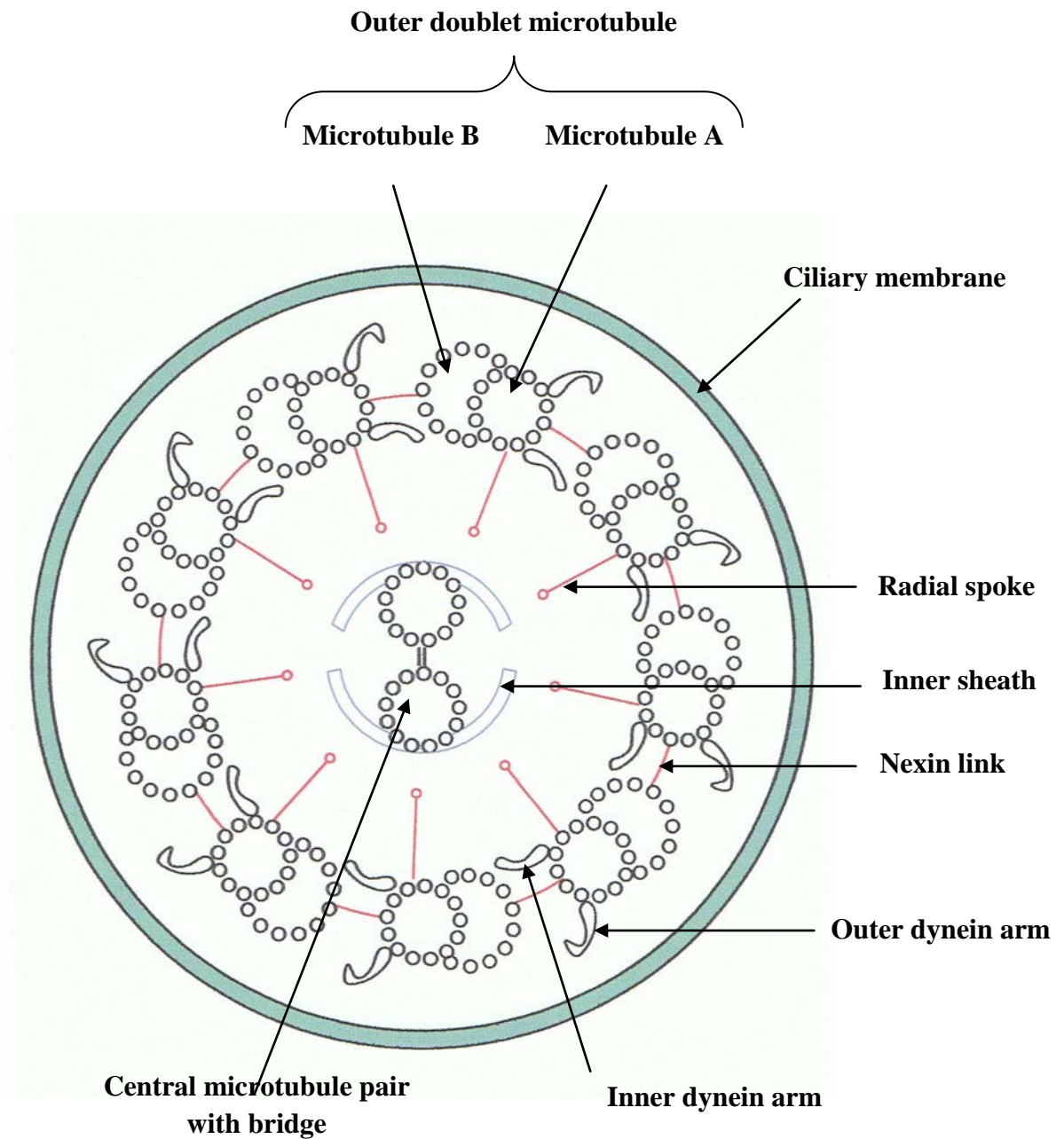


**Figure 1.1** The normal ciliary ultrastructure illustrating the classical '9+2' arrangement. Two central microtubules (central pair) are enclosed within a central sheath to form the central axis of the axoneme. This is surrounded by nine microtubule doublets. The doublets consist of an A and B microtubule. Each doublet is connected by nexin links to the next. From the A doublet, inner and outer dynein arms project to the adjacent doublet. Radial spokes connect the central sheath to the outer microtubule doublets.

### ***1.3.1 Ciliary membrane***

Ciliary axonemes are ensheathed by a membrane that extends from, and is continuous with, the plasma membrane. However, the ciliary membrane is structurally and functionally distinct from the cell membrane. The ciliary membranes of all cilia contain specific ion channels and receptor proteins that initiate signalling pathways that ultimately lead to regulating differentiation, migration, and cell growth during development and adulthood (Satir and Christensen 2007).

Within the ciliary membrane of mammalian respiratory cilia are two transmembrane complexes. The first is the ciliary crown (Figure 1.2 A) which was first observed in the mouse oviduct (Dirksen and Satir 1972) and subsequently in thymic cysts of nude mice (Cordier 1975), and in the mammalian trachea (Kuhn and Engleman 1978). The ciliary crown is composed of two regions: An electron dense cap tightly bound to the central and each peripheral subfibre A microtubule. Dense filaments radiate from this cap to the second region, the plate or ciliary crown. The crown is composed of 3 to 7 fibres (bristles) that project out onto the ciliary membrane, have a mean length of 31nm, width of 9nm and show a periodic structure (Dentler and LeCluyse 1982, Foliguet and Puchelle 1986). The crown is only present on fully mature cilia, suggesting it may function as a cap to prevent further ciliary elongation (Kuhn and Engleman 1978, Dentler and LeCluyse 1982). It has been suggested that the ciliary crown may be involved with several functions associated with microtubule assembly, as well as ciliary transport and mucociliary transport (Foliguet and Puchelle 1986).

The second transmembrane complex is the ciliary necklace (Figure 1.2 B and C), which consists of multiple strands of intramembrane particles extending distally 0.25  $\mu\text{m}$  from

the base of the cilium. The necklace is formed from membranous particles in two to six parallel rows, 30nm apart, at the base of the ciliary shaft (Gilula and Satir 1972, Dute and Kung 1978, Thai *et al.* 2002). The ciliary necklace may have a role in energy transduction or timing of the ciliary beat, by regulating localised membrane permeability (Gilula and Satir 1972). It may also assist in attaching the basal body to the transition zone and ciliary membrane (Dentler 1981, Arima *et al.* 1985). Evidence to support this has come from experiments using calcium shock treatment to cause deciliation. A calcium binding protein, centrin, is found in the area of the ciliary necklace and following calcium shock it was found that the cilia broke at a point above the ciliary necklace (Dentler 1981, Satir and Sleight 1990, Wanner *et al.* 1996).

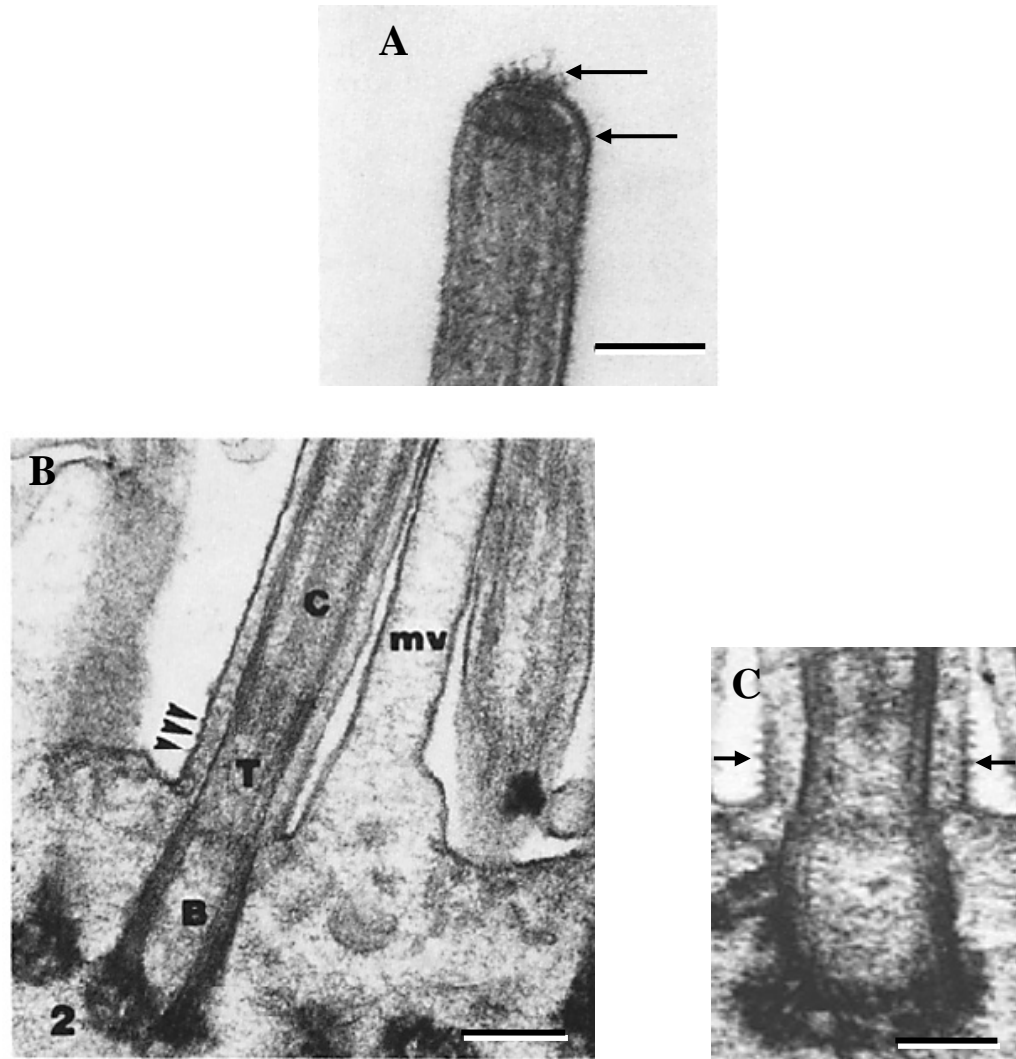


**Figure 1.2 (A) Organisation of the surface glycocalyx on the tips of oviduct cilia.** The top arrow is pointing to the ciliary crown and the bottom arrow is pointing to the ciliary cap. Scale bar represents 100 $\mu$ m. **(B) Longitudinal section of cilia showing the structure of the ciliary membrane in the transition region.** The arrows indicate the regularly arranged surface proteins found on the membrane in this region. C = longitudinal section of cilia; B= basal body, MV= microvillus and T= transition region. Scale bar represents 100 $\mu$ m. **(C) Longitudinal section through the base of the cilia.** The arrows are pointing to six regularly spaced projectors that are extending from the membrane from both sides of the cilium. Scale bar represents 100 $\mu$ m. Taken from (Anderson and Hein 1977).

### ***1.3.2 Microtubular structures***

The microtubules of the 9 + 2 axoneme polymerise from tubulin heterodimers composed of  $\alpha$ - and  $\beta$ -tubulin subunits (Nogales 1999) with the fast polymerising (+) end at the ciliary tip. The dimers organise in a linear pattern with a slight helical pitch (Carson and Collier 1988).

#### **Central pair**

The central pair of microtubules (Figure 1.1) are two single asymmetric microtubules that are biochemically distinct (Porter and Sale 2000) and each has a wall composed of 13 protofilaments (Afzelius 2000). The distal portion of the central pair terminates in the ciliary crown (Dentler 1981) and the proximal portion ends in the axosome (Dute and Kung 1978). A double bridge spanning 8nm, which repeats every 14nm, is found between the two central microtubules (Warner 1976).

#### **Peripheral microtubule doublets**

The two microtubules of each peripheral pair are more complex than the central pair and are constructed from two subfibres, A and B (Figure 1.1). Subfibre A is a complete microtubule composed of 13 parallel protofilaments (A1-A13) onto which the inner and outer dynein arms attach. Subfibre B is incomplete and contains only 10 protofilaments (B1-B10). Three intermediate filament proteins, known as tectins A, B and C, as well as linker proteins, originally named Sp77 and Sp83 in the sea urchin, are found in the midwall area common to both the A and B microtubules (Downing and Sui 2007). Tectin has been shown to be important in the structural stability of the microtubule doublet, and may control ciliary length (Hagiwara *et al.* 2000). It is thought that the linker might regulate axoneme movement by undergoing significant conformational

changes (Downing and Sui 2007). The B microtubule unit ends at the ciliary tip, however the A microtubule continues as a single filament and attaches to the ciliary crown (Dentler 1981). The base of the microtubule doublet attaches to a complex known as the ciliary necklace (Satir and Sleight 1990). Figure 1.3 gives a detailed image of the relationship between microtubule doublets and other proteins in the axoneme.

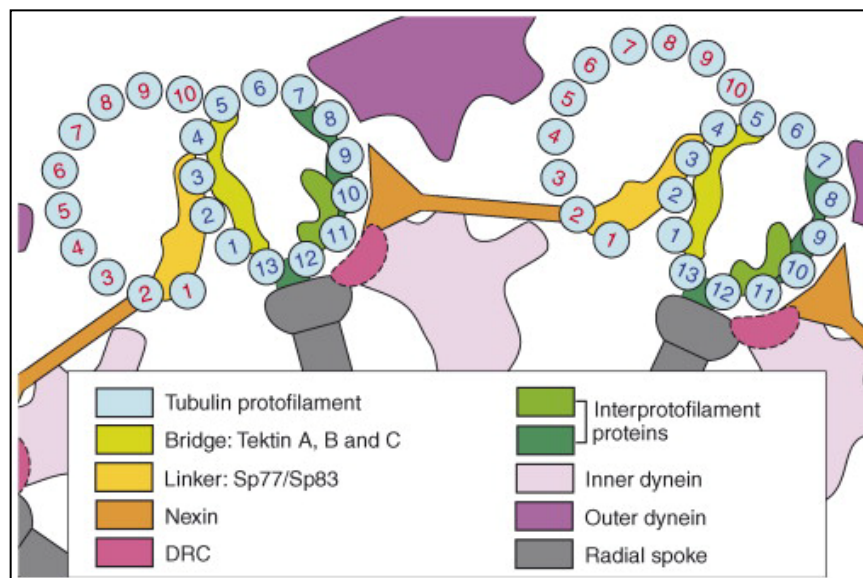


**Figure 1.3 Schematic showing the relationship between microtubule doublets and other proteins in the axoneme.** Subfibre A is a complete microtubule composed of 13 parallel protofilaments onto which the inner and outer dynein arms attach (numbers 1 to 13 in blue). Subfibre B is incomplete and contains only 10 protofilaments (numbers 1 to 10 in red). Locations of dynein arms, tubulin protofilaments and other proteins within the doublets, including nexin, tektin and linker proteins are given. The numbers represent the subunits. DRC=Dynein regulatory complex. Taken from (Downing and Sui 2007).

### **1.3.3 Microtubule associated proteins**

#### **1.3.3.1 Dynein arms**

Dynein is a high molecular protein and functions as a motor to generate the force needed for motility. The force is generated through adenosine triphosphate hydrolytic activity sites, which are conserved within nucleotide binding motifs called P-loops (Gibbons 1995). In the axoneme, dynein complexes are visualised as inner or outer “arms” and are attached to the A tubule and project towards the B tubule of each microtubule doublet (Figure 1.1 and 1.3). Both dynein arms are present on each of the nine peripheral microtubule doublets. During ciliary beating the dynein arms interact with adjacent microtubules and move the microtubules relative to each other.

Dyneins are members of a large family composed of axonemal and cytoplasmic dyneins, which are classified according to their size, as heavy, intermediate and light chains. Around two-thirds of the C-terminal heavy chain makes up the motor domain. The N-terminal region of the heavy-chain interacts with different intermediate and light chains to form either an outer or inner dynein arm. As the dynein arms are highly conserved across phyla, the green ciliated alga, *C. reinhardtii*, has served as an important tool for understanding the function and structure of human cilia (Gibbons 1995, Harrison and King 2000).

#### **1.3.3.2 Radial spokes**

The membrane sheath surrounding the central microtubule pair is joined to the outer doublets with T-shaped radial spoke proteins. Each radial spoke consists of a "stalk" and "head" and these structures are made up of many protein subunits (Yang *et al.* 2001).

Radial spokes are known to contain at least 17 different proteins, 5 are located in the head and 12 make up the stalk (Yang *et al.* 2001). Figure 1.1 shows the stalk structure of radial spokes binding to the A-tubule of each microtubule doublet, with the spoke head facing in towards the centre of the axoneme (Yang *et al.* 2001, Yang *et al.* 2006). Radial spokes are known to play a role in the movement of the cilium and also influence the bending pattern of the cilium. It has been shown that mutant organisms, that lack functioning radial spokes, have immotile cilia (Yang *et al.* 2006). It is not understood how radial spokes carry out their functions, although they are thought to interact with both the central pair microtubules and the dynein arms. RSP3, is one of the radial spoke subunits and an anchor protein, which is thought to hold a protein kinase A that interacts with dynein arms and regulates ciliary beating (Figure 1.4) (Wirschell *et al.* 2008).

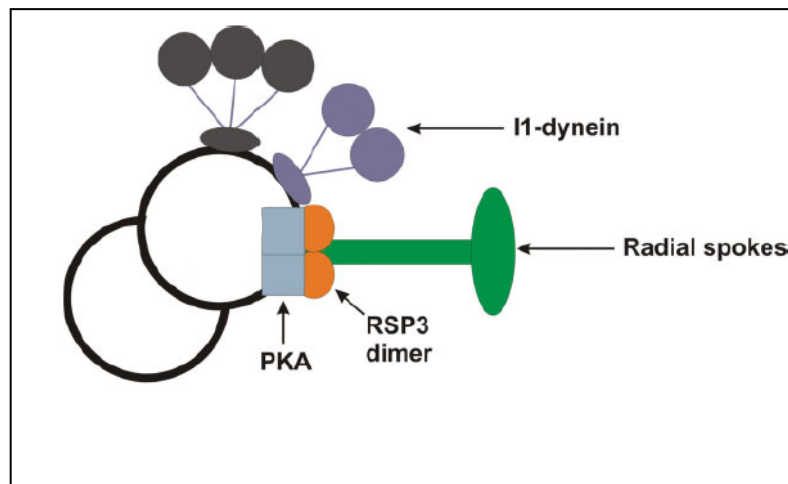


**Figure 1.4 Model showing the RSP3 dimer at the base of the radial spoke stalk.** RSP3 is required for anchoring the radial spoke to the A tubule of the outer doublet. PKA=protein kinase A. Adapted from (Wirschell *et al.* 2008).

### **1.3.3.3 Nexin links**

The adjacent outer doublet microtubules are connected by a flexible linker protein called nexin. Figure 1.3 shows nexin linking the A9-A11 protofilaments of the A tubule in one doublet to the B2 protofilament in the adjacent B-tubule doublet (Nicastro *et al.* 2006, Sui and Downing 2006). Nexin is proposed to be part of the regulatory process that maintains a regular ciliary beat (Woolley 1997). It is thought that due to the zigzag structure and its close relationship to the dynein regulatory complex, the stretching of nexin may play a role in the regulation and coordination of the dynein arms (Woolley 1997).

### **1.3.3.4 Dynein regulatory complex**

The dynein regulatory complex is thought to mediate signals between dynein arms, nexin links and radial spokes to regulate ciliary beating (Gardner *et al.* 1994, Meeks and Bush 2000, Porter and Sale 2000). This complex is a group of seven polypeptides, several of which are clustered on subfibre A, located at the tip of the base of the second radial spoke in close association with the inner dynein arm (Figure 1.3) (Gardner *et al.* 1994, Woolley 2000).

### **1.3.3.5 Other microtubule associated proteins**

Dynein is not the only molecular motor within the ciliary axoneme. The proteins kinesin and myosin have been associated with inner singlet microtubules and the basal bodies, respectively (Wanner *et al.* 1996). Other molecular processors and messenger systems have also been identified as structural components within the axoneme (Smith 2002). Examples are kinases, phosphatases and calcium binding proteins that are bound to the

axoneme and are thought to have a role in ciliary function. Table 1.1 lists these molecules.

**Table 1.1 Kinases, phosphatases and calcium binding proteins bound to the ciliary axoneme.**

| <b>Kinase</b>             | <b>Location</b>   |
|---------------------------|---|
| Protein kinase A          | axoneme (Smith 2002)  |
| A-kinase anchor proteins  | central microtubules and radial spokes (Kultgen <i>et al.</i> 2002) |
| Calmodulin binding kinase | radial spokes (Porter and Sale 2000)                                |
| Casein kinase             | outer doublets (Kultgen <i>et al.</i> 2002)                         |
| Centrin/catractin         | inner dynein arms (Smith 2002)                                      |

### **1.3.3.6 Basal body**

At the base of the cilium is the basal body, which is held within the apical domain of the cell cytoplasm by a macromolecular complex. The basal body consists of nine microtubule triplets; each triplet is composed of one complete A tubule and incomplete B and C tubules (Haimo and Rosenbaum 1981).

## ***1.4 Mechanism of motion***

The beat pattern of cilia is asymmetric and consists of two main strokes: a fast forward effective stroke (power stroke), followed by a slower recovery stroke (Chilvers and O'Callaghan 2000a). During the effective stroke the cilium is fully extended and during

the recovery stroke the cilia bends 90° and sweeps back to the starting point (Figure 1.5) (Chilvers and O'Callaghan 2000a). The mechanism of ciliary motion depends on the molecular motors (outer and inner dynein arms) built into the axoneme which act to produce force that cause the doublet microtubules to slide with respect to one another (Satir 1989). The C terminus of B1, B4 and B5 tubules of the microtubule A doublet (Figure 1.3) have been shown to be critical for this interaction as antibodies against these structures have been shown to inhibit the movement of isolated bovine axonemes (Vent *et al.* 2005). Analysis of ciliary beating patterns in patients with PCD has revealed that mammalian cilia regulate their bending form by means of inner arms and their frequency by means of outer dynein arms (de Iongh and Rutland 1995, Chilvers *et al.* 2003a). The central pair divides the axoneme into opposite halves. The motors on one side of the axoneme are mainly active during the effective stroke while the motors on the other side are predominantly active during the recovery stroke (Antunes and Cohen 2007). The stroke orientation is dictated by the orientation of the basal body of the axoneme (Satir 1999, Lee *et al.* 2005). In addition, ciliary activity accelerates in response to a variety of chemical (Wong *et al.* 1990, Jain *et al.* 1993), mechanical (Sanderson and Dirksen 1986), hormonal (Sanderson and Dirksen 1989, Jain *et al.* 1995, Gheber *et al.* 1998) and thermal stimuli (Mwimbi *et al.* 2003), through second messenger cascades resulting in alterations of the phosphorylation status of axonemal proteins (Wang and Satir 1998, Zagoory *et al.* 2002, Gertsberg *et al.* 2004).

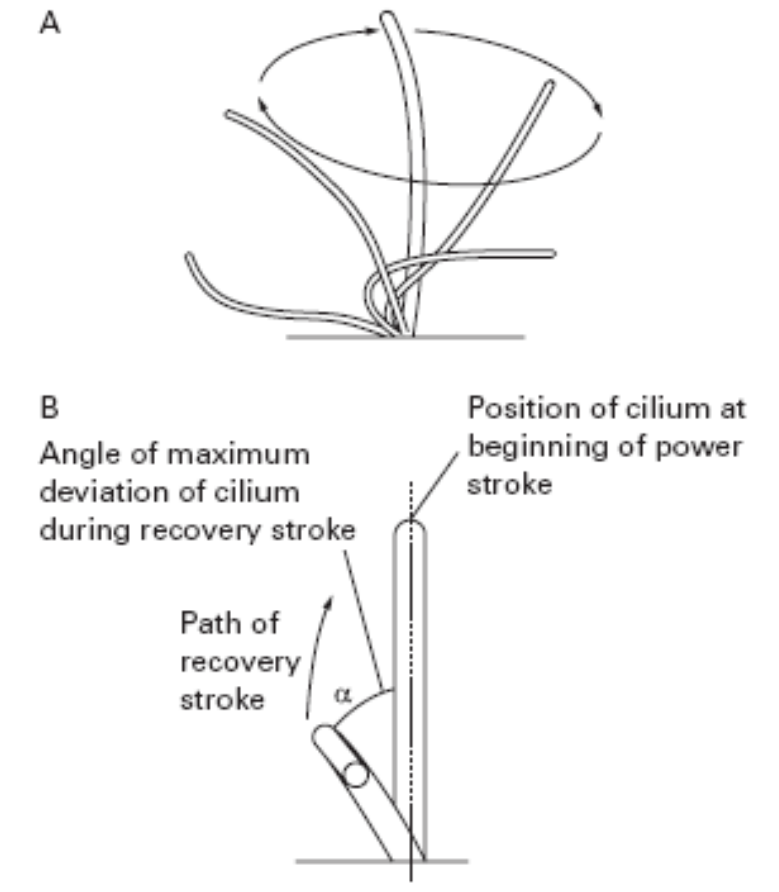


**Figure 1.5** Planes of view used to observe and record the ciliary beat cycle and beat frequency. (A) Side profile of the ciliary beat pattern. (B) Beat angle  $\alpha$ , the cilium is viewed beating forward from the plane of the paper. The beat angle is formed by the point of maximum deviation of the cilium during the recovery stroke from the path the cilium travels during the power stroke. Taken from (Chilvers and O'Callaghan 2000a).

## ***1.5 Ciliogenesis***

Ciliogenesis is a complex series of events involving the production and docking of basal bodies at the apical membrane, followed by generation of the ciliary axoneme (Pan *et al.* 2007). More and more mutations in genes with roles in ciliogenesis have been implicated in human diseases (Ibanez-Tallon *et al.* 2003). Environmental factors such as respiratory viruses and cigarette smoke also affect cilia, causing ciliary loss and require intact mechanisms of ciliogenesis for repair (Sisson *et al.* 1994, Look *et al.* 2001, Ibricevic *et al.* 2006). Mechanistically, many concepts of ciliogenesis and cilia assembly are based on the analysis of transmission electron micrographs from developing ciliated airways provided over a quarter of a century ago (Sorkin 1968).

One of the earliest known steps marking the onset of ciliogenesis is the generation of centrioles through a process that requires  $\gamma$ -tubulin nucleation (Dutcher 2003). The centrioles then become basal bodies upon docking at the apical membrane of the cell, where axoneme assembly follows (Pan *et al.* 2007). This stage requires an active remodelling of the cytoskeleton to provide a dense actin net or web at the apical membrane for basal body docking (Pan *et al.* 2007). The establishment of this actin net in ciliated airway epithelial cells relies heavily on small GTPases, and particularly RhoA (Pan *et al.* 2007). Some genes that regulate ciliogenesis have been identified. Transcription factor Foxj1 is required for docking basal bodies at the apical membrane and subsequent axoneme production (Brody *et al.* 2000, You *et al.* 2004). It has also been shown to promote RhoA activity and is required for apical actin localisation (Pan *et al.* 2007). Transcription factor, hepatocyte nuclear factor 3/forkhead homolog 4 (HFH-4), has been shown to be involved in regulating the morphogenesis of

mammalian motile cilia (Brody *et al.* 2000). Transcription factors TTF1 and Foxa2 (HNF-3 $\beta$ ) have also been shown to be expressed in ciliated epithelial cells prior to ciliogenesis (Stahlman *et al.* 1998).

Axoneme assembly occurs as multiprotein complexes are transported along the microtubules bidirectionally for assembly and maintenance of cilia in a process termed intraflagella transport (Kozminski *et al.* 1993). Intraflagella transport studies have revealed that dyneins, and other building blocks of cilia, dock at the basal body while awaiting transport to the distal axoneme by kinesin motor proteins (Brody 2004). After the cargo is deposited and axonemal turnover products picked up, the complexes are moved back towards the base by a cytoplasmic dynein (Rosenbaum and Witman 2002, Scholey 2003). This process in which proteins are loaded onto the intraflagella transport particles at the ciliary base, and are transferred across the ciliary compartment, is known as compartmentalisation ciliogenesis (Avidor-Reiss *et al.* 2004). The intraflagella transport process also controls ciliary length. Figure 1.6 shows a schematic of intraflagella transport. Mutations or deficiencies in intraflagella transport components are hypothesised to be the basis of defects in sensory cilia in some forms of polycystic kidney disease and retinitis pigmentosa (Brody 2004, Wilson 2004, Zhang *et al.* 2004). In motile cilia, mutations in dyneins may also result in a “traffic jam” at the basal body or proximal axoneme, leading to failed transport of ciliary motor proteins and subsequently a PCD phenotype (Fliegauf *et al.* 2005). These studies emphasise the impact of a dynein mutation and provide one mechanism for failure of dynein arm formation in PCD. For more information see the review by Eggenschwiler *et al.* (2007).

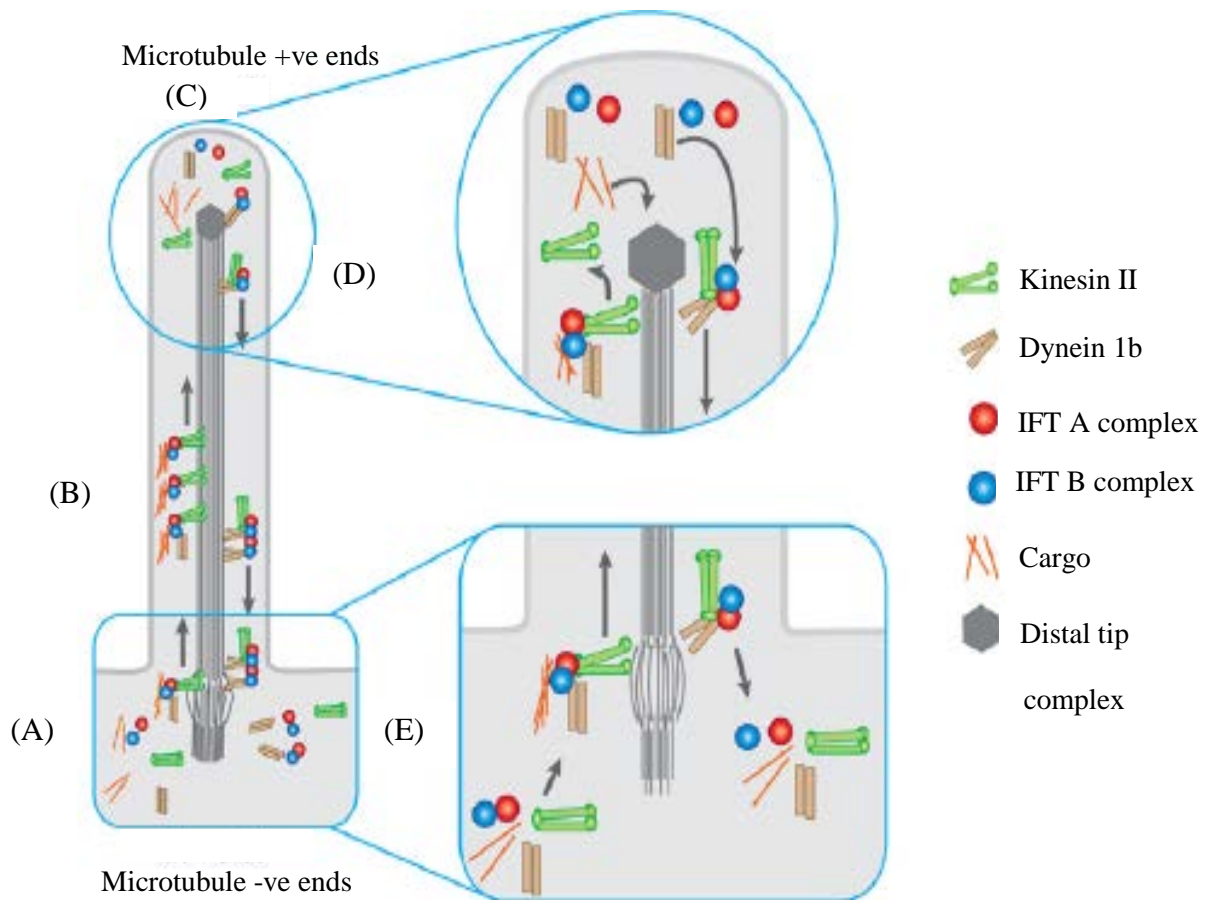


**Figure 1.6 Diagram showing the main features of intraflagella transport.** (A) IFT complexes and the associated cargo required for cilia assembly and maintenance gather around the base of the growing cilium awaiting transport to the distal tip. (B) Transport to the distal tip is powered by the motor protein kinesin II. This is known as anterograde transport (transport of molecules from the cell body, mediated by kinesins). (C) Once at the distal tip complex, the anterograde cargo is unloaded, turnover cargo is picked up, and the kinesin II motor is inactivated for transport back to the cytoplasm. (D) Then the cytoplasmic dynein 1b, itself an anterograde cargo protein, is activated to power the retrograde trip back to the cytoplasm. Retrograde transport involves the transport of molecules back to the cell and is mediated by dynein proteins. (E) At the base, the retrograde apparatus is disassembled, potentially allowing IFT components to be reused. Adapted from (Eggenchwiler and Anderson 2007).

## ***1.6 Ependymal cilia***

The ependyma is a single, uninterrupted, layer of squamous to columnar ciliated cells that lines the cerebral ventricles, cerebral aqueducts and the central canal of the spinal cord (Del Bigio 1995). Figure 1.7 shows the ciliated ependymal cells from the fourth ventricle of a rat brain. Ependymal cells arise from the germinal matrix in the developing brain surrounding the ventricular system (Sturrock and Smart 1980, Gould *et al.* 1990). Each ependymal cell has approximately 40 cilia, approximately 8  $\mu\text{m}$  long, that beat continuously at a frequency of around 40 Hz (Del Bigio 1995, O'Callaghan *et al.* 1999), moving the CSF and cellular debris close to the ventricular wall in the direction of CSF flow (Cathcart and Worthington 1964, Shimizu and Koto 1992). Other recognised functions of the ciliated ependymal cells include, acting as neural stem cells (Johansson *et al.* 1999), and locally mixing the CSF thus minimising the unstirred CSF layer over the ependyma and optimizing the distribution of neuronal messengers in the CSF (Roth *et al.* 1985). By keeping the surface of the brain and aqueducts clear of debris the ciliated ependymal cells may have a role in host defence (Mohammed *et al.* 1999, Hirst *et al.* 2003).

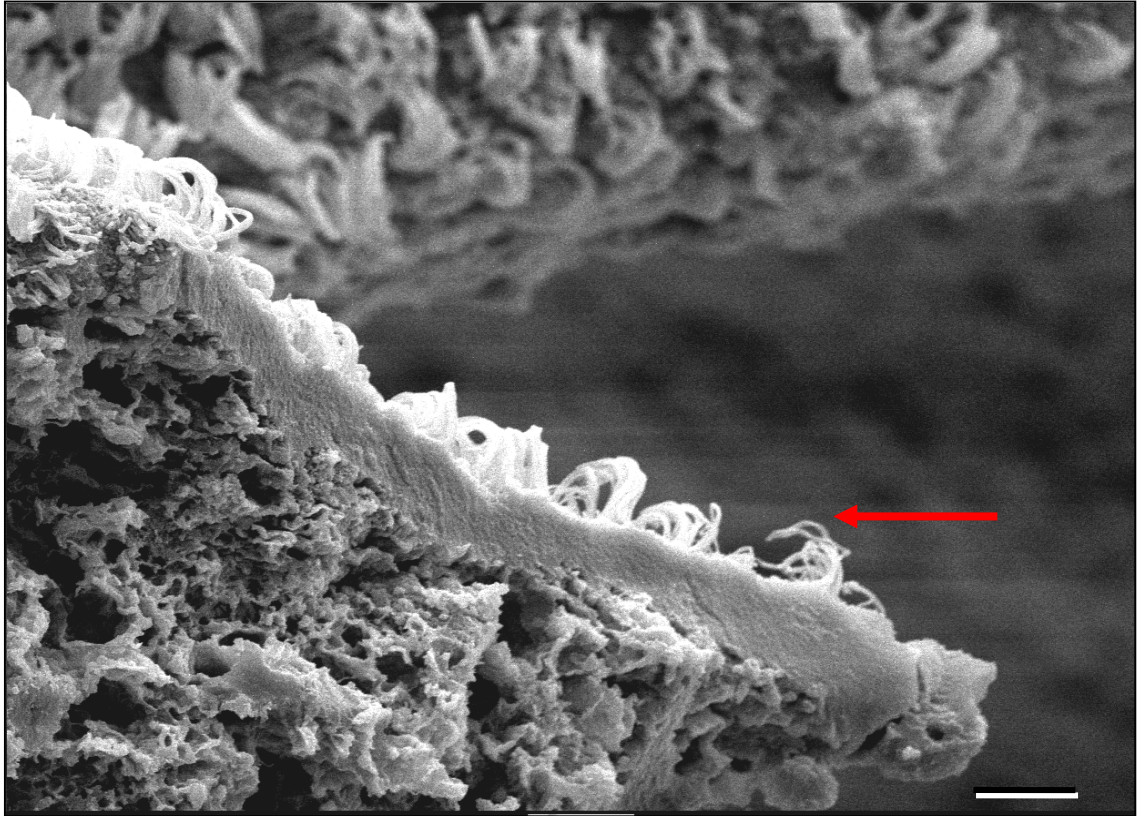


**Figure 1.7 Scanning electron micrograph of ciliated ependyma of the fourth ventricle in a rat brain.** The arrow is pointing to cilia. The brain slice is 200 $\mu$ m thick. Scale bar represents 100  $\mu$ m. This image was taken by Andrew Rutman, University of Leicester.

### **1.6.1 Cerebral spinal fluid (CSF)**

The cerebrospinal fluid (CSF) is located within the ventricles, spinal canal, and subarachnoid spaces (Han and Backous 2005). The CSF is secreted from two sources at the rate of 0.35 ml/min (Jorgensen 1988). First it is actively secreted by the choroid plexus, present in each of the four ventricles and second, as the CSF travels along the brain vasculature, it picks up an additional contribution of volume derived from the products of brain metabolism (Bradbury and Lumsden 1979). The CSF makes up 10-20% of brain weight (Bradbury and Lumsden 1979). The choroid plexus has an epithelial lining with highly vascularised tissue and forms a barrier between the CSF and blood by tight junction coupling (Grondona *et al.* 1998). CSF moves within the ventricles and subarachnoid spaces under the influence of hydrostatic pressure generated by its production (Johanson *et al.* 2008). The movement of CSF through the ventricular system occurs from the lateral ventricles to the third ventricle via the foramen of Munro, then through the Sylvain aqueduct to the fourth ventricle and finally into the cisterna magna of the subarachnoid space and the central canal of the spinal cord (Figure 1.8) (Picketts 2006). CSF fluid is then removed through the arachnoid villi into the venous circulation (Picketts 2006).

The CSF has many roles including, acting as a cushion for the brain, allowing the distribution of neuroactive substances, and is the "sink" that collects the waste products produced by the brain (Han and Backous 2005). It is thought that the flow of CSF may also be crucial for neuronal function, although it is not known how the direction of CSF movement in the ventricles is established, or its associated functional consequences (Killer *et al.* 2007). Recently, Sawamoto *et al.* found that the CSF flow correlated with the planar polarity of the ependymal cells that line the ventricles and the orientation of

neuroblasts migration (Sawamoto *et al.* 2006). Also, the chemorepulsive factors present in the choroid plexus are distributed in a gradient that corresponds to the direction of CSF flow and neuronal migration (Sawamoto *et al.* 2006). Neuroblasts in the adult brain are formed in the subventricular zone and then travel to their final destination in the olfactory bulb. In Tg737<sup>orpk</sup> mutant mice, which have severe defects in ciliary motility, the CSF flow is abnormal and only around 9% of the neuroblasts generated in the subventricular zone reach the olfactory bulb (Sawamoto *et al.* 2006). Therefore, Sawamoto and colleagues proposed that the coordinated beating of the ependymal cilia, and thus the CSF flow, produces a chemorepulsive gradient in the subventricular zone that may help guide neuroblasts towards the olfactory bulb.

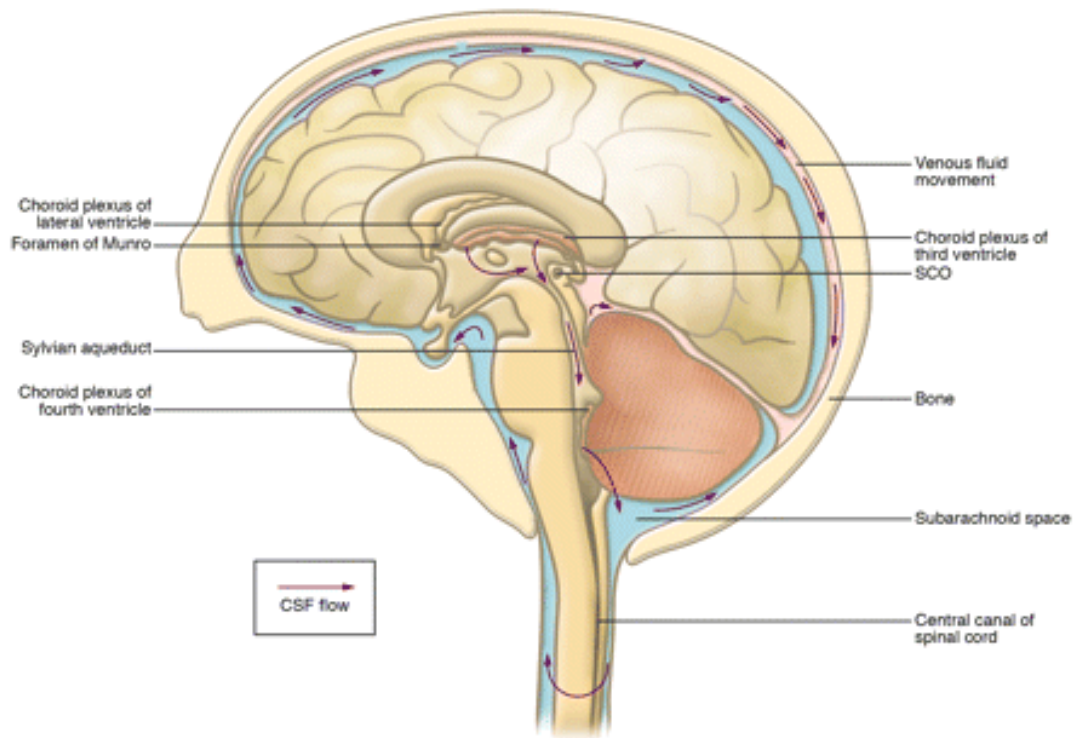


**Figure 1.8 Diagrammatic section through the human brain showing the CSF flow.** The movement of CSF through the ventricular system occurs in a rostral-caudal direction, from the lateral ventricles to the third ventricle via the foramen of Munro, then through the Sylvian aqueduct to the fourth ventricle and finally into the cistern magna of the subarachnoid space and the central canal of the spinal cord. CSF fluid is then removed through the arachnoid villi into the venous circulation. Taken from Picketts (2006).

---

### **1.6.2 Regulation of ciliary beat frequency (CBF) and CSF flow in the ependyma**

It is thought that the CBF is regulated by an increase in cytosolic  $\text{Ca}^{2+}$  levels (Nguyen *et al.* 2001). Nguyen and colleagues have shown that the CBF of ciliated ependymal cells is mediated by the activation of serotonin (5-HT) receptors, resulting in  $\text{IP}_3$  (inositol 1,4,5-triphosphate) mediated release of  $\text{Ca}^{2+}$  from intracellular  $\text{Ca}^{2+}$  stores (Nguyen *et al.* 2001). The initial elevation of cytosolic  $\text{Ca}^{2+}$  levels then causes a prolonged increase of intracellular  $\text{Ca}^{2+}$  due to the opening of  $\text{Ca}^{2+}$  release-activated  $\text{Ca}^{2+}$  (CRAC) channels in the plasma membrane (Nguyen *et al.* 2001). It is also thought that the binding of ATP to a purinergic receptor, which activates adenylate cyclase to generate cAMP, inhibits ciliary beating (Nguyen *et al.* 2001, Monkkinen *et al.* 2007). Figure 1.9 presents a model by Nguyen *et al.* (2001) for these pathways. Other regulatory mediators of CBF include the  $\text{G}\alpha_{i2}$  G protein, which is localised in the ventricular regions including the ependymal cilia (Monkkinen *et al.* 2007). Monkkinen and colleagues have shown that knockdown of  $\text{G}\alpha_{i2}$  by specific antisense oligonucleotides, resulted in ciliary stasis on cultured rat ependymal cells *in vitro* and hydrocephalus in the rat *in vivo* (Monkkinen *et al.* 2007). This demonstrates an essential role of  $\text{G}\alpha_{i2}$  in ciliary function and CSF volume (Monkkinen *et al.* 2007). Other studies have also demonstrated a role for pituitary adenylate cyclase-activating polypeptide type 1 receptor (PAC1) in the regulation of CSF circulation and development of hydrocephalus (Lang *et al.* 2006, Picketts 2006). Activation of PAC1 receptors with pituitary adenylate cyclase-activating polypeptide, has also recently been shown to reduce ciliary beat frequency and ciliary amplitude in primary cultures of rat brain ependymal cilia (Mnkkonen *et al.* 2008).

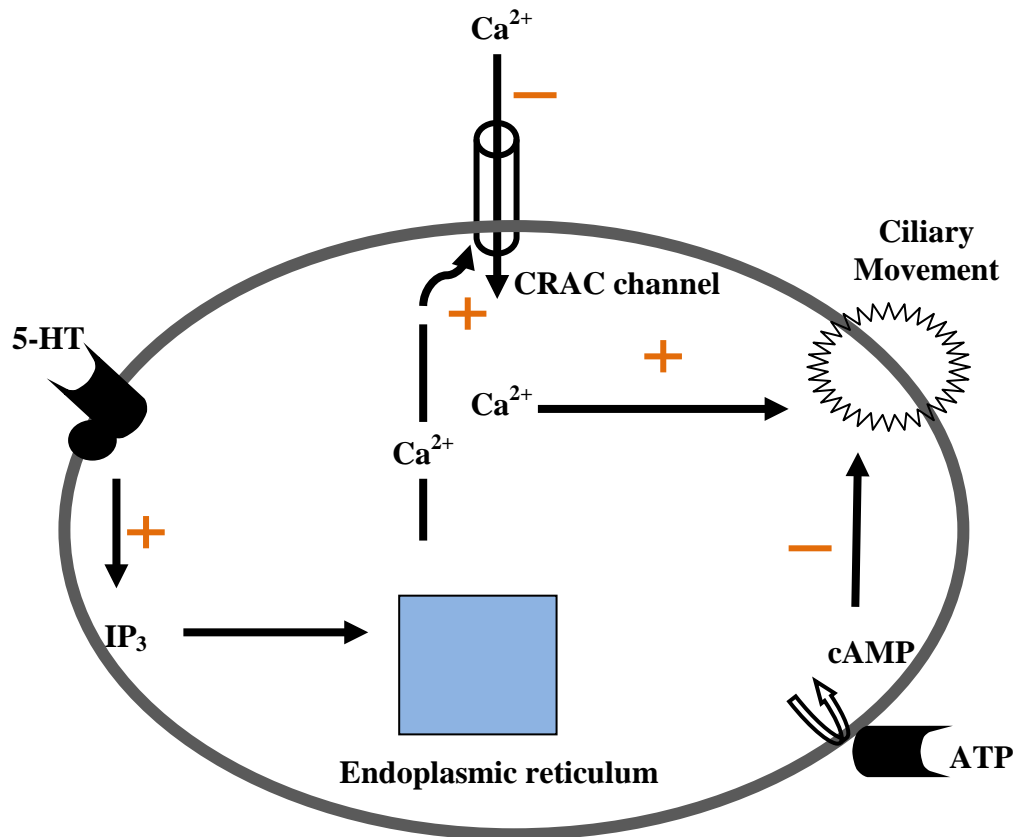


**Figure 1.9 Two independent pathways, involving 5-HT and ATP, with opposing effects on ciliary beating of ependymal cells.** In the first pathway exposure to 5-HT increases ciliary beating by activating a 5-HT receptor, that triggers the generation of intracellular IP<sub>3</sub>, which releases Ca<sup>2+</sup> from intracellular Ca<sup>2+</sup> stores. The released Ca<sup>2+</sup> mediates the opening of CRAC channels that results in the influx of Ca<sup>2+</sup> from the extracellular environment. The increases in Ca<sup>2+</sup> ultimately increase CBF by an as yet unidentified mechanism. In contrast in the second pathway, ATP binding activates the production of intracellular cAMP, which inhibits CBF by a still to be identified mechanism. Adapted from (Nguyen *et al.* 2001).

---

### **1.6.3 Ependymal ciliary defects and disease**

Abnormal movement of the ependymal cilia, and thus the CSF flow, has been strongly linked to the development of hydrocephalus (Shimizu and Koto 1992, Picco *et al.* 1993, Hirst *et al.* 2003, Ibanez-Tallon *et al.* 2004, Banizs *et al.* 2005, Sawamoto *et al.* 2006). Hydrocephalus is a progressive pathological condition characterised by excessive accumulation of CSF in the brain ventricles. Hydrocephalus can be caused in a number of ways; impaired CSF flow, excess CSF production or lack of CSF reabsorption (Bruni *et al.* 1985, Garton and Piatt 2004). Damage of the ciliated ependyma by bacteria such as *S. pneumoniae* or *L. monocytogenes* can also lead to hydrocephalus (Grafe *et al.* 2001, Hirst *et al.* 2003).

Hydrocephalus is also seen in patients and small animals with primary ciliary dyskinesia (Koto *et al.* 1987a, Koto *et al.* 1987b). Primary ciliary dyskinesia is an inherited condition in which all of the cilia are immotile or beat in a dyskinetic fashion (Chodhari *et al.* 2004), making them inefficient in propelling fluid or mucus (see part B of the introduction). Further insight into the connection between dysfunctional cilia and the development of hydrocephalus was recently demonstrated. Banizs and colleagues have shown that severely dysfunctional and malformed cilia in the choroid plexus resulted in disturbed cAMP-regulated chloride transport, leading to excess CSF production and hydrocephalus (Banizs *et al.* 2005). Also, Omran and colleagues have shown that dysfunction of the axonemal dynein heavy chain (Mdnah5) inhibited ependymal flow leading to hydrocephalus formation (Ibanez-Tallon *et al.* 2004). An inhibitor of ciliary movement, metavanadate, has also been shown to induce hydrocephalus in rats (Nakamura and Sato 1993).

---

## ***1.7 Lung/ Respiratory cilia***

The lung is the largest epithelial surface exposed to the environment and is constantly at risk of exposure to respiratory pathogens and toxic environmental agents (Chilvers and O'Callaghan 2000b). The respiratory epithelium primarily consists of two types of cells, mucus producing goblet cells and ciliated cells (80%) (Antunes and Cohen 2007). Epithelial basal cells have the potential to divide and differentiate and are the main airway epithelial progenitor cells from which ciliated columnar epithelial cells, goblet cells and clara cells derive (Inayama *et al.* 1988, Hong *et al.* 2004). Basal cells have a cobblestone like appearance and do not extend up to the surface layer; consequently the respiratory epithelium has a pseudostratified structure (Widdicombe *et al.* 1985, Liedtke 1988) (Figure 1.10).

Approximately, 200 cilia project from the respiratory cell surface (Rhodin 1966), with a density of around  $6-8\mu\text{m}^{-2}$  (Figure 1.11). Each cilium is approximately 6-7  $\mu\text{m}$  long in the trachea and 2-3  $\mu\text{m}$  long in the lower airways (Wanner *et al.* 1996, Houtmeyers *et al.* 1999), although the width of the cilium is constant, at around 0.2-0.3 $\mu\text{m}$  in diameter (Breeze and Wheeldon 1977, Sleight *et al.* 1988, Kim *et al.* 1997). However, recent research suggests that the ciliary length is maintained in the distal airways with normal ciliary beat frequency and beat pattern (personal communication with Professor Chris O'Callaghan). The respiratory epithelium provides a protective barrier and is composed of two surface liquid layers: the periciliary liquid layer which is a watery fluid that surrounds the cilia on the apical surface of the ciliated cell and provides an ideal environment (low viscosity) for cilia to beat at a frequency of 11 to 14 Hz (Salathe *et al.* 1997, Knowles and Boucher 2002, Chilvers *et al.* 2003b), and the mucus layer which is

rich in mucins and overlays the periciliary layer (Matsui *et al.* 1998a). The vast majority of the ciliary stroke occurs in the periciliary fluid with only the distal tip of the cilia when fully extended making contact with the outer mucus layer.

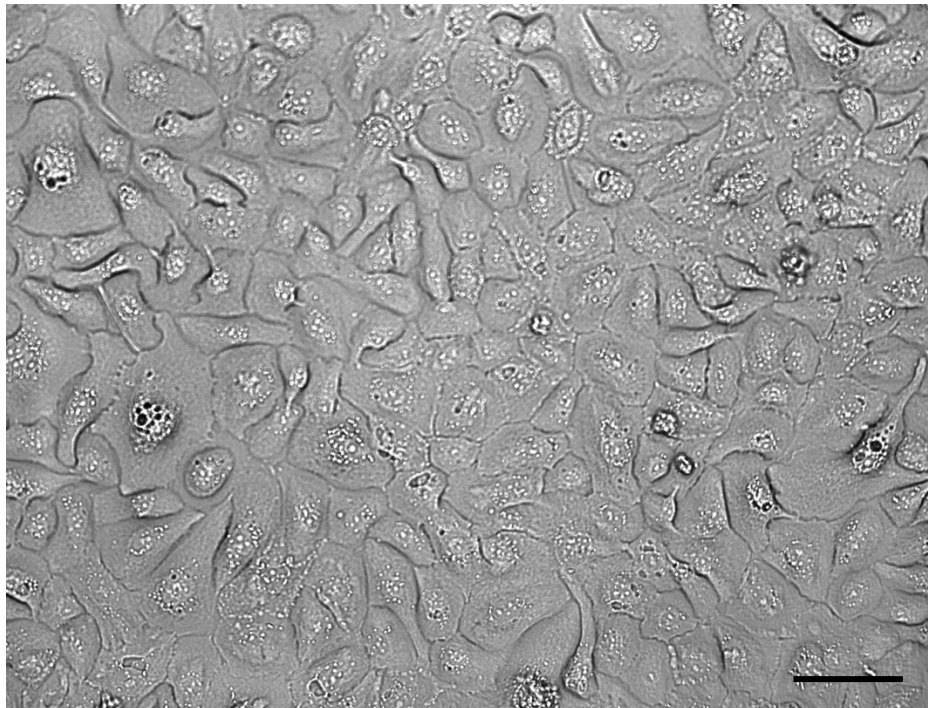


**Figure 1.10** Light microscope image showing the cobblestone appearance of Human respiratory basal cells in culture. Scale bar represents 20 $\mu$ m.

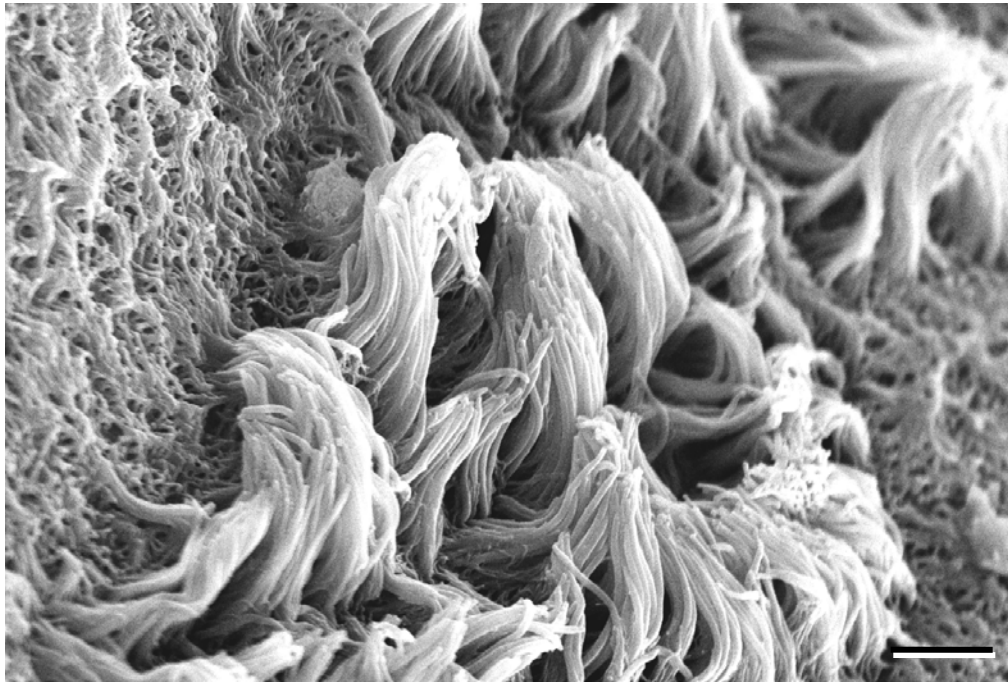


**Figure 1.11 Scanning electron micrograph of human ciliated respiratory epithelium.** Scale bar represents 100 $\mu$ m. Taken by Andrew Rutman, University of Leicester.

### ***1.7.1 Respiratory mucus and mucociliary clearance***

The lung and nasal passages are constantly at risk of exposure to respiratory pathogens and toxic environmental agents, and have evolved a very effective defence system (Stannard and O'Callaghan 2006). A primary innate airway defence mechanism is via the mechanical clearance of mucus and microbes trapped therein (Boucher 1994b, Boucher 1994a, Wanner *et al.* 1996).

Mucus is produced by goblet cells and submucosal glands found in the surface epithelium of the upper and lower respiratory tract (Antunes and Cohen 2007). They secrete high molecular weight mucous glycoprotein's, termed mucins, to protect the epithelial lining from the battery of dust, fumes, microorganisms and other inhaled debris (Antunes and Cohen 2007). The mucins are the product of at least two distinct

genes, MUC5AC and MUC5B (Verdugo *et al.* 1983b) and these proteins mix with other proteins, lipids and glycoconjugate components in fluid to form mucus. Mucus is approximately 1% NaCl, 1% free protein and 1% mucins, with the remainder being water (Houtmeyers *et al.* 1999). Additionally, mucus contains innate immunity proteins, such as lactoferrin and lysozyme which aid in the local immune defences (Sleigh *et al.* 1988). Mucus interacts with the tips of beating cilia and is moved towards the mouth and swallowed. Particles trapped in the mucus are thereby removed from the airways, a process termed mucociliary clearance (Wanner *et al.* 1996). This requires appropriate mucus/periciliary fluid production and coordinated ciliary activity to function effectively (Wanner *et al.* 1996)

The lung also possesses an additional mechanism, namely cough clearance, to clear mucus from the lung. This is independent of ciliary action. However, the periciliary liquid layer has been shown to be an important contributor to the efficiency of cough clearance (Zahm *et al.* 1989). In particular, the lubricating function of the periciliary liquid layer facilitates mucus movement along airway surfaces in response to cough (Knowles and Boucher 2002). Various studies have demonstrated complex interactions among cilia, the periciliary liquid layer and the mucins in the mucus layer (Matsui *et al.* 1998a, Matsui *et al.* 1998b).

### **1.7.2 Regulation of CBF in the airways**

Regulation of ciliary beat frequency is important as it has a direct effect on mucociliary clearance. For some time, it has been thought that the engagement of the ciliary tip with the mucus layer in the airway is critical for adequate mucociliary clearance (Salathe 2007). Tarran and colleagues have shown that the periciliary fluid level appears to

remain reasonably stable if mucus is present, and the addition of fluid to the system seems to swell the mucus layer, with little influence on the periciliary fluid level (Tarran *et al.* 2001). However, the efficiency of mucus transport is improved by the addition of fluid to the system (Tarran *et al.* 2001). Pseudohypoaldosteronism is a genetic disease resulting in an increased amount of airway surface liquid, and mucociliary clearance in these patients is the highest measured (Kerem *et al.* 1999). These data therefore suggest that mucociliary clearance in the airways does not operate at full capacity under normal conditions.

When measured *in vitro*, human respiratory cilia beat at approximately 12–15 Hz at body temperature. Cilia seem to beat in a coordinated manner (metachronal waves), although the mechanism for this coordination is still speculative (Braiman and Priel 2008). It has been suggested that the close spatial relationship of cilia is important for some coordinated beating (Salathe 2007). Also, as at least in part the environment in which cilia beat consists of fluid, significant hydrodynamic forces must exist between beating cilia. It is thought that these hydrodynamic interactions are the most important factor for ciliary coordination on epithelial surfaces (Gheber *et al.* 1998) and may explain why the lengths of metachronal waves are limited (Sanderson and Sleight 1981, Gheber and Priel 1989).

The changes in airway CBF *in vivo* are mediated mainly through the stimulation of receptors by naturally released ligands. Most effects stem from the activation of G protein-coupled receptors (e.g., P2Y<sub>2</sub>, adenosine, bradykinin, and muscarinic acetylcholine receptors), although mechanical influences may also play a role (Sanderson *et al.* 1994). Also, ATP (Homolya *et al.* 2000, Kawakami *et al.* 2004),

acetylcholine (Racke and Matthiesen 2004) and hyaluronan (Lieb *et al.* 2000, Forteza *et al.* 2001) are a few of the known, endogenously produced, molecules that regulate human CBF from the luminal side of the airway.

### **1.7.2.1 Regulation of CBF by cyclic nucleotides**

Cyclic adenosine monophosphate (cAMP) and cyclic guanosine monophosphate (cGMP) are both cyclic nucleotide messengers with regulatory roles for ciliary beat frequency (Wanner *et al.* 1996, Wyatt *et al.* 1998). Cyclic AMP is synthesised by activation of adenylyl cyclase following receptor stimulation (Wyatt *et al.* 1998). Intracellular increases in cAMP concentration cause an increase in ciliary beat frequency (Di Benedetto *et al.* 1991b, Wyatt *et al.* 1998). This is thought to occur via activation of cAMP-dependent protein kinase A, which then alters phosphorylation of specific axonemal target proteins, such as the dynein light chains (Lansley *et al.* 1992, Wanner *et al.* 1996, Uzlaner and Priel 1999). There are numerous lines of evidence linking protein kinase A and a cAMP-dependent phosphorylation-mediated event to CBF increases in the mammalian cilium. First, an A-kinase anchoring protein has been found in human airway cilia (Kultgen *et al.* 2002). Also, protein kinase A and protein kinase A activity have been found in mammalian cilia from multiple species (Salathe *et al.* 1993, Sisson JH 2000, Wyatt and Sisson 2001, Kultgen *et al.* 2002).

Cyclic GMP has been shown to be involved in CBF regulation, at least in some mammalian species (Geary *et al.* 1995, Wyatt *et al.* 1998, Uzlaner and Priel 1999, Zhang and Sanderson 2003). However, how cGMP regulates CBF remains unknown and it is not as well understood as the cAMP-dependent pathway.

### **1.7.2.2 Role of protein kinase C**

Protein kinase C is resident in the cell membrane and is activated by diacyl glycerol, a bi-product formed when inositol triphosphate is generated from the hydrolysis of phosphatidylinositol 4,5- bisphosphate (Poole *et al.* 2004). In contrast to protein kinase A, protein kinase C activation causes a reduction in beat frequency and this observation has been consistent in all mammalian cilia examined (Wanner *et al.* 1996, Wong *et al.* 1998, Wyatt *et al.* 2000).

### **1.7.2.3 Role of calcium in ciliary beat regulation**

Intracellular calcium,  $[Ca^{2+}]_i$ , plays a key role in regulating ciliary beat frequency and is tightly controlled (Briman *et al.* 1998, Uzlaner and Priel 1999). Elevation of  $[Ca^{2+}]_i$  is associated with an increase in CBF (Verdugo 1980, Girard and Kennedy 1986, Sanderson and Dirksen 1989, Villalon *et al.* 1989, Sanderson *et al.* 1990, Di Benedetto *et al.* 1991a, Lansley *et al.* 1992, Salathe and Bookman 1995). Similarly, a fall in  $[Ca^{2+}]_i$  causes a decrease in CBF (Salathe and Bookman 1995, Wanner *et al.* 1996). The calcium that mediates the increase in CBF can stem from either intracellular stores or from calcium influx through the plasma membrane (Salathe *et al.* 1997, Barrera *et al.* 2004). There is still no agreement how calcium regulates CBF but several mechanisms have been proposed. One of the suggested mechanisms in calcium mediated regulation of CBF involves calmodulin and a calcium/calmodulin-dependent kinase, as calmodulin inhibitors blocked calcium-mediated increases in CBF (Verdugo *et al.* 1983a, Di Benedetto *et al.* 1991a). However, calcium/calmodulin-dependent kinase targets have not been found in mammalian cilia and the calmodulin inhibitors used in previous studies were found to be ciliotoxic (Salathe 2007). Also, other calmodulin inhibitors

have been shown not to inhibit calcium's ability to increase CBF (Salathe and Bookman 1999). Thus, these data do not support a role for calcium/calmodulin-dependent kinase and calmodulin in calcium's regulation of mammalian CBF.

#### **1.7.2.4 Regulation of CBF by intracellular pH**

Sutto and colleagues have shown that relatively small changes of intracellular pH, have profound effects on CBF and these changes influence the axoneme directly (Sutto *et al.* 2004). Their data show that intracellular alkalization results in faster ciliary beating in human tracheobroncal epithelial cells, whereas intracellular acidification attenuates CBF (Sutto *et al.* 2004). There is also evidence for direct axonemal beat regulation by intracellular pH. Keskes *et al* have shown that human spermatozoa lacking outer dynein arms failed to exhibit higher beat frequency during mild alkalisation, in contrast to normal spermatozoa (Keskes *et al.* 1998). This suggests that the outer dynein arm activity, which is determining ciliary frequency, may be directly sensitive to pH.

#### **1.7.3 Nitric Oxide in the respiratory tract**

The presence of nitric oxide in the respiratory tract was first demonstrated by the discovery of nitric oxide in exhaled air (Gustafsson *et al.* 1991). Nitric oxide is a signaling molecule, produced from L-arginine by nitric oxide synthases (cNOS) present in epithelial cells (Asano *et al.* 1994, Watkins *et al.* 1998). Three mammalian isoforms have been identified: nNOS (neuronal NOS), iNOS (inducible NOS) and eNOS (endothelial NOS) and all are expressed within the respiratory tract (Moncada and Higgs 1993). eNOS and nNOS are primarily expressed in endothelial and neuronal cell types, respectively, and require calcium and calmodulin for their activation. These two isoforms are highly dependent on increases in intercellular  $Ca^{2+}$  for enzyme activation

(Gaston *et al.* 1994). In the bronchial epithelium, eNOS is localized at the basal membrane of ciliary microtubules, and mediates regulation of ciliary beat frequency (Li *et al.* 2000, Gertsberg *et al.* 2004). nNOS generates nitric oxide as a major mediator of smooth muscle relaxation (Belvisi *et al.* 1992).

The third isoform, iNOS, is induced during inflammatory conditions and is present in cells of the inflammatory immune system (Alderton *et al.* 2001). Patients with allergic rhinitis have been shown to have increased iNOS in nasal epithelial cells, suggesting a role in affecting the inflammatory process (Kawamoto *et al.* 1999). iNOS activity has also been reported to promote airway epithelial cell migration and wound repair following epithelial injury (Bove and van der Vliet 2006). Although under normal conditions iNOS is continuously expressed in human airway epithelial cells (Guo *et al.* 2000).

Within the nose and respiratory tract the postulated functions of nitric oxide include antimicrobial activity (Croen 1993, Braun *et al.* 1999) and upregulation of ciliary motility (Jain *et al.* 1993, Runer *et al.* 1998).

#### ***1.7.4 Respiratory ciliary dysfunction and disease***

Mucociliary clearance relies on normal ciliary function and mucus composition, and diseases arise if any of its components are compromised (Antunes and Cohen 2007). The abnormal movement of airway cilia is seen in patients with primary ciliary dyskinesia (PCD). This is due to various ultrastructural defects (Chilvers *et al.* 2003a), resulting in the dyskinetic cilia markedly reducing the ability of cilia to propel fluid or mucus (impaired mucociliary clearance). As a result PCD patients often present with chronic airway infections and recurrent middle ear infections (Eliasson *et al.* 1977).

Other conditions such as an influenza infection can also lead to impaired mucociliary clearance leading to secondary ciliary dyskinesia (Marcelo *et al.* 2009). Also, in patients with cystic fibrosis the height of the periciliary layer is significantly reduced, due to abnormal mucus production, leading to impaired mucociliary clearance and therefore facilitating the persistent growth of bacterial pathogens (De Rose 2002). Figure 1.12 shows an electron microscope image of healthy human ciliated epithelium and Figure 1.13 shows damaged epithelium as a result of disease.

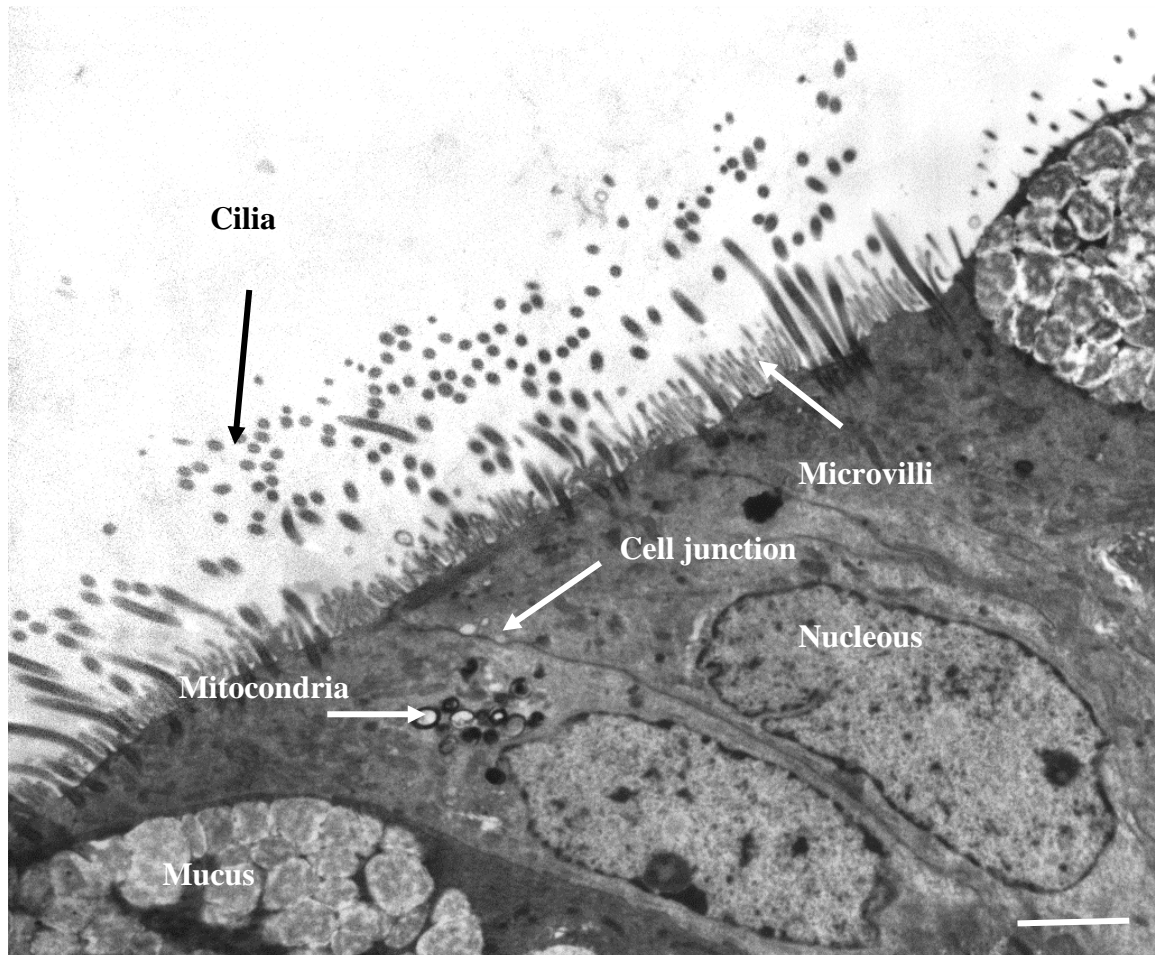


**Figure 1.12** Transmission electron microscopy image of healthy ciliated human airway epithelium. The cell membrane is intact. The scale bar represents 2 $\mu$ m. Taken by Andrew Rutman (NCG PCD clinical referral service in Leicester).

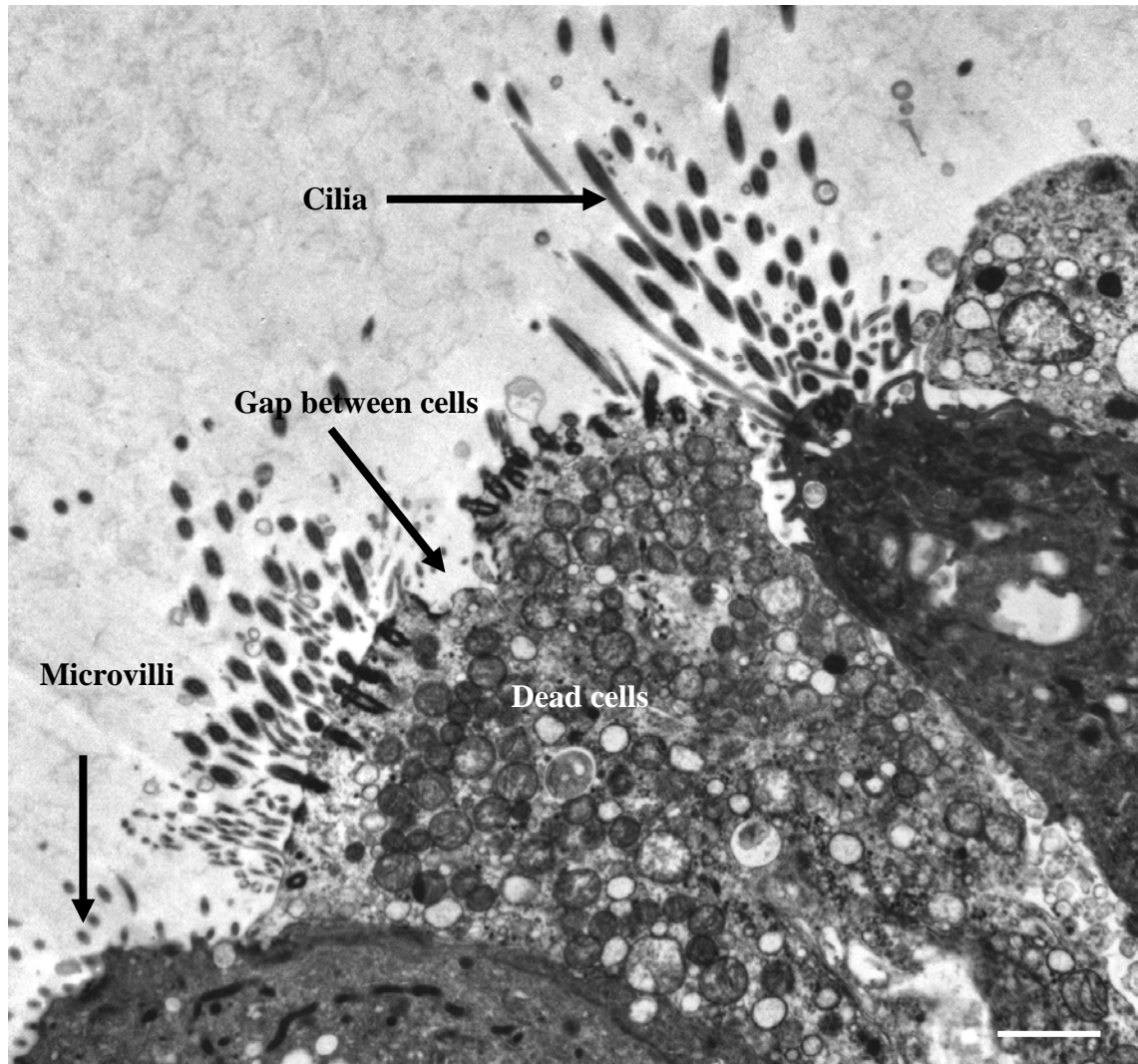


**Figure 1.13** Transmission electron microscopy image of damaged ciliated human airway epithelium. The cells are dying and separating from one another. The scale bar represents 2 $\mu$ m. Taken by Andrew Rutman (NCG PCD clinical referral service in Leicester).

---

## **Part B: Primary Ciliary Dyskinesia (PCD)**

### ***1.8 History***

The first people to describe a syndrome of sinusitis, bronchiectasis and situs inversus were Siewert in 1904 and Kartagener in 1935 (Meeks and Bush 2000). This triad is known as Kartagener's syndrome and is caused by a congenital reduction or absence of ciliary function (Meeks and Bush 2000). In 1976, Afzelius was the first to associate this triad with structural defects in the dynein arms of the respiratory tract cilia (Afzelius 1976). He coined the term "immotile cilia syndrome". Primary ciliary dyskinesia is now the preferred term as it is now recognised that ciliary motility is not always absent, but can be reduced and the cilia may move in a dyskinetic fashion in this condition (Greenstone *et al.* 1988).

### ***1.9 Pathophysiology***

Respiratory cilia have the most relevance in the pathophysiology of primary ciliary dyskinesia (Schidlow 1994). The epithelia of the upper and lower respiratory tract is covered with motile cilia that function to constantly move inhaled particles, cell debris, and microbes towards the throat (Fliegauf *et al.* 2007). This process is termed mucociliary clearance. Due to lack of mucociliary clearance in PCD patients, recurrent infections of the upper and lower respiratory tract ultimately cause permanent lung damage such as bronchiectasis (Meeks and Bush 2000, Geremek and Witt 2004). Deficiencies in dynein arms on the outer microtubular doublets of cilia are the most common ciliary abnormality associated with PCD (Afzelius 1976). There are a number of other deficiencies including a lack of the inner or outer dynein arms, or a complete or

partial lack of both inner and outer dynein arms (Chao *et al.* 1982). Less common causes of PCD have also been reported such as, a radial spoke defect (Sturgess *et al.* 1979) a lack of central core structures in cilia (Afzelius 1979), and a microtubular transposition (Sturgess *et al.* 1980). Electron microscopy images from cross sections of the ciliary axoneme from a healthy subject and PCD patients are shown in Figures 1.14, 1.15 and 1.16. Table 1.2 summarises the reported axonemal defects associated with PCD. It is likely that due to the multiple polypeptides that compose the cilium, further defects exist which are beyond the resolution of the electron microscope (Chao *et al.* 1982, Biggart *et al.* 2001).

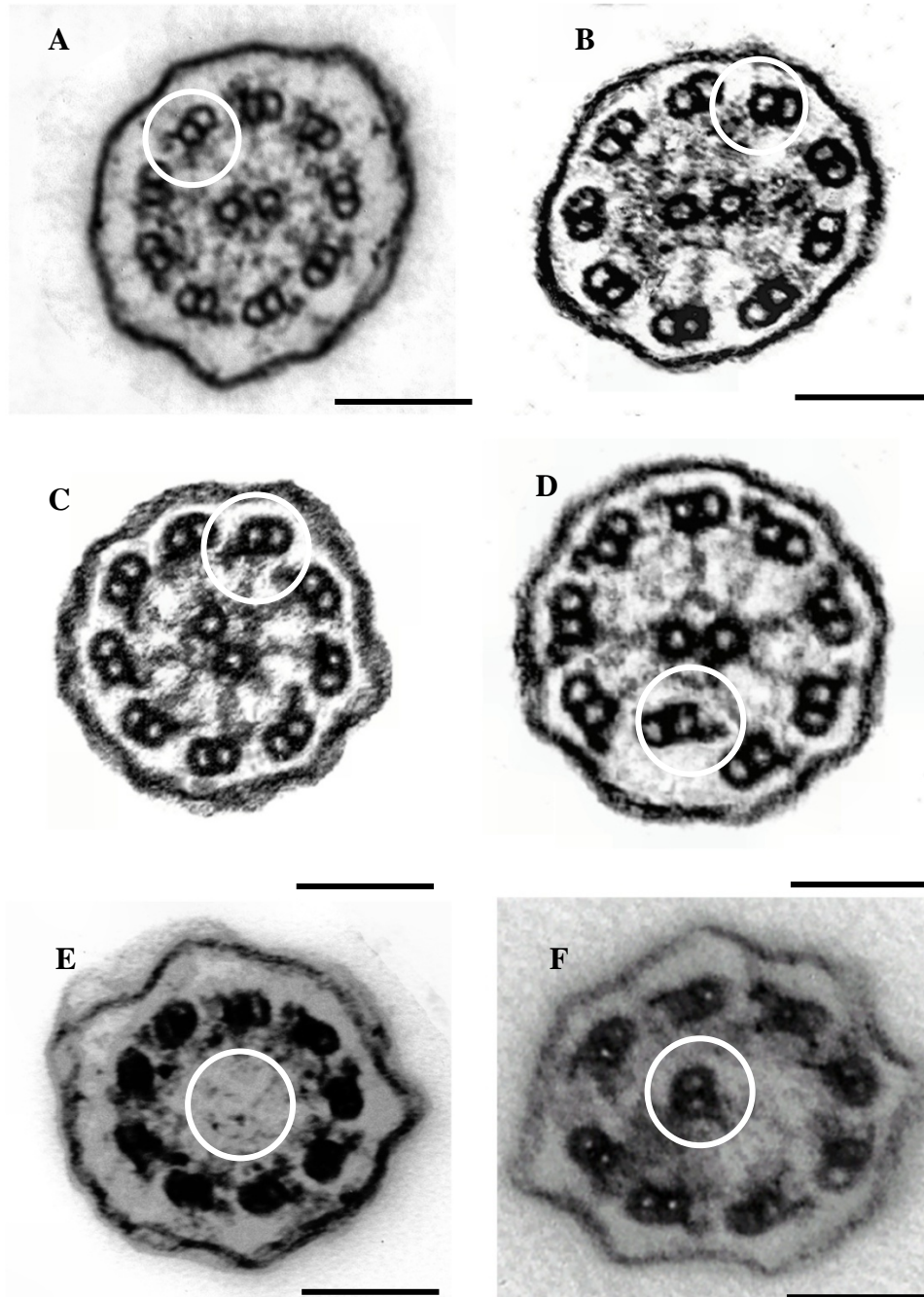


**Figure 1.14** Transmission electron microscopy images of a cross section through the axoneme of cilia from human airway epithelial cells. The cross sections reveal A) the classic 9+2 microtubule structure from a normal individual. Nine peripheral microtubule pairs with their associated inner and outer dynein arms surround the central microtubule pair (circled area). B) Axoneme from a PCD patient demonstrating absent inner and outer dynein arms (circled area). C) Axoneme from a PCD patient demonstrating absent outer dynein arms (circled area). D) Axoneme from a PCD patient demonstrating absent inner dynein arms and axonemal transposition due to radial spoke defect (circled area). E) Axoneme from a PCD patient demonstrating central microtubular agenesis, in which the central microtubule pair is absent (circled area). F) Axoneme from a PCD patient demonstrating ciliary transposition. A peripheral outer microtubule doublet and its dynein arms have transposed to the centre of the axoneme to replace the absent central microtubule pair (circled area). Bar is 100 nm. Taken by Andrew Rutman (NCG PCD clinical referral service in Leicester).

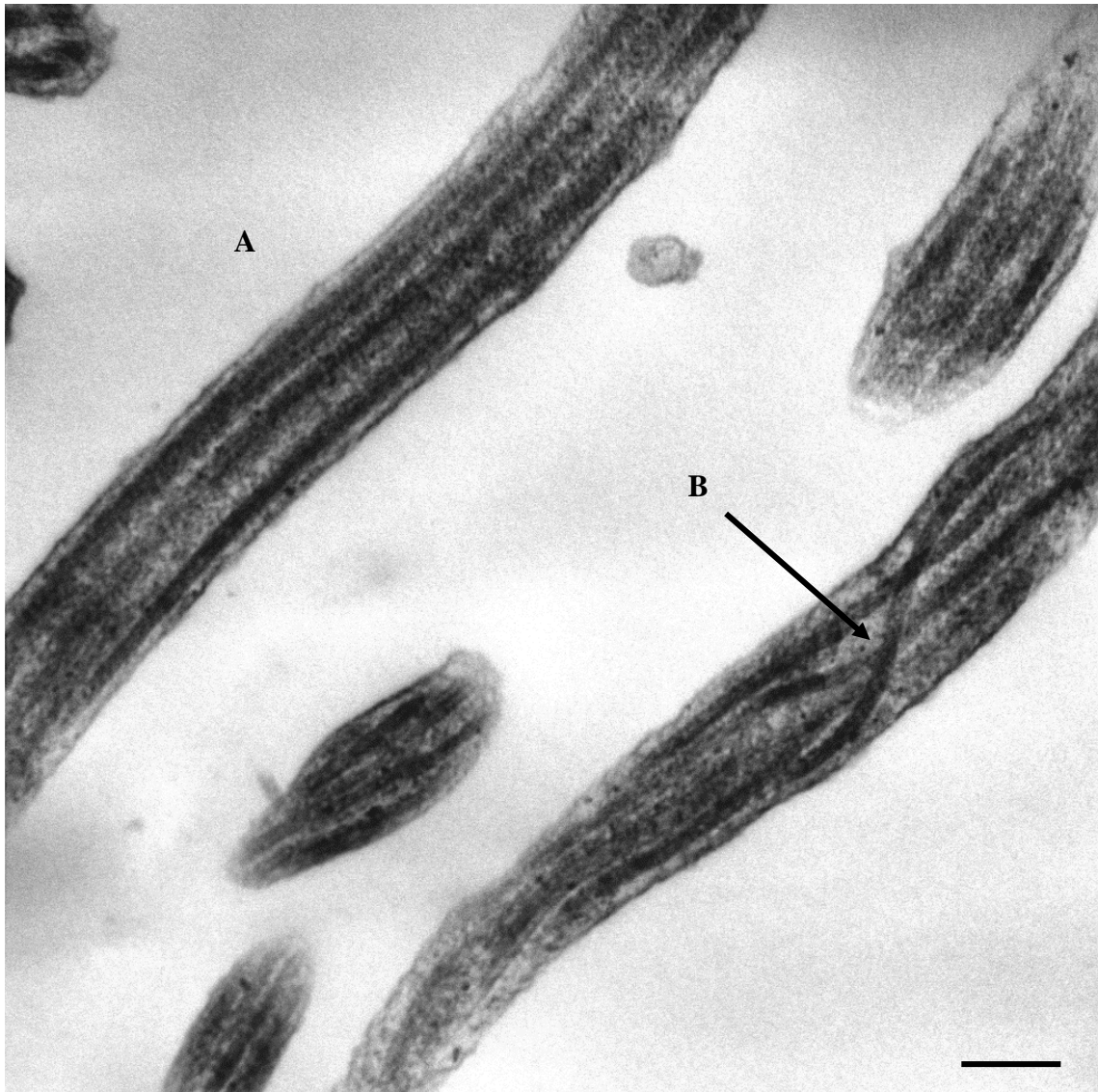


**Figure 1.15** Transmission electron microscopy image of cilia from human airway epithelial cells. The longitudinal sections reveal A) normal peripheral microtubule structures. B) abnormal axoneme demonstrating ciliary transposition. A peripheral outer microtubule doublet have transposed to the centre of the axoneme (arrow). The scale bar represents 100 nm. Taken by Andrew Rutman (NCG PCD clinical referral service in Leicester).

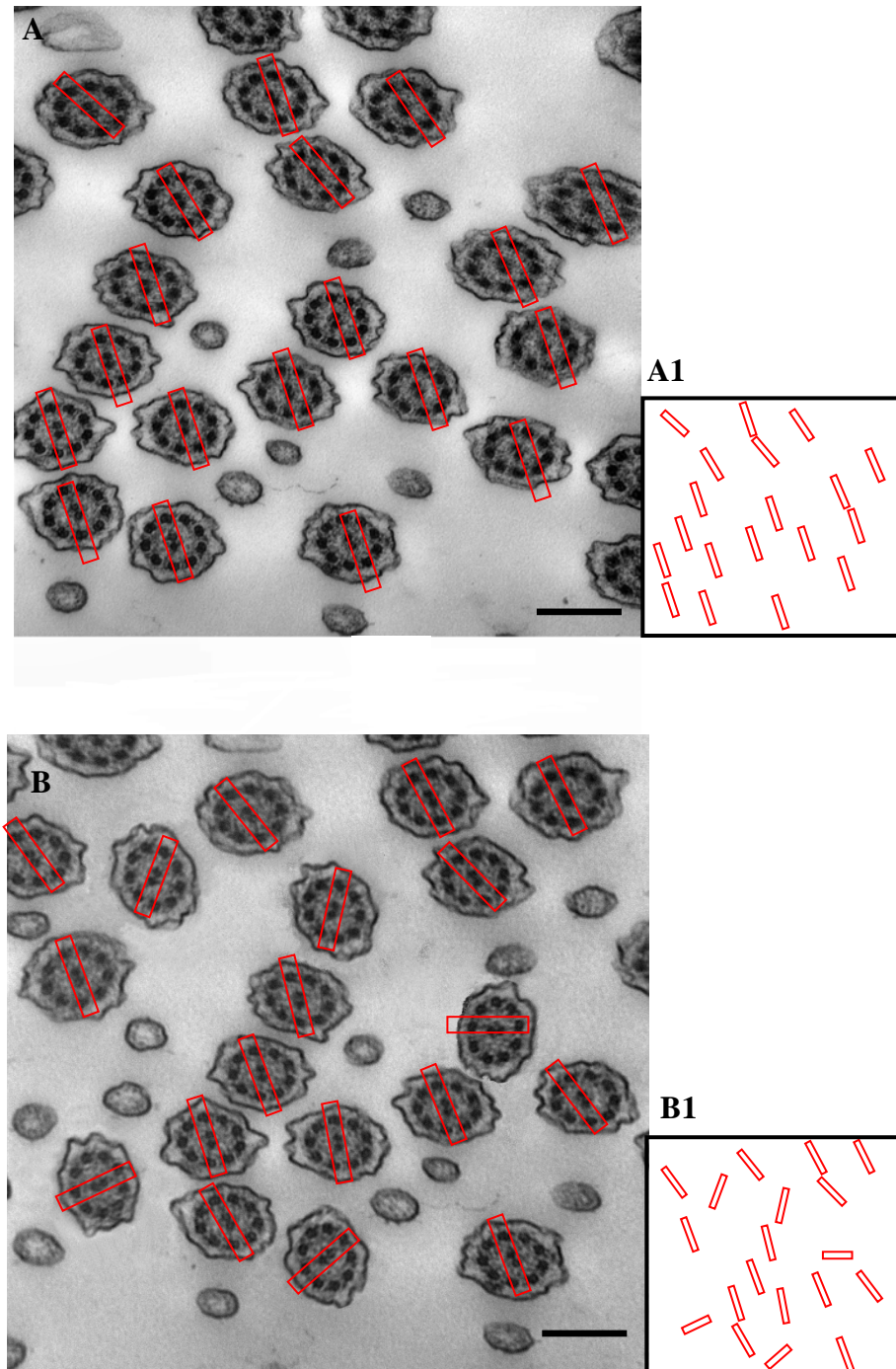


**Figure 1.16** Electron microscopy images of cilia from human airway epithelial cells. A rectangular box has been placed surrounding the central pair axoneme to show ciliary orientation. The cross sections reveal A) normal ciliary orientation. B) abnormal ciliary orientation from a PCD patient. A1 and B1) for clarity the axonemes have been removed and the ciliary orientation displayed. Taken by Andrew Rutman (NCG PCD clinical referral service in Leicester).

Table 1.2 Reported axonemal defects associated with PCD

| <u>Structure</u>          | <u>Defect</u>                            | <u>Reference</u>  |
|---------------------------|--|---|
| <b>Dynein arms</b>        | No outer                                 | (Neustein <i>et al.</i> 1980, Levison <i>et al.</i> 1983)   |
|                           | No inner                                 | (Greenstone <i>et al.</i> 1988)                             |
|                           | No outer and inner                       | (Afzelius 1976, Pedersen and Mygind 1976)                   |
| <b>Axoneme structures</b> | Ciliary disorientation                   | (Rutman <i>et al.</i> 1993, Rayner <i>et al.</i> 1996)      |
|                           | Transposition defects                    | (Sturgess <i>et al.</i> 1980)                               |
|                           | Abnormally long                          | (Afzelius <i>et al.</i> 1985, Niggemann <i>et al.</i> 1992) |
|                           | Abnormally short                         | (Rautiainen <i>et al.</i> 1991)                             |
|                           | Ciliary aplasia                          | (Richard <i>et al.</i> 1989, DeBoeck <i>et al.</i> 1992)    |
|                           | Central microtubular agenesis            | (Stannard <i>et al.</i> 2004)                               |
|                           | Defective radial spokes/inner arm defect | (Sturgess <i>et al.</i> 1979, Antonelli <i>et al.</i> 1981) |
| <b>Basal apparatus</b>    | Abnormal                                 | (Lungarella <i>et al.</i> 1985)                             |

These ultrastructural abnormalities within the ciliary axoneme, result in cilia that are either stationary or beat in a slow dyskinetic fashion. Slow motion videos (S1-S3) of beating respiratory cilia are given in appendix A (see CD with thesis) showing normal (S1), dyskinetic (S2) and static cilia (S3). Evidence from humans and *Chlamydomonas* suggests that the outer dynein arms mainly determine ciliary beat frequency and force, whereas inner dynein arms appear to determine ciliary bending pattern (Zariwala *et al.* 2007). Ineffective movement of the cilia leads to impairment in the mucociliary clearance, resulting in mucous retention. This leads to recurrent chest infections, progressing to chronic sinusitis and bronchiectasis which are the leading causes of morbidity and mortality in PCD patients (Rossman and Newhouse 1988). The main reason for recurring infections in PCD patients is an increased burden of bacteria in the middle ear, paranasal sinuses and airway (Rossman and Newhouse 1988).

Congenital disorders, such as retinal degeneration, hydrocephalus, sensory hearing deficits, and mental retardation, have also been reported in PCD patients (Ibanez-Tallon *et al.* 2003). Around half of PCD patients exhibit *situs inversus* (Afzelius 1976). This is due to dysfunction of the monocilia at the embryonic node which are responsible for the establishment of left-right asymmetry during early development (Nonaka *et al.* 1998, McGrath and Brueckner 2003).

PCD patients often have fertility issues, in male patients reduced fertility is due to sperm dysmotility and/or reduced sperm count (Afzelius and Eliasson 1983, Munro *et al.* 1994). Female patients with PCD may have fertility problems due to the lack of ciliary movement in the Fallopian tubes (Zariwala *et al.* 2007). Also, in some older patients lithoptysis (stone expectoration) and pulmonary calcium deposition have been observed (Kennedy *et al.* 2007).

### **1.10 Genetics and inheritance**

The incidence of primary ciliary dyskinesia is approximately one in 10,000-20,000, although the precise incidence is not known (Afzelius 1976). As primary ciliary dyskinesia exhibits an autosomal recessive pattern of inheritance, the disease prevalence increases where consanguineous marriages are customary and those that are isolated for geographical or cultural reasons (Jeganathan *et al.* 2004, O'Callaghan 2004). The incidence of PCD has been reported to be one in 2,200 people, in British Asian populations where there is a high rate of consanguineous marriages (O'Callaghan *et al.* 2009).

As mentioned, PCD is usually inherited in an autosomal recessive pattern, although some rare cases of autosomal dominant or X-linked inheritance are known (Narayan *et al.* 1994, Iannaccone *et al.* 2003, Krawczynski *et al.* 2004, Moore *et al.* 2006). An association between X-linked recessive retinitis pigmentosa (RPGR) and sensory hearing deficits with PCD have also been identified (Moore *et al.* 2006). In addition, Budny *et al.* (Budny *et al.* 2006) described a single family with a new syndrome that is caused by oral-facial-digital syndrome type 1 (OFD1) mutation and characterised by X-linked recessive mental retardation, macrocephaly and PCD.

PCD is caused by mutations in one or more of a number of different genes and is therefore genetically heterogeneous (Blouin *et al.* 2000, Chodhari *et al.* 2004, Geremek and Witt 2004). Due to the molecular complexity of the axonemes of cilia and sperm there are a large number of potential candidate genes. Table 1.3 lists genes identified as responsible for PCD. The majority of the genes identified so far encode outer dynein arm components (Wilkerson *et al.* 1994, Pennarun *et al.* 1999, Bartoloni *et al.* 2002,

Olbrich *et al.* 2002), whereas only one gene has been shown to be required for cytoplasmic preassembly of axonemal dyneins (Omran *et al.* 2008). Further studies are needed to identify other genes responsible for PCD patients.

**Table1.3 Genes identified as responsible for PCD.** Adapted from Barbato *et al.* (2009).

| <u>Gene</u>   | <u>Locus</u>     | <u>Electron Microscopy</u>             | <u>Exons</u> | <u>Hot spot</u>   | <u>Phenotype</u>              | <u>Reference</u>               |
|---------------|------------------|--|--------------|---|-------------------------------|--------------------------------|
| <i>DNAH5</i>  | 5p15-p14         | Outer dynein arm                       | 79+1         | exons 34, 50, 63, 76, 77<br>c. 10815delT founder mutation | PCD+Kartagener syndrome       | (Olbrich <i>et al.</i> 2002)   |
| <i>DNAI1</i>  | 9p13-p21         | Outer dynein arm                       | 20           | exons 13, 16, 17<br>IVS1 + 3insT founder mutation         | PCD+ Kartagener syndrome      | (Pennarun <i>et al.</i> 1999)  |
| <i>DNAH11</i> | 7p15.3-21        | Normal                                 | 82           | exon 52   | PCD+ Kartagener syndrome      | (Bartoloni <i>et al.</i> 2002) |
| <i>DNAI2</i>  | 17q25            | Outer dynein arm                       | 14           | exon 11   | PCD+ Kartagener syndrome      | (Loges <i>et al.</i> 2008)     |
| <i>TXNDC3</i> | 7p14.1           | Outer dynein arm                       | 18           | Not known   | Kartagener syndrome           | (Sadek <i>et al.</i> 2003)     |
| <i>RPGR</i>   | Xp21.1<br>Xp11.4 | variable                               | ~25          | Not known   | PCD with retinitis pigmentosa | (van Dorp <i>et al.</i> 1992)  |
| <i>KTU</i>    | 14q21.3          | Outer dynein arm &<br>inner dynein arm | 3            | Not known   | PCD+ Kartagener syndrome      | (Omran <i>et al.</i> 2008)     |
| <i>OFD1</i>   | Xp22             | Not known                              | 23           | Not known   | PCD with mental retardation   | (Budny <i>et al.</i> 2006)     |
| <i>RSPH9</i>  | 6p21.1           | Radial spoke                           | 5            | exon 5<br>c.801_803delGAA founder mutation                | PCD+ Kartagener syndrome      | (Castleman <i>et al.</i> 2009) |
| <i>RSPH4A</i> | 6q22.1           | Radial spoke                           | 6            | Not known   | PCD+ Kartagener syndrome      | (Castleman <i>et al.</i> 2009) |

A brief description of the genes identified as responsible for PCD is given below. For a more detailed description the reader is referred to (Barbato *et al.* 2009).

**DNAH5:** The *DNAH5* gene located on human chromosome 5p15.2 encodes a heavy chain dynein. Within the critical genetic region on chromosome 5p15, the human ortholog (*DNAH5*) of the *Chlamydomonas*  $\gamma$ -heavy chain was identified (Olbrich *et al.* 2002). Mutations in the *Chlamydomonas* ortholog result in slow-swimming algae with ultrastructural outer dynein arm defects (Wilkerson *et al.* 1994). Mutations in *DNAH5* have been regularly associated with outer dynein arm defects, randomization of left-right asymmetry and male infertility (Olbrich *et al.* 2002, Fliegauf *et al.* 2005, Hornef *et al.* 2006). It is thought that *DNAH5* mutations predominantly cause outer dynein arm defects (Hornef *et al.* 2006).

**DNAI1:** *DNAI1* is a gene for a human axonemal dynein intermediate chain 1 and is located on chromosome 9p21-p13 (Pennarun *et al.* 1999). All mutations in the *DNAI1* gene are associated with outer dynein arm defects (Pennarun *et al.* 1999, Guichard *et al.* 2001, Zariwala *et al.* 2001, Zariwala *et al.* 2006).

**DNAH11:** Homozygous mutations in the *DNAH11* gene on human chromosome 7, can cause PCD (Bartoloni *et al.* 2002). Mutational analysis, by direct sequencing, revealed a homozygous nonsense mutation (R2852X) in exon 52 in a patient with cystic fibrosis, *situs inversus* and severe respiratory phenotype. However, electron microscopy revealed normal respiratory cilia axonemes without any apparent ciliary ultrastructural defects (Olbrich *et al.* 2002). Most recently, in a second family the R2852X mutation was also reported with no apparent ciliary ultrastructural defects (Schwabe *et al.* 2008).

However, high-speed video microscopy revealed a hyperkinetic dyskinetic ciliary beating pattern in the affected members of the family (Schwabe *et al.* 2008).

**DNAI2**: Loges *et al.* (Loges *et al.* 2008) identified homozygous loss-of-function DNAI2 mutations in four individuals from a family with PCD and outer dynein arm defects. Protein expression analysis of the outer dynein arm intermediate chain DNAI2 showed sublocalization throughout respiratory cilia. Electron microscopy showed that respiratory cells from these patients lacked DNAI2 protein expression and exhibited outer dynein arm defects.

**KTU**: Chromosome 14 open reading frame 104 gene (KTU) was first identified in a mutant medaka fish, and has also been found to be mutated in two PCD families with both inner and outer dynein arm deficiencies (Omran *et al.* 2008). This protein is required for cytoplasmic pre-assembly of dynein arm complexes before intraflagellar transport carries them to the ciliary compartment. This mutation leads to immotile respiratory cilia and sperm tails (Barbato *et al.* 2009).

**TXNDC3**: This gene represents the human ortholog of the sea urchin intermediate chain 1 gene that encodes a component of sperm outer dynein arms (Olbrich *et al.* 2002, Sadek *et al.* 2003). In 47 patients with either functional or ultrastructural ciliary abnormalities, screening of the eighteen TXNDC3 exons revealed sequence variants in only one patient (Afzelius 1976). The girl had chronic respiratory disease and situs ambiguous. The ciliary beat frequency appeared normal, and transmission electron microscopy revealed that 66% of her respiratory cilia had shortened or absent outer dynein arms (Afzelius 1976). The disease probably results from the unusual

combination of a nonsense mutation and a common intronic variant found in 1% of control chromosomes (Afzelius 1976).

**RPGR:** Retinitis Pigmentosa is a genetically heterogeneous disorder in which abnormalities of the photoreceptors on the retinal pigment epithelium lead to progressive loss of vision (van Dorp *et al.* 1992). Patients with X-linked Retinitis Pigmentosa have been shown to have mutations in *RPGR* (RP guanosine triphosphatase regulator). *RPGR* is expressed in human rods and cones and is essential for photoreceptor maintenance and viability. The *RPGR* gene is located on chromosome Xp21.1 and families in which RP cosegregated with PCD have been shown to harbour mutations in *RPGR* (van Dorp *et al.* 1992, Dry *et al.* 1999, Hong *et al.* 2003, Iannaccone *et al.* 2003, Zito *et al.* 2003, Hong *et al.* 2005, Moore *et al.* 2006). Ultrastructural analysis showed diverse abnormalities of ciliary structure, including outer dynein arm defects with or without inner dynein arm defects, and central-complex and nexin linked defects (Zariwala *et al.* 2007).

**OFDI:** Oral-facial-digital type 1 syndrome is an X-linked dominant human development disorder characterised by digital abnormalities, mental retardation, craniofacial malformations and male lethality (Ferrante *et al.* 2001). Mutations in *OFDI*, a gene located on chromosome Xp22, are responsible for this disorder (Budny *et al.* 2006). Budny *et al.* (2006) reported a large Polish family with a novel X-linked recessive mental retardation syndrome comprised of macrocephaly together with ciliary dysfunction in males. High speed video microscopy later confirmed PCD with severely disorganized ciliary beat pattern in an index case. Linkage analysis in the affected families led to the identification of a frame shift mutation in the *OFDI* gene (Budny *et al.* 2006).

---

**RSPH9 and RSPH4A**: These genes were recently discovered using whole-genome single-nucleotide polymorphism based linkage analysis in seven consanguineous families with PCD and central-microtubular-pair abnormalities (Castleman *et al.* 2009). Their study identified positional candidate genes, *RSPH9* on chromosome 6p21.1 and *RSPH4A* on chromosome 6q22.1. Both *RSPH9* and *RSPH4A* encode protein components of the axonemal radial spoke head. Investigation of the effect of knockdown or mutations of *RSPH9* orthologs in zebrafish and *Chlamydomonas* indicate that radial spoke head proteins are important in maintaining normal movement in motile, "9+2"-structure cilia and flagella (Castleman *et al.* 2009). Disturbance in function of these genes was not linked to defects in left-right axis determination in humans or zebrafish (Castleman *et al.* 2009).

### ***1.11 Associations with primary ciliary dyskinesia***

#### **Nitric Oxide**

An interesting PCD phenotype that is possibly related to ciliary function is low nasal and exhaled nitric oxide. Several studies have shown that individuals of all ages with PCD have 10-20% of the normal nitric oxide levels in their lower airways (Wodehouse *et al.* 2003, Corbelli *et al.* 2004, Noone *et al.* 2004). Interestingly, in parents of the PCD patients who are obligate heterozygote's, nasal nitric oxide levels were intermediate between levels in PCD and normal individuals (Noone *et al.* 2004). These low levels of nitric oxide are found regardless of the underlying ciliary ultrastructural defect (Lundberg *et al.* 1994, Karadag *et al.* 1999, Narang *et al.* 2002, Wodehouse *et al.* 2003, Noone *et al.* 2004). There are two other known conditions with reduced airway nitric oxide concentrations: cystic fibrosis (Balfour-Lynn *et al.* 1996) and systemic sclerosis

with pulmonary hypertension (Kharitonov *et al.* 1997). This is in contrast to other causes of bronchiectasis and diseases such as asthma, where raised levels of exhaled nitric oxide have been reported (Kharitonov and Barnes 2000).

The mechanisms behind the low levels of nitric oxide in PCD are not fully understood and further studies are needed to determine whether these low values are primary or secondary to the cilia defect. Possible explanations are that the production of nitric oxide is absent or the diffusion of nitric oxide into the airway lumen is reduced in some way (Lundberg *et al.* 1994). If the low levels are due to reduced production, this could be explained by deficient nitric oxide synthesis in the superficial structures of the nasal airways (§1.7.3). Recently it has been shown that some PCD patients exhibit a polymorphism in the promoter of iNOS and a missence mutation in exon 7 of eNOS (Zhan *et al.* 2003). As mentioned in §1.7.3, eNOS is localized at the basal membrane of ciliary microtubules and mediates regulation of ciliary beat frequency (Li *et al.* 2000). Also in another study it was confirmed that the levels of both nNOS and eNOS are very low in children with PCD (Narang *et al.* 2002). Therefore, it is possible that ciliary dysfunction and impaired nitric oxide synthesis seen in PCD could be interrelated. However, the situation may not be straight forward. Despite low levels of nasal and exhaled nitric oxide in children with PCD, the levels of exhaled nitric oxide metabolites ( $\text{NO}_2^-$ ,  $\text{NO}_3^-$  and S-nitrosothiol) did not differ from levels in healthy controls (Csoma *et al.* 2003). Also when Loukides and colleagues administered arginine, the precursor of nitric oxide, as an aerosol into the nose, the mean ciliary beat frequency in both healthy controls and in PCD patients with a baseline ciliary beat frequency less than 8Hz increased (Loukides *et al.* 1998). However, the PCD nitric oxide levels were still lower than the normals.

Another hypothesis for these low nitric oxide levels stems from the observation of low levels of nitric oxide production by myocytes in patients with Duchennes muscular dystrophy. It has been suggested that mutations in the dystrophin gene result in uncoupling of nitric oxide synthase from the contractile apparatus, with loss of function by some mechanism yet to be determined (Jain *et al.* 1993). Cilia, like myocytes, also contain mechanochemical ATPases and it may be that loss of ciliary function results in reduced nitric oxide synthase output by a similar mechanism (Jain *et al.* 1993). Also, recently it was shown that the expression of muscle membrane-associated nitric oxide synthase (NOS1) was significantly impaired in Duchene muscular dystrophy (Straub *et al.* 2002). Therefore indirectly suggesting that NOS1 may contribute significantly to fractional exhaled nitric oxide, in healthy children (Straub *et al.* 2002).

#### **Neonatal respiratory distress**

Infants with PCD may present unexplained respiratory distress in the neonatal period and require ventilation (Whitelaw *et al.* 1981, Holzmann *et al.* 2000, Coren *et al.* 2002).

#### **Neurological**

Unexplained hydrocephalus within the neonatal period and mental retardation in older children has been reported (Greenstone *et al.* 1984, De Santi *et al.* 1990, al-Shroof *et al.* 2001). These abnormalities may be due to abnormalities of ependymal cilia lining the ventricular surface resulting in impaired flow of cerebrospinal fluid (O'Callaghan *et al.* 1999, Ibanez-Tallon *et al.* 2004).

### **Leukocytes**

Microtubules are found within leucocytes and are thought to assist with cell motility (Koh *et al.* 2003). PCD patients have been shown to have abnormal neutrophil orientation, migration and chemotaxis (Valerius *et al.* 1983, Fiorini *et al.* 2000, Koh *et al.* 2003).

### **Other associations**

Other associations seen with PCD are trachea-oesophageal fistula (Engesaeth *et al.* 1993), oesophageal stricture and midgut volvulus (Ozgen *et al.* 2000), gastro-oesophageal reflux (Engesaeth *et al.* 1993), polycystic kidneys (Saeki *et al.* 1984), complex congenital heart disease (Pedersen and Stafanger 1983, Engesaeth *et al.* 1993) and biliary atresia (Gershoni-Baruch *et al.* 1989).

## ***1.12 Diagnosis of primary ciliary dyskinesia***

It is thought that early diagnosis of PCD is likely to have a significant effect on both short term and long term morbidity (Ellerman and Bisgaard 1997, Noone *et al.* 2004). Currently, the diagnosis of PCD is based on the presence of typical clinical phenotypes, plus specific ultrastructural defects of cilia identified by transmission electron microscopy. However, as secondary inflammation and infection can produce ciliary defects which may result in a misdiagnosis of PCD, one should be extremely cautious in making a diagnosis if the clinical symptoms do not fit. When our understanding of genetic mutations associated with PCD is better understood and definitive genetic methods are developed, genetic tests may become a fast and effective way to diagnose PCD.

Diagnosis of PCD is often delayed, despite the presence of typical symptoms early in life (Coren *et al.* 2002). This is in part due to the symptoms presented in PCD (cough, rhinitis, secretory otitis media) being common in children (Bush *et al.* 1998) and mimicking clinical features of other respiratory diseases, such as asthma or cystic fibrosis. Various studies have shown that despite the early onset of PCD respiratory symptoms shortly after birth, the mean age of PCD diagnosis is around 4 years of age (Bush *et al.* 1998, Coren *et al.* 2002, Noone *et al.* 2004). Chronic cough, persistent early onset rhinitis, and situs inversus are common clues to underlying PCD, that may lead to poor feeding and failure to thrive (Ferkol and Leigh 2006). For details of the conventional diagnosis of PCD, see the recent review by Bush *et al.* (Bush *et al.* 2007).

### **Part C: Pathogenic bacteria**

Although the majority of bacteria are beneficial or harmless, some are responsible for global diseases. An important feature of pathogenic bacteria is their virulence factors. These virulence factors are essential for causing disease and interact directly with the host tissues or conceal the bacterial surface from host's defence mechanisms (Tuomanen 1999, Gosink *et al.* 2000).

This thesis focuses on the pathogenic bacteria *Streptococcus pneumoniae* and *Listeria monocytogenes*. *S. pneumoniae* asymptotically colonizes the human naso-pharynx but also accounts for approximately one-quarter of community acquired pneumonia in both children and adults (Fernandez-sabe 2003). Also, *S. pneumoniae* is one of the most common bacteria isolated from the respiratory tract of patients with PCD (Xu *et al.* 2008). *L. monocytogenes* is an intracellular pathogenic bacterium that invades the ciliated brain parenchyma leading to meningitis (Seeliger 1986, McLauchlin 1997).

Bacterial pathogens, including *L. monocytogenes* and *S. pneumoniae*, are known to form structured populations of microorganisms, adhered and embedded in an extracellular matrix consisting mainly of exopolysaccharides (biofilms) (Hall-Stoodley and Stoodley 2009). It is thought that these biofilm structures protect the bacteria from host immune responses as well as different antimicrobials (Stewart 2001). Bacterial biofilms have been shown to occur in a sequential process generally involving, 1) initial attachment of individual cells to the surface 2) formation of aggregates 3) further cell proliferation and biofilm maturation (Allegrucci *et al.* 2006).

Below a more detailed description of each bacterium is given.

### ***1.13 Streptococcus pneumoniae: The pneumococcus***

*S. pneumoniae* (often referred to as the pneumococcus) is a Gram-positive, encapsulated, haemolytic, coccus of approximately 1µm in diameter (Bannister 1996). The *Streptococcus* genus comprises over 250 species, which include several human pathogens. *S. pneumoniae* was first isolated more than 120 years ago (Sternberg 1981), yet today it remains a major cause of morbidity and mortality in both the developing and developed worlds.

*S. pneumoniae* is the causative agent of several infectious diseases, including pneumonia, septicaemia, meningitis and otitis media (Magee and Yother 2001). In addition, pneumococci have been reported in a variety of other diseases including arthritis, osteomyelitis, endocarditis, endophthalmitis, abscesses, necrotising fasciitis, and sinusitis (Oggioni *et al.* 2006).

The mortality and morbidity caused by pneumococcal infection is very high in the developed world and alarmingly high in the developing world (Greenwood 1999, Lesinski *et al.* 2001). This is despite the use of antibiotics to which the pneumococcus is sensitive and the use of steroids as an adjunctive therapy (Hirst *et al.* 2003). According to The World Health Organisation (WHO), *S. pneumoniae* claims around 1.6 million lives per year worldwide, mainly in young children, immunocompromised patients and the elderly (Attali *et al.* 2008). In the United Kingdom, *S. pneumoniae* is the most common bacterial respiratory pathogen, causing community acquired pneumonia, which in patients with concurrent pneumococcal septicaemia has mortality rates of more than 20% (Balakrishnan *et al.* 2000, Lim *et al.* 2001).

### **1.13.1 Pneumococcal carriage and colonisation**

Like many microorganisms, carriage plays an important role in the aetiology of pneumococcal disease (Obaro 2001). Pneumococcal infections begin with the colonisation of the nasopharynx, which allows progression of pneumococci into the lower parts of the respiratory tract, ultimately leading to systemic disease (Rayner *et al.* 1995, Barthelson *et al.* 1998). Furthermore, colonisation of pneumococci in the upper respiratory tract serves as a key reservoir of transmission to other susceptible individuals (Kadioglu *et al.* 2002). The scale of colonisation can differ between individuals, although up to 40% of the general population are thought to carry it in small numbers (Austrian 2000, Tuomanen and Masure 2000). The carriage rate of pneumococci can vary from 5 to 70% depending on the age of onset, the environment of the host, and the presence of underlying respiratory infections (Austrian 1986, Obaro *et al.* 1996, Wu *et al.* 1997). Examples of host tissue ligands that the pneumococci have been suggested to bind include, the platelet-activating factor receptor (pafR) that has

been suggested to serve as a ligand in the lung (Tuomanen 2000) and the polymeric immunoglobulin receptor (pIgR) with a same role in the nasopharynx (Sollid *et al.* 1987).

### **1.14 *S. pneumoniae* virulence factors**

A number of virulence factors have been described for pneumococci, although we do not know which interact with cilia. During the course of this study, attention was paid to pneumococcal virulence factors, pneumolysin and the neuraminidase, NanA. Therefore, a summary of some of the literature regarding these virulence factors is given below.

#### **1.14.1 *Pneumolysin***

Pneumolysin is a 53Kd protein and the major pneumococcal toxin that is produced by all clinical isolates of *S. pneumoniae* (Kalin *et al.* 1987, Paton *et al.* 1993). Pneumolysin forms oligomers that embed in the lipid-bilayer of target cells leading to the creation of pores in the target cell membranes (Paton *et al.* 1993, Rossjohn *et al.* 1998). This leads to cell lysis and contributes to the invasive capacity of pneumococci (Gilbert *et al.* 1999). As pneumolysin is inhibited by cholesterol, this suggests that membrane cholesterol is the receptor for this toxin (Paton *et al.* 1986, Andrew *et al.* 1997, Rossjohn *et al.* 1998).

Analysis of the primary amino acid sequence of pneumolysin does not reveal a distinctive secretion signal sequence (Mitchell 2004). It was previously suggested that for pneumolysin release and thus virulence, the cells needed to undergo autolysis (Berry *et al.* 1989a). Autolysis is characterized by cell wall degradation by a peptidoglycan hydrolase (autolysin). However, in the recent years it has been demonstrated that

pneumolysin can be released independently of autolysin (Balachandran *et al.* 2001, Price and Camilli 2009).

Pneumolysin exhibits a wide range of activities that are consistent with a role in virulence. This is supported by studies *in vivo and in vitro* showing that pneumolysin-deficient pneumococci exhibit reduced virulence in the mouse, with slower growth in the lungs and delayed development of the cellular inflammatory response (Canvin *et al.* 1995, Kadioglu *et al.* 2000, Hirst *et al.* 2008). Mice infected with pneumolysin deficient pneumococci were shown to have reduced mortality and morbidity compared with the wild-type pneumococci (Berry *et al.* 1989b). Also, Kadioglu *et al.* have shown that in a mouse model of acute pneumonia, the absence of pneumolysin was associated with significantly lower numbers of pneumococci in the nasopharynx, trachea, and lungs (Kadioglu *et al.* 2002). Furthermore, Feldman and colleagues demonstrated that injection of recombinant pneumolysin into the rat lung resulted in severe pneumonia that was identical to that caused by the injection of *S. pneumoniae* (Feldman *et al.* 1991).

A few studies have investigated the impact of pneumolysin on human respiratory mucosa. Pneumolysin has been shown to be cytotoxic to bronchial epithelial cells. In organ cultures with air interface, after 48 hours of infection with pneumococci, the ciliary beat frequency was reduced, tight junctions disrupted and ciliary disorganization and epithelial damage occurred (Rayner *et al.* 1995). This disruption reduced the ability of ciliated epithelial cells to clear mucus from the lower respiratory tract, thus, facilitating propagation of pneumococci (Rayner *et al.* 1995). Pneumolysin has also shown to be important for colonization. Pneumolysin-deficient pneumococci have been

shown to attach significantly less well to respiratory epithelial cells (Rubins *et al.* 1998, Kadioglu *et al.* 2002).

The role of pneumolysin has also been studied using ciliated ependymal cells. Ciliated ependymal cells cover the ventricular surface of the brain and cerebral aqueducts separating the neuronal tissue from cerebrospinal fluid which is infected in meningitis (See §1.6). Using both *ex vivo* and *in vivo* studies, Hirst *et al* showed that pneumolysin inhibited ciliary beat frequency or was very toxic to the ependymal cells, causing opening of the gap junctions between the cells (Mohammed *et al.* 1999, Hirst *et al.* 2000b, Hirst *et al.* 2003). The effects of pneumococci seen *ex vivo* were abolished with an anti-pneumolysin antibody (Hirst *et al.* 2004b). Also more recently, Hirst *et al* have shown that to cause meningitis in the adult rat, pneumococci need to produce pneumolysin, confirming the important role of pneumolysin in the pathogenesis of pneumococcal meningitis (Hirst *et al.* 2008). Friedland and colleagues reported that in rabbits a pneumolysin deficient strain caused less meningeal inflammation than that induced by the parent wild-type strain (Friedland *et al.* 1995). A summary of the *in vitro* activities of pneumolysin is listed in Table 1.4.

**Table 1.4 Examples of *in-vitro* biological properties of pneumolysin.** Adapted from (Hirst *et al.* 2004a).

| <u>Activity</u>  | <u>Reference</u>                 |
|--|----------------------------------|
| Inhibition of polymorphonuclear cell respiratory burst, random migration and chemotaxis  | (Paton and Ferrante 1983)        |
| Inhibition of mitogen-induced proliferation and antibody production by human lymphocytes | (Ferrante <i>et al.</i> 1984)    |
| Activation of classical complement pathway   | (Boulnois <i>et al.</i> 1991)    |
| Lysis of erythrocytes  | (Mitchell <i>et al.</i> 1989)    |
| Inhibition of ciliary beat of respiratory mucosa   | (Feldman <i>et al.</i> 1990)     |
| Toxic to pulmonary alveolar epithelial cells   | (Rubins <i>et al.</i> 1993)      |
| Stimulation of TNF- $\alpha$ and IL-1 $\beta$ production from human monocytes            | (Houldsworth <i>et al.</i> 1994) |
| Activation of phospholipase A <sub>2</sub> in pulmonary endothelial cells                | (Rubins <i>et al.</i> 1994)      |
| Separation of epithelial cell tight junctions  | (Rayner <i>et al.</i> 1995)      |
| Initiates nitric oxide production from macrophages                                       | (Braun <i>et al.</i> 1999)       |
| Reduces ciliary beat frequency of cerebral ependymal cells                               | (Hirst <i>et al.</i> 2000b)      |
| Induces production of IFN- $\gamma$ in spleen cells                                      | (Baba <i>et al.</i> 2002)        |
| Induces synthesis and release of IL-8 from neutrophils                                   | (Cockeran <i>et al.</i> 2002)    |
| Generates multiple conductance pores in the membrane of nucleated cells                  | (El-Rachkidy <i>et al.</i> 2008) |
| Induces polymorphonuclear leukocyte migration across the pulmonary endothelium           | (Moreland and Bailey 2006)       |

### **1.14.2 Neuraminidases**

Neuraminidases (also known as sialidases) are one of the key virulence factors of pneumococci as they remove sialic acid from host cell-surface glycans, thus unmasking certain receptors to facilitate pneumococcal adherence and colonization (Paton *et al.* 1993, Kadioglu *et al.* 2008). Sialic acid is a generic term for a large family of nine-carbon monosaccharides of naturally occurring analogues of *N*-acetylneuraminic acid.

*S. pneumoniae* encodes at least three neuraminidase genes, *nanA*, *nanB* and *nanC* (Camara *et al.* 1994, Berry *et al.* 1996), with a recent study revealing *nanA* to be present in all clinical strains (Pettigrew *et al.* 2006). Neuraminidase A is highly expressed at the transcriptional level (Berry *et al.* 1996, Manco *et al.* 2006), and its expression is up-regulated upon interaction with host cells (LeMessurier *et al.* 2006, Oggioni *et al.* 2006, Song *et al.* 2008). Yesilkaya *et al.* recently have shown that neuraminidase A also plays an important role in mucin utilization and that growth of pneumococci in mucin resulted in an increase in NanA transcription (Yesilkaya *et al.* 2008). A NanA deficient pneumococcus did not grow when mucin was used as the sole carbon source (Yesilkaya *et al.* 2008). Gene-knockout studies in mouse models have shown that both NanA and NanB are important for survival of the pneumococci in the respiratory tract and the blood stream (Manco *et al.* 2006). Further support for a role for NanA in pneumococcal survival in the host comes from Pettigrew *et al.* (2006), who analysed the distribution of neuraminidase genes among 342 pneumococcal paediatric clinical and carriage isolates and found that the *nanA* gene was present in 100% of the *S. pneumoniae* strains. Whereas *nanB* and *nanC* were present in 96% and 51% of strains examined, respectively (Pettigrew *et al.* 2006). This high prevalence of *nanA* suggests that it is an essential gene for survival and pathogenesis in all pneumococcal strains (Pettigrew *et al.*

2006). Other studies have also suggested that NanA mutants colonise the rodent respiratory tract less efficiently than wild-type strains (Orihuela *et al.* 2004, Tong *et al.* 2005). Moreover, recently using an *in vitro* model of biofilm formation incorporating human airway epithelial cells, Parker *et al.* demonstrated that small-molecule inhibitors of NanA blocked biofilm formation (Parker *et al.* 2009).

### ***1.14.3 Other pneumococcal virulence factors***

Other examples of pneumococcal virulence factors are listed below with a brief description. Reviews of these can be found in (Jedrzejewski 2007, Kadioglu *et al.* 2008). Figure 1.17 shows these virulence factors on the pneumococcus.

#### **Capsule**

In *S. pneumoniae* the polysaccharide capsule is an important virulence factor by virtue of its antiphagocytic activity (Tuomanen and Masure 1997). These polysaccharides form a negative shell around the bacterium (Kamerling 2000a), which provides protection against phagocytosis and acapsular mutants have been shown to be avirulent (Tuomanen and Masure 1997). *S. pneumoniae* expresses at least 90 different polysaccharide (PS) capsules one at a time (Henrichsen 1995). Differences in the composition of the capsular types is thought to be responsible for alteration in virulence, although the reason for this remains unknown (Kamerling 2000a). Each pneumococcal serotype is defined by the antigenic structure of the capsular material. The serotyping technique, known as the Quellung (Neufeld) reaction, causes pneumococci to appear to swell in the presence of specific antiserum (Heineman 1973).

**Hyaluronidase (Hyl)**

Hyaluronidase is a major surface protein (Berry *et al.* 1994). It breaks down the hyaluronic acid component of mammalian connective tissue and extracellular matrix (Humphrey 1948). The degradation of hyaluronic acid is thought to aid bacterial spread and colonisation, as demonstrated by in other microorganisms (Fitzgerald and Repesh 1987).

**N-acetyl-muramoyl-L-alanine amidase (LytA)**

LytA is the main autolysin in the pneumococcus (Lopez *et al.* 1997). LytA-negative mutants have been shown to have reduced virulence in murine models of bacteraemia, pneumonia and meningitis (Berry *et al.* 1989a, Canvin *et al.* 1995, Hirst *et al.* 2008).

**Pneumococcal surface protein A (PspA)**

PspA is located on the cell surface of pneumococci (McDaniel *et al.* 1984, Yother and White 1994) and found in every characterised pneumococcal strain (Crain *et al.* 1990). There is evidence suggesting that PsaA has at least two virulence functions. These include inhibition of killing pneumococci by host lactoferrin and inhibition of complement C3 activation and decomposition of C3 fragments (Tu *et al.* 1999, Ren *et al.* 2003, Shaper *et al.* 2004). PspA is variable in structure as PspA from different isolates usually differ in molecular weight varying from ~67 to 99 kDa (Waltman *et al.* 1990).

**Pneumococcal surface antigen A (PsaA)**

PsaA is a 37-kDa divalent metal-ion-binding lipoprotein genetically conserved among all *S. pneumoniae* serotypes (Morrison *et al.* 2000) and is essential for *S. pneumoniae*

virulence (Berry and Paton 1996). PsaA is the lipoprotein component of an ATP-binding cassette transport system (Dintilhac *et al.* 1997) and this complex transports manganese ions and mutations in *psaA* cause decreased adhesion to cells, decreased virulence, and increased sensitivity to oxidative stress (Berry and Paton 1996, Ogunniyi *et al.* 2000, Marra *et al.* 2002). Immunization with PsaA was shown to protect mice against nasopharyngeal carriage and lung colonization (Briles *et al.* 2000a, Briles *et al.* 2000b).

### **PiaA and PiuA**

These are the lipoprotein metal binding components of ATP-binding cassette transporter operons that mediate iron uptake in pneumococci. Mutations in either *piaA* or *piuA* lead to decreased virulence in models of pneumonia and bacteraemia. Although the double mutant has shown to be attenuated to a greater extent (Brown *et al.* 2002).

### **Pneumococcal adhesion and virulence A (PavA) and B (PavB)**

Pneumococci have several types of adhesins that bind to fibronectin, including PavA and PavB. Both are essential for virulence and are thought to be involved in bacterial colonization and spread from the nasopharynx and lungs to the blood stream and the nervous system (Pracht *et al.* 2005).

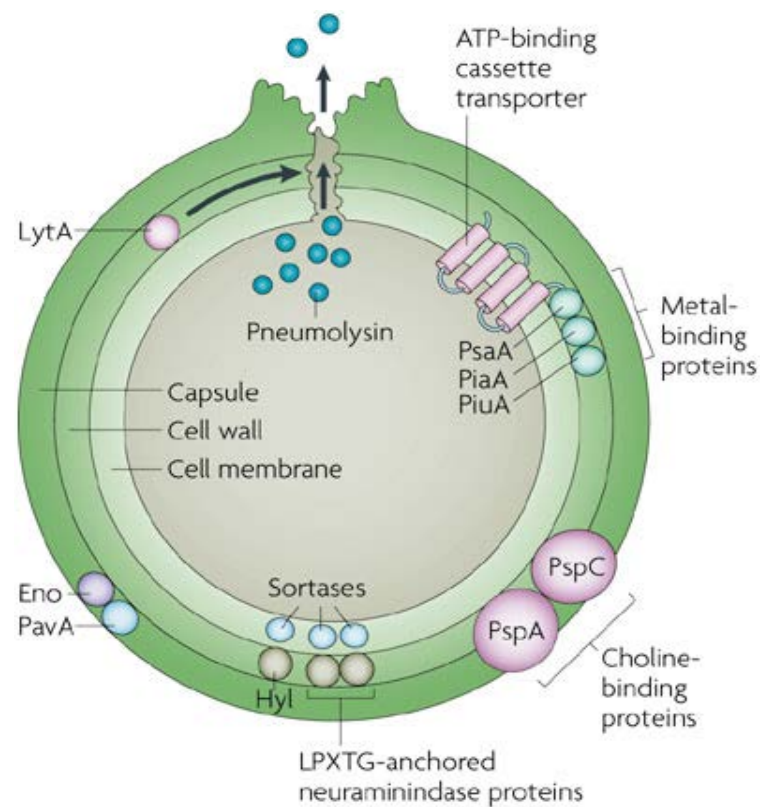


**Figure 1.17 *Streptococcus pneumoniae* virulence factors.** Diagram showing important virulence factors of pneumococci. These include: the capsule and cell wall; pneumolysin; LPXTG-anchored surface proteins, including Hyaluronidase (Hyal) and neuraminidase proteins; choline-binding proteins, including pneumococcal surface proteins A and C (PspA and PspC) and autolysin A (LytA); metal-binding lipoproteins including, pneumococcal surface antigen A (PsaA), pneumococcal iron acquisition A (PiaA) and pneumococcal iron uptake A (PiuA); Fibronectin binding proteins including, pneumococcal adhesion and virulence A (PavA) and enolase (Eno). Taken from (Kadioglu *et al.* 2008).

### **1.15 *Listeria monocytogenes***

*Listeria monocytogenes* is a Gram positive, non-spore forming, facultative intracellular bacillus, first discovered as a causative agent of septicaemia in rabbits (Murray 1926). It was later discovered to be a human pathogen, in 1929, when a case of listeriosis was identified in Denmark (Vazquez-Boland *et al.* 2001b). Listeriosis can result from ingesting contaminated food products and mainly affects immunocompromised patients, such as those with AIDS, pregnant women and newborns (Jurado *et al.* 1993). Listeriosis results in death in 25-30% cases, as it manifests as gastroenteritis, meningitis, encephalitis, mother-to-mother infections and septicaemia (Hamon *et al.* 2006). However, the incidence of human listeriosis is very low, with around 2-8 sporadic cases annually per million population in the United States and Europe (Farber and Peterkin 1991, Tappero *et al.* 1995). In epidemic situations, the incidence in the target population has been shown to increase by a factor of 3 to 10 (Schlech *et al.* 1983, Linnan *et al.* 1988, Schwartz *et al.* 1989). The diverse clinical manifestation of infection with *L. monocytogenes* reflects its ability to cross three tight barriers in the human host. Following ingestion, *L. monocytogenes* crosses the intestinal barrier by invading the intestinal epithelium, thereby gaining access to internal organs (McLauchlin 1997). When *L. monocytogenes* crosses the blood-brain barrier, this results in infection of the meninges and the brain, and in pregnant women, crossing the fetoplacental barrier leads to infection of the fetus (Seeliger 1986, McLauchlin 1997).

#### **1.14.1 *Intracellular infectious cycle and associated virulence factors***

*L. monocytogenes* has two distinct lifestyles: saprophytic, primarily in decaying vegetation in soil and parasitic in the tissues of mammals and birds, in which it can

cause serious foodborne illness (listeriosis) (Gray and Killinger 1966, Vazquez-Boland *et al.* 2001a).

The infectious cycle begins with adhesion of the bacterium to the surface of the eukaryote cell following penetration into the host cell. *L. monocytogenes* enters nonphagocytic cells in a zipper-like entry mechanism, in that the bacteria are engulfed, by gradually sinking into dip like structures in the host cell surface (Vazquez-Boland *et al.* 2001a). During this process the target cell membrane closely surrounds the bacterial cell, as seen in Figure 1.16 A. The initial attachment to host cells requires *L. monocytogenes* ligands to recognise eukaryotic receptors, including the transmembrane glycoprotein E-cadherin, the Met receptor for hepatocyte growth factor (HGF), the C1q complement component, and components of the extracellular matrix such as heparin sulphate, proteoglycans and fibronectin (Niemann *et al.* 2004). The listerial ligands identified are surface proteins, which include internalin A and B (InlA and InlB), the actin polymerising protein ActA, and p60 (Cossart and Lecuit 1998, Lecuit *et al.* 1999, Lecuit *et al.* 2001).

Thirty minutes after entry, the bacteria disrupts the phagosome membrane; a process that is essential for listerial intracellular survival and proliferation (Goebel and Kreft 1997). The bacteria escape by secreting a pore-forming haemolysin known as Listeriolysin-O (LLO) (Figure 1.16 B) (Kuhn *et al.* 1988, Portnoy *et al.* 1988, Gedde *et al.* 2000). Also, a phosphatidylinositol-specific phospholipase C (PI-PLC) contributes to escape from the phagosome (Wadsworth and Goldfine 1999, Goldfine *et al.* 2000, Wadsworth and Goldfine 2002). When in the cytoplasm, the bacteria replicate with a doubling time of approximately 1 hour and host actin polymerises at one end of the bacterium, facilitating movement through the host cytosol (Figure 1.16 C and D)

(Tilney and Portnoy 1989, Tilney *et al.* 1990, Kocks *et al.* 1993). This actin filament-based movement depends on a listerial membrane anchored surface protein ActA (Domann *et al.* 1992, Kocks *et al.* 1992). Some bacteria eventually come into contact with the cell plasma membrane at which point they produce protrusions into neighbouring cells (Figure 1.16 E). These protrusions are engulfed in a new vacuole, creating a double membrane vacuole, and the process starts over again (Figure 1.18 F and G). Two additional enzymes contribute to the cell-to-cell spread. A phosphatidylcholine-specific phospholipase C (PC-PLC), which breaks down the double membrane vacuole (Vazquez-Boland *et al.* 1992), and a Zn-dependent metalloprotease that processes the PC-PLC propeptide to a mature form (Yeung *et al.* 2005).

*L. monocytogenes* infection has been a useful model for evaluation of the host-pathogen cellular interactions and cell biology: see the following reviews (Pamer 2004, Hamon *et al.* 2006).

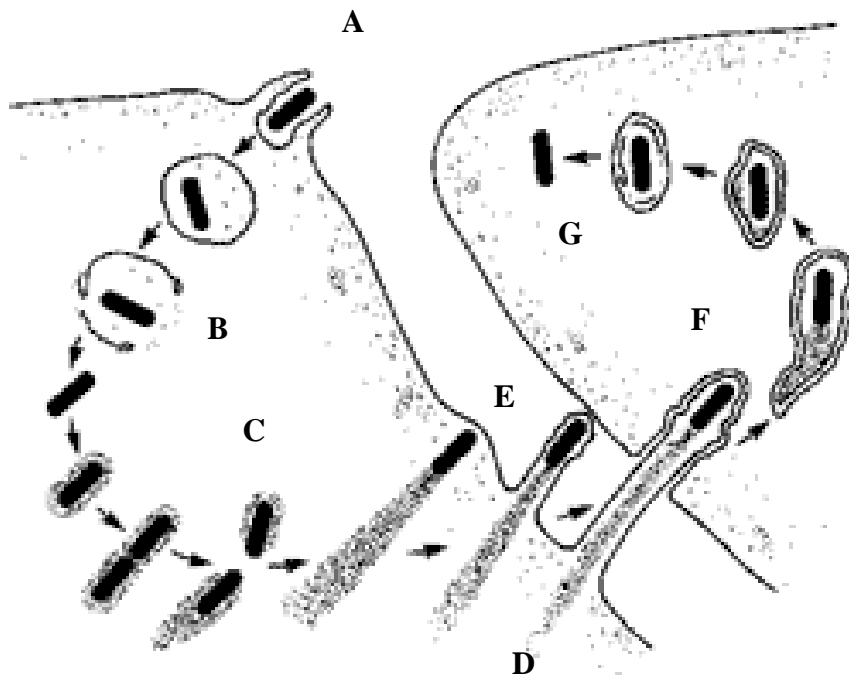


**Figure 1.18** Scheme of the intracellular life cycle of *Listeria* spp. A) entry of *Listeria* into the host cell by induced phagocytosis B) *Listeria* escaping from the host phagosomes C) cytosolic replication D) recruitment of host cell actin to facilitate movement throughout the cytosol E) formation of protrusions into neighbouring cells F) formation of a double membrane phagosome G) escape from the secondary phagosome and reinitiating of the cycle. Taken from Vazquez-Boland *et al*, 2001.

---

### 1.15.2 PrfA: the regulatory switch for virulence

The expression of genes required for invasion, intracellular survival and listerial cell to cell spread is dependent upon a transcriptional activator known as PrfA (positive regulatory factor A) (Mengaud *et al.* 1991, Chakraborty *et al.* 1992, Freitag *et al.* 1992). It is thought that PrfA serves as a switch enabling *L. monocytogenes* transition from the outside environment into an animal host (Freitag 2006). A summary of some of the information regarding PrfA activity and regulation is given below.

The absolute requirement of PrfA for *L. monocytogenes* virulence has been demonstrated, as has the requirement for several genes within the PrfA regulon (Leimeister-Wachter *et al.* 1990, Freitag *et al.* 1993). Strains with mutations within the PrfA gene failed to replicate within the cytosol of host cells or failed to spread into adjacent cells (Leimeister-Wachter *et al.* 1990, Mengaud *et al.* 1991). These mutants also were severely attenuated for virulence in murine models of listeriosis (Leimeister-Wachter *et al.* 1990).

PrfA was first identified as a regulatory factor required for listeriolysin-O transcription and has since been shown to regulate the expression of a large number of bacterial gene products directly associated with virulence (Scorti *et al.* 2007). To date, only 10 of the 2,853 coding sequences of the *L. monocytogenes* EGDe genome (Glaser *et al.* 2001) have been confirmed to be directly regulated by PrfA (Milohanic *et al.* 2003, Marr *et al.* 2006). A list of these 10 genes and their function is given in Table 1.5. These genes are organised into seven transcriptional units, of which four are clustered together in LIPI-1, a pathogenicity island essential for *Listeria* virulence (Figure 1.19). The other three PrfA dependent transcriptional units include *inlAB* (encodes internalins A and B), *inlC* and

the *hpt* locus and are present at different points of the *L. monocytogenes* chromosome (Figure 1.17). See review by (Vazquez-Boland *et al.* 2001b) and (Portnoy *et al.* 2002) for a more detailed description of listerial pathogenesis and virulence determinants.

Table 1.5 List of genes regulated directly by PrfA and their function.

| <u>Gene</u> | <u>Putative function</u>  | <u>Reference</u>                  |
|-------------|---|-----------------------------------|
| <i>llo</i>  | Encodes the haemolysin listeriolysin O, a pore forming toxin that causes disruption of the phagocytic vacuole   | (Armstrong and Sword 1966)        |
| <i>plcA</i> | Encodes phosphatidylinositol-specific phospholipase C and together with <i>prfA</i> cooperate with LLO and PlcB in phagocytic vacuole disruption        | (Goldfine <i>et al.</i> 1995)     |
| <i>prfA</i> | Encodes positive regulatory factor A  | (Chakraborty <i>et al.</i> 1992)  |
| <i>mpl</i>  | Encodes a metalloprotease involved in the extracellular maturation of the <i>plcB</i> product (Zinc metalloproteinase precursor)                        | (Poyart <i>et al.</i> 1993)       |
| <i>actA</i> | Encodes the actin-polymerising surface protein A, which mediates bacterial actin-based motility and cell to cell spread                                 | (Kocks <i>et al.</i> 1992)        |
| <i>plcB</i> | Encodes a phospholipase C with a broad substrate range that cooperates with LLO in disruption of the phagosome and lysis of the double membrane vacuole | (Smith <i>et al.</i> 1995)        |
| <i>hpt</i>  | Encodes a hexose phosphate transporter required for rapid bacterial growth in the host cell cytosol   | (Chico-Calero <i>et al.</i> 2002) |
| <i>inlC</i> | Encodes internalin C a secreted internalin homologue required for virulence in mouse. Its role in pathogenesis is yet to be determined                  | (Engelbrecht <i>et al.</i> 1996)  |
| <i>inlA</i> | Encodes internalin A, a surface protein that mediates invasion of non-phagocytic cells  | (Hamon <i>et al.</i> 2006)        |
| <i>inlB</i> | Encodes internalin B, a surface protein that mediates invasion of non-phagocytic cells  | (Hamon <i>et al.</i> 2006)        |

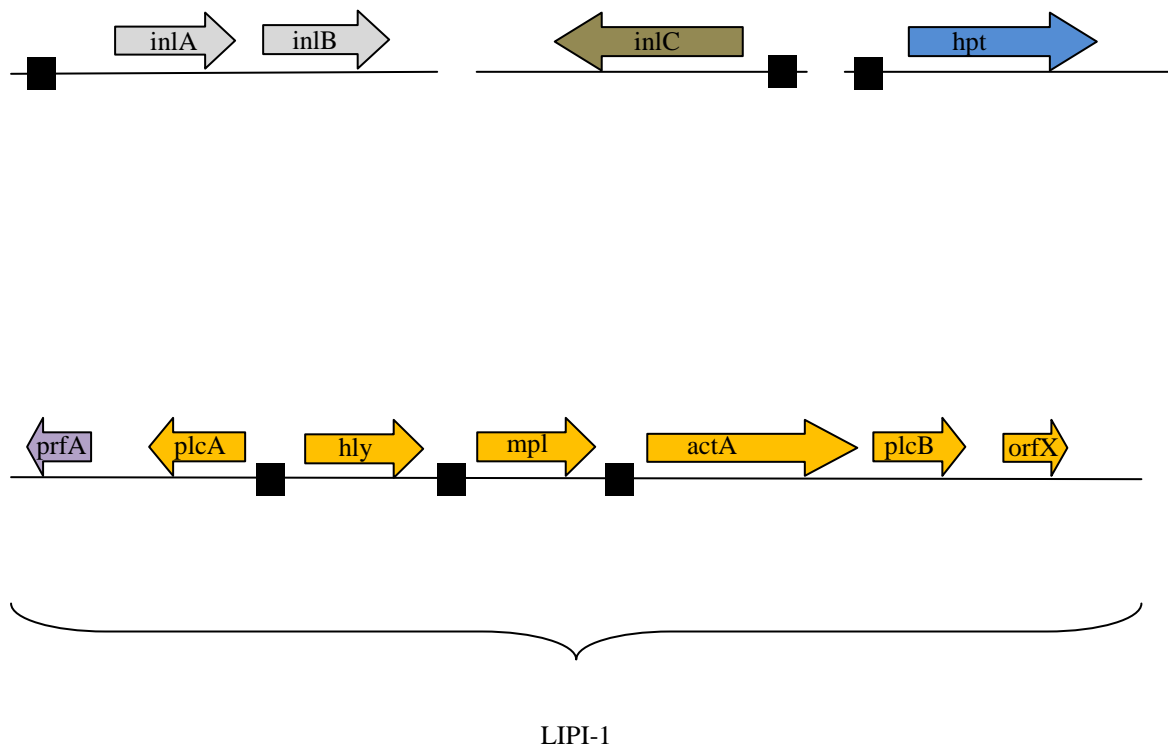


**Figure 1.19 The PrfA virulon of *L. monocytogenes*.** The Figure shows the physical organisation of the listerial pathogenicity island-1 (LIPI-1) genes and the three other PrfA regulated loci, *inlA*, *inlB*, *inlC* and *hpt*, in the *L. monocytogenes* EGDe genome. Genes pointing to the right are on the positive strand and the PrfA boxes are indicated by black squares. (Adapted from Scotti *et al*, 2007).

### ***1.16 Outline of this thesis***

This thesis initially focused on learning the techniques associated with growing rat brain ciliated ependymal cells in culture and measuring ciliary beat frequency and ciliary beat amplitude. This was because ependymal cilia are easy to obtain, cheap and quick to culture. Also, preliminary experiments in our group had shown an interesting interaction of *Listeria* with ependymal cells. Therefore, the interaction of *Listeria* with ependymal cilia was further investigated and these results are presented in Chapter three. The rest of this thesis focuses on the main topic of interest which was to study the interaction between pneumococci and human respiratory cells in healthy and PCD cultures and the results are presented in chapters four and five. The sequence of experiments was logical, as they enabled me to develop my expertise in studying ciliary interactions with bacteria in the ependymal cells. Then when I became fully competent in the study of cilia in the laboratory, the precious human ciliated tissue was used.

Chapter two provides details of the materials and methods used to culture ependymal and respiratory ciliated cells and various methods used to measure the interaction of *Listeria* and pneumococci with these cells. The aim of Chapter six was to contextualise the findings of this thesis with the known literature and to provide the reader with an indication of future research ideas.

Little is known about the importance of ciliary dysfunction in PCD patients in terms of the direct interaction of respiratory pathogens with host respiratory cells. This project therefore underlines the holistic investigation of the role of cilia in defending respiratory cells against respiratory pathogens, specifically *Listeria* and pneumococci. The hypotheses tested in this thesis will be:

- A) That *Listeria* form aggregates in the presence of ciliated ependymal cells
- B) That PCD patients are more susceptible to pneumococcal infection, due to low nitric oxide levels and absent/reduced mucociliary clearance

Aspects of the underlying mechanisms of respiratory infections in PCD patients will also be undertaken. The hypothesis tested will be:

- C) That pneumococcal damage to respiratory cells is pneumolysin dependent

Also, mechanistic investigations in the ability of respiratory cells from PCD patients to fight bacterial challenge will be undertaken. The hypothesis tested will be:

- D) Due to conditioning of the PCD epithelium to recurrent infections they have up-regulated cytokine and chemokines levels.

**CHAPTER TWO - MATERIALS  
AND METHODS**

## 2.1 Chemicals

Unless stated in the text all chemicals were from Sigma-Aldrich Ltd (UK), tissue culture media from Invitrogen (UK) and Sigma-Aldrich Ltd (UK) and bacterial growth media from Oxoid Ltd (UK).

## 2.2 Bacterial growth media

Culture media were prepared in deionised water, autoclaved at 121°C for 15 minutes at 1.5 bar pressure and stored at room temperature until used. A list of growth media used for *L. monocytogenes* and *S. pneumoniae* is shown in Table 2.1.

**Table 2.1 Media composition for bacterial cultures**

| Medium                     | Composition  | Bacteria                | Oxoid Product number |
|----------------------------|--|-------------------------|----------------------|
| Tryptone Soya broth (TSB)  | Tryptone Soya Broth, 3% (w/v)                                    | <i>L. monocytogenes</i> | CM0876               |
| Tryptone Soya Agar (TSA)   | Tryptone Soya Agar, 4% (w/v)                                     | <i>L. monocytogenes</i> | CM0131               |
| Brain Heart Infusion (BHI) | Brain Heart Infusion, 3.7% (w/v)                                 | <i>S. pneumoniae</i>    | BO0366               |
| Blood Agar Base (BAB)      | Blood Agar Base, 4.0% (w/v)                                      | <i>S. pneumoniae</i>    | CM0055               |
| Blood Agar (BA)            | Blood Agar Base, 95% (v/v).<br>Defibrinated horse blood, 5% v/v) | <i>S. pneumoniae</i>    | CM0055<br>SF0050C    |

---

### ***2.3 Preparation of tryptone soya agar and blood agar plates***

Once autoclaved, the tryptone soya agar and blood agar were allowed to cool to ~50°C. To the blood agar base, 5% v/v defibrinated horse blood was added. If antibiotics were required (see §2.5), the appropriate amount was added at ~40°C. The agar was then poured (~15ml) into 90mm single vent Petri dishes and left to set and dry at room temperature and then stored at 4°C for up to 6 months.

### ***2.4 Bacterial strains and growth conditions***

Table 2.2 lists all the bacterial strains used in this thesis.

*Listeria monocytogenes* was inoculated (by spreading 500µl volume) on to tryptone soya agar plate and incubated overnight at 37°C. The next day, colonies were used to inoculate 200ml tryptone soya broth which was incubated overnight at 37°C with shaking at 200 rpm. The next day the OD<sub>500</sub> was adjusted by adding tryptone soya broth until it was between 0.8-1.0 (equivalent to mid exponential phase). The culture was then separated into universal tubes (10ml per tube) containing 10% v/v glycerol and frozen at -70°C until required. Numbers of viable bacteria in the stock (10ml universal tubes) were determined by colony counting on tryptone soya agar plates (§2.7). Before use, frozen stocks were thawed at room temperature and the bacteria were sedimented (4,000 X g for 10 min) and re-suspended in 10 ml medium 199 (experimental buffer) and diluted to the required concentration. For growth of EGDe  $\Delta prfA$  and 10403S  $\Delta prfA$ , 5mg/ml erythromycin was added to the tryptone soya agar and tryptose soya broth.

*Streptococcus pneumoniae* was grown on blood agar plates in a CO<sub>2</sub> jar (BBL GasPak system, USA). A candle was lit and placed inside the jar, the lid tightly closed and

incubated at 37°C overnight. The candle was placed to create anaerobic conditions by eliminating any oxygen present. Colonies from the blood agar plate were used to inoculate 100ml BHI which was then incubated overnight at 37°C. The next day the OD<sub>500</sub> was adjusted by the adding BHI until it was between 0.8-1.0 (equivalent to mid exponential phase). The culture was then separated into Eppendorf tubes (1ml per tube) containing 10% v/v glycerol and frozen at -70°C until required. Numbers of viable bacteria in the stock were determined by colony counting on blood agar plates (§2.7). Before use, frozen stocks were thawed at room temperature and the bacteria were then sedimented (4,000 X g for 10 min) and re-suspended in 1ml basal epithelial base medium (BEBM, Lonza, UK) and diluted to the required concentration.

**Table 2.2 Bacterial strains used in this thesis.** The following strains were chosen because they were either reference strains, or they were mutated in genes thought to be involved in or to regulate host cell attachment.

| <b>Bacterial Strain</b>                             | <b>General description</b>  | <b>Source or reference</b>   |
|---|---|--|
| <i>L. monocytogenes</i> 10403S                      | wild-type laboratory strain   | (Freitag <i>et al.</i> 1993)   |
| <i>L. monocytogenes</i> C52                         | wild-type laboratory strain   | (Mueller and Freitag 2005)   |
| <i>L. monocytogenes</i> EGDe                        | wild-type laboratory strain   | (Murray 1926)  |
| <i>L. monocytogenes</i> 10403S $\Delta$ <i>prfA</i> | <i>prfA</i> gene disrupted by integration of <i>Tn</i> 917 in a 10403S background                     | Kindly provided by Professor Dan Portnoy, University of California, USA          |
| <i>L. monocytogenes</i> EGDe $\Delta$ <i>prfA</i>   | <i>prfA</i> gene disrupted by integration of pAUL51-10 in a EGDe background                           | Kindly provided by Professor Trinad Chakraborty, University of Giessen, Germany. |
| <i>L. monocytogenes</i> 10403S $\Delta$ BAP         | <i>BAP</i> gene disrupted by integration of pSJ004  | (Jordan <i>et al.</i> 2008)  |
| <i>S. pneumoniae</i> (D39)                          | Wild type laboratory strain, serotype 2   | National Collection Type. Culture 7466, London, UK                               |
| <i>S. pneumoniae</i> D39 $\Delta$ PLY               | Serotype 2 strain with deletion of pneumolysin gene   | (Berry <i>et al.</i> 1989b)  |
| <i>S. pneumoniae</i> (TIGR4)                        | wild-type laboratory strain, serotype 4   | Kindly provided by Tim Mitchell, University of Glasgow, UK                       |
| <i>S. pneumoniae</i> D39 $\Delta$ NanA              | <i>NanA</i> gene disrupted by integration of <i>pR</i> 410 in a D39 background                        | (Yesilkaya <i>et al.</i> 2008)   |
| Irradiated <i>S. pneumoniae</i> (D39)               | Pneumococci were killed by exposure to a source of cobalt 60 at approximately 250 Gray/hr for 4 hours | Kindly done by Graham Eaton, Dept. of Biochemistry University of Leicester, UK.  |

## 2.5 Antibiotics and media supplements

All media supplements are shown in Table 2.3. Those dissolved in water were filter-sterilised through a 0.2 µm acrodisc filter (Acrodisc, Gelman Laboratories, USA), aliquoted and stored at -20°C.

**Table 2.3 Antibiotics and media supplements.**

| Media supplements | Stock                | Final concentration in medium |
|-------------------|----------------------|-------------------------------|
| Erythromycin      | 100 mg/ml in ethanol | 150 µg/ml                     |
| Gentamicin        | 100 mg/ml in water   | 150 µg/ml                     |
| Penicillin        | 10000 IU/ml in water | 100 IU/ml                     |
| Streptomycin      | 10000 mg/ml in water | 150 µg/ml                     |
| Fungizone         | 1250 mg/ml in water  | 2.5 µg/ml                     |

## 2.6 Serotyping pneumococci

Serotyping was done by the capsular reaction test (Quellung reaction) using diagnostic pneumococcal antiserum (Heineman 1973). A loop of overnight culture of *S. pneumoniae* was smeared onto a microscope slide and allowed to air-dry. 10µl 1 % w/v methylene blue in water was placed onto a coverslip and mixed with 10µl of undiluted specific anti-pneumococcal capsular polysaccharide antiserum (Statens Serum Institute, Copenhagen, Denmark). A coverslip was then placed onto the slide. Bacteria were

examined under x1000 oil objective and were compared to a control slide prepared with heat-inactivated foetal calf serum (non-immune serum). Heat inactivation of foetal calf serum was performed by raising the temperature of the serum to 56°C for 30 minutes. Bacteria were counted as reactive if the capsule was distinctly outlined around the blue stained cells.

### ***2.7 Viable counts***

Viable counts were calculated as average colony forming units (cfu) formed from duplicate 50 µl volumes plated onto an appropriate agar plate (Miles and Misra 1938), following ten-fold serial dilutions in sterile PBS. The cfu/ml was determined by the following equation;  $\text{cfu/ml} = y \times 10^d \times 20$ , where y is the average colony count in 50µl and d is the dilution factor.

### ***2.8 Ependymal cell culture***

An adaptation (Hirst *et al.* 2000a) of a previously described method (Weibel *et al.* 1986) was used to grow the ependymal cells. Eight-well (25 x 35 mm) tissue culture trays (Fisher Scientific, UK) were coated with bovine fibronectin (1µg/cm<sup>2</sup>) (Sigma-Aldrich, UK) and were incubated at 37°C in 5% v/v CO<sub>2</sub> for 2 hours before use. Newborn (1 to 2 day old) Wistar rats (Biomedical Services, University of Leicester, UK) were killed by cervical dislocation and their brains were removed. The cerebellum was removed, as were small (3 mm) edge regions of the frontal cortex and the left and right cortical hemispheres of the brain. The remaining brain regions (containing ependymal cells and ventricles) were mechanically dissociated by passing the tissue through an 18-gauge needle in 2 ml of 20mM Hepes buffered medium199. Dissociated tissue from each brain

was seeded into the wells of 25 x 35 mm tissue culture trays (500 µl/well): each well contained 2 ml of serum-free minimum essential medium containing penicillin (100 IU/ml), streptomycin (100 µg/ml), fungizone (2.5 µg/ml), bovine serum albumin (5 µg/ml), insulin (5 µg/ml), transferrin (10 µg/ml), selenium (5 µg/ml) (Invitrogen, UK) and from day 3 onward, thrombin (0.5 IU/ml) (Sigma-Aldrich, UK). The medium was completely replaced on day 3 after seeding. Thereafter, the adherent ependymal cells were fed by the replacement of 2 ml of medium, three times a week (Hirst *et al.* 2000a). The ciliated ependymal cell colonies were identified at day 5 by visual identification of beating cilia using an inverted microscope and were used for experiments when cells were between 14-17 days old (Weibel *et al.* 1986).

### ***2.9 Infection of ependymal cells***

Before use, the medium from the ependymal cell cultures was completely removed from each well and the cells were washed 5 times with warm phosphate buffered saline before 1ml of 20mM Hepes buffered medium 199 was added to each well. For infection, 1ml of *L. monocytogenes* suspension ( $2 \times 10^8$  cfu/ml) was added to give a final concentration of  $10^8$  cfu/ml.

### ***2.10 Nasal respiratory cell culture***

The details of all the reagents used for the respiratory cell cultures are given in Table 2.4.

### **2.10.1 Subjects**

Subjects diagnosed with primary ciliary dyskinesia (n=50) from the diagnostic clinic at Leicester United Kingdom were used. Healthy controls (n=60) were recruited from staff and by local advertising at the University of Leicester. PCD was diagnosed based on the consensus recently published by Bush and colleagues (Barbato *et al.* 2009). Normal subjects were non smokers who had no history of respiratory disease for at least 6 weeks at the time of study. The study protocol was approved by the Leicestershire and Rutland Regional Ethics Committee and written informed consent was obtained from all subjects.

### **2.10.2 Collagen coating**

PureCol solution of collagen was prepared as a 1% w/v solution in phosphate buffered saline (500µl in 50ml phosphate buffered saline). A sufficient volume of PureCol solution was added to completely cover the surface of plates, flasks, glass-slides and transwells where appropriate. After incubating for 5 hours at room temperature, they were washed with nano pure water, left to air dry and then stored in a sealed bag at room temperature until used.

**Table 2.4 List of reagents used for the respiratory cell culture.**

| <b>Reagents</b>                                   | <b>Source/Catalogue number/info.</b> |
|---|--------------------------------------|
| Hepes buffered medium 199                         | Invitrogen, UK, 21180-021            |
| PureCol solution (collagen)                       | Nunclon, Holland, 5409               |
| Bronchial epithelial cell base medium (BEBM);     | Lonza, Switzerland, CC-3171          |
| Dubco minimal essential media (DMEM)              | Invitrogen, UK 41966-029             |
| Trypsin/EDTA                                      | Sigma, UK, T3924                     |
| (BEGM SingleQuotes) contains:                     | Lonza, Switzerland,T3924             |
| Bovine pituitary extract (BPE)                    | CC-4009                              |
| Insulin, bovine                                   | CC-4021                              |
| Hydrocortisone (HC);                              | CC-4031                              |
| Gentamycin Sulfate and Amphotericin-B (GA-1000)   | CC-4081                              |
| Retinoic Acid                                     | CC-4085                              |
| Transferrin                                       | CC-4205                              |
| Tri I odothyronine (T3)                           | CC-4211                              |
| Epinephrine                                       | CC-4221                              |
| Epidermal growth factor, human recombinant (hEGF) | CC-4230                              |
| Nunc 8-well tissue culture chambers               | Fisher, UK, 177402                   |
| T80 Flasks  | Sigma, UK, 156499                    |
| 12-well plates                                    | Sigma, UK, 150628                    |
| Clear transwells                                  | Corning, USA, 3460                   |
| Trans retinal (100mg)                             | Sigma, UK, R-7632                    |

### **2.10.3 Brush biopsy**

Nasal brushing is the most common and least invasive method for sampling ciliated epithelium (Rutland *et al.* 1981, MacCormick *et al.* 2002). After blowing the nose, a 2mm nylon cytology brush was used to brush the side of the nasal turbinate in an anterior and posterior direction and then withdrawn. Typically, a good biopsy yielded about 1mg of ciliated tissue. Each tissue strip contained rows of 10-50 ciliated cells. The epithelial strips obtained were then dislodged by agitating in 2ml of 20mM HEPES buffered medium 199 (pH 7.4), containing penicillin (100 IU/ml), streptomycin (100 µg/ml) and fungizone (2.5 µg/ml), and kept in the fridge overnight. This allowed time for the antibiotics and fungizone to work and clear any potential deep cellular infections.

### **2.10.4 Basal cells**

An adaptation of a previously described method was used to grow respiratory basal cells (Gray *et al.* 1996). The brush biopsy contained a heterogeneous population of both differentiated and undifferentiated respiratory epithelial cells. The contents of the brush biopsy (unknown number of cells) was placed in a collagen-coated well from a 12 well plate in 1ml of basal epithelial growth medium (BEGM) (BEBM+SingleQuots see Table 2.5), containing penicillin (100 IU/ml), streptomycin (100 µg/ml) and fungizone (2.5 µg/ml), at 37°C. The basal cells were fed every other day by removing the medium and replacing it with 1ml BEGM. When the cells were 90 to 100% confluent (after 7-10 days) the entire medium was removed and the cells were washed with 0.3ml Trypsin/EDTA solution (0.5g porcine trypsin and 0.2g EDTA per liter of Hanks' Balanced Salt Solution with phenol red) and left at room temperature for about 2-3

minutes, occasionally agitating the tray. As soon as the cells began to detach, they were suspended by pipetting the Trypsin/EDTA solution over the cell surface. Cells were then placed in a 15ml tube containing 1ml BEGM to inactivate the trypsin. The well surface was then washed with 3ml of BEGM (to recover all the cells) and this also was placed in the 15ml centrifuge tube. The cells were then centrifuged (2,000 X *g* for 10 min) and the supernatant was removed. The pellet was resuspended in 1ml BEGM, making sure that there were no clumps by vigorous pipetting. The cell suspension was then added to a T80 (80cm<sup>2</sup>) collagen-coated flask containing 14ml BEGM. When the cells in the T80 flask were 90 to 100% confluent (up to 4-7 days), the entire medium was removed and the cells were washed with 1.4ml Trypsin/EDTA solution and left at room temperature for about 2-3 minutes, agitating the flask occasionally. As soon as the cells detached, 8ml BEGM was added and the cells were suspended by pipetting the medium over the cell surface. The cell suspension was pipetted into a 15ml tube and the cells were centrifuged for 5 minutes at 4,000*g*. The supernatant was removed and the pellet resuspended in 1.8ml BEGM. Half of the cell supernatant was used for basal cell studies (900  $\mu$ l) in which the cells were either divided between the wells of a 12-well collagen coated plate (70  $\mu$ l in each well) or up to 20 wells of 8-well collagen coated glass chamber slides (40  $\mu$ l in each well). The basal cells were fed with fresh BEGM medium, 1ml in the 12-well plates and 400 $\mu$ l in the 8-well glass chamber slides, every other day until confluent monolayers were obtained. Confluent 12 well plate wells contained  $\sim 10^7$  cells and the glass chamber slides contained  $\sim 10^5$  cells.

The other half of the basal cell suspension was used for air liquid interface cultures (§ 2.10.5).

---

### ***2.10.5 Air liquid interface (ALI) cultures***

An adaptation of a previously described method was used to grow respiratory ciliated cells (Gray *et al.* 1996). For the ALI cultures 0.25ml of basal cell suspension ( $\sim 1 \times 10^3$  cells/cm<sup>2</sup>) from the T80 flasks (see §2.10.4) was added into four collagen-coated transwell inserts (0.4 µm pore size, 1.2cm<sup>2</sup> diameter) of a 12-well plate with 1ml BEGM on the basolateral side. Until confluent, the cells were fed with BEGM every other day by replacing medium on the apical and basal surfaces (300µl and 850µl respectively). When the basal cells reached confluency the medium was removed from the apical surface, exposing the cells to air, and the medium was also removed from the basolateral well and replaced with 700ul of air liquid interface (ALI) medium [50:50 BEBM and DMEM (400nM glucose)] containing penicillin (100 IU/ml), streptomycin (100 µg/ml), fungizone (2.5 µg/ml) and 10 nM *trans*-retinoic acid. Cells were fed every other day by replacing the basolateral ALI medium completely. Mucus was produced from the apical surface within the first two weeks and the first cilia emerged from cultures from day 16 onwards. The apical surface of the cells was washed with 0.3ml PBS if the cells were producing excess mucus. Fully mature cilia were present after 3 weeks in culture and the transwell contained  $\sim 2 \times 10^5$  cells.

### ***2.10.6 Transepithelial electrical resistance measurements***

To confirm the presence of mature healthy epithelium, transepithelial electrical resistance (TEER) measurements were made using a chopstick EVOM voltohmmeter (World Precision Instruments, Sarasota, FL, USA) after temporary addition of 0.5 ml of culture medium to the upper insert.

### ***2.11 Infection of basal and ciliated respiratory cells***

Before infecting the basal and respiratory cells, BEGM and ALI media containing antibiotics were replaced with BEBM for 2 hours. Cells were then washed twice with BEBM and infected with *S. pneumoniae* ( $10^7$  cfu). Basal cells were infected for 4 hours with pneumococci that were diluted to the required concentration in 400 $\mu$ l BEBM. Ciliated respiratory cells were infected for 2 hours with pneumococci that were diluted to the required concentration in 200 $\mu$ l BEBM.

### ***2.12 Interaction between microspheres and cilia***

Positive, negative and neutral microspheres (Table 2.5) were diluted in relevant tissue culture medium and added to the ciliated cells (BEBM for respiratory cells and Hepes 199 for ependymal cells). The surface charge of these microspheres was kindly measured by Professor Samuel Lai, Department of Chemical & Biomolecular Engineering, Johns Hopkins University, Baltimore, USA.

**Table 2.5 List of microspheres used in this study and their details.**

| <b>Microsphere charge</b> | <b>Details</b>   | <b>Source</b>  |
|---------------------------|--|--|
| Positive                  | Melamine formaldehyde, 1.53 $\mu$ M diameter, surface charge of 24 +/- 1 mV. | microspheres-nanospheres, Cold Spring, NY, USA   |
| Negative                  | Silicon oxide, 1.42 $\mu$ M diameter, surface charge of -98 +/- 3 mV         | microspheres-nanospheres, Cold Spring, NY, USA   |
| Neutral                   | latex microspheres, surface charge of 0 mV                                   | Kindly donated by Prof. Samuel Lai Dept. of Chemical & Biomolecular Engineering, Johns Hopkins University, Baltimore, USA. |

### ***2.13 Measurement of ciliary beat frequency (CBF)***

Ciliary beat frequency was measured as previously described (Mohammed *et al.* 1999, Hirst *et al.* 2000a). For better resolution of cilia, the transwell inserts were placed on a purpose-made Perspex cassette containing four wells with fixed cover slips containing 500 $\mu$ L of BEBM. Trays of ependymal cells and the transwells on the Perspex cassette were placed in a humidified (80 - 90% humidity) thermostatically controlled (37°C) incubation chamber on a light microscope stage (Diphot; Nikon) and left to equilibrate for 30 minutes. Using probes the solution temperature (Fluke 52 II thermometer, Everett, Washington, USA) and pH (Fisher, UK) was measured. All CBF measurements were made with the solution temperature between 36.5 and 37.5° C and the pH between

7.35 and 7.45. For viewing the ciliated respiratory cells and for the ependymal cells, a 50x water immersion lens a 32x lens objective were used respectively. Beating of cilia was recorded (magnification x320) using a Troubleshooter 1000 high speed video camera (Lake Image Systems Ltd, UK) at 500 frames per second. All video files were created using the AVI video format. For viewing the AVI files, MiDAS 4.0 player software (<http://www.xcitex.com/html/downloads.php>) was used. Video sequences were played back either at reduced frame rates or frame by frame, and ciliary beat frequency was determined by timing a pre-selected number of individual ciliary beat cycles. At each time point, measurements of ten individual cilia from the same colony of cells were made.

### ***2.14 Measurement of ciliary beat amplitude***

High-speed video recordings were made as described in section 2.13. From the slow motion replay of the video recordings it was possible to determine the maximum forward position of the cilia tip and the maximum backward position of the ciliary tip. The distance travelled between these two points was measured, in mm, on a display screen (10inch screen) and was defined as the ciliary beat amplitude.

For each experiment, five different regions of ciliated ependyma (approximately 60 $\mu$ m x 140 $\mu$ m) and respiratory cilia (approximately 50  $\mu$ m x 100  $\mu$ m) were chosen at random. From each area, five measurements of ciliary beat amplitude were made. In some experiments where bacterial aggregates covered the cilia five readings were taken from cilia covered by these aggregates and five readings from cilia outside these areas. The amplitude of the ciliary beat in the control, which was not exposed to bacteria, was defined as 100%.

### ***2.15 Measurement of bacterial aggregation***

Still video files were obtained at the end of the experiments. From still photographs, projected onto the laptop screen, the perimeter of bacterial aggregates associated to the cells was traced onto acetate sheets. Using a grid, the percentage of ciliated tissue covered by bacterial aggregates was determined for each sample. The grid contained 100 squares and each square represented 1% coverage. Five different areas of ciliated cells were chosen at random.

### ***2.16 Scanning electron microscopy***

Scanning electron microscopy was done in collaboration with Andrew Rutman (University of Leicester). Ependymal cells were fixed with 4% v/v glutaraldehyde in Sorensen's phosphate buffer (0.1M, pH 7.4) before centrifugation for 5 minutes at 223g (Hirst *et al.* 2000a). The pellet was then re-suspended in fresh Sorensen's buffer for 1 hour and rinsed twice with distilled water. The cells were post-fixed in 1% w/v osmium tetroxide for 1 hour, after which the sample was centrifuged (5 minutes, at 223g). Cells were washed gently in fresh Sorensen's buffer 3 times and re-centrifuged. The samples were then transferred into Bijou pots (7ml) and dehydrated through a graded ethanol series; 50% v/v for 5 minutes, 70% v/v for 5 and then 15 minutes, followed by 90% v/v and 100% for 5 and 15 minutes. The samples were then rinsed with neat hexamethyldisilazane (HMDS) for 30 minutes and then immersed in fresh HMDS which was allowed to evaporate overnight, leaving the cells fixed to aluminium scanning electron microscope stubs (Agar scientific). These were then sputter-coated with gold prior to examination.

---

### ***2.17 Immunohistochemical characterisation of basal cells***

Confluent basal cells, grown in glass chamber slides, as described in §2.10.4, were fixed with 4% w/v paraformaldehyde in phosphate buffered saline for 10 minutes at room temperature. The cells were then washed with 200µl phosphate buffered saline for 20 minutes with three buffer changes. The last wash was replaced with 1ml 3% w/v BSA (Bovine serum albumin) in phosphate buffered saline and left for 10 minutes at room temperature and then washed three times with phosphate buffered saline. Cells were stained for 2 hours with 200µl mouse anti-cytokeratin peptide 14 (CK14) monoclonal antibody (Sigma, UK.C8791), at a dilution of 1:200 in 1% w/v BSA in PBS at 37°C (Jakiela *et al.* 2008). After three washes in phosphate buffered saline, FITC-Goat anti-mouse IgG, A, M (Zymed laboratories, 65-6411) was diluted 1:50 in 1% w/v BSA in phosphate buffered saline and was added for 2 hours at 37°C. During the final 10 minutes, 1:1000 Hoechst stain (Sigma Aldrich, UK, H6024) was added to stain the nuclei. After 3 washes with PBS, the chamber was removed and a few drops of mountant (80% v/v glycerol, 3% w/v n-propyl gallate in phosphate buffered saline) was placed onto the slide, covered with a size 1.5 coverslip and sealed with nail varnish. The cells were then visualised using a Nikon eclipse TE2000-U microscope.

## ***2.18 Fluorescent labeling of basal and ciliated cells infected with pneumococci***

### **Pneumococcal infected basal cells**

Bacterial, cytoplasmic and nuclear staining of basal cells was performed prior to infection studies. 2µg/ml Hoechst (Invitrogen, UK) was diluted in 300 µl of BEBM and left in the dark covering the cells for 20 minutes (Mocharla *et al.* 1987). The basal cells were then rinsed twice with BEBM.

After the nuclei staining, the plasma membrane of the cells was stained with 1,1'-dioctadecyl-3,3,3',3'-tetramethylindocarbocyanine perchlorate (DiI; DiIC18, Invitrogen, UK) (Honig and Hume 1986). DiI (3µl of a 1mM solution) was diluted in 300µl of the appropriate medium which was added to the cells for 20 minutes at 37°C. After incubation, the cells were washed three times with fresh medium.

Bacterial stocks were prepared as described in §2.4. *S. pneumoniae* stock cultures (1ml) were spun at 600x *g* for 10 minutes and re-suspended in 1ml BEBM. The bacteria were stained using mixed isomers 5-and-6-carboxy-2',7'-dichlorofluorescein diacetate succinimidyl ester (CFSE; Invitrogen, UK) (Breeuwer *et al.* 1996). CFSE (3µl of a 1mM stock solution) was added to 1ml of bacterial suspension and incubated at 37°C for 45 minutes. The bacterial suspension was then centrifuged as before and the pellet washed three times by re-suspension in an equal volume of BEBM medium to remove excess dye. The basal cells were infected with the stained pneumococci as mentioned in §2.11.

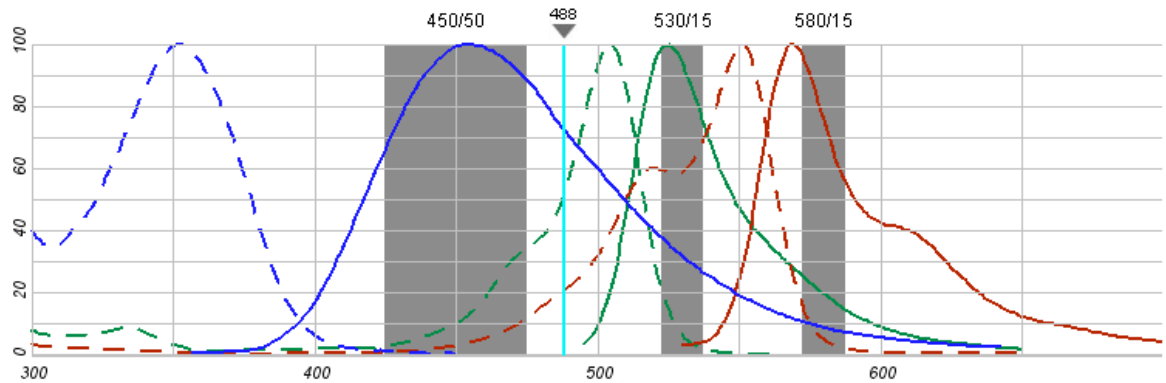
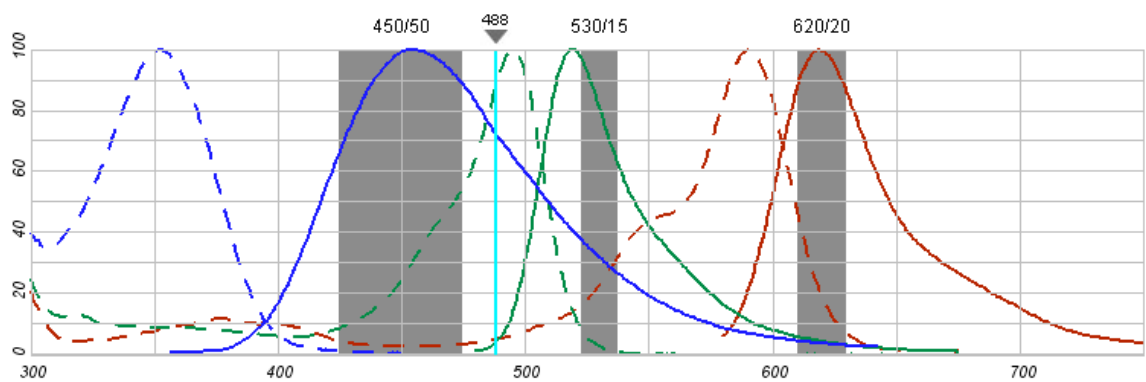
---

**Pneumococcal infected ciliated cells**

After each experiment, cells were fixed with 4% w/v paraformaldehyde overnight at 4°C. The next day, cells were washed with 200µl PBS for 20 minutes with three buffer changes. After the last wash 1ml 3% w/v BSA in PBS was added and left for 10 minutes at room temperature and then washed three times with PBS. Cilia were labelled with mouse anti-acetylated tubulin antibody (Sigma, UK, T6793) diluted 1:1000 and pneumococci were labelled with rabbit anti-type 2 pneumococcal capsule antibody (Statens serum institute, USA, 16745) diluted 1:40 in 1% w/v BSA in PBS. A 200 µl solution of these primary antibodies diluted in 3% w/v BSA in PBS were added to the cells for 2 hours at 37°C. After three washes in 200µl PBS, antibodies bound to the tubulin protein of cilia were detected using goat anti-mouse alexafluor 594 (Invitrogen, UK, A-11020) diluted 1:250 in 1% w/v BSA in PBS. Antibodies bound to the pneumococcal capsule were detected using FITC goat anti-rabbit IgG (Abcam, ab6717) diluted 1:250 in 1% w/v BSA in PBS. A 200µl solution of these secondary antibodies diluted in 1% w/v BSA in PBS was added to the cells for 2 hours at 37°C. During the final 10 minutes, 1:1000 Hoechst stain (Sigma Aldrich, UK, H6024) was added to stain the nuclei. After 3 washes with PBS, the membranes were excised from inserts using a scalpel and mounted invertedly onto slides. After adding a few drops of mountant (80% v/v glycerol, 3% w/v n-propyl gallate in PBS) onto the membrane the cells were covered with a size 1.5 coverslip and sealed with nail varnish.

Figure 2.2 A and B are spectrums showing the fluorescent excitation and emission maxima for each of the fluorophores used in the basal and ciliated respiratory studies, respectively. Each peak is distinct and thus could be used for the studies.

The respiratory basal and ciliated cells were viewed with a Leica TCS SP5 laser scanning confocal microscope (X 63 Plan-APOCHROMAT 1.4 numerical aperture oil DIC lens or X 40 Plan- NEOFLUAR 1.3 numerical aperture oil DIC lens). The lasers for scanning were an Argon laser (488 nm), DPSS (561 nm) and blue diode laser (405 nm).

**A****B**

**Figure 2.2 Fluorescence Spectra used to confirm the compatibility of the fluorophores used.** The X-axis is the relative intensity and the Y-axis the wavelength. The light blue line in both images represents the 488 laser. The peaks are representative of the absorption (dashes) and fluorescence emission (unbroken) spectra. The grey bands show the emission band for each fluorophores/ analyses window. A) fluorophores used for basal cell studies. Green is the CFSE stained bacteria, red is the DiI stained basal cells and blue the Hoechst stained nuclei B) fluorophores used for ciliated cell studies. Green is the FITC labelled bacteria, red is cilia labelled with anti mouse secondary alexafluor 594 and blue the Hoechst stained nuclei. Obtained from Invitrogen website, the link is given below.

<http://www.invitrogen.com/site/us/en/home/support/Research-Tools/Fluorescence-SpectraViewer.html>

### **2.19 Image analysis software**

To create a 3D surface representation of confocal z stack series from both infected basal and ciliated cells a '3D volume render image' using the blend mode of Imaris software was generated (Bitplane AG, Switzerland, <http://www.bitplane.com>).

Using the Surpass feature of Imaris it was possible to create 3D surfaces for each fluorescence channel. In this study 3D surfaces were only created for the cytoplasm (red-DiI) and nuclei (blue, Hoechst). Also, using the 'spot object' feature of Surpass, 1  $\mu\text{m}$  (bacteria) fluorescent objects were automatically recreated as spots, regardless of the overall intensity. Thus, it was possible to define each bacterium adhered to the cells as a 1 $\mu\text{m}$  spot. Imaris detects an automatic threshold at which to insert the spots. The number of spots in each image is calculated automatically. Also, by making the red channel 20% transparent it was possible to locate those spots hidden by the cytoplasm. Using a Leica laser scanning confocal microscope (X 63 objective) five random areas were imaged by obtaining z sections. Each z section was approximately 0.4 $\mu\text{m}$ . The data from the five random areas were added together and represented as a ratio of adhered bacteria per cell. Only bacteria in close proximity to the red channel were included in the calculation. Web training for each feature used is available at <http://www.bitplane.com/go/web-training>.

### **2.20 Assay of nitric oxide in culture**

As described in §2.12, respiratory cells were infected with *S. pneumoniae*. Nitric oxide (NO•) concentration in culture media was measured using a chemiluminescence analyser (model 280, Sievers Instruments, Boulder, CO, USA) as previously described

---

(Tsang *et al.* 2002). Briefly, nitric oxide was rapidly converted to nitrite ( $\text{NO}_2^-$ ) and nitrate ( $\text{NO}_3^-$ ) in liquid medium.  $\text{NO}^\bullet$  was measured by chemiluminescence by reducing  $\text{NO}_2^-$  and  $\text{NO}_3^-$  in the presence of vanadium (III) chloride. Between 5-10 $\mu\text{l}$  of cell supernatant was injected into the first chamber of the Sievers chemiluminescence analyzer, where  $\text{NO}_3^-$  and  $\text{NO}_2^-$  were reduced by vanadium (III) chloride (in 1 mol/L HCl) back to  $\text{NO}^\bullet$ . The latter was neutralised in 1M NaOH in the second chamber to remove HCl vapours from entering the  $\text{NO}^\bullet$  analyzer.  $\text{NO}^\bullet$  was mixed with ozone in the third chamber to produce ground-state  $\text{NO}_2$  and excited-state  $\text{NO}_2^*$ . The latter then emitted a photon on returning to the ground state and the photon was detected by a photomultiplier. Software supplied by the manufacturer allowed instant conversion of the photon reading to the corresponding concentration of  $\text{NO}^\bullet$ . A 100mM nitrate solution was used to prepare a standard curve.

### ***2.20.1 Preparation of the glass vessel***

Figure 2.3 shows the assembled nitric oxide analyser apparatus. Before taking measurements, the valves of the glass vessel were closed. Then 15-20 ml of fresh 1M NaOH was added through the tap labelled 3 on the diagram. The cap labelled 4 on the diagram was then removed and 4-5 ml of saturated vanadium in HCl was added into the vessel. Before closing the cap, a new inoculation disk was inserted. The last stage was to turn on the two water baths, one was filled with ice cold water and the other was filled with water at 95°C.

### ***2.20.2 Preparation of the standards and unknown samples***

To prepare for inoculation of standards and test samples, all valves to the glass vessel were closed. The nitrogen cylinder was turned on and the pressure set to 5-8 psi. The

valves were then turned in the following order, to avoid surge of pressure in the analyser. First, valve 1 from the nitrogen cylinder, valve 2 between the vanadium vessel and NaOH trap, valve 3 from the NaOH trap to the NO• analyser, which was opened very slowly. The voltage of the NO• analyser rose when the pressure increased from the glass vessel after opening valve 3 and then slowly fell to around 10mV. Regulating valve 4, on the glass vessel was then turned on until a pressure reading of 5.7-5.8 psi was obtained in the NO• analyser. The apparatus was then ready for use.

For sample analysis, first 100µl of ultra pure water was injected through disc A (Figure 2.3). The peak on the recorder screen raised and fell back to the baseline before the next sample was added. Standard solutions (100µl) were then analysed in the order 200nM, 400nM, 600nM, 800nM and 1 µM nitrate. The test samples were then analysed. If the height of the peak obtained for 100µl of a test sample was outside the standard range, 40µl of sample was injected into the analyser. At the end of the run the valves were turned off in the order 3, 2 and 1. The vanadium waste was collected into a beaker by opening the outlet valve. All the pressure tubing was removed and rinsed with ultra pure water. The NaOH vessel was also rinsed and stored containing 15-20ml of ultra pure water.

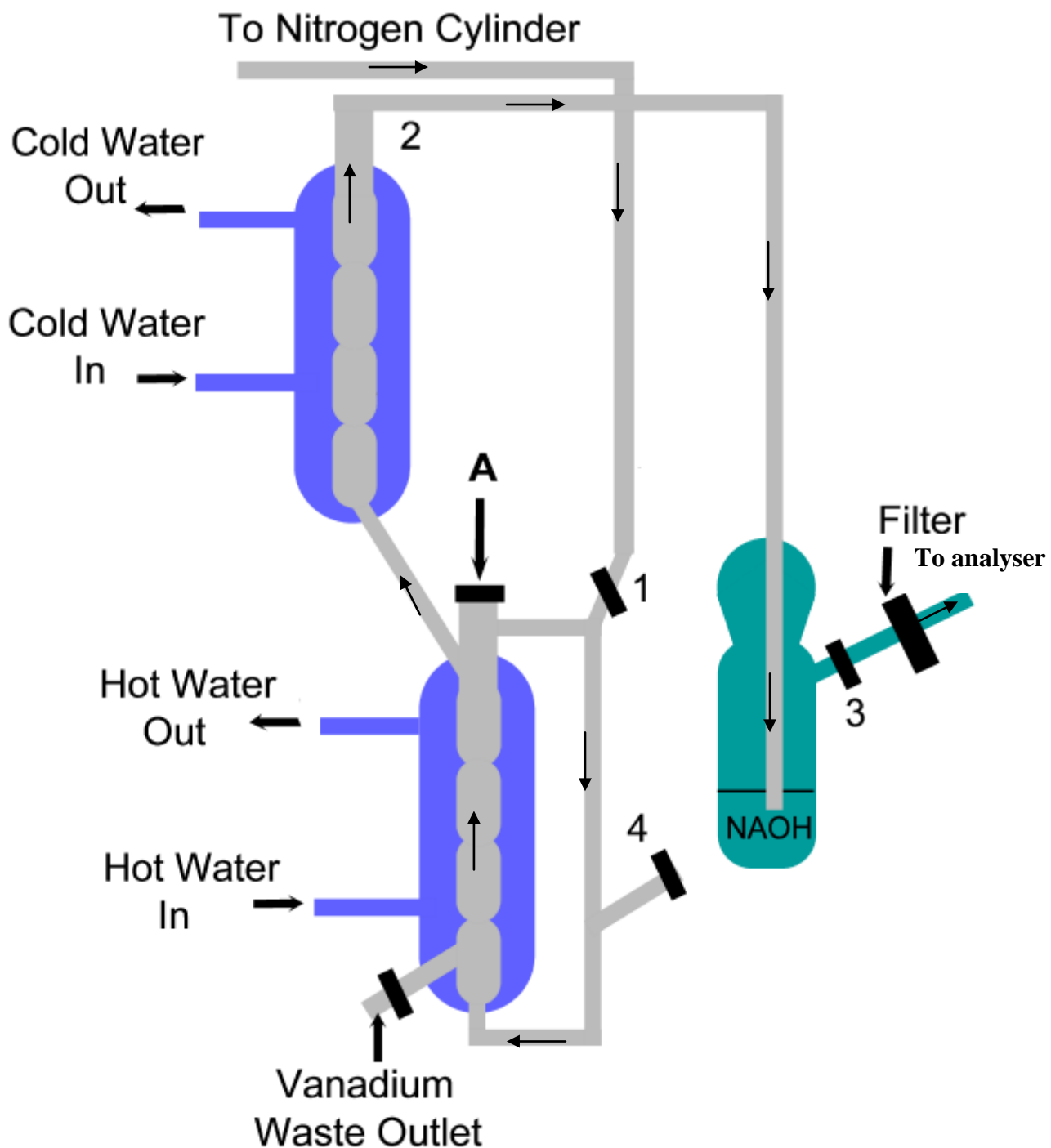


**Figure 2.3** Diagram of the nitric oxide analyser glasswear. “A” shows the injection point. The numbers indicate different valves (1) the valve from the nitrogen cylinder, (2) the valve between the vanadium vessel and the NaOH trap, (3) the valve from the NaOH trap to the NO<sup>•</sup> analyser and (4) the regulating valve on the glass vessel.

### **2.21 Trypan blue assay**

Trypan blue binds to DNA inside the cell and is a simple method to measure cell viability (Freshney 1987). Viable cells with intact membranes exclude trypan blue and are not coloured, whereas, dead cells absorb the stain and appear blue. A basal cell suspension of 20 $\mu$ l (§2.10.4) was placed in an eppendorf tube and added to 20 $\mu$ l of 0.4% w/v trypan blue solution (Sigma, T-8154). Of this suspension 10 $\mu$ l was added to the chamber of a C-Chip disposable hemocytometer (Digital Bio, Korea) and using a light microscope, the number of live and dead cells counted within 2-3 minute.

### **2.22 Measurement of cell viability**

Damage to respiratory basal and ciliated cells following incubation with *S. pneumoniae* was determined by measurement of lactate dehydrogenase (LDH) release. The lactate dehydrogenase assay is a means of measuring membrane integrity as a function of the amount of cytoplasmic LDH released into the culture medium, as a result of cell death. The assay is based on the reduction of NAD by LDH. The resulting reduced NAD (NADH) is utilized in the stoichiometric conversion of a tetrazolium dye. The resulting coloured compound is measured spectrophotometrically. If the cells are lysed prior to assaying the medium, an increase or decrease in cell numbers results in a concomitant change in the amount of substrate converted. This indicates the degree of cytotoxicity caused by the test material, in this case pneumococci. If cell-free aliquots of the medium from cultures given different treatments are assayed, then the amount of LDH activity can be used as an indicator of relative cell viability as well as a function of membrane integrity.

LDH in the cell culture supernatant was measured by an *in vitro* assay kit (Sigma, UK). The cells were removed by centrifuging (at 250g for 4 minutes) and 50µl of supernatant transferred to a well of a flat-bottomed microtitre plate. To prepare the enzymatic lactate dehydrogenase assay mixture equal amounts of LDH assay substrate, cofactor and dye solution were mixed together. Of this assay mixture 100µl was then added to each well of the flat-bottomed plate containing the cell culture supernatant. The plate was then covered with aluminium to protect from light and incubated for 30 minutes at room temperature. 1 M HCL (15µl) was added to each well to stop the enzymatic reactions.

To measure the total LDH from infected cells, 1/10 volume of LDH assay lysis solution per well (40 µl) was added to the cells and incubated at 37°C for 45 minutes. The cells were then centrifuged and 50µl transferred to a well of a flat bottomed plate followed by the same enzymatic analysis mentioned above.

Using an ELISA plate reader the absorbance was measured at a wavelength of 490nm. The background absorbance was also measured at 690 nm and this value was subtracted from the primary wavelength measurement. The results were presented as a percentage of the LDH released from the fully lysed control wells.

### ***2.23 Adherence assay***

An adaptation of a previously described method was used to determine the adherence of pneumococci to basal cells (Cundell *et al.* 1995). Basal cells were infected with 10<sup>7</sup> cfu pneumococci for 4 hours at 37°C (§2.12). To remove the loosely adhered bacteria after the incubation period, the supernatant was removed and the glass slide was separated from the plastic chamber. The glass slide was gently placed vertically in 50ml PBS for 1

minute. The slide was then removed and placed into another pot containing 50ml PBS for 1 minute. This procedure was repeated 5 times. After the last wash, the cells were dislodged from the slide by the addition of 200  $\mu$ l 0.1% v/v trypsin for 5 minutes and then re-suspended in BEBM medium. Bacteria were counted by colony counting.

### **2.24 Invasion assay**

An adaptation of a previously described method was used to assess the ability of pneumococci to invade basal cells (Cundell *et al.* 1995). Basal cells were infected with  $10^7$  cfu pneumococci for 4 hours at 37°C (§2.12). After the incubation period, the cell supernatant was removed and the cells were treated with 50 $\mu$ g/ml gentamicin in BEBM medium for two hours to remove extracellular pneumococci. The cells were dislodged from the slide by the addition of 200  $\mu$ l 0.1% v/v trypsin for 5 minutes and then re-suspended in BEBM medium. Viable intracellular bacteria were quantified by plating lysed cells for colony counting (§2.7).

### **2.25 Chemokine and cytokine analysis**

Chemokines and cytokines were measured using a 96-well multi spot assay (Meso Scale Discovery [MSD], Maryland, USA) according to the manufacturer's instructions. Briefly, the assay employs a sandwich immunoassay format where capture antibodies are coated in a single spot, or in a patterned array, on the bottom of the wells of a multi-spot plate (Figure 2.4). Samples or standards are incubated in the multi-spot plate, and each cytokine binds to its corresponding antibody spot. When a potential is applied to the electrode, bound labelled sulpho tag produces light and this is proportional to the amount of inflammatory proteins in the sample. Unknown samples are calculated by

comparing their light emitted to that of a known amount of the protein on the standard curve.

Cytokines were measured using a human Th<sub>1</sub>/Th<sub>2</sub> standard 10 spot plate (Catalog number N01010A-1) and human chemokines were measured using a high band MS6000 10 spot plate (Catalog number N01001B-1), using SECTOR Imager 6000 (MSD, Maryland, USA). For more details follow the following link. ([http://www.mesoscale.com/CatalogSystemWeb/Documents/Human\\_96\\_well\\_Base.pdf](http://www.mesoscale.com/CatalogSystemWeb/Documents/Human_96_well_Base.pdf)). The lower limit of detection was 1 pg/ml.

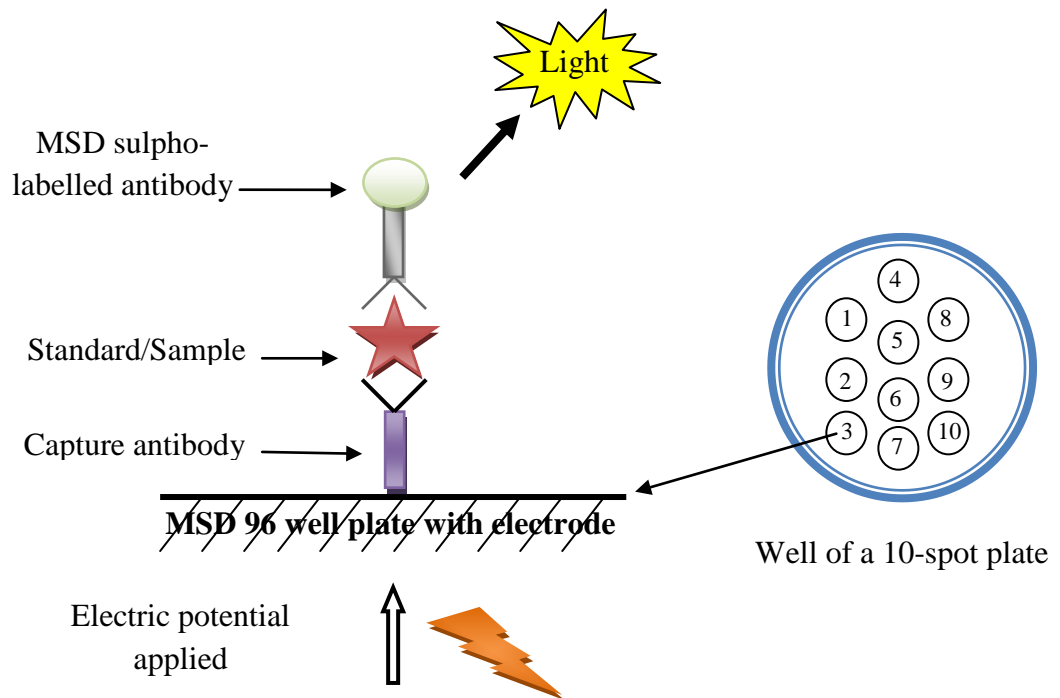


**Figure 2.4. Schematic showing the antibody sandwich system in MSD assays.** Cytokine capture antibody is pre-coated on specific spots of a multi-spot plate. Sample or standards are incubated in the multi-spot plate, and each cytokine binds to its corresponding antibody spot. When a potential is applied to the electrode, bound labelled sulpho tag produces light and this is proportional to the amount of inflammatory proteins in the sample. Unknown samples are calculated by comparing their light emitted to that of a known amount of the protein on the standard curve.

### ***2.26 Statistical analysis***

Statistical analysis was performed using GraphPad Prism 5 (GraphPad, San Diego, CA, USA). The cytokine and chemokine data were analysed using one way analysis of variance (Kruskal–Wallis test) and expressed as median  $\pm$  inter quartile range (IQR). The rest of the data were analysed by using repeated measures one way analysis of variance (ANOVA) and expressed as the mean  $\pm$  standard deviation. Between groups comparisons were performed using the nonparametric Mann-Whitney U-test. Within group comparisons were performed using a paired t-test. A p-value of  $<0.05$  was taken as the threshold for statistical significance. Advice on the use of statistical analyses was given by Dr John Bankart (Statistician, Department of Health Sciences, University of Leicester, UK).

**CHAPTER THREE – RESULTS**  
**(ependymal cilia and *Listeria*)**

### **3.1 Overview**

*Listeria monocytogenes* is a food-borne pathogen that, if ingested, has the potential to enter the systemic circulation and move from the blood to penetrate the blood-brain barrier to cause meningitis and meningoencephalitis, especially in the unborn and newborn infant (Seeliger 1986, McLauchlin 1997). The risk of listeriosis is also markedly increased in immunocompromised patients, such as those with AIDS (Jurado *et al.* 1993).

In meningitis, bacteria in the cerebrospinal fluid are separated from the neuronal tissue adjacent to the ventricular system and aqueducts, by the ependyma. The ependyma is a single, uninterrupted, layer of ciliated cells that lines the cerebral ventricles, cerebral aqueducts and the central canal of the spinal cord. Each ependymal cell has approximately 40 cilia that beat continuously at a frequency of around 40 Hz, moving the CSF close to the ventricular wall, in the direction of CSF flow (Shimizu and Koto 1992). In addition, the ependymal cilia are thought to act as a barrier to pathogen infection of the underlying neuronal tissue (Del Bigio 1995). Prior to the entry of *Listeria* into the cells of the brain the bacteria need to overcome this mechanical beating of the cilia. Abnormal movement of the ependymal cilia has been strongly linked to the development of hydrocephalus (Picco *et al.* 1993, Monkkonen *et al.* 2007).

During meningitis caused by *L. monocytogenes*, bacteria have been shown to be present inside ependymal (Michelet *et al.* 1999) and neuronal (Drevets *et al.* 2004) cells, as well as in the cerebrospinal fluid (Michelet *et al.* 1999, Deckert *et al.* 2001, Remer *et al.* 2001). However, the details of *L. monocytogenes* attachment to ciliated ependymal cells and subsequent invasion are poorly understood. To improve our understanding of the

patho-physiology of listerial meningitis, the effect of different strains of *L. monocytogenes* on ependymal cilia was studied.

### ***3.2 Interaction of wild-type L. monocytogenes and ciliated ependymal cells***

Wild-type *L. monocytogenes* 10430S ( $10^8$  cfu), were incubated with ciliated ependymal cells for three hours. Ciliary beat frequency (CBF) measurements were carried out at defined times, after infection. During the first 30 minutes, the CBF was between 42 Hz and 35 Hz and then stayed constant at around 40 Hz. However, after three hours the cells started to detach from the tissue culture tray and for this reason, a three hour time course was chosen for the subsequent experiments.

Ependymal cells from newborn Wistar rats were grown in culture until optimal ciliation was reached (14-17 days) (Hirst *et al.* 2000a). Figure 3.1A is a low magnification electron micrograph showing individual ependymal cells with tufts of cilia. Figure 3.1B is a high magnification of ciliated rat ependymal cells *in vitro* at 15 days in culture. As mentioned in section 1.6 each ependymal cell has approximately 40 cilia, approximately 8µm long and beat continuously at a frequency of around 40 Hz. A slow motion video of beating ependymal cilia (Video S4) is given in Appendix A (See CD accompanied with the thesis). Ciliated ependymal cells were then incubated with wild-type strains of *L. monocytogenes* for three hours at 37°C. The behaviour of both the ependymal cilia and the *Listeria* was altered in these co-cultures but the alterations were dependent on the strain of *L. monocytogenes*.

The first strain studied was *L. monocytogenes* 10403S. In the presence of ependymal cells the bacteria aggregated and by three hours about 11% of the surface area of the

ependymal cell culture was covered by listerial aggregates that were attached to the underlying cilia (Table 3.1, and Appendix A video S5). Scanning electron microscopy revealed that the vast majority of the 10403S aggregates consisted of bacteria within an extracellular material (Figure 3.2A). The scanning electron microscopy image in Figure 3.2B shows strands of material between the individual 10403S bacteria after three hours of co-culture with ependymal cells. Occasional aggregates of bacteria associated with cilia, but without extracellular material, were also present (Figure 3.2C).

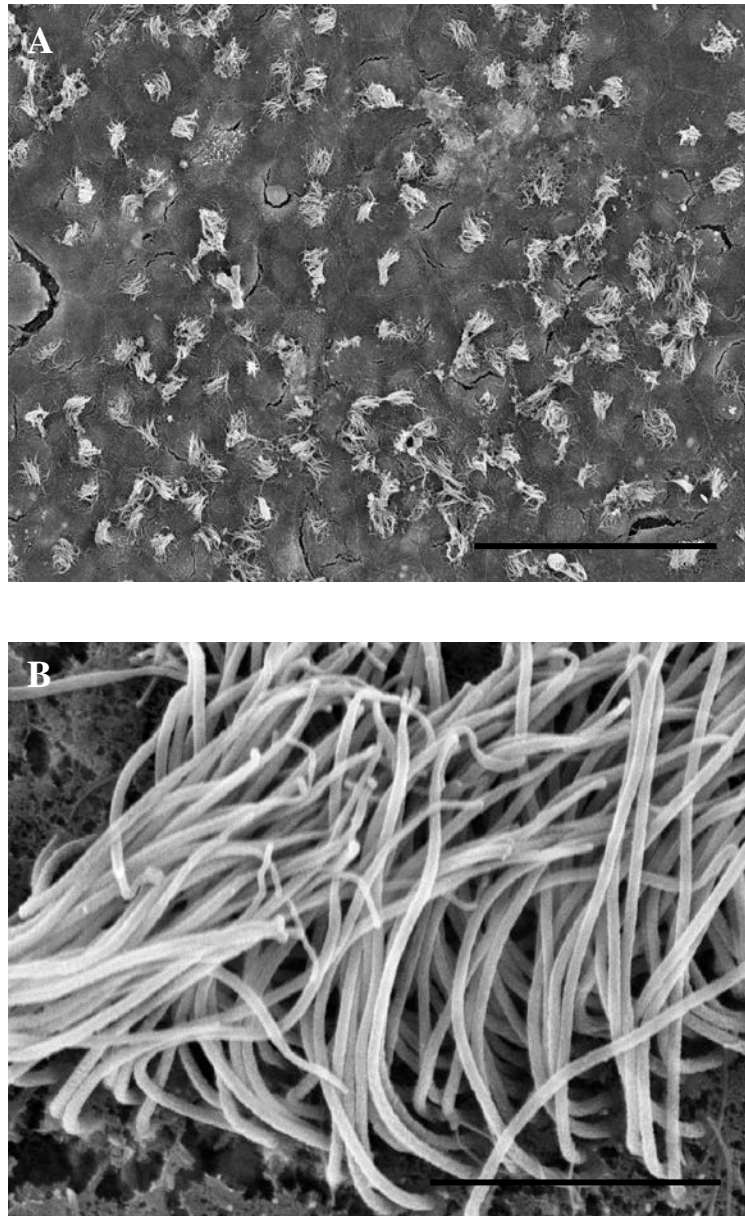


**Figure 3.1 Scanning electron microscope images.** (A) low magnification of ciliated rat ependymal cells *in vitro*. Scale bar represents 50 $\mu$ m, (B) high magnification of cilia on an ependymal cell *in vitro*. Scale bar represents 5 $\mu$ m.

**Table 3.1 Ependymal ciliary beat frequency and percentage of tissue covered with bacterial aggregates in the presence of extracellular material.**

| <i>L. monocytogenes</i><br>strain | ciliary beat frequency<br>(Hz) | % of tissue covered by bacterial<br>aggregates in the presence of<br>extracellular material |
|-----------------------------------|--------------------------------|---|
| Control                           | 41±2                           | NLA   |
| 10403S                            | 44±5                           | 11±3**  |
| C52                               | 16±2*                          | NLA   |
| EGDe                              | 46±5                           | 62±10***  |
| 10403SΔ <i>prfA</i>               | 42±3                           | NLA   |
| EGDeΔ <i>prfA</i>                 | 41±2                           | NLA   |
| 10403sΔ <i>BapL</i>               | 41±2                           | 12±3  |

Rat ciliated ependymal cells were incubated with *L. monocytogenes* strains *in vitro* for 3 hours before ciliary beat frequency was measured. Data are the mean ± standard deviation of 8 experiments. \* Significantly different (p<0.05) from the control (non-infected ependymal cells). Also, percentage of tissue covered with bacterial aggregates in the presence of extracellular material was measured. \*\* Significantly different from the C52 (p<0.05) and wild type EGDe (p<0.001) and \*\*\* indicates significant difference from 10403S and C52 (p<0.001). NLA: No listerial aggregates.

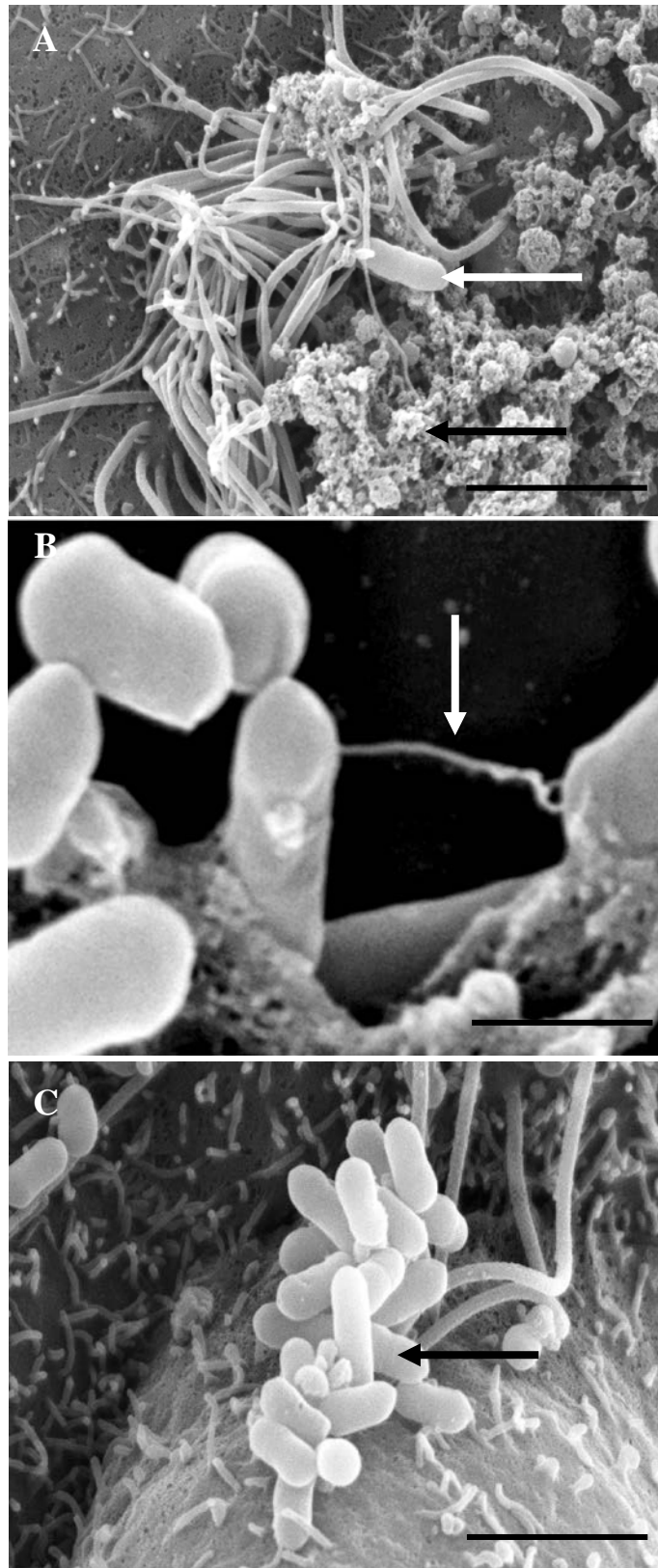


**Figure 3.2 Scanning electron microscope images.** (A) *L. monocytogenes* strain 10403S on ciliated ependymal cells. Areas with extracellular material (black arrow) and bacteria (white arrow). Scale bar represents 2 $\mu$ m, (B) A strand of extracellular material (arrow) between cells of *L. monocytogenes*. Scale bar represents 1 $\mu$ m, (C) *L. monocytogenes* strain 10403S aggregate on a ciliated ependymal cell. The arrow is pointing to an aggregate. No extracellular material is visible. The scale bar represents 2 $\mu$ m.

At three hours post-infection there was no significant difference ( $p>0.05$ ) in the ciliary beat frequency of cells incubated with 10403S or the medium alone control (Table 3.1). However, the amplitude of the beating cilia covered by bacterial aggregates was significantly reduced (36% below that of the control value,  $p<0.001$ , Table 3.2). The ciliary beat amplitude of cilia not covered by bacterial aggregates was also reduced compared to control but to a much lesser extent (88% of the control value,  $p<0.001$ , Table 3.2).

**Table 3.2 Ependymal ciliary beat amplitude inside and outside the listerial aggregates.**

| <i>L. monocytogenes</i> strain | Mean ciliary beat amplitude outside the listerial aggregates (% of control) | Mean ciliary beat amplitude inside the listerial aggregates (% of control) |
|--------------------------------|---|--|
| Control                        | 100±0   | NA   |
| 10403S                         | 88±6*   | 36±4 <sup>#</sup>  |
| C52                            | 61±4**  | NLA  |
| EGDe                           | 81±6*   | 36±3 <sup>#</sup>  |
| 10403SΔ <i>prfA</i>            | 80±6*   | NLA  |
| 10403sΔ <i>BapL</i>            | 89±4*   | 41±4 <sup>#</sup>  |
| EGDeΔ <i>prfA</i>              | 77±2*   | NLA  |
| EGDe 2 hours                   | 89±3*   | 62±6 <sup>***</sup>  |

Data are the mean ± standard deviation of 5 experiments. All the data shown are after three hours infection except the last row which is at two hours post infection. \* Significantly different from the control ( $p<0.05$ ). \*\* Significantly different from other wild-type strains and the control ( $p<0.05$ ).

<sup>#</sup> Significantly different from the ciliary beat amplitude outside the listerial aggregates. <sup>\*\*\*</sup> Significantly different from the ciliary beat amplitude inside the listerial aggregates of EGDe at three hours ( $p<0.001$ ). There were no significant differences in the ciliary beat amplitude outside the listerial aggregates between the mutants and their respective wild-type control ( $p>0.05$ ). NA: not applicable. NLA: no listerial aggregates.

To investigate if the findings with *L. monocytogenes* 10403S were strain specific, the study was repeated with two other wild-type strains of *L. monocytogenes*, C52 and EGDe. After three hours incubation with C52, in contrast to 10403S there was a significant reduction in ciliary beat frequency ( $P < 0.001$ , Table 3.1). The bacteria were seen to be attached to and moving in time with the beat of the cilia but no extracellular material or bacterial aggregates were seen. The amplitude of the cilia after incubation with C52 was significantly reduced (61%,  $P < 0.001$ , Table 3.2) compared to the control value and the other wild-type strains studied.

After three hours incubation with EGDe, there was no decrease ( $p > 0.05$ ) in ciliary beat frequency compared to the control (Table 3.1). Incubation with the EGDe strain, during the first two hours, resulted in chains of bacteria attaching to the cilia, moving at the same beat frequency as the cilia (Appendix A video S6). After three hours, large areas of bacteria were aggregated in an extracellular material (Appendix A video S7). Approximately 61% of the surface area of the ependymal cell culture was covered by listerial aggregates in association with extracellular material. This observation was significantly greater ( $p < 0.001$ ) than with 10403S. Figure 3.3A shows large areas of extracellular material and EGDe bacteria. Figure 3.3B shows a large clump of EGDe bacteria. Where aggregates were present, there was a 64% reduction in ciliary amplitude ( $P < 0.001$ , Table 3.2). Where cilia were not covered by listerial aggregates, the ciliary beat amplitude was decreased by 19% ( $P < 0.001$ , Table 3.2). The reduction in ciliary amplitude appeared to be dependent on the size of the bacterial aggregates. The ciliary amplitude at 3 hours co-culture with EGDe was markedly reduced compared to the amplitude after 2 hours (Table 3.2), at which time the bacterial aggregates were smaller. Incubation of each bacterial strain and spent supernatant (supernatant from a previous

experiment) did not result in bacterial aggregate formation, indicating that bacterial aggregates and extracellular material formed as a result of contact between the ependymal cells and the bacteria.

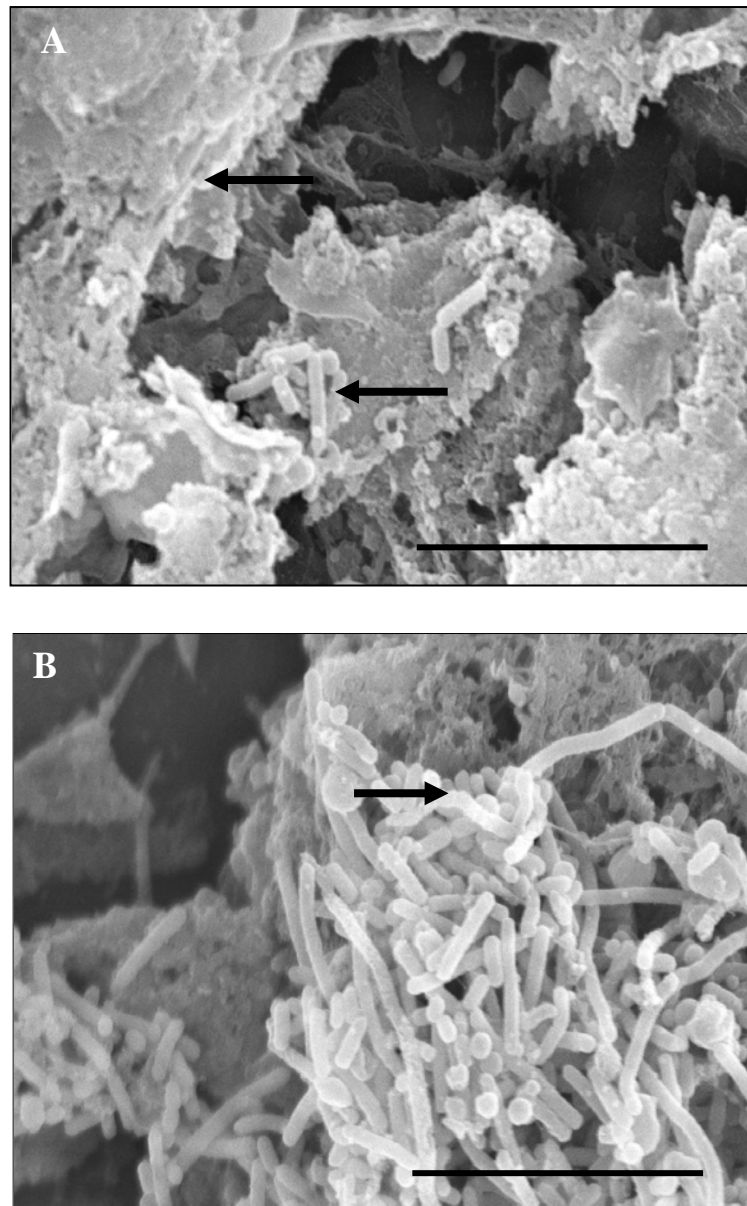


**Figure 3.4 Scanning electron microscope images.** (A) The presence of a thick layer of extracellular material on ciliated ependymal cells after incubation with *L. monocytogenes* strain EGDe. The top arrow is pointing to an area with extracellular material and the bottom arrow to an aggregate of bacteria. Scale bar represents 10 $\mu$ m, (B) *L. monocytogenes* EGDe aggregate in the presence of extracellular material. The arrow is pointing to an area of extracellular material. Scale bar represents 10 $\mu$ m.

### **3.3 Role for PrfA?**

The expression of gene products that facilitate invasion, replication and bacterial cell to cell spread is dependent upon a transcriptional activator known as PrfA (positive regulatory factor A) (§1.15.2) (Mengaud *et al.* 1991, Chakraborty *et al.* 1992, Freitag *et al.* 1992). Ciliated ependymal cells were incubated with  $\Delta prfA$  mutants of EGD<sub>e</sub> and 10403S for three hours at 37°C. The C52  $\Delta prfA$  mutant was not available. In contrast to the wild type strains, no aggregates or extracellular material were observed with the  $\Delta prfA$  mutants. As with the wild-types, the mutants had no effect on ciliary beat frequency ( $p > 0.05$ , Table 3.1). Although there was significant reduction in ciliary beat amplitude of the cells incubated with EGD $\Delta prfA$  and 10403S $\Delta prfA$  compared to the control ( $P < 0.001$ , Table 3.2), it was not significantly different ( $P > 0.05$ ) from their respective wild-type strains (Table 3.2).

### **3.4 Role for biofilm associated protein?**

Various genes have been identified that are important for listerial attachment to surfaces. The biofilm associated protein (*bap-L*) has recently been identified as being involved in the attachment of *Listeria* to cells (Jordan *et al.* 2008). Mutations in this gene have previously been shown to significantly reduce the ability of *Listeria* to adhere to polystyrene (Jordan *et al.* 2008). Ciliated ependymal cells were incubated with a 10403S mutant that lacked the biofilm associated protein ( $\Delta BapL$ ). This mutant had no effect on the ciliary beat frequency (Table 3.1) and the surface area of the ependymal cell culture was covered by listerial aggregates that were attached to the underlying cilia (Table 3.2). There was no significant difference ( $p > 0.05$ ) in the percentage of tissue covered by 10403S and  $\Delta BapL$  aggregates in the presence of extracellular material. Also, similar to the wild-type strain, the amplitude of the beating cilia covered by

bacterial aggregates was markedly reduced (41% of the control value,  $P < 0.001$ , Table 3.2) compared to the control. Furthermore, also similar to the wild-type strain, the ciliary beat amplitude of cilia not covered by bacterial aggregates was reduced (89% of the control value,  $P < 0.001$ , Table 3.2) compared to control.

**CHAPTER FOUR– RESULTS**  
**(respiratory cilia and pneumococci)**

## 4.1 Overview

*Streptococcus pneumoniae* (pneumococcus) asymptotically colonizes the human naso-pharynx but also accounts for approximately one-quarter of community acquired pneumonia in both children and adults (Fernandez-sabe 2003). It has previously been shown that pneumococci and pneumolysin, the pore forming toxin released on lysis of pneumococci, damage the lining of the airway and the mucociliary escalator of healthy epithelium (Feldman *et al.* 1992, Rayner *et al.* 1995, Kadioglu *et al.* 2002). In the United Kingdom, *S. pneumoniae* is the most common bacterial respiratory pathogen, causing community acquired pneumonia, which in patients with concurrent pneumococcal septicaemia has mortality rates of more than 20% (Balakrishnan *et al.* 2000, Lim *et al.* 2001). *S. pneumoniae* is also one of the most common bacteria isolated from the respiratory tract of patients with primary ciliary dyskinesia (PCD) (Xu *et al.* 2008). PCD is a genetic disorder and is caused by one of a number of different ciliary defects, each of which results in ineffective ciliary function (Schidlow 1994). Respiratory cilia have the most relevance in the pathophysiology of primary ciliary dyskinesia (Schidlow 1994). Motile cilia covering the epithelia of the upper and lower respiratory tract function to constantly move inhaled particles, cell debris, and microbes towards the throat (Fliegauf *et al.* 2007). Because PCD patients lack mucociliary clearance, recurrent infections of the upper and lower respiratory tract eventually cause permanent lung damage such as bronchiectasis in these patients (Meeks and Bush 2000, Geremek and Witt 2004). There has been a distinct lack of fundamental research into the pathophysiology of upper and lower airway infection in patients with PCD primarily due to poor diagnostic facilities and a paucity of respiratory tissue and consequently samples available for experimental purposes. Therefore, little is known on the

interaction of pathogens and human ciliated airway epithelial cells in PCD. In order to determine if PCD patients are more susceptible to pneumococcal damage, the interactions of pneumococci with ciliated respiratory epithelium from PCD patients and healthy individuals was investigated.

PCD is also associated with extremely low levels of nasal and exhaled nitric oxide (Lundberg *et al.* 1994, Karadag *et al.* 1999, Narang *et al.* 2002, Wodehouse *et al.* 2003, Noone *et al.* 2004). The mechanism that is responsible for the low levels of nitric oxide in PCD is not fully understood. Nitric oxide has been shown to be involved in the up-regulation of ciliary motility (Jain *et al.* 1993, Runer *et al.* 1998), it also has antimicrobial effects (Braun *et al.* 1999), including killing pneumococci (Runer *et al.* 1998). Reduced amounts of nitric oxide can complicate the interpretation of data on interaction of pneumococci with PCD patients. As a result this study also determined how exposure to pneumococci alters nitric oxide production by the respiratory epithelium of PCD patients and healthy controls.

#### ***4.2 Establishment of air-liquid interface epithelial cell cultures***

As mentioned in §2.10.5, after seeding  $\sim 10^3$  basal cells/cm<sup>2</sup> to obtain a confluent monolayer, the cells were exposed to air and only fed from the basolateral side. Mucus was produced from the apical surface within the first two weeks and the first cilia emerged from day 16 onwards. The number of differentiated ciliary cells gradually increased, and, in the majority of inserts, 30 to 50% of the surface was ciliated after 30 days of culture. Figure 4.1 summarises this process. Figure 4.2 shows scanning electron microscopy images of full length cilia and early stage ciliogenesis where cilia are not full length. After  $\sim 28$  days the formation of mature epithelium was confirmed by visual

inspection and the measurement of transepithelial electrical resistance (TEER) (Appendix A video S8). Figure 4.3 shows the experimental set up during the measurement of transepithelial electrical resistance. Cultures with a TEER measurement between ~950-1600 ohms/cm<sup>2</sup> were considered stable (when looked at under the microscope no breaks were observed in the epithelial layer) and ready for use in subsequent experiments. Table 4.1 summarises the TEER readings from 10 cultures.

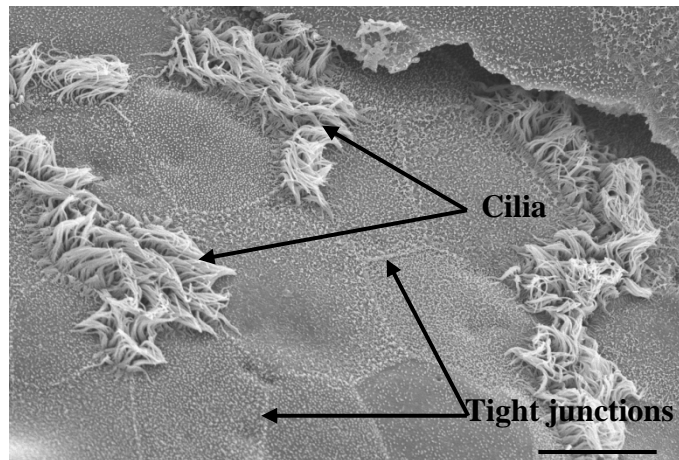
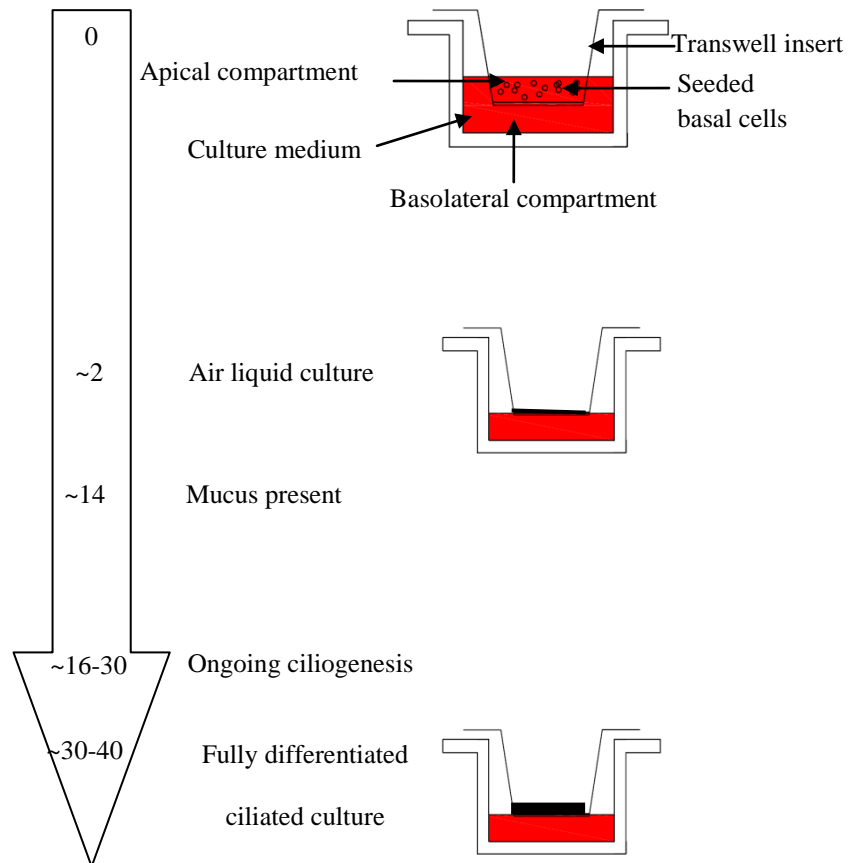


**Figure 4.1 Air-liquid interface culture of differentiated nasal epithelial cells.** Initially cultures were submerged basally and apically and by day 2 a confluent monolayer was obtained. At this point the cells were exposed to air and only fed from the basolateral side. By day 14, mucus was produced from the apical surface and the first cilia started to emerge from day 16 onwards. The cultures were used in studies after 30-40 days of culture. The numbers in the arrow above represent the number of days after seeding basal cells in the transwell insert. The SEM image was taken by Andrew Rutman, University of Leicester. Scale bar represents 20  $\mu\text{m}$ .

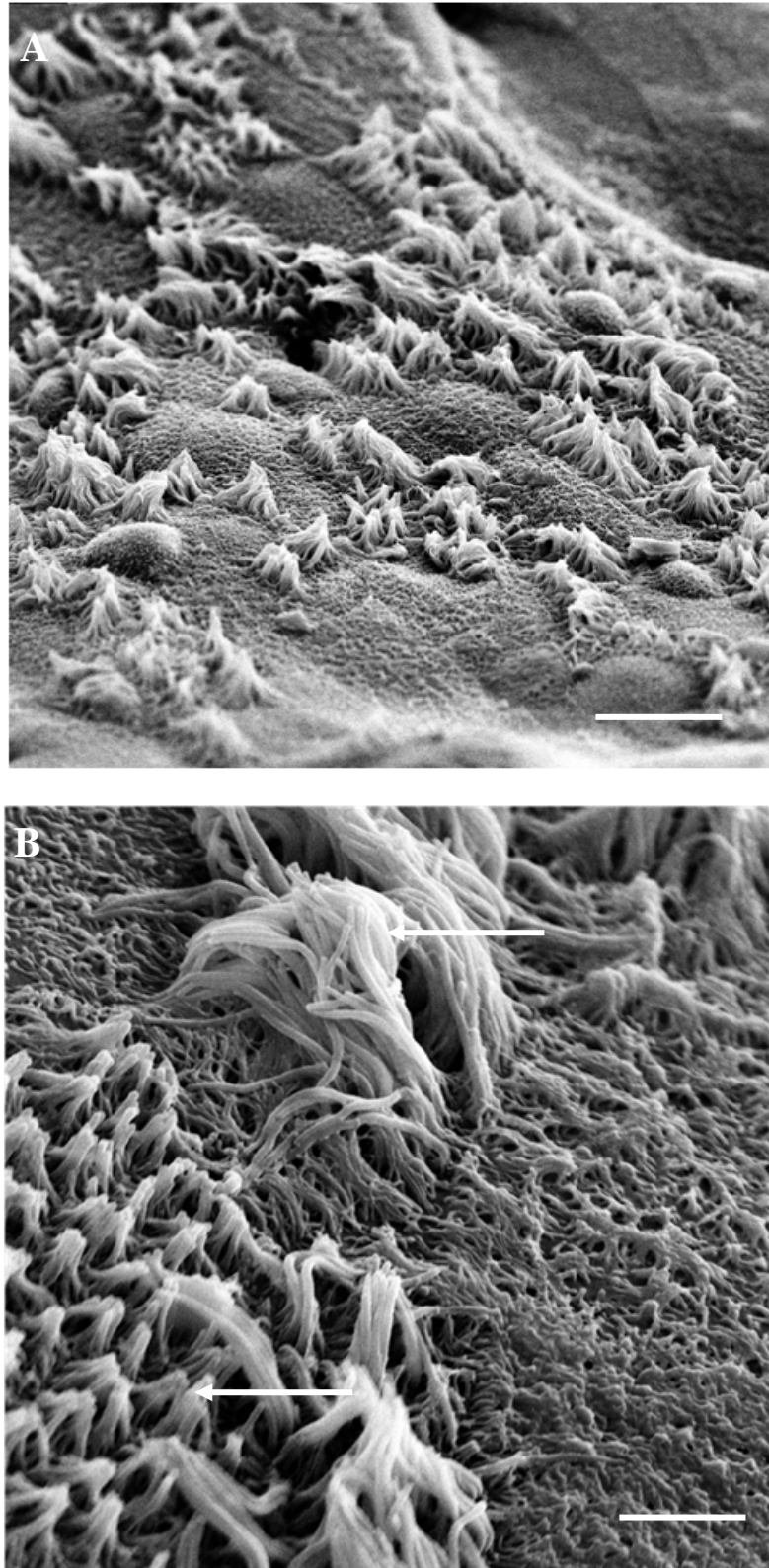


**Figure 4.2 Human respiratory cilia from air-liquid tissue culture.** A) low magnification of full length cilia (fully grown). Scale bar represents 1000  $\mu\text{m}$ . B) higher magnification, top arrow is pointing to full length cilia and the bottom arrow is pointing to cilia undergoing early ciliogenesis, where cilia are not fully grown. Scale bar represents 100  $\mu\text{m}$ . These images were taken by Andrew Rutman, University of Leicester.

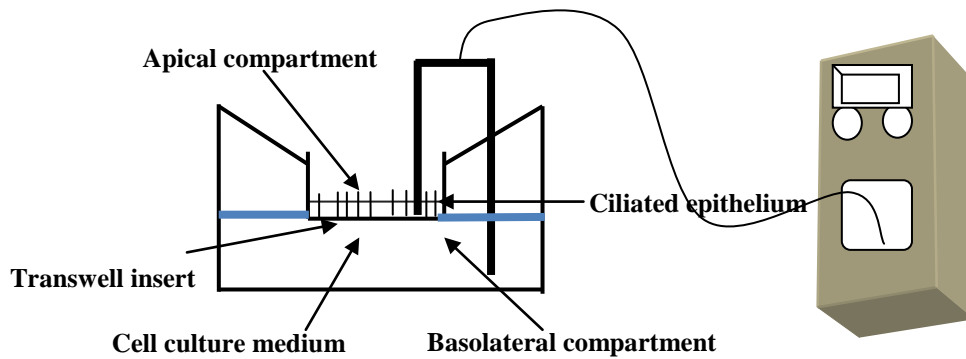


**Figure 4.3** Experimental set-up showing a transwell filter insert, covered by ciliated epithelium, during measurement of transepithelial electrical resistance using a chopstick electrode on an electrical volt Ohm meter.

**Table 4.1** Transepithelial electrical resistance (TEER) readings from 10 air-liquid interface cultures.

| Culture number | TEER $\Omega/\text{cm}^2$ (mean $\pm$ SD) |
|----------------|---|
| Culture 1      | 1069 $\pm$ 320                            |
| Culture 2      | 1437 $\pm$ 185                            |
| Culture 3      | 989 $\pm$ 102                             |
| Culture 4      | 956 $\pm$ 116                             |
| Culture 5      | 978 $\pm$ 22                              |
| Culture 6      | 1343 $\pm$ 355                            |
| Culture 7      | 1103 $\pm$ 108                            |
| Culture 8      | 1243 $\pm$ 121                            |
| Culture 9      | 968 $\pm$ 53                              |
| Culture 10     | 1614 $\pm$ 393                            |

## 4.2 Interaction of wild type *S. pneumoniae* with ciliated respiratory cells

Wild-type *S. pneumoniae* D39, at a concentration of  $10^7$  cfu were incubated with ciliated respiratory cells for 4 hours. Ciliary beat frequency (CBF) measurements were carried out at defined times, namely 0, 60, 120, 180 and 240 minutes after infection (Figure 4.4). During the four hour period, the CBF of infected cultures was between 13-16 Hz (Figure 4.4). This was not significantly different from the control cells ( $p>0.05$ ). Despite a normal CBF, after two hours the cells started to lift off from the culture insert. Figure 4.5 shows the transepithelial resistance of control and infected cultures at 0, 2 and 4 hours. The transepithelial resistance of the 4 hour infected cultures was significantly different from the control and 2 hour infected cultures ( $p<0.001$ ). These data indicate that at four hours the epithelial layer is losing its integrity. As a result, a two hour time course was chosen for the subsequent set of experiments.

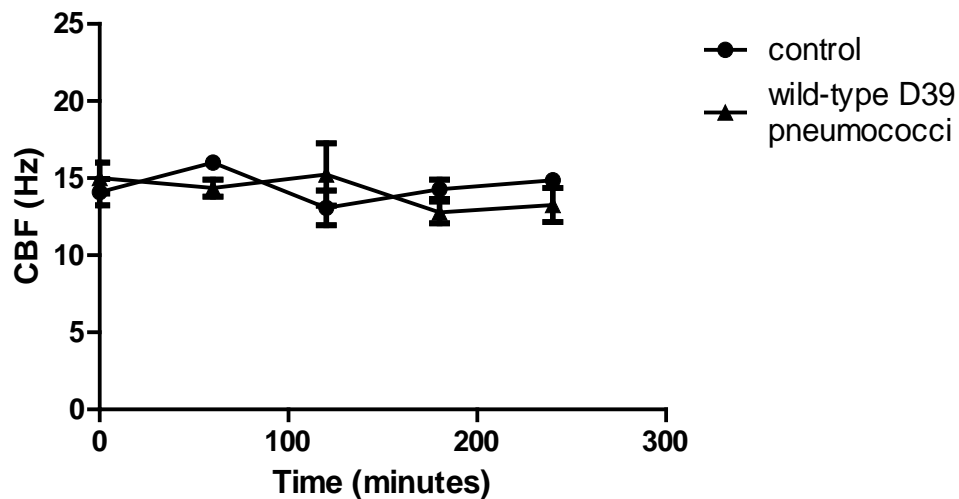


**Figure 4.4** Ciliary beat frequency measurements of respiratory ciliated cells incubated in BEBM medium alone (control) or with  $10^7$  cfu *S. pneumoniae* D39. Each point is the mean  $\pm$  standard deviation of 3 individual readings with cells from different healthy individuals.

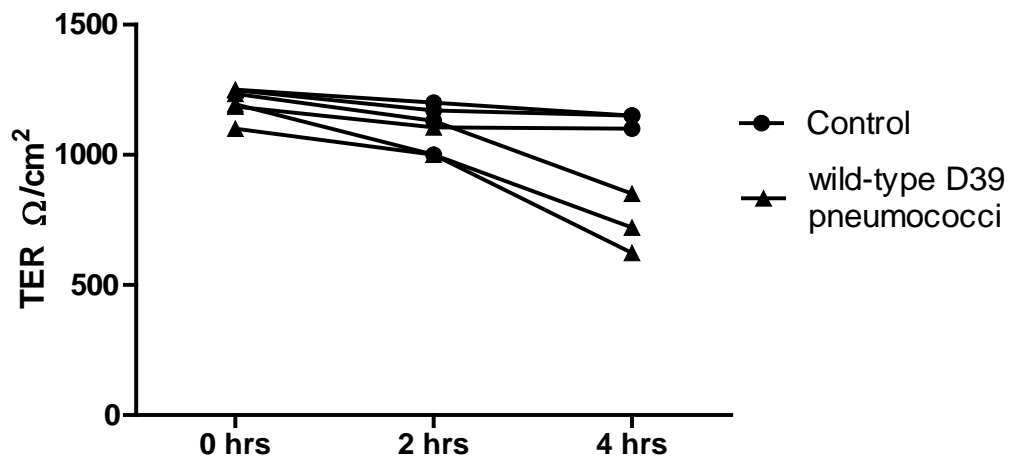


**Figure 4.5** Transepithelial electrical resistance (TEER) readings from control and *S. pneumoniae* infected air-liquid interface cultures. Respiratory ciliated cells were incubated with BEBM medium as the control or  $10^7$  cfu D39. Each line corresponds to cells from a different healthy individual. The TEER readings of the infected cells at 4 hours were significantly different from the control at 4 hours and both 2 hour values ( $P < 0.001$ ).

The first strain studied was *S. pneumoniae* D39. In the presence of respiratory cells the pneumococci attached to the cilia and by two hours about 6% of the surface area of the respiratory cell culture was covered by pneumococcal aggregates that were attached to the cilia (Table 4.2, and Appendix A video S9). At two hours post-infection there was no significant difference ( $P > 0.05$ ) in the ciliary beat frequency of cells incubated with D39 or the medium alone control (Table 4.2). However, the amplitude of the beating cilia covered by bacterial aggregates was markedly reduced (43% of the control value,  $P < 0.001$ , Table 4.3). The ciliary beat amplitude of cilia not covered by bacterial aggregates was also reduced compared to control but to a much lesser extent (89% of the control value,  $P < 0.001$ , Table 4.3).

**Table 4.2 Respiratory ciliary beat frequency and percentage of tissue covered with bacterial aggregates.**

| <i>S. pneumoniae</i> strain | ciliary beat frequency<br>(Hz) | % of tissue covered by bacterial<br>aggregates |
|-----------------------------|--------------------------------|--|
| Control                     | 15.7±1                         | NA   |
| D39                         | 14.9±1.5                       | 6±1.6*   |
| TIGR4                       | 15.6±2                         | 5.7±1*   |
| D39ΔPLY                     | 14.2±0.6                       | 5.3±2*   |
| D39 ΔNanA                   | 14.1±2                         | NPA  |

Respiratory ciliated cells were incubated with *S. pneumoniae* strains *in vitro* for 2 hours before ciliary beat frequency was measured. Also, percentage of tissue covered with bacterial aggregates was measured.

\* Significantly different ( $p < 0.05$ ) from the control (non-infected respiratory cells). NA: Not applicable.

NPA: No pneumococcal aggregates. Data are the mean  $\pm$  standard deviation of 6 experiments.

**Table 4.3 Respiratory ciliary beat amplitude inside and outside the pneumococcal aggregates.**

| <i>S. pneumoniae</i> strain | Mean ciliary beat<br>amplitude outside the<br>pneumococcal<br>aggregates<br>(% of control) | Mean ciliary beat<br>amplitude inside the<br>pneumococcal<br>aggregates |
|-----------------------------|--|---|
| Control                     | 100±0  | NA  |
| D39                         | 89±7*  | 43±8**  |
| TIGR4                       | 88±5*  | 46±5**  |
| D39ΔPLY                     | 90±2*  | 41±9**  |
| D39Δ NanA                   | 87±3   | NA  |

Data are the mean  $\pm$  standard deviation of 6 experiments. \* Significantly different from the control ( $p < 0.05$ ). \*\* Significantly different from the respective ciliary beat amplitude outside the pneumococcal aggregates ( $p < 0.001$ ). There were no significant differences in the ciliary beat amplitude outside the pneumococcal aggregates between different bacterial strains ( $p > 0.05$ ). NA: not applicable. Data are the mean  $\pm$  standard deviation of 6 experiments.

In order to view pneumococcal attachment to cilia in more detail, the cilia and bacteria were fluorescently labelled and viewed using a confocal microscope (§2.18). Figure 4.6a shows a confocal image of a pneumococcal infected ciliated culture. The bacteria appear to be attached to the tip of the cilia. Using Imaris image analysis software (§2.19) a 3D surface reconstruction of figure 4.6a shows this attachment in more detail (Figure 4.4b and c). The bacteria appear to be bound to the side of the cilia towards the tip. Figure 4.6d shows a clump of pneumococci attached towards the tip of the cilia. Interestingly, only one bacterium from the bacterial aggregate is in contact with the cilia (Figure 4.6d).

To investigate if the findings with *S. pneumoniae* D39 were strain specific and related to the pore forming toxin pneumolysin; the study was repeated with another wild-type strain of *S. pneumoniae*, TIGR4 and the pneumolysin deficient mutant D39 $\Delta$ PLY. After two hours incubation with TIGR4 and D39 $\Delta$ PLY, similar to D39 there was no reduction in ciliary beat frequency ( $P>0.05$ , Table 4.2). The bacteria were seen to be attached to and moving in time with the beat of the cilia and covering around 5% of the surface area of the respiratory cell culture. Also similar to D39, the ciliary beat amplitude of cilia not covered by bacterial aggregates was reduced compared to control and reduced even further where the beating cilia were covered by bacterial aggregates (Table 4.3). Next the role of another pneumococcal virulence factor, neuraminidase A (NanA) was investigated. Similar to D39 there was no reduction in ciliary beat frequency ( $P>0.05$ , Table 4.2). The  $\Delta$ NanA pneumococci were seen to be attached to the cilia although interestingly, no bacterial aggregates were observed. The ciliary beat amplitude was also significantly reduced compared to the control (Table 4.3).

To determine if viable bacteria were necessary for adherence to cilia and aggregate formation, pneumococci were killed using irradiation (§2.4). To insure the pneumococci were dead, they were plated onto blood agar plates and no bacteria were recovered. This study showed that the dead pneumococci were still able to adhere to the cilia, although they did not aggregate.

#### ***4.2.1 Studing the surface charge of cilia***

In this study the charge of the respiratory ciliary surface was investigated using microspheres. Positive, negative and neutral microspheres were added to the respiratory and ependymal ciliated cells. The positively charged melamine formaldehyde and negatively charged silicon oxide microspheres (microspheres-nanospheres, Cold Spring, NY, USA) both attached to the cilia (video S10 and S11 in Appendix A). The surface charge of these microspheres was measured and silica particles had a surface charge of  $-98 \pm 3$  mV, whereas melamine particles had a surface charge of  $24 \pm 1$  mV (§2.25). Interestingly, neutral latex microspheres did not bind to the cilia. A summary of all the data is given in table 4.4.

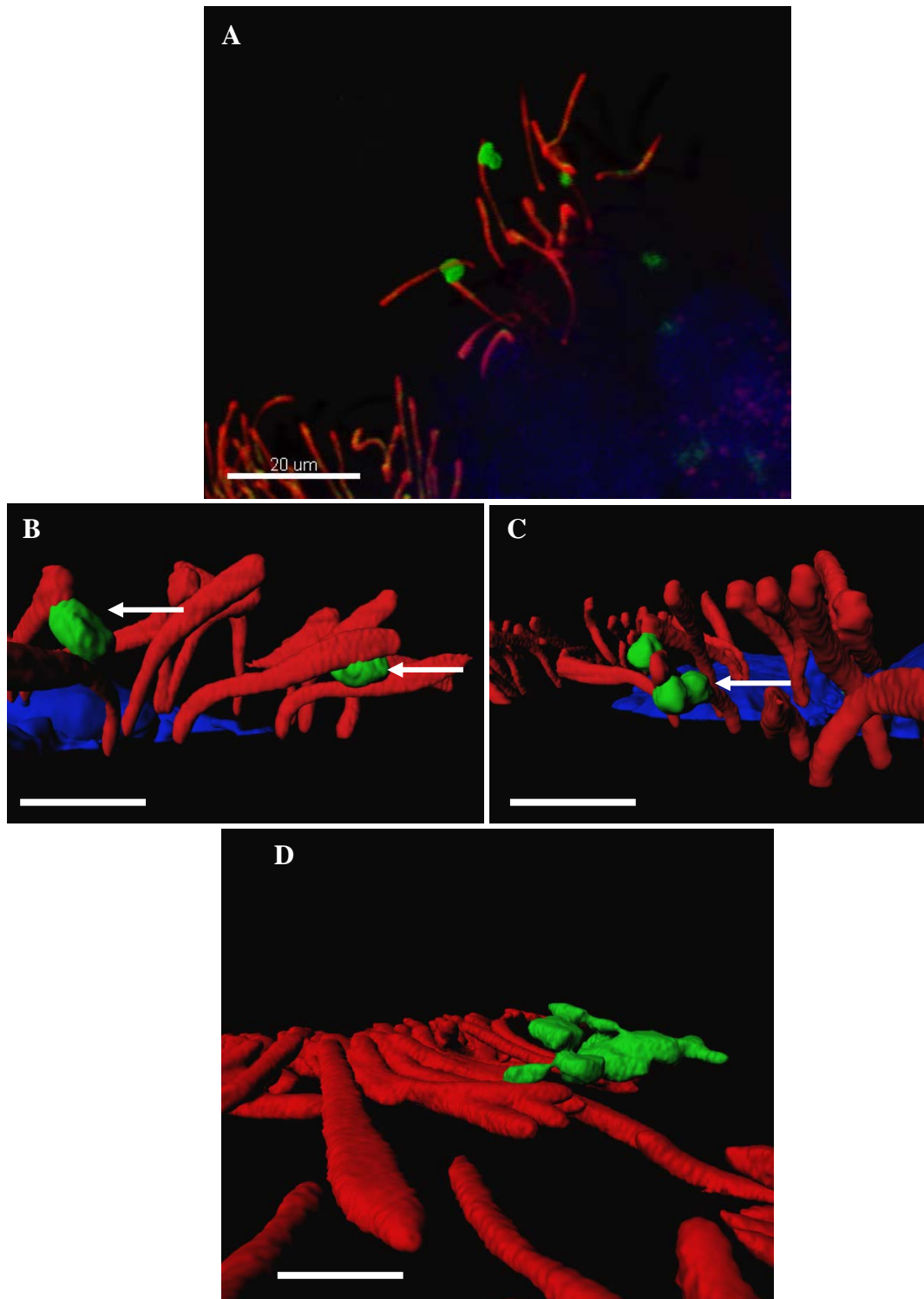


**Figure 4.6 Confocal images processed by Imaris software of pneumococci attached to respiratory cilia.** A) '3D volume render image' using the blend mode of Imaris software, showing pneumococci (in green) attached towards the tip of the cilia (in red). Bar is 20µm. B, C and D are images generated using the surpass feature of Imaris to create 3D surfaces for each fluorescence channel. B and C show the bacteria attached towards the tip and at the side of the cilia (see arrows) C) shows an aggregate of pneumococci attached to the cilia. Nuclei are in blue. Bar is 100 µm. Immunostaining was performed as described in §2.18.

**Table 4.4 Pneumococcal and abiotic particle attachment to respiratory and ependymal cilia and the formation of aggregates. N=5,**

| Bacterial strain or particle                | Attachment | Aggregate formation |
|---|------------|---------------------|
| D39   | +          | +                   |
| TIGR4                                       | +          | +                   |
| D39 $\Delta$ PLY                            | +          | +                   |
| D39 $\Delta$ NanA                           | +          | -                   |
| Dead D39                                    | +          | -                   |
| Positively charged<br>melamine microspheres | +          | -                   |
| Negatively charged<br>silica microspheres   | +          | -                   |
| Neutral latex particles                     | -          | -                   |

### ***4.3 Cytotoxicity of ciliated respiratory cells induced by pneumococci***

Cytotoxicity to ciliated respiratory cells was determined by measuring the release of lactate dehydrogenase (LDH) after exposure of the cells to *S. pneumoniae* strain D39. Ciliated cultures from both PCD and healthy individuals were grown in transwell inserts as previously described (§2.10.5). After two hours incubation with pneumococci there was a significant difference ( $p < 0.05$ ) in LDH release from infected healthy normal and PCD ciliated cells, compared to the control (uninfected cells) (Table 4.5). There was no significant difference ( $p > 0.05$ ) in LDH release from infected PCD ciliated cells and infected healthy controls (Table 4.5).

**Table 4.5 LDH release (% of fully lysed) as a measurement of cell damage.**

| <i>S. pneumoniae</i> strain | Normal  | PCD      |
|-----------------------------|---------|----------|
| Control                     | 8.1±3.4 | 4.8±3.8  |
| 10 <sup>7</sup> D39         | 11±3.8* | 6.9±3.8* |

Respiratory ciliated cells from healthy normal and PCD patients were incubated with *S. pneumoniae* D39 *in vitro* for two hours. Data are given as a percentage of the fully lysed cells (100%). \*Significantly different from the respective control (ciliated cells incubated with BEBM medium),  $P < 0.05$ . There was no significant difference ( $p > 0.05$ ) between normal and PCD patients. Data are the mean  $\pm$  standard deviation of 6 experiments.

#### ***4.4 Nitric oxide release from ciliated respiratory cells***

The nitric oxide released into the supernatant by cultured ciliated cells from PCD patients, was not significantly different ( $P > 0.05$ ) from the healthy controls (Figure 4.7). There was also no difference in nitric oxide levels in PCD patients once infected. However, there was an increase in nitric oxide levels in normal ciliated cells after incubation with 10<sup>7</sup> cfu D39 pneumococci for two hours at 37°C (Figure 4.7).

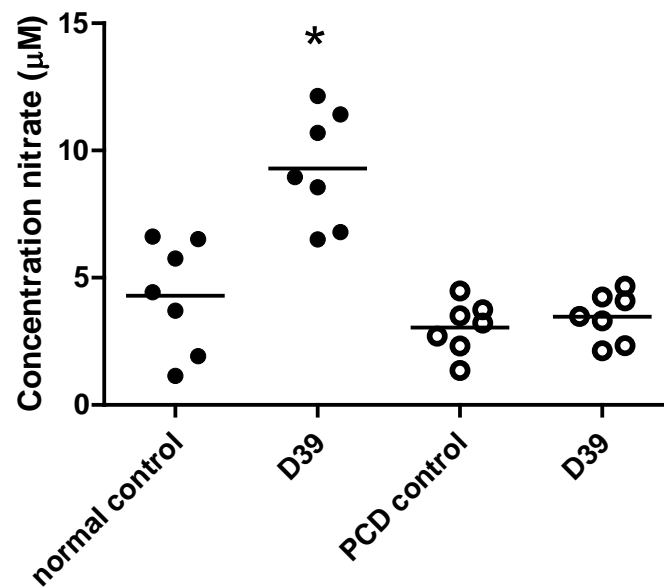


**Figure 4.7** Nitric oxide (measured as nitrate) release from ciliated cells after incubation with  $10^7$  cfu wild type pneumococcal strain D39. Each point represents cells from an individual donor. The full circles represent normal donors and hollow circles PCD patients. \* indicates significant difference from the control and PCD data ( $P < 0.001$ ). The horizontal line is the mean.

It was then of interest to investigate if the increased nitrate levels seen in Figure 4.7 affected the viability of pneumococci. Therefore, D39 pneumococci at a concentration of  $10^7$  cfu were incubated with  $10\mu\text{M}$  sodium nitrate (value from Figure 4.7) or BEBM medium (as a control) for 2 hours at  $37^\circ\text{C}$ . To determine viability, after 2 hours pneumococci were plated onto blood agar plates. This was repeated three times and no difference was observed between the bacteria recovered from incubation with sodium nitrate and the control (Table 4.6).

**Table 4.6 Colony counts of recovered pneumococci (cfu/ml) after incubation with 10 $\mu$ M sodium nitrate. The control pneumococci were incubated in BEBM medium.**

| Pneumococci incubated with<br>BEBM (covtrol) | Pneumococci incubated<br>with sodium nitrate |
|--|--|
| 1 x 10 <sup>7</sup>                          | 1 x 10 <sup>7</sup>                          |
| 1.6x 10 <sup>7</sup>                         | 3 x 10 <sup>7</sup>                          |
| 1.2 x 10 <sup>7</sup>                        | 8 x 10 <sup>6</sup>                          |

#### ***4.5 Number of recovered pneumococci following two hour exposure to PCD and healthy ciliated respiratory cells***

After infecting PCD and healthy ciliated cultures with pneumococci for 2 hours, the supernatant and the cultures were re-suspended in 200 $\mu$ l BEBM medium. Following ten-fold serial dilutions in PBS, the recovered supernatant was plated onto blood agar plates. This experiment was repeated with 4 PCD and 4 healthy ciliated cultures. Significantly more pneumococci ( $p < 0.05$ ) were recovered from the healthy ciliated cultures (Table 4.7).

**Table 4.7 Colony counts of recovered pneumococci (cfu/ml) after infection of normal and PCD ciliated epithelial cells.**

| Normal               | PCD               |
|----------------------|-------------------|
| $4.4 \times 10^{6*}$ | $1 \times 10^6$   |
| $5 \times 10^{6*}$   | $3.5 \times 10^5$ |
| $6.2 \times 10^{6*}$ | $4.4 \times 10^5$ |
| $6.5 \times 10^{6*}$ | $2 \times 10^6$   |

\*Significantly different ( $p < 0.05$ ) from the recovered pneumococci of PCD ciliated cultures.

#### ***4.6 Pneumococcal induced chemokine release from ciliated cells***

A panel of nine chemokines were chosen and measured after incubation of the cells with *S. pneumoniae* (Eotaxin, Eotaxin-3, IL-8, IP-10, MCP-1, MCP-4, MDC, MIP-1 $\beta$  and TARC). Whilst extrapolating the data, PCD patients with a static ciliary phenotype appeared to have higher values to other PCD phenotypes, thus the PCD patients were separated into two groups, static and non-static. There was a significant difference ( $p < 0.05$ ) in the resting levels of six of the chemokines studied from ciliated cells cultured from PCD patients (non-static group) compared to healthy volunteers (Eotaxin, IP-10, MCP-1, MDC, MIP-1b and TARC) (Table 4.8). Whereby, PCD ciliated cells showed higher levels of chemokine release ( $p < 0.05$ ). This is compared to a significant increase ( $p < 0.05$ ) in the resting levels of all of the chemokines studied from ciliated cells cultured from ciliary static PCD patients compared to healthy volunteers and the non-static PCD group (Table 4.8).

All chemokines released by PCD static ciliated cells following two hour incubation with  $10^7$  cfu *S. pneumoniae* were significantly higher ( $p < 0.05$ ) compared to healthy ciliated

cells following the same stimulation with *S. pneumoniae*. Except for IL-8 and Eotaxin-3, the non-static PCD ciliated cells following stimulation with pneumococci had similar increased levels of chemokines compared to the healthy volunteers. Interestingly, the cells from the static PCD group after incubation with pneumococci showed higher ( $p<0.05$ ) levels in 5 chemokines (Eotaxin, Eotaxin-3, IL-8, MDC and TARC) compared to the cells from non static PCD patients.

In healthy volunteers following infection of the ciliated cells with pneumococci a slight increase in several chemokines (IP-10, MDC, MIP-1 $\beta$  and TARC) was observed compared to the uninfected control. Also, exposure of PCD ciliated cells (non static group) to pneumococci resulted in increased eotaxin compared to the uninfected control. Furthermore, exposure of PCD static ciliated cells to pneumococci resulted in increased levels of Eotaxin, IL-8 and MDC compared to the uninfected control. Graphs from each chemokine assayed in this study, is given in appendix B, where PCD data are divided according to their phenotype (static and non-static).

Table 4.8 Chemokine release by ciliated respiratory cells from healthy controls and PCD patients in response to *S. pneumoniae*.

| Chemokine<br>pg/ml | Healthy controls |                         | PCD patients        |                         |                            |                             |
|--------------------|------------------|-------------------------|---------------------|-------------------------|----------------------------|-----------------------------|
|                    | control          | 10 <sup>7</sup> cfu D39 | Non statics cilia   |                         | Static cilia               |                             |
|                    |                  |                         | Control             | 10 <sup>7</sup> cfu D39 | Control                    | 10 <sup>7</sup> cfu D39     |
| <b>Eotaxin</b>     | 26(0-107)        | 123(90-135)             | <b>170(76-352)</b>  | <b>265(122-520)*</b>    | <b>519(378-674)#</b>       | <b>742(475-820)*#</b>       |
| <b>Eotaxin-3</b>   | 3269(1234-3878)  | 2240(1699-3058)         | 3162(2054-4923)     | 4515(2342-11800)        | <b>12523(9870-19020)#</b>  | <b>13511(9628-16282)#</b>   |
| <b>IL-8</b>        | 2795(1140-5725)  | 3082(1894-4660)         | 2501(1100-4933)     | 3810(1564-19860)        | <b>20735(15500-25742)#</b> | <b>26516(20452-32633)*#</b> |
| <b>IP-10</b>       | 189(112-213)     | 270(209-322)*           | <b>345(231-617)</b> | <b>438(295-894)</b>     | <b>779(550-1199)#</b>      | <b>1024(649-1443)</b>       |
| <b>MCP-1</b>       | 12(10-18)        | 21(18-39)               | <b>90(30-98)</b>    | <b>71(38-124)</b>       | <b>111(100-193)#</b>       | <b>129(101-235)</b>         |
| <b>MCP-4</b>       | 190(163-295)     | 236(160-292)            | 270(205-319)        | <b>271(219-649)</b>     | <b>661(450-698)#</b>       | <b>713(598-805)</b>         |
| <b>MDC</b>         | 200(187-226)     | 296(244-344)*           | <b>458(314-699)</b> | <b>491(374-946)</b>     | <b>971(800-1476)#</b>      | <b>1356(1101-1907)*#</b>    |
| <b>MIP-1β</b>      | 0                | 5(3-6) *                | <b>11(4-14)</b>     | <b>15(6-40)</b>         | <b>33(25-76)#</b>          | <b>67(34-80)</b>            |
| <b>TARC</b>        | 69(21-84)        | 84(68-121) *            | <b>108(102-236)</b> | <b>187(97-472)</b>      | <b>531(250-631)#</b>       | <b>605(526-964)#</b>        |

Data are median± inter quartile range of 10 PCD (5 statics and 5 non statics) and 10 healthy normal donors. \*significantly different (p<0.05) from respective control. # significantly different from same data in the non statics. Significant differences (P<0.05) from same data in the healthy control ciliated cells, are highlighted in bold.

#### ***4.7 Pneumococcal induced cytokine release from ciliated cells***

The data for cytokine release in response to *S. pneumoniae* are given in Table 4.9. In total 10 different cytokines were measured; INF $\gamma$ , IL-10, IL-4, IL-13, IL-5, IL-1 $\beta$ , IL-2, TNF $\alpha$ , IL12p70 and IL-6. Similar to the chemokine data PCD patients with a static ciliary phenotype seemed to have higher cytokine readings, thus they were separated into two groups (static and non-static).

There was a significant difference ( $p < 0.05$ ) in the resting level of IL-6 from ciliated cells cultured from PCD patients (non-static group) compared to healthy volunteers (Table 4.9). Whereby, PCD cells released higher levels of IL-6 ( $p < 0.05$ ). This is compared to significantly higher values ( $p < 0.05$ ) in the resting levels of INF $\gamma$ , IL-10, IL-13, IL-5, TNF $\alpha$ , IL12p70 and IL-6 from ciliated cells cultured from ciliary static PCD patients compared to healthy volunteers and the non-static PCD group (Table 4.9).

Except for IL-4 and IL-12 all cytokines released by PCD static ciliated cells following two hour incubation with *S. pneumoniae* were significantly higher ( $p < 0.05$ ) compared to healthy ciliated cells following the same stimulation with *S. pneumoniae*. In non-static PCD ciliated cells following stimulation with pneumococci only IL-6 and IL-10 had increased levels of chemokines compared to the healthy volunteers. Interestingly, the cells from the static PCD group after incubation with pneumococci showed higher levels in 4 cytokines (IL-6, INF $\gamma$ , IL-5 and IL-13) compared to the cells from non static PCD patients.

In healthy volunteers following infection of the ciliated cells with pneumococci no increase in cytokine levels was observed compared to the uninfected control. However, exposure of PCD ciliated cells (non static group) to  $10^7$  cfu pneumococci resulted in

increased IL-6 and IL-10 compared to the uninfected control. Furthermore, exposure of PCD static ciliated cells to  $10^7$  cfu pneumococci resulted in increased levels of IL-6, IL-10 and IL-1 $\beta$  compared to the uninfected control. Graphs from each cytokine assayed in this study, is given in appendix B, where PCD data are divided according to their phenotype (static and non-static).

**Table 4.9** Cytokine release by ciliated respiratory cells from healthy controls and PCD patients in response to *Streptococcus pneumoniae*.

| Cytokine<br>pg/ml             | Healthy controls |                         | PCD patients        |  |                          |   |
|-------------------------------|------------------|-------------------------|---------------------|--|--------------------------|---|
|                               | control          | 10 <sup>7</sup> cfu D39 | Control             | Non statics cilia<br>10 <sup>7</sup> cfu D39 | Control                  | Static cilia<br>10 <sup>7</sup> cfu D39 |
| <b>IL-6</b>                   | 187(137-258)     | 186(60-358)             | <b>695(381-937)</b> | <b>2539(1209-3526)*</b>                      | <b>5000(4000-6303) #</b> | <b>15481(10000-20209)* #</b>            |
| <b>IL-10</b>                  | 36(27-57)        | 35(27-53)               | 43(35-58)           | <b>90(72-119)*</b>                           | <b>87(38-111) #</b>      | <b>120(92-146)*</b>                     |
| <b>INF<math>\gamma</math></b> | 69(52-85)        | 69(41-102)              | 57(39-76)           | 78(4-102)                                    | <b>109(78-165) #</b>     | <b>109(78-128) #</b>                    |
| <b>IL-1<math>\beta</math></b> | 16(10-20)        | 18(11-26)               | 6(6-13)             | 13(9-26)                                     | <b>21(18-30) #</b>       | <b>27(24-38)*</b>                       |
| <b>IL-4</b>                   | 6(3-10)          | 6(3-8)                  | 4(3-5)              | 6(3-6)                                       | 6(3-18)                  | 7(4-27)                                 |
| <b>IL-5</b>                   | 13(10-15)        | 9(8-13)                 | 13(9-16)            | 12(10-21)                                    | <b>21(16-29) #</b>       | <b>25(20-40) #</b>                      |
| <b>IL-2</b>                   | 20(14-26)        | 18(13-36)               | 22(16-33)           | 38(20-51)                                    | 43(21-54)                | <b>45(40-70)</b>                        |
| <b>IL-13</b>                  | 48(39-68)        | 61(50-69)               | 54(43-91)           | 51(43-91)                                    | <b>100(86-137) #</b>     | <b>110(90-153) #</b>                    |
| <b>IL-12p70</b>               | 14(0-21)         | 18(10-31)               | 17(12-23)           | 18(10-31)                                    | <b>40(28-48) #</b>       | 29(16-40)                               |
| <b>TNF<math>\alpha</math></b> | 91(71-94)        | 83(55-94)               | 82(56-125)          | 77(34-127)                                   | <b>151(125-196) #</b>    | <b>145(123-200)</b>                     |

Data are median (inter quartile range) of 10 PCD (5 statics and 5 non statics) and 10 healthy normal donors. \*significantly different (p<0.05) from respective control.

# significantly different from same data in the non statics. Significant differences (P<0.05) from same data in the healthy control ciliated cells, are highlighted in bold.

**CHAPTER FIVE – RESULTS  
(Respiratory basal cells and  
pneumococci)**

## **5.1 Overview**

In order to achieve successful infection bacteria must overcome multiple obstacles. In the majority of cases, this requires bypassing the first line of host defence, the barrier provided by epithelial surfaces. During the course of a respiratory infection the ciliated epithelium is damaged, cilia striped away and the basal cells become exposed. PCD is commonly associated with recurrent airway infections that are thought to be caused, at least in part, by impaired mucociliary clearance. Infections of the airway commonly cause destruction of the columnar epithelial cells, thus exposing the sensitive underlying basal cells of the airway to bacterial toxins and host inflammatory mediators. Nasal epithelial basal cells are the main airway epithelial progenitor cell from which ciliated columnar epithelial cells, goblet cells and clara cells derive, however, little is known on the interaction of *S. pneumoniae* and human basal airway epithelial cells in PCD. The basal cells are known to react to infectious stimuli by releasing inflammatory mediators but these responses are uncharacterised in PCD or during pneumococcal infection.

In order to determine if the respiratory epithelial cells of PCD patients were more susceptible to pneumococcal damage the interactions of pneumococci with basal respiratory cells from PCD patients and normal individuals were investigated.

## 5.2 Basal cell culture

Initially, from the basal cell suspension mentioned in §2.10.4, cells were divided between the wells of a 12-well plate coated with collagen (see §2.10.3). Between 60-80  $\mu\text{l}$  of basal cell suspension (contained  $\sim 4 \times 10^4$  cells) was added to each well containing 1ml of BEGM. The cells were fed with fresh BEGM medium every other day and by day 13-15 the cells were fully confluent. Only when the cells in the well had reached confluency ( $\sim 10^6$  cells), were they used in experiments. Table 4.1 follows the progression in cell confluency in 10 patients over 15 days.

| Patients | Day 3 | Day 5 | Day 7 | Day 9 | Day 11 | Day 13 | Day 15 |
|----------|-------|-------|-------|-------|--------|--------|--------|
| 1        | 15%   | 60%   | 80%   | 90%   | 100%   |        |        |
| 2        | 15%   | 50%   | 85%   | 90%   | 98%    | 100%   |        |
| 3        | 5%    | 5%    | 8%    | 10%   | 40%    | 85%    | 100%   |
| 4        | 8%    | 5%    | 15%   | 30%   | 90%    | 75%    | 100%   |
| 5        | 8%    | 9%    | 10%   | 40%   | 55%    | 70%    | 100%   |
| 6        | 5%    | 7%    | 15%   | 60%   | 70%    | 70%    | 100%   |
| 7        | 3%    | 6%    | 9%    | 45%   | 50%    | 60%    | 100%   |
| 8        | 5%    | 10%   | 25%   | 65%   | 80%    | 90%    | 100%   |
| 9        | 6%    | 8%    | 15%   | 50%   | 80%    | 90%    | 100%   |
| 10       | 5%    | 20%   | 45%   | 60%   | 90%    | 100%   |        |

**Table 5.1 Progress in basal cell confluency in wells of a 12-well plate over 15 days.** Basal cells were seeded at day 1 and every other day by visual inspection, an estimated percentage of cell confluency was recorded. By day 15 the majority of cells were 100% confluent. This data was recorded in 10 patients.

After the initial experiments, the majority of the experiments were carried out in Nunc 8-well tissue culture chambers. Each chamber slide was coated with collagen (see §2.10.2). Around 40-60  $\mu\text{l}$  of basal cell suspension (contained  $\sim 10^4$  cells) from a confluent T80 flask (see § 2.10.4) was added to each chamber that contained 400  $\mu\text{l}$  of

BEGM. By day 3 the majority of the wells were confluent ( $\sim 2 \times 10^4$  cells) and if not they were fed with fresh BEGM medium. In contrast to the first method, using this method it was possible to get up to 20 confluent wells per patient. Table 4.2 follows the progression in cell confluency in 10 patients for up to 5 days. To ensure that before the start of any experiment the basal cells were viable, trypan blue was added to the confluent basal cells from 10 patients. Greater than 95% viability was found in every case.

### ***5.3 Characterisation of basal cells***

Immunohistochemical staining of the basal cells and immunofluorescence was used to characterise basal cells. Single-cell basal layers were stained with the anti-cytokeratin peptide 14 monoclonal antibody, ck-14. Immunohistochemical staining for cytokeratin has been routinely used to identify basal cells (Zabner *et al.* 1996, Nakajima *et al.* 1998, Jakiela *et al.* 2008). The ck-14 antibody reacts specifically with the basal layer of the laryngeal epithelium (Zabner *et al.* 1996). Figure 4.1A shows Ck-14 positive cells (red). To ensure there was no non-specific binding the secondary antibody was incubated on the cells in the absence of the primary antibody (Figure 4.1B).

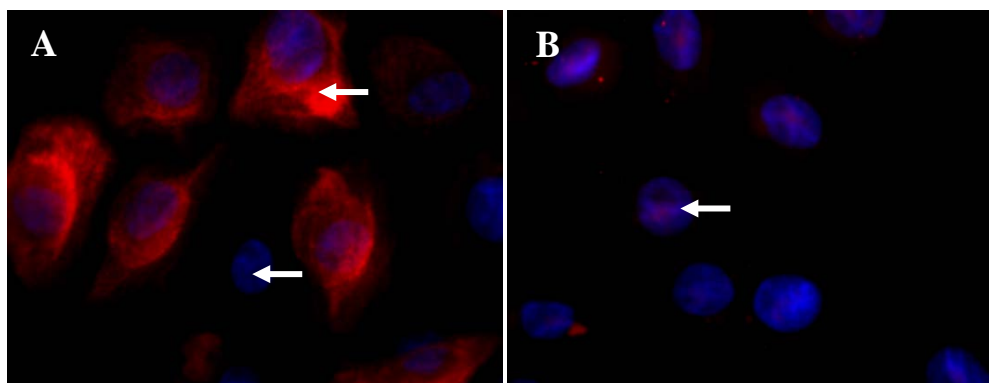


**Figure 5.1** immunofluorescent images showing the expression of ck-14 in basal respiratory epithelial cells; A) basal cells stained with anti-CK-14 antibody (anti-mouse-IgM, red), the top arrow is pointing to a CK14<sup>+</sup> cell and the bottom arrow to a CK14<sup>-</sup> cell. B) Basal cells only stained with the secondary antibody. The nuclei are stained with Hoechst (Blue). Original magnification x600.

#### ***5.4 Cytotoxicity of basal cells induced by pneumococci***

Cytotoxicity was determined by measuring the release of lactate dehydrogenase (LDH) after exposure to *S. pneumoniae* strain D39 and  $\Delta$ PLY. Respiratory basal cells were grown in glass chamber slides as previously described (§2.10.4). After four hours incubation there was no significant difference ( $p > 0.05$ ) in LDH release from uninfected basal cells and cells of both normal and PCD patients incubated with  $10^6$  cfu/ml D39 bacteria. However, LDH release after infection with  $10^8$  and  $10^7$  cfu/ml wild-type D39 was significantly different from the control and from each other ( $p < 0.001$ , Table 4.3). Interestingly, there was no significant difference in LDH release from normal and PCD basal cells either before or after exposure to pneumococci ( $p > 0.05$ ). Basal cells that were infected with the pneumolysin deficient mutant  $\Delta$ PLY at the same concentrations as the wild-type had significantly less ( $p < 0.001$ , Table 4.3) LDH release than cells incubated with the wild type D39 bacteria.

**Table 5.3.** LDH release (% of fully lysed) as a measurement of cell damage.

| <i>S. pneumoniae</i> strain | Normal     | PCD       |
|-----------------------------|------------|-----------|
| Control                     | 4.4±3.4    | 4.1±2.7   |
| 10 <sup>8</sup> D39         | 32.8±4.7 * | 38.8±5.5* |
| 10 <sup>8</sup> ΔPLY        | 2.4±1.1    | 2.2±0.8   |
| 10 <sup>7</sup> D39         | 13.7±5.5** | 14±6.5**  |
| 10 <sup>7</sup> ΔPLY        | 1.1±1.6    | 2.0±3.1   |
| 10 <sup>6</sup> D39         | 5±2.1      | 6±2.8     |
| 10 <sup>6</sup> ΔPLY        | 4±2.4      | 2.5±1     |

Respiratory basal cells from PCD and normal patients were incubated with *S. pneumoniae* D39, a pneumolysin negative mutant, ΔPLY, *in vitro* for four hours. Data are given as a percentage of the fully lysed cells (100%). \*Significantly different from the control (Basal cells incubated with BEBM medium),  $p < 0.001$ . \*\* Significantly different from the control and cells infected with 10<sup>8</sup> D39 cfu/ml,  $p < 0.001$ . Data are the mean ± standard deviation of 6 experiments.

### ***5.5 Pneumococcal adhesion and invasion of respiratory basal cells***

As mentioned in § 2.23 and § 2.24, after infecting the basal cells with 10<sup>7</sup> cfu D39 for 4 hours, the medium and the chamber was removed from the glass slide. The glass slide was inverted vertically in successive 60ml polypropylene containers (sterilised by irradiation, Fisher, FB51806) of PBS to remove the loosely adhered bacteria. The number of recovered bacteria from each wash is given in Figure 4.2. By the 5<sup>th</sup> wash no bacteria were recovered from the PBS. The remaining bacteria were assumed to be adhered and the basal cells were removed using 0.1% w/v trypsin, resuspended in BEBM and plated on blood agar plates. 0.1% trypsin was shown not to kill pneumococci. The number of bacteria adhered in a well to both PCD and normal basal

cells are given in Figure 4.3. There was no significant difference ( $p>0.05$ ) in the number of adhered bacteria in PCD and normal basal cells. Viable intracellular bacteria were quantified by plating lysed cells for colony counting after treatment with  $50\mu\text{g/ml}$  gentamicin for two hours to remove extracellular pneumococci (Cundell *et al.* 1995). This experiment was repeated with basal cells from 10 PCD patients and 10 normals and no bacteria were recovered. To ensure the gentamicin killed the pneumococci,  $10^7$  cfu D39 pneumococci were incubated with  $50\mu\text{g/ml}$  gentamicin for 2 hours and then plated on blood agar plates. This was repeated 3 times and no bacteria were recovered.

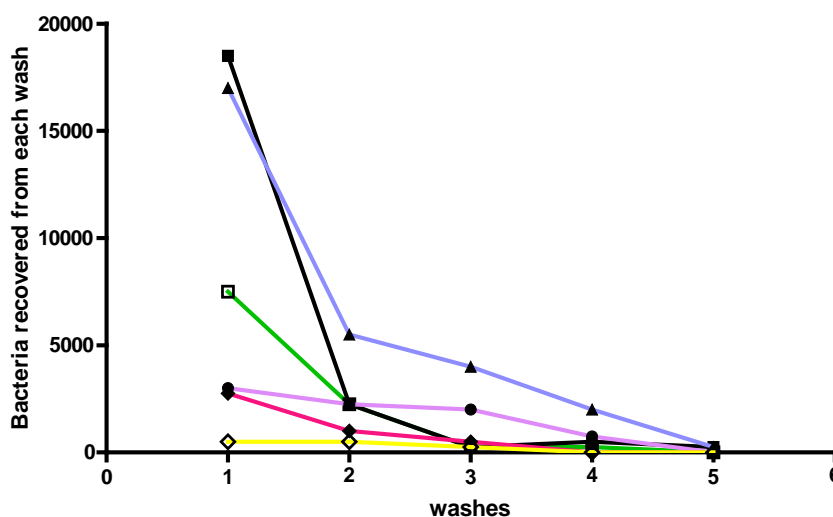


**Figure 4.2** Graph showing the number of bacteria recovered from each wash of glass chamber slide. This experiment was repeated six times with different basal cells (indicated by the different colours). By the 5<sup>th</sup> wash no bacteria were detected in the wash solution.

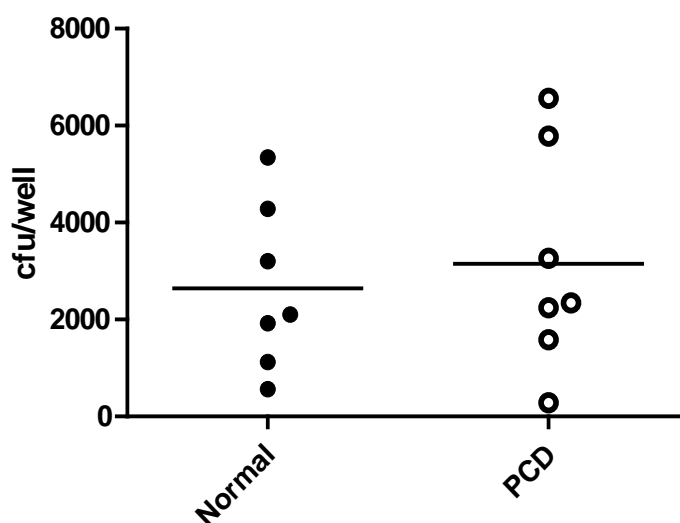


**Figure 4.3** Graph showing the number of bacteria adhered to basal cells from normal and PCD individuals. Each point represents a separate individual and the horizontal line is the mean.

A second method, using confocal microscopy and Imaris image analyses, was also used to study adhesion and invasion of pneumococci to basal cells (§2.19). Briefly, bacteria, nuclei and the cytoplasm were stained before infecting the cells with the bacteria (§2.17 and 18). The CFSE stain did not affect the viability of the pneumococci after 4 hours, as assayed by colony counting. After 4 hours the cells were washed with PBS, fixed with 4% w/v paraformaldehyde and viewed using a Leica SP5 laser scanning confocal microscope. Random areas from each well (n=5) were imaged by obtaining 4  $\mu\text{m}$  z sections. Figure 4.4a is a confocal image of infected basal cells, created using the 3D volume render and blend mode function of Imaris. In figure 4.4b the blue and red channels were rebuilt using the 3D surface option of Imaris and the spot object feature was used for the green channel. As seen in Figure 4.4c, by making the red channel 20% transparent (cytoplasm) it was possible to visualise the internal number of spots (bacteria). Thus the number of adhered and internal bacteria was quantified. The data

from the five random areas were combined together to calculate the number of adhered and internal bacteria per cell.

Figure 4.5 shows a graph with adhered and internal bacteria per cell for PCD patients and normals. Similar to the results using colony counts, there was no significant difference in the bacteria adhered to basal cells from normal and PCD individuals. Interestingly, in contrast to the first method, internal pneumococci were detected in this method. Furthermore, the number of internal pneumococci were significantly more ( $p < 0.01$ ) in healthy individuals basal epithelium.

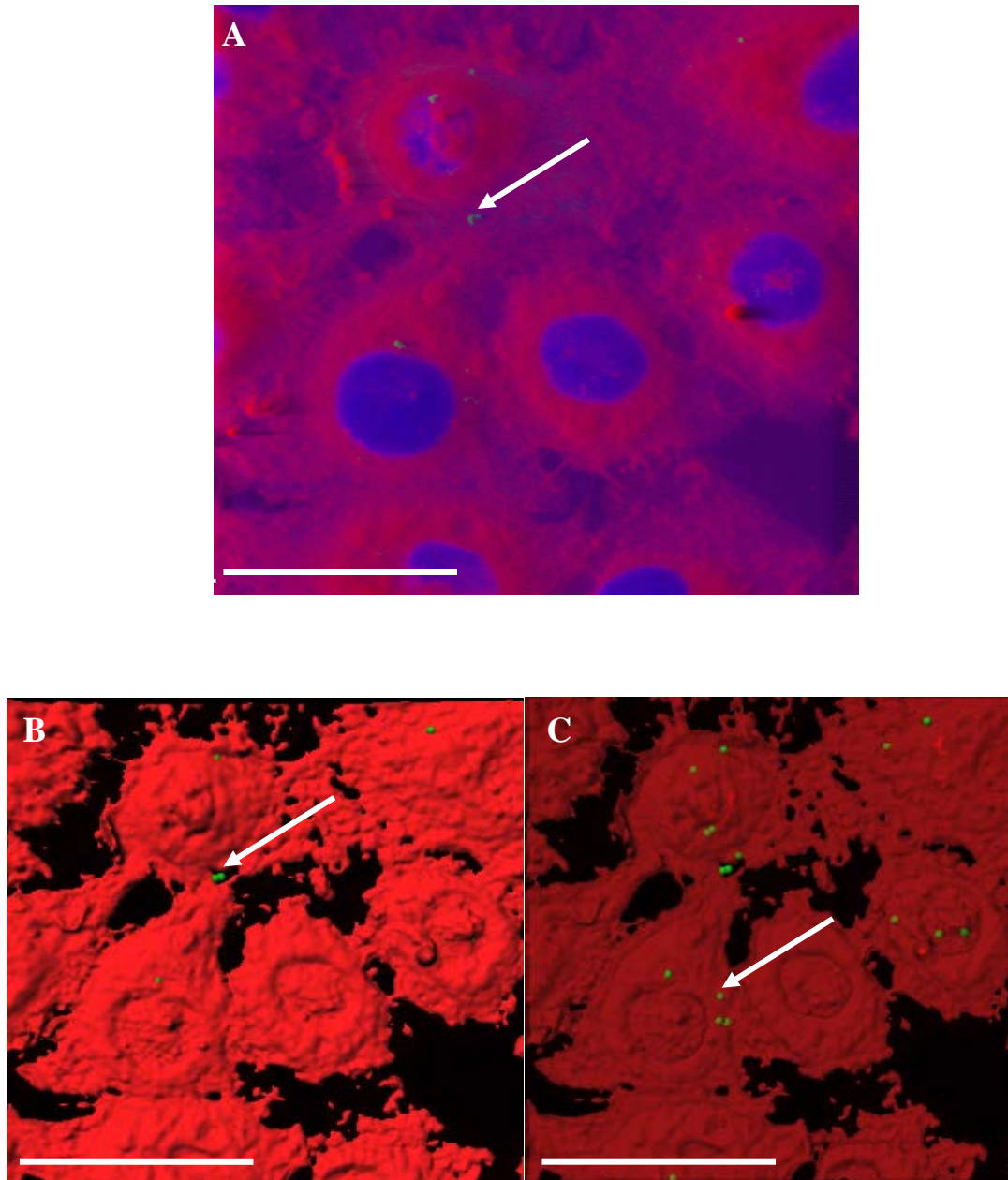
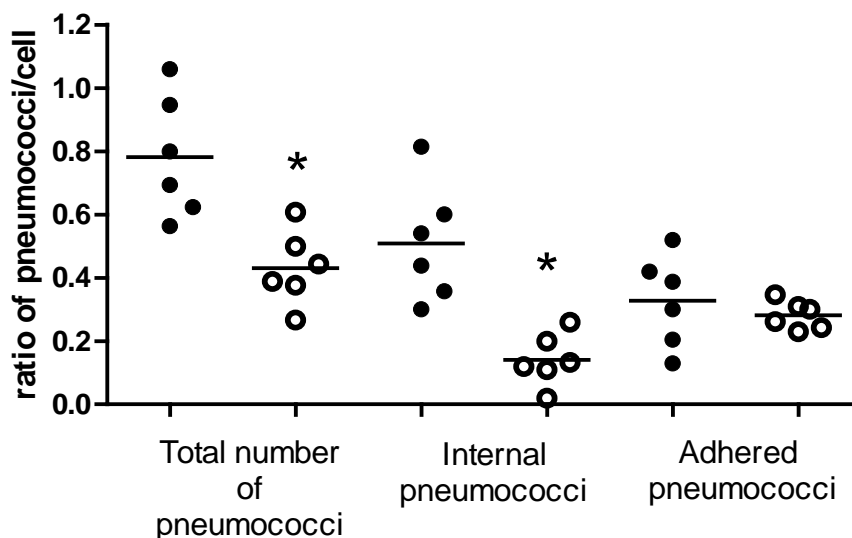


Figure 4.4 Confocal images of infected basal cells A) Imaris blend image showing the pneumococci in green, nuclei blue and the cytoplasm red. B) Analysis of image A using 3D and 'spot object' features in Imaris software. Each bacterium is shown as a 1  $\mu\text{m}$  spot in green. C) Using the transparent feature in Imaris software the cytoplasm in image B has been made transparent to observe the internal bacteria. The arrows are pointing to bacteria (spots). Scale bar represents 20  $\mu\text{m}$ . Immunostaining was performed as mentioned in §2.18.



**Figure 4.5** shows the ratio of pneumococci per cell counted from the confocal images. The full circles are normal patients and hollow circles are PCD patients. There was no significant difference in the number of adhered bacteria with normal and PCD basal cells. Normal patients had more internal bacteria compared to the healthy basal cells.\* significantly different from respective normal ( $p < 0.05$ ).

### 5.6 Nitric oxide release from basal cells

Respiratory basal cells were infected with *S. pneumoniae* as described in §2.11. Nitric oxide production was measured using a chemiluminescence analyser as described in §2.20. Briefly, solution nitrate ( $\text{NO}_3^-$ ) was reduced to nitric oxide with vanadium (III), and the nitric oxide was then detected by gas-phase chemiluminescence after reaction with ozone.

#### Standard curve

Using the height of the peak after injecting 100 $\mu\text{l}$  of different standard solutions of sodium nitrate a standard curve was produced (Figure 4.6). Unknown nitric oxide concentrations (nM x-axis) were interpolated from their peak heights (mm y-axis).

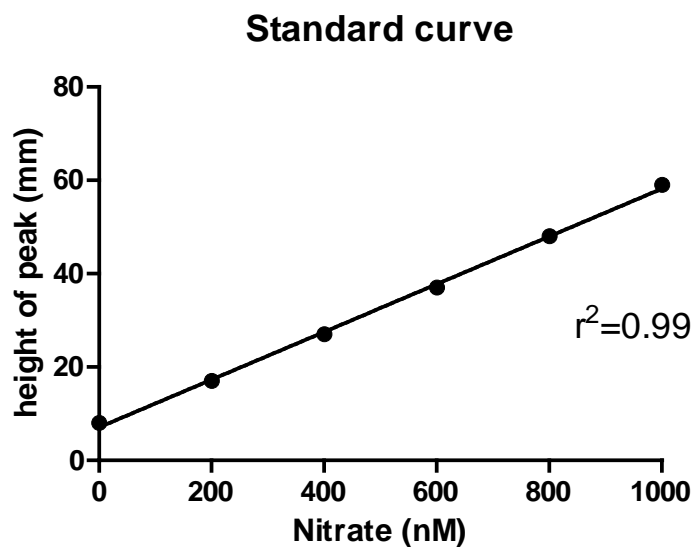
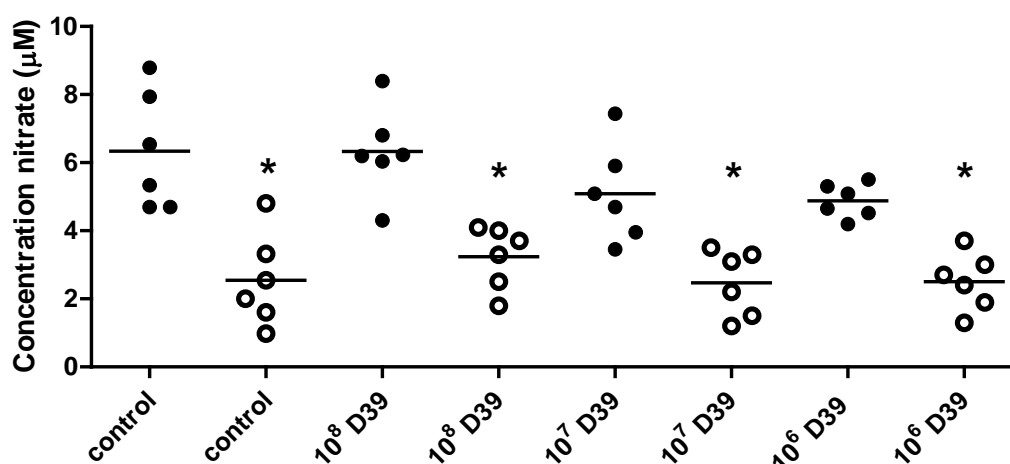


**Figure 4.6 Standard curve of chemiluminescence vs. nitrate concentration.** Each point represents the mean of 3 individual readings. The regression coefficient ( $r^2$ ) is 0.99.

The nitric oxide release from cultured basal cells from PCD patients was significantly lower than that from cells of healthy controls (Figure 5.7). However, there was no increase ( $p>0.05$ ) in nitric oxide levels released from normal and PCD patient's basal cells after incubation with  $10^6$ ,  $10^7$  and  $10^8$  cfu/ml pneumococci for four hours at  $37^\circ\text{C}$  (Figure 5.7).



Figure

5.7 Nitric oxide (measured as nitrate) release from basal cells after incubation with the wild type pneumococcal strain D39. Each point represents cells from an individual donor. The full circles represent a normal donor and the hollow circles PCD patients. \* indicates significant difference from the respective normal ( $p < 0.001$ ). The horizontal lines are the means.  $n=6$ .

### 5.7 Pneumococcal induced chemokine release from basal cells

In total nine different chemokines were measured; Eotaxin, Eotaxin-3, IL-8, IP-10, MCP-1, MCP-4, MDC, MIP-1b and TARC. There was no difference in the resting levels of these mediators from basal cells cultured from PCD patients and healthy volunteers (Table 5.4). Furthermore, following exposure to  $10^7$  cfu pneumococci, there was no difference in chemokines released from PCD and control basal cells (Table 4.4). Of the nine cytokines analysed only IL-1 $\beta$  and TNF $\alpha$  were above the limit of detection. Both these cytokines were slightly increased following pneumococcal infection of the basal cells (IL-1 $\beta$ , 3 (0-8) and TNF $\alpha$ , 2 (1-5)).

**Table 4.4. Chemokine release by basal cells from healthy controls and patients with PCD, in response to *Streptococcus pneumoniae*.**

| Chemokine<br>pg/ml | Healthy patients |                                 | PCD patients  |                                 |
|--------------------|------------------|---------------------------------|---------------|---------------------------------|
|                    | control          | 10 <sup>7</sup> cfu pneumococci | control       | 10 <sup>7</sup> cfu pneumococci |
| <b>Eotaxin</b>     | 64 (51-75)       | 75 (70-93)**                    | 64 (56-85)    | 88 (69-113)                     |
| <b>Eotaxin-3</b>   | 715 (476-793)    | 1054 (834-1190)**               | 828 (637-910) | 1142 (1012-1467)**              |
| <b>IL-8</b>        | 3 (2-3)          | 15 (5-35)                       | 2 (2-3)       | 45 (19-49)**                    |
| <b>IP-10</b>       | 290 (272-355)    | 377 (347-404)**                 | 340 (323-374) | 387 (351-479)**                 |
| <b>MCP-1</b>       | 5 (4-5)          | 6 (5-8)**                       | 5 (4-7)       | 6 (5-10)**                      |
| <b>MCP-4</b>       | 53 (37-65)       | 75 (64-101)**                   | 67 (45-77)    | 99 (85-123)**                   |
| <b>MDC</b>         | 289 (248-335)    | 358 (332-378)**                 | 326 (312-373) | 439 (326-453)**                 |
| <b>MIP-1b</b>      | 0                | 3 (1-4)**                       | 0             | 2 (1-7)                         |
| <b>TARC</b>        | 17 (2-41)        | 41(25-65)                       | 34 (16-56)    | 41 (25-74)                      |

Data as median (IQR). \*\* Significantly different from respective control. No significant differences between PCD and healthy patients data.n=6.

**CHAPTER SIX - DISCUSSION**

---

In this chapter the results from chapters three to five will be discussed.

### ***6.1 The behaviour of *L. monocytogenes* and ciliated rat ependymal cells is altered during their co-culture***

In this study the effect of *L. monocytogenes* on ependymal cilia was investigated to improve understanding of the pathophysiology of listerial meningitis. Three aspects of the results are noteworthy: the strain-specific effect of list *Listeria* eria on the ependyma, the presence of aggregates of *Listeria* on the cilia and the dissociation of ciliary beat frequency from beat amplitude.

#### **The effect of ciliated ependymal cells on *Listeria***

Adherence of pathogens to host cells is pre-requisite for cell invasion (Hultgren *et al.* 1985, Rubino *et al.* 1993). In this study *Listeria* attached to ependymal cells and the unexpected observation was the extensive aggregation of the *Listeria* attached to cilia. The adhesion of *Listeria* to ependymal cilia and the marked aggregation of *Listeria* with the formation of extracellular material may help to explain why CSF samples taken clinically from patients with listerial meningitis contain relatively small numbers of *Listeria*. Aggregates were only found physically attached to the cilia with no aggregates in the culture medium or in spent culture medium. It seems that signalling events are occurring, presumably after initial cilium/ *Listeria* attachment, which leads to more bacteria binding. In some instances extracellular material was visible and where present it may contribute to the formation of the aggregate but this material is not a prerequisite for aggregation because aggregates were found in the absence of this material. Other studies have also shown that *L. monocytogenes* produce extracellular

---

material (Marsh *et al.* 2003, Jordan *et al.* 2008) and using ruthenium red (a carbohydrate stain) have shown it contains polysaccharides (Borucki *et al.* 2003).

A strain-specific pattern was seen with bacterial aggregation around cilia, with EGDe showing the greatest aggregation but there was no aggregation of C52. Bacterial aggregates were most often seen in the presence of extracellular material. The reasons for these strain differences are not clear. Although, considerable inter-strain variation in listerial phenotype has been reported before, for example, in adhesion to abiotic surfaces (Borucki *et al.* 2003) and in response to sodium chloride and low pH (Adriao *et al.* 2008). Those results, and the data from this study, indicate that caution must be observed when extrapolating from results with a single strain of *L. monocytogenes*.

The observation that the formation of aggregates and extracellular material was abolished in two *prfA* mutants indicates that genes within the regulon of the central virulence regulator, PrfA, are involved. The absolute requirement of PrfA for *L. monocytogenes* virulence has been demonstrated before, as has the requirement for several genes within the PrfA regulon (Leimeister-Wachter *et al.* 1990, Freitag *et al.* 1993), but the explanation of how the regulon determines the effects reported here remains to be determined. To my knowledge there are no PrfA regulatory genes that have been shown to be involved in aggregate formation. To determine the genes involved in this process, studies using mutants of known PrfA-regulated genes could be useful (see Table 1.5 for a list of these genes). Also, for finding unknown PrfA-regulated genes, promoter mapping methods such as ChIP-chip (Aparicio *et al.* 2004) could be used. Chromatin immunoprecipitation (ChIP) is a powerful method to measure protein–DNA interactions *in vivo*, and it can be applied on a genomic scale with

---

microarray technology (ChIP-chip) (Wade *et al.* 2007). For more information into the ChIP-chip method, the reader is referred to a recent review by Wade *et al.* (2007).

Bacterial pathogens, including *L. monocytogenes*, are known to form structured populations of microorganisms, adhered and embedded in an extracellular matrix consisting mainly of exopolysaccharides (biofilms) (Hall-Stoodley and Stoodley 2009). It is thought that these biofilm structures protect the bacteria from host immune responses as well as different antimicrobials (Stewart 2001). Bacterial biofilms have been shown to occur in a sequential process generally involving, 1) initial attachment of individual cells to the surface 2) formation of aggregates 3) further cell proliferation and biofilm maturation (Allegrucci *et al.* 2006). Therefore, it is possible that the aggregates seen in this study are controlled by the same genes that have been shown to be important for biofilm formation. In light of these data, the role of the cell wall-anchored biofilm associated protein (Bap) was investigated in aggregate formation. Bap has been implicated in biofilm formation of *S. aureus* (Cucarella *et al.* 2001) and recently been shown to be involved in biofilm formation of *L. monocytogenes* to abiotic surfaces (Jordan *et al.* 2008). However, the work from this study using the 10403S $\Delta$ BapL mutant suggests that Bap does not have a role in listerial aggregate formation. For more information on listerial biofilms see the recent reviews by Bayles and Moscoso (Bayles 2007, Moscoso *et al.* 2009).

### **The effect of *Listeria* on ciliated ependymal cells**

The introduction of high speed digital video imaging has allowed measurement of the amplitude of beating cilia in an ependymal culture system and simultaneous determination of their ciliary beat frequency (Chilvers and O'Callaghan 2000a, Chilvers

---

*et al.* 2003b). At a concentration seen in the rat brain during listerial meningitis (Michelet *et al.* 1999, Deckert *et al.* 2001, Remer *et al.* 2001), the three wild-type *L. monocytogenes* strains studied decreased the ciliary amplitude. However, only strain C52 significantly reduced ciliary beat frequency. The inhibition of ciliary beat frequency by C52, a strain in which PrfA is in a constitutively activated state (Kreft and Vazquez-Boland 2001, Marsh *et al.* 2003), indicates that expression of the PrfA regulon prior to exposure of the ependymal cells, affects ciliary functioning. The genes under the regulation of the PrfA regulon control the expression of genes whose products are essential for virulence. As these products are up-regulated in the C52 strain, this may explain the toxic effect it has on cilia compared to other strains studied.

Interestingly, a dissociation of ciliary beat frequency from beat amplitude was observed, in that amplitude could be reduced without an effect on frequency. Such dissociation has not been reported before. For cilia associated with listerial aggregates, a ‘drag’ effect due to the attached aggregates is likely to contribute to decreased amplitude. However, this does not explain the reduced ciliary beat amplitude observed outside the listerial aggregates. One explanation could be that the viscosity of the medium surrounding the ependymal cilia is increased. Johnson and colleagues (Johnson *et al.* 1991) found that increasing the viscosity on respiratory and oviductal cilia resulted in unpredictable ciliary activity; cilia stopped beating, slowed down or seemed to beat more quickly with a short amplitude. Insight into the mechanism of autoregulation of ciliary beat frequency following exposure to changes in viscosity was provided by Andrade and colleagues (Andrade *et al.* 2005). They found that changes in mucous viscosity activate vanilloid 4-like (TRPV4) channels that elevate intracellular  $Ca^{+2}$ . As mentioned in §1.6.2, the release of  $Ca^{+2}$  from intracellular  $Ca^{+2}$  stores, increases the CBF

---

of ciliated ependymal cells. Therefore, Andrade and colleagues proposed that elevated intracellular  $\text{Ca}^{+2}$  at high viscous loads may allow cilia to adapt to a wide range of viscosities. However, these points do not explain the maintenance of beat frequency seen in this study. Indeed, one may expect an increase in frequency if amplitude was reduced. An unchanged frequency of the beat stroke, even when the distance travelled (amplitude) decreases, suggests there is a fixed timing of intra-cilium events between ciliary strokes.

## ***6.2 The behaviour of *S. pneumoniae* and ciliated respiratory cells is altered during their co-culture***

In this thesis an *in vitro* model of differentiated nasal epithelium was used to analyze the interaction between pneumococci and ciliated respiratory epithelial cells. Three aspects of the results are noteworthy: binding of pneumococci and the formation of pneumococcal aggregates on the cilia, dissociation of ciliary beat frequency from the beat amplitude and the pneumolysin-dependent toxic effect of pneumococci on the cells.

### **6.2.1 The effect of respiratory ciliated cells on *S. pneumoniae***

#### **Pneumococcal binding to cilia**

One of the key mechanisms to bacterial pathogenesis is their ability to adhere to mucosal surfaces (Boyle and Finlay 2003). In the study reported here, some of the added pneumococci were found to bind to respiratory cilia. Therefore, it appears that pneumococcal binding to cilia may aid its colonisation of the respiratory tract, where it would normally be cleared by mucociliary transport.

---

After observing the pneumococcal binding to cilia the mechanism of this adherence was further investigated. The role of pneumococcal virulence factors, specifically pneumolysin and neuraminidase A (NanA) was investigated. Pneumolysin is the major pneumococcal toxin, but from this work, at the two hour time point of this study, it appears to have no role in pneumococcal binding to respiratory cilia. Pneumococcal neuraminidases also are key virulence factors. It has been proposed that they aid adherence by removing terminal sialic acid from host cell-surface glycans, thus unmasking certain receptors to facilitate pneumococcal adherence and colonization (Paton *et al.* 1993, Kadioglu *et al.* 2008). However, in this study the pneumococcal NanA mutant was found to bind to the cilia, thus ruling out NanA as the sole adhesion factor. To determine if viable bacteria were necessary for adherence to cilia, pneumococci were killed using irradiation and then added to ciliated cells. This study showed that the dead pneumococci were still able to adhere to the cilia. This is in agreement with previous data demonstrating that heat-killed *B. Bronchiseptica* were able to adhere to ciliated canine tracheal cells (Bemis and Wilson 1985).

It is noteworthy that several other bacterial pathogens target ciliated cells for adherence, including *Mycoplasma pneumoniae* (Krunkosky *et al.* 2007), *Mycoplasma hypopneumoniae* (Hsu *et al.* 1997), *Klebsiella pneumoniae* (Fader *et al.* 1988), *Pseudomonas aeruginosa* (Mewe *et al.* 2005), *Moraxella catarrhalis* (Balder *et al.* 2009), *Bordetella pertussis* (Tuomanen *et al.* 1988) and *Bordetella bronchiseptica* (Anderton *et al.* 2004, Edwards *et al.* 2005). Some of these authors suggest that the binding of bacteria to cilia is due to bacterial adhesins (surface proteins of the pathogen) and toxins. For example, Edwards *et al.* (2005) have shown that loss of any of the three identified adhesins (filamentous hemagglutinin, fimbriae, or pertactin) or the

---

multifunctional toxin (CyaA) from *B. bronchiseptica* reduced the bacterium's capacity to bind to cilia. In another study, P97 (a 97-kDa outer membrane associated protein) was shown to have a direct role in adherence of *M. hypopneumoniae* to porcine cilia (Hsu *et al.* 1997). Fader *et al.* (1988) have demonstrated that adherence of *K. pneumoniae* to ciliated hamster tracheal cells is mediated by Type 1 Fimbriae. Type 1 fimbriae are adhesion structures expressed by many Gram-negative bacteria and have been shown to facilitate adherence to mucosal surfaces and inflammatory cells *in vitro*. Balder *et al.* (2009) demonstrated that the *M. catarrhalis* surface protein hag (a key adherence factor), is responsible for the tropism of *M. catarrhalis* for ciliated normal human bronchial epithelial (NHBE) cells. Others have suggested a role for receptors (surface carbohydrates of the target host cell) in the adherence of bacteria to cilia. For example, Krunkosky *et al.* (2007) demonstrated that *M. pneumoniae* infection of differentiated NHBE cells resulted in stimulation of intercellular adhesion molecule 1 (ICAM-1) gene expression.

All the above studies were in Gram-negative bacteria and thus may be different from the mechanism of the Gram-positive pneumococcus. However, the above studies suggest that a complex set of adhesins and receptors are involved in bacterial adherence to cilia. Thus, future work could include investigating major pneumococcal adhesins that have previously been shown to be important in direct or indirect pneumococcal binding to surfaces. These include, hyaluronidase, LytA, PspA, PsaA, PavA and PavB which have been described in §1.14.3. Furthermore, to determine the receptors involved in pneumococcal adherence to cilia, studies would include antibody staining for the presence of receptors that have been shown to be important for pneumococcal adherence to the cell surface and then blocking those receptors with antagonists. These

---

receptors include, ICAM-1 (Murdoch *et al.* 2002) , Toll like receptors 2 and 4 (Malley *et al.* 2003, Knapp *et al.* 2004), platelet-activating factor receptor (PafR) (Tuomanen 1997) and poly-immunoglobulin receptor (pigR)(Zhang *et al.* 2000).

Interestingly, the bacteria mentioned above have been shown to bind to different regions on the cilia. For example, *M. hypopneumoniae* has been shown to adhere at the tips and along the length of the cilia (Blanchard *et al.* 1992), whereas others have shown that *M. catarrhalis* only associated with the tips of cilia (Balder *et al.* 2009). *B. pertussis* and *M. pneumoniae* (Krunkosky *et al.* 2007) have been shown to associate primarily with the base of the ciliary shaft, whereas *P. aeruginosa* preferentially locates at the tip. Taken together, these studies indicate that receptors for all these pathogens are probably clustered either at the ciliary tip or at the base of the ciliary shaft, specifically the sialic rich regions termed the ciliary crown and necklace. In this study pneumococci appeared to bind to the side of the cilia towards the tip (Figure 4.6b and c) suggesting this is where the receptors for pneumococci are present.

A possible explanation for Gram-positive pneumococci not binding to sialic rich regions on the cilia may be due to the presence of the negatively charged capsule. The pneumococcal polysaccharide capsule that has been shown to reduce the entrapment of pneumococci in mucus (Nelson *et al.* 2007), by repulsing the negatively charged sialic acid rich mucopolysaccharides that are found in mucus (Kamerling 2000b). Thus, it is also possible that the negatively charged pneumococci are repused from attaching to the negatively charged tip and the base of the cilia. To confirm this hypothesis future work would include the use of the pneumococcal un-capsulated R6 strain to determine if this strain binds to similar regions as the D39 capsulated strain. However, this hypothesis would only work if the sides of the cilium were positively charged. In this study with

---

use of charged microspheres both positive and negatively charged sites were detected on the respiratory ciliary surface. However, using light microscopy it was not clear where these beads were binding to the cilia. Further work would include the use of fluorescently labelled charged particles with the use of confocal microscopy combined with 3D reconstruction using Imaris image analysis software.

### **Formation of pneumococcal aggregates towards the ciliary tip appears to be NanaA dependent**

As described previously, pneumococcal aggregates were seen attached to respiratory cilia. To my knowledge no other study has reported the presence of pneumococcal aggregates on cilia. As seen in Figure 4.6, it seems that initial cilium/pneumococcal attachment, may lead to more bacterial binding and the formation of aggregates. The presence of bacterial aggregates adhered to cilia has previously been demonstrated (Blanchard *et al.* 1992). In their study, Blanchard *et al.* (1992) showed that *M. hypopneumoniae* adhered to ciliated cells that line the epithelial tract, forming microcolonies at the tips of the cilia (Blanchard *et al.* 1992).

To determine if the pneumococcal aggregate phenomenon was strain specific, a pneumococcal serotype 4 strain TIGR4, was compared to the results obtained from the serotype 2 D39 strain. Also, the pneumococcal pneumolysin mutant,  $\Delta$ PLY, was used to study the role of this toxin in aggregate formation. Both TIGR4 and  $\Delta$ PLY showed no differences in their interaction with cilia compared to the D39 strain (all bacterial numbers were  $10^7$  cfu). Furthermore, although dead bacteria were found to bind to the cilia they did not form any aggregates. This suggests that for aggregate formation the pneumococci need to be viable.

---

Previous studies have shown that mutants deficient in NanA are less virulent than the wild-type pneumococci in mice (Mitchell *et al.* 1997) and that loss of NanA impaired pneumococcal persistence in the nasopharynx (§1.14.2) (Tong *et al.* 2000, Orihuela *et al.* 2004, Manco *et al.* 2006). Consequently, the role of NanA in pneumococcal aggregate formation was investigated and it was found to be NanA dependent. NanA is highly expressed at the transcriptional level (Berry *et al.* 1996, Manco *et al.* 2006), and its expression is up-regulated upon interaction with host cells and in the lung cells (LeMessurier *et al.* 2006, Oggioni *et al.* 2006, Song *et al.* 2008). A recent study demonstrated that the *S. pneumoniae* neuraminidase A is involved in biofilm formation on plastic (Parker *et al.* 2009). In their study using an *in vitro* model of biofilm formation, incorporating human airway epithelial cells, Parker *et al.* (2009) demonstrated that the nanA mutant had a significantly reduced capacity to form biofilms compared to the wild-type pneumococci. Furthermore, they showed that the nanA mutant only attached to the microtitre wells and did not form macrostructures, as seen with the wild-type, and small-molecule inhibitors of NanA blocked biofilm formation (Parker *et al.* 2009). Also, in another study the expression of nanA has been shown to be up regulated when *S. pneumoniae* are in a biofilm phenotype (Oggioni *et al.* 2006). Interestingly, a *P. aeruginosa* neuraminidase mutant has also shown a reduction in its ability to colonise the respiratory tract which was correlated with diminished biofilm production (Soong *et al.* 2006).

To further confirm the role of NanA in bacterial aggregate formation, gene expression studies would be of benefit. A recent study by Uchiyama *et al.* (2009) has shown that NanA activity can be independent of its enzymatic activity. In their study the contribution of pneumococcal NanA in invasion of human brain endothelial cells

---

involved an adhesin function, in which the N-terminal lectin-like domain played a critical role, and a small but significant contribution was due to its sialidase activity. Therefore, to confirm the role of NanA in aggregate formation a future experiment would include repeating the experiment with a mutant of the NanA protein which has deletions in its active enzymatic sites. Furthermore, the expression of the capsular polysaccharide has been shown to be essential for pneumococcal colonisation (Allegrucci *et al.* 2006). Therefore, in support of this information it would be interesting to see if the R6 unencapsulated pneumococcal strain forms bacterial aggregates.

### **6.2.2 The effect of *S. pneumoniae* on respiratory ciliated cells**

In the presence of wild-type pneumococcal strains a dissociation of ciliary beat frequency from beat amplitude was observed, in that amplitude could be reduced without an effect on beat frequency. The amplitude of cilia under the bacterial aggregates was reduced further compared to the cilia outside the aggregates. This suggests that for cilia covered by pneumococcal aggregates, a 'drag' effect due to the attached aggregates may contribute to the decreased amplitude. This is a likely explanation as the NanA mutant did not form aggregates and the ciliary amplitude was only slightly reduced. The reduction of ciliary amplitude outside the aggregates was not due to the toxin pneumolysin as the pneumolysin negative strain also reduced the amplitude. The studies mentioned here suggest that there are two mechanisms behind the reduction of ciliary amplitude. One that is due to the presence of bacteria and is not due to the toxin pneumolysin and a second method that is mechanical and reduces the amplitude further (presence of bacterial aggregates). Table 6.1 summarises these pneumococcal strains and their effect on the cilia.

However, these proposed mechanisms do not explain how the cilia maintain their ciliary beat frequency once their amplitude is reduced. These observations are similar to the *Listeria* infected ependymal cells. And as mentioned in §6.1 an unchanged frequency of the beat stroke, even when the distance travelled (amplitude) decreases, may suggest there is a fixed timing of intra-cilium events between ciliary strokes.

Table 1.6 Summary of the pneumococcal strains that produced aggregates and their effect on the ciliary beat amplitude

| <b>Pneumococcal strain</b> | <b>Pneumococcal aggregates</b> | <b>ciliary beat amplitude</b> | <b>ciliary beat amplitude under the pneumococcal aggregates</b> |
|----------------------------|--------------------------------|-------------------------------|---|
| Wild type D39              | present                        | reduced                       | further reduced   |
| D39 $\Delta$ PLY           | present                        | reduced                       | further reduced   |
| D39 $\Delta$ NanA          | absent                         | reduced                       | Not applicable  |

In the study reported here toxicity to the respiratory epithelium was measured by LDH release and was dependent on the pneumococcal concentration and pneumolysin. This is agreement with previous studies suggesting that pneumolysin is cytotoxic to ciliated epithelial cells (Rayner *et al* 1995).

---

### ***6.3 Comparisons between healthy normal and PCD basal and ciliated respiratory cells in their response to pneumococci***

#### ***6.3.1 Respiratory cells from PCD patients show no increase in nitric oxide production following infection with pneumococci***

In PCD patient's nasal nitric oxide is low and this may be related to ciliary function. Nitric oxide is an important signalling molecule produced from L-arginine by nitric oxide synthases (NOS) present in epithelial cells (Asano *et al.* 1994, Watkins *et al.* 1998). Three mammalian NOS isoforms have been identified: nNOS (neuronal NOS), iNOS (inducible NOS) and eNOS (endothelial NOS) and all are expressed within the respiratory tract (Moncada and Higgs 1993). Within the nose and respiratory tract the postulated functions of nitric oxide include antimicrobial activity (Croen 1993, Braun *et al.* 1999), regulation of ciliary motility (Jain *et al.* 1993, Runer *et al.* 1998) and down regulation of the proinflammatory cytokine response (Walley *et al.* 1999).

Studies have consistently revealed low levels of exhaled nitric oxide in primary ciliary dyskinesia; the low levels being attributed principally to the reduced bronchial iNOS activity rather than the alveolar eNOS (Paraskakis *et al.* 2007, Shoemark and Wilson 2009). In another study it was confirmed that the levels of both nNOS and eNOS are very low in children with PCD (Narang *et al.* 2002). There have been no reports in nitric oxide levels released from PCD ciliated cells in culture. In the study reported here, nitric oxide released into the supernatant from non-infected ciliated cultures of PCD patients was not significantly different from healthy normal ciliated cultures. This was an unexpected result as nitric oxide released from non-infected PCD basal cells was significantly reduced

compared to non-infected healthy normal basal cells. The reasons for these differences in nitric oxide levels between the basal and ciliated PCD cells are unclear.

Following infection with pneumococci, in healthy normal ciliated cells increased levels of nitric oxide were detected. These are in keeping with previous studies that have reported nitric oxide levels are increased once cells are exposed to bacterial products for example, LPS (Weinberg *et al.* 1994, Cook and Cattell 1996). Interestingly, in PCD ciliated cultures nitric oxide levels were not increased after infection with pneumococci. This suggests that PCD patients may have a problem with iNOS stimulation, as iNOS is responsible for increases in nitric oxide during infections (Weinberg *et al.* 1994). The data from a recent study supports this hypothesis, as some PCD patients have been shown to exhibit a polymorphism in the promoter of iNOS (Zhan *et al.* 2003). Therefore, it is possible that a lack of increase in nitric oxide levels seen in this study following pneumococcal infection could in part be due to genetic abnormalities in the iNOS gene. Furthermore, as seen in Figure 6.1 activation of the transcription factor nuclear factor kappa B (NF- $\kappa$ B) pathway by bacterial antigens results in iNOS production. Thus any functional problems relating to the NF- $\kappa$ B pathway could also result in reduced nitric oxide production following bacterial stimulation.

In both normal and PCD basal cell cultures no increases in nitric oxide were detected after infection of the cells with pneumococci. This may suggest that only fully differentiated ciliated cells express iNOS and are capable of increasing iNOS expression.

---

### ***6.3.2 Respiratory cells from PCD patients have increased levels of cytokine and chemokines compared to respiratory cells from healthy individuals***

Given that pneumococci are one of the most common pathogens isolated from PCD patients, the cytokine and chemokine profile of respiratory cells from PCD patients infected with pneumococci was investigated. In the study reported here, there was no increase in cytokines and a slight increase in four of the chemokine levels after infection of healthy ciliated cells with pneumococci for two hours. However, ciliated cells from PCD patients released higher levels of some cytokine and chemokines, compared to healthy ciliated cells, both before and after infection with pneumococci. Furthermore, in PCD ciliated cultures there was an increase in some cytokine and chemokine levels after infection of the cells with pneumococci. Whilst extrapolating the data, it was of great interest to find that ciliated cell cultures from PCD patients with a static ciliary phenotype, released higher levels of both cytokine and chemokines compared to the other PCD phenotypes that had some ciliary movement. Before discussing these cytokine and chemokines in more detail it is important to understand how they are regulated.

The first physical barrier in the conducting airway which an inhaled microorganism, such as *S. pneumoniae*, encounters is the respiratory epithelium. Once in contact with the lung epithelium, pneumococci are detected by specific immune receptors (Koedel *et al.* 2003, Opitz *et al.* 2004), that are capable of activating transcription factors such as the ubiquitous transcription factor nuclear factor-kappaB (NF- $\kappa$ B) (Greene and McElvaney 2005, Schmeck *et al.* 2006, Chapman *et al.* 2007). NF- $\kappa$ B serves as a master switch, transactivating various proinflammatory and chemotactic cytokines such as IL-6 and IL-8 and also up-regulates the production of mediators of the innate immune

response such as nitric oxide (Strieter *et al.* 2003, Schmeck *et al.* 2004). Nitric oxide has been shown to inhibit proinflammatory cytokine expression by down regulating NF- $\kappa$ B that binds to the promoter region of these proinflammatory cytokine genes (Walley *et al.* 1999). Activation of NF- $\kappa$ B by pneumococci has been demonstrated both *in vitro* and in animal models (Spellerberg *et al.* 1996, Amory-Rivier *et al.* 2000, Schmeck *et al.* 2004, Jones *et al.* 2005). Figure 6.1 shows a proposed schematic diagram of the pneumococcal stimulated NF- $\kappa$ B pathway resulting in activation of proinflammatory cytokines and nitric oxide.

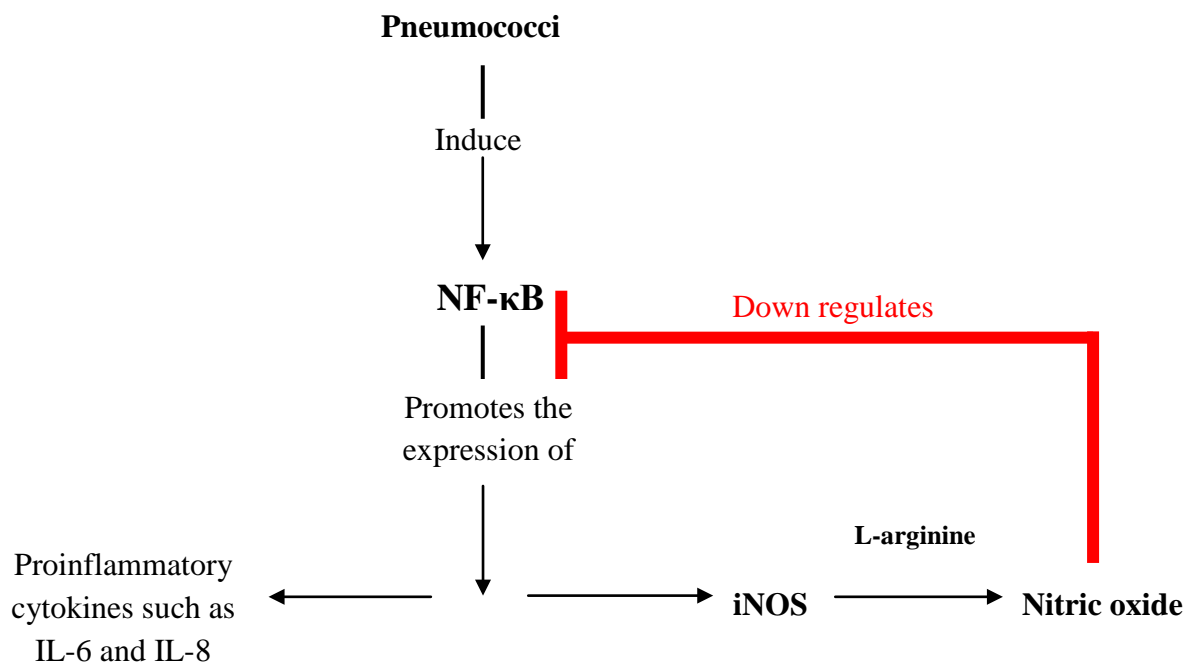


**Figure 6.1 Proposed schematic diagram showing the early immune responses to pneumococci.** Following exposure to pneumococci, specific immune receptors are activated that result in the activation of NF- $\kappa$ B. NF- $\kappa$ B is a protein complex that promotes the expression of proinflammatory mediators such as L-6, IL-8, and nitric oxide. iNOS is produced from L-arginine by constitutive nitric oxide synthase. Nitric oxide has been shown to inhibit proinflammatory cytokine expression by down regulating NF- $\kappa$ B that binds to the promoter region of these proinflammatory cytokine genes (shown in red).

---

In the study reported here, increased levels of cytokine and chemokines were only detected in PCD pneumococcal infected ciliated cultures. The increased levels of proinflammatory cytokines, such as IL-6 and IL-8, from PCD ciliated cell cultures suggests that the NF- $\kappa$ B signalling pathway (Figure 6.1) has been activated. This may imply that at 2 hours, PCD cultures are more sensitive to pneumococcal exposure compared to healthy ciliated cultures that did not show any increases in proinflammatory cytokines. It may be possible that efficient mucociliary clearance in the healthy cell cultures, as opposed to PCD cell cultures, is preventing the pneumococci to adhere and infect the cells and thus mount an inflammatory response. This is further supported by the fact that PCD ciliated cultures with a static phenotype had higher levels of cytokine and chemokines compared to non static PCD cultures where there was some ciliary movement and thus pneumococcal clearance. These data may suggest that a complete lack of mucociliary clearance further induces the release of pro-inflammatory mediators, although it remains to be resolved why this is the case. It would be interesting to decipher if PCD patients with a static ciliary phenotype suffer from more infections than the non static PCD patients, as this has not been confirmed in clinical studies.

Another explanation for a lack of increase in proinflammatory mediators in healthy ciliated cultures, may be due to the increased levels of nitric oxide detected in the healthy cultures following pneumococcal infection reported in this study. Nitric oxide has been shown to down-regulate the inflammatory response (Kerr *et al.* 2004, Marriott *et al.* 2006) by decreasing the amount of NF- $\kappa$ B available for binding to the regulatory region of proinflammatory cytokine genes (Walley *et al.* 1999). As pneumococcal infected PCD ciliated cells did not result in any up regulation of nitric oxide this may

---

result in over expression of NF- $\kappa$ b and thus proinflammatory cytokines. A similar pattern of increased expression of proinflammatory cytokines, including IL-6 and IL-8, as a result of abnormalities within the NF- $\kappa$ b pathway has been demonstrated in epithelial cells from patients with Cystic fibrosis (CF) and is thought to contribute to the excessive inflammatory response in CF (Scheid *et al.* 2001). CF patients like PCD patients suffer from recurrent chest infection and some patients have low nasal nitric oxide levels (Steagall *et al.* 2000, Gomez and Prince 2007). Therefore, it is possible that PCD patients may also have abnormalities within the NF- $\kappa$ b pathway and this may explain the lack of an increase in nitric oxide and increased proinflammatory cytokines.

The biggest increase detected in proinflammatory cytokines following pneumococcal infection of PCD ciliated respiratory cells was in IL-6. Increased IL-6 levels have been associated with a range of diseases and is often linked to the severity of the disease (Barnes 2009). Interestingly, the highest levels of IL-6 were detected in the cultures from the static PCD group. Therefore, it would be of interest to decipher if PCD patients with a static ciliary defect show more severe respiratory symptoms compared to other PCD patients. Blocking proinflammatory cytokines including IL-6 with monoclonal antibodies has proven to be of clinical beneficial in other chronic inflammatory diseases such as rheumatoid arthritis and inflammatory bowel syndrome (Nishimoto and Kishimoto 2006). Therefore, it is possible that a similar approach may be useful in patients with PCD.

The study reported here is the first to investigate a detailed cytokine and chemokine profile for PCD ciliated cultures. Currently, there is only one study in the literature that has investigated IL-8 and TNF- $\alpha$  levels in nasal lavage fluid from PCD patients compared to subjects with no respiratory problems (McShane *et al.* 2004). These

---

authors found that IL-8 levels were increased in PCD patients. This is in keeping with the data reported here as, PCD patients with a static ciliary phenotype had increased levels of IL-8. However, McShane and colleagues do not mention the phenotype of their PCD patients.

In summary, understanding the inflammatory response in PCD may allow determination of mechanisms of tissue damage, and even allow monitoring of therapy. Furthermore, the phenotype of the PCD patients seems to be important when assaying the inflammatory response.

#### ***6.3.4 Pneumococcal adhesion and invasion of respiratory basal cells; a comparison between basal cells from healthy normal and PCD patients***

Infections of the airway commonly cause destruction of columnar epithelial cells, thus exposing the sensitive underlying basal cells of the airway to bacterial toxins and host inflammatory mediators (Mygind and Wihl 1977). *S. pneumoniae* is one of the most common pathogens isolated from the sputum of children and adults with PCD (Ellerman and Bisgaard 1997). Thus, it was of interest to see if PCD basal cells are more susceptible to infection by *S. pneumoniae* compared to healthy normal basal cells. Thus, the ability of pneumococci to adhere and invade basal cells was compared in the two groups, using two different methods.

Using either colony count or microscopy no differences were observed in pneumococci adhered to PCD and normal basal cells. However, the number of bacteria detected by microscopy was 1000- fold greater than by colony counting. On average, as seen in Figure 5.5, the ratio of pneumococci per cell was 0.3. Since, the number of basal cells in a well at confluence was  $\sim 10^5$  one may expect to have recovered  $\sim 10^4$  pneumococci

---

from each well. However, the average number of bacteria recovered by colony counting was  $\sim 10^3$  (Figure 5.3). The reasons for these differences are not known and require further investigation.

The gentamicin protection assay (invasion assay) used in this study was based on several observations made in the 1970s, whereby bacteria that were internalized inside cells were shown to be protected by antibiotics on the cell surface (Mandell 1973, Vaudaux and Waldvogel 1979). Although, this assay can severely underestimate the number of intracellular bacteria as it is based on the recovery of viable bacteria after their internalization by eukaryotic cells, and does not account for internal bacteria being killed by the eukaryotic cells (Booth *et al.* 2003). Furthermore, prolonged treatment with high concentrations of gentamicin may lead to significant endocytotic uptake of the antibiotic and thus eventually contribute to the killing of intracellular bacteria (Pils *et al.* 2006). Therefore, in some studies the antibiotic protection assays have been used in parallel with microscopic evaluation of infected samples to detect both viable and killed intracellular bacteria (Heesemann and Laufs 1985, Drevets and Elliott 1995). As a result in this study two methods were used to detect internal pneumococci.

Depending on the method used to study internal pneumococci, different observations were recorded in that internal pneumococci were only detected using confocal microscopy. Possible explanations for these different observations are; 1) gentamicin has killed the internal bacteria and therefore no bacteria are recovered in the colony count. If in this study the permeability of the cells is increased in some way, it would allow the gentamicin to penetrate the cells and kill the internal bacteria. 2) The detected pneumococci from confocal microscopy images are not viable 3) the pneumococci are viable but they are not culturable. Previously it was thought that bacteria are dead when

they are no longer able to grow in culture media. However, in the recent years many bacteria have been shown to lose their culturability, but remain viable and potentially are able to multiply (Oliver 2005). Although to my knowledge, this viable but non culturable state has not previously been reported in pneumococci. Therefore, further experiments are required to determine if pneumococci are capable of losing their culturability. For more details on the viable but non culturable state of bacteria, see the recent review by Oliver (2005).

Another interesting observation from the confocal images was the number of internal pneumococci in normal and PCD basal cells. In healthy basal cells five times more pneumococci were detected compared to PCD basal cells. One explanation for this could be the presence of higher levels of nitric oxide in healthy normal basal cells. As nitric oxide has been shown to up-regulate the Paf receptor, which once activated internalises the pneumococci (Tuomanen 2000). To confirm this, antibody or gene expression studies would be useful to determine if there is an up-regulation of Paf in healthy respiratory basal cells compared to basal cells from PCD patients.

Another possibility stems from the observation that some viruses (Sodeik *et al.* 1997, Suomalainen *et al.* 1999) and bacteria (Clausen *et al.* 1997, Hu and Kopecko 1999, Kim *et al.* 2001) use host cell microtubules and cytoplasmic dynein proteins to promote their invasion, replication and movement in host cells. Dynein proteins that are anchored to the ciliary axoneme and help drive coordinated beating of cilia have been shown to be defected in PCD patients. Therefore, it is possible that PCD patients may also have defects in cytoplasmic dynein proteins. If so, these data may explain the reduced number of internalised pneumococci observed in PCD basal cells from the study presented here. However, currently no studies have investigated abnormalities in

cytoplasmic dyneins in PCD patients and also linked pneumococcal invasion to cytoplasmic dynein proteins.

### **Summary**

Table 6.2 summarises the differences between basal and ciliated cultures from PCD and healthy individuals in context to the experiments carried out in this thesis. From the results of this study one cannot conclusively say that PCD patients are more susceptible to pneumococcal infection. Although, the low nitric oxide levels and high levels of inflammatory mediators observed in the PCD ciliated epithelium may aid pneumococcal infection.

Table 6.2 Summary of experiment carried out on ciliated and basal respiratory cultures from healthy and PCD individuals and their differences.

| <b>Cells</b>          | <b>LDH release</b> | <b>Baseline nitric oxide levels</b> | <b>Nitric oxide release after pneumococcal infection</b> | <b>Chemokines levels</b> | <b>Cytokines levels</b> | <b>Adhered pneumococci</b>           | <b>Pneumococcal invasion</b>      |
|-----------------------|--------------------|-------------------------------------|--|--------------------------|-------------------------|--------------------------------------|-----------------------------------|
| <b>Ciliated cells</b> | No difference      | No difference                       | Increased in Healthy cultures                            | Higher in PCD cultures   | Higher in PCD cultures  | More recovered from healthy cultures | Experiment not done               |
| <b>Basal cells</b>    | No difference      | Higher in healthy cultures          | No increase in both groups                               | No difference            | Not detected            | No difference                        | More detected in healthy cultures |

**APPENDIX A**

---

In all videos the beating cilia were recorded (32x objective) using a troubleshooter 1000 high speed video camera (Lake Image Systems Ltd, UK) at 500 frames per second. Video sequences were played back at a reduced frame rate. For viewing the AVI files, MiDAS 4.0 player software should be used <http://www.xcitex.com/html/downloads.php>

The details of the videos attached in the CD accompanied with the thesis are as follows:

**Video S1-S3. Human respiratory cells from a nasal brushing**

Slow motion videos of normal beating human respiratory cilia (S1), dyskinetic cilia (S2) and static cilia (S3).

**Video S4. Rat brain ciliated ependymal cells after incubation in tissue medium 199 for three hours (negative control)**

A slow motion video of beating cilia on ependymal cells. Note the distance travelled by the tip of each cilium; this is the ciliary amplitude.

**Video S5. Rat brain ciliated ependymal cells after incubation with wild- type *L. monocytogenes* strain 10403S for three hours**

This slow motion video shows the listerial aggregates attached to and moving at the same frequency as the cilia. Compared to the control, the ciliary amplitude is markedly reduced where associated with the bacterial aggregates.

**Video S6. Rat brain ciliated ependymal cells after incubation with wild- type *L. monocytogenes* strain EGDe for two hours**

This slow motion video shows long chains of the EGDe bacterial strain attached to and moving at the same frequency as the cilia. The bacteria appear to form a network over

---

the underlying cilia. The ciliary beat frequency is normal, however the amplitude of the ciliary beat is reduced compared to the control.

**Video S7. Rat brain ciliated ependymal cells after incubation with wild- type *L. monocytogenes* strain EGDe for 3 hours**

This slow motion video shows large areas of bacteria aggregated to extracellular material and covering the cilia on ependymal cells. The bacteria are moving at the same frequency as the cilia. The ciliary beat frequency is normal but the ciliary beat amplitude is dramatically reduced compared to the control.

**Video S8. Human ciliated respiratory cells in culture after incubation in BEBM tissue culture medium for two hours (negative control)**

Slow motion video of beating cilia on respiratory cells.

**Video S9. Human ciliated respiratory cells in culture after incubation with wild type *S. pneumoniae* strain D39 for two hours**

This slow motion video shows a small pneumococcal aggregate attached to the cilia. The bacteria are moving at the same frequency as the cilia. The ciliary beat frequency is normal but the ciliary beat amplitude is reduced compared to the control.

**Video S10. Rat brain ciliated ependymal cells after incubation with positively charged melamine beads**

Slow motion video of melamine beads attached to ependymal cilia.

---

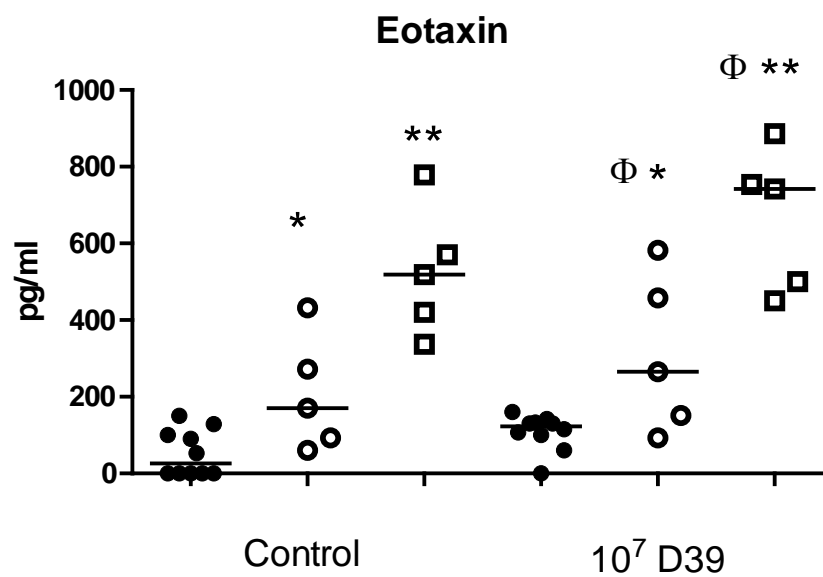
**Video S11. Rat brain ciliated ependymal cells after incubation with negatively charged silica beads**

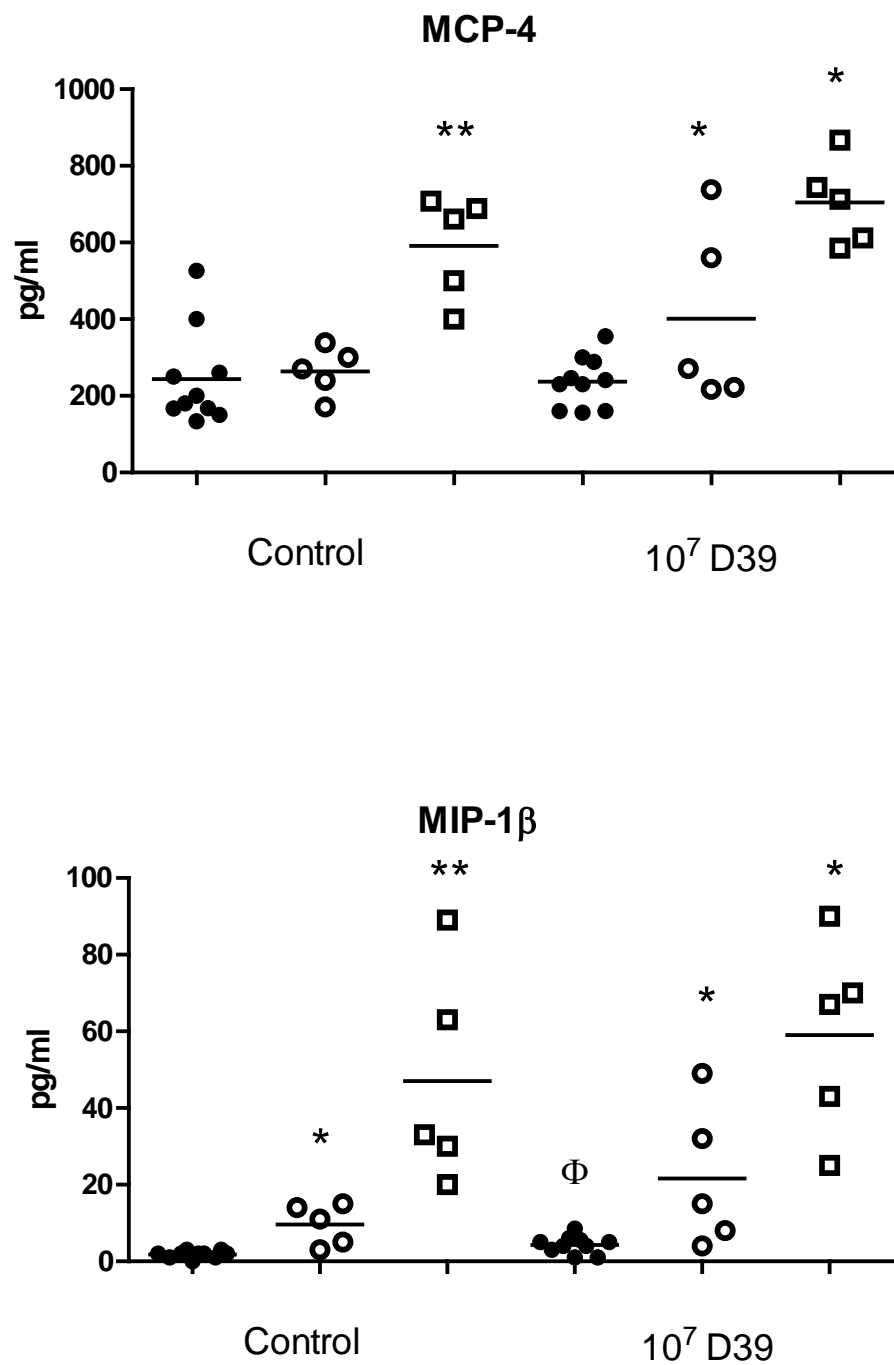
Slow motion video of silica beads attached to ependymal cilia.

**APPENDIX B**

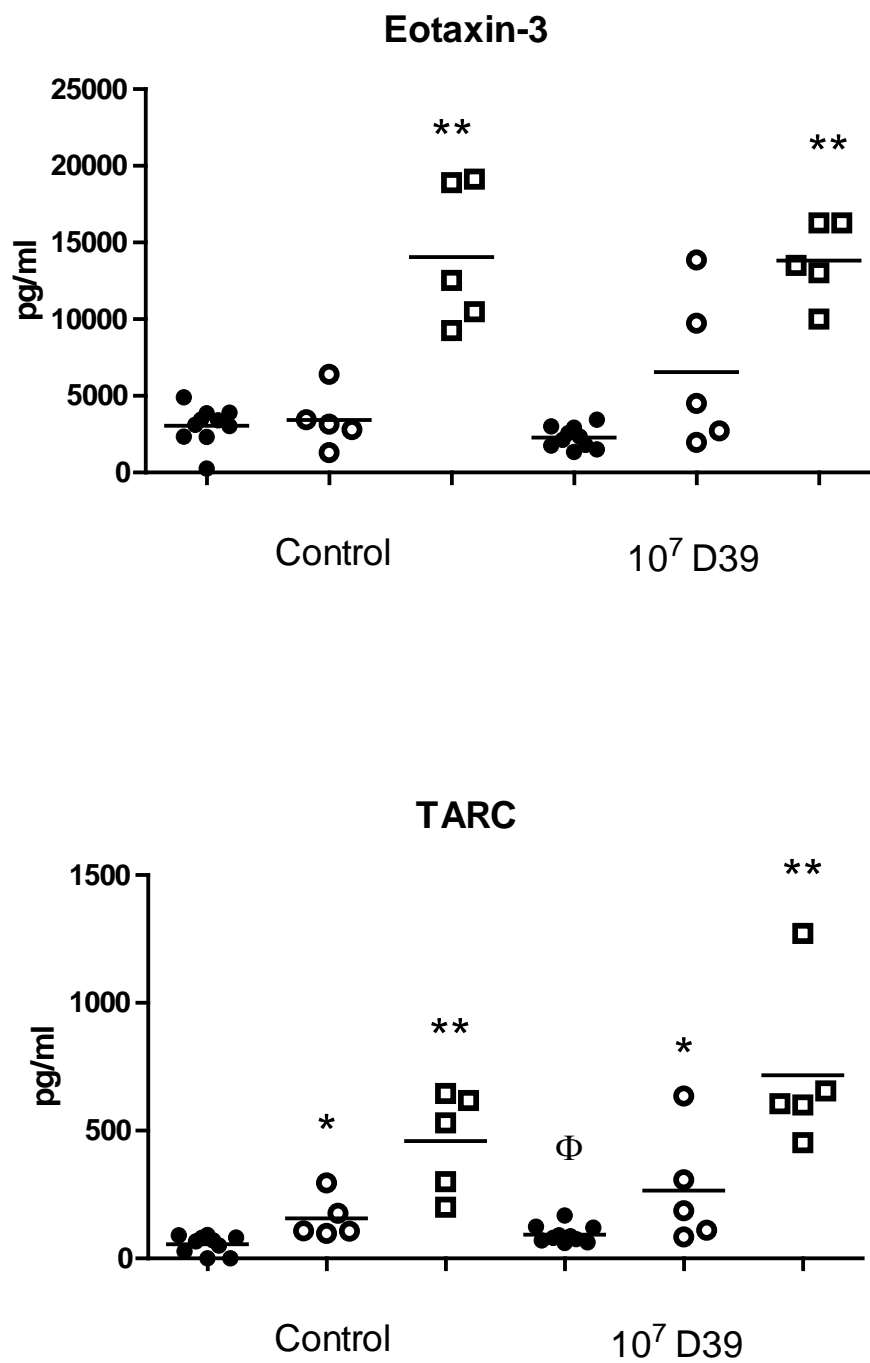
Graphs related to §4.6 and §4.7, showing the chemokine and cytokine release by ciliated respiratory cells from healthy control and PCD patients in response to pneumococci. On the graphs each full circle represents a healthy normal ciliated culture. The hollow circles represent PCD non static ciliated cultures and the hollow squares PCD static cultures.

\*Significantly different from the same data in the healthy control ciliated cultures. \*\* Significantly different from the same data in the control and the non static PCD cultures.  $\Phi$  significantly different from respective control.

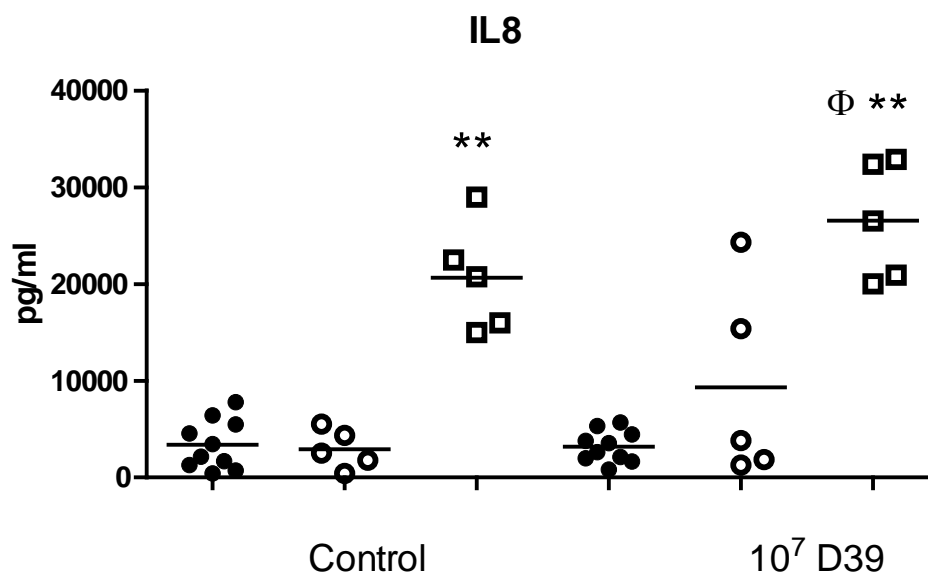
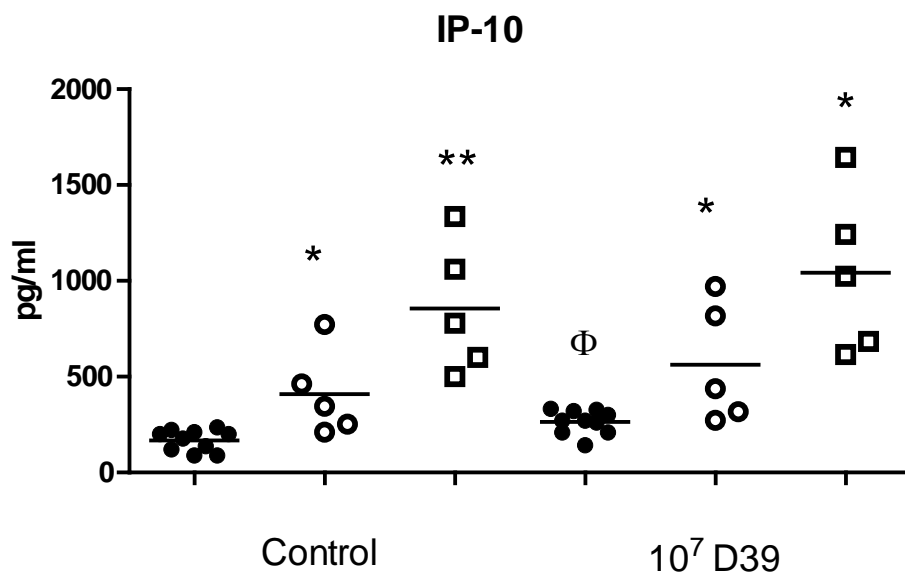




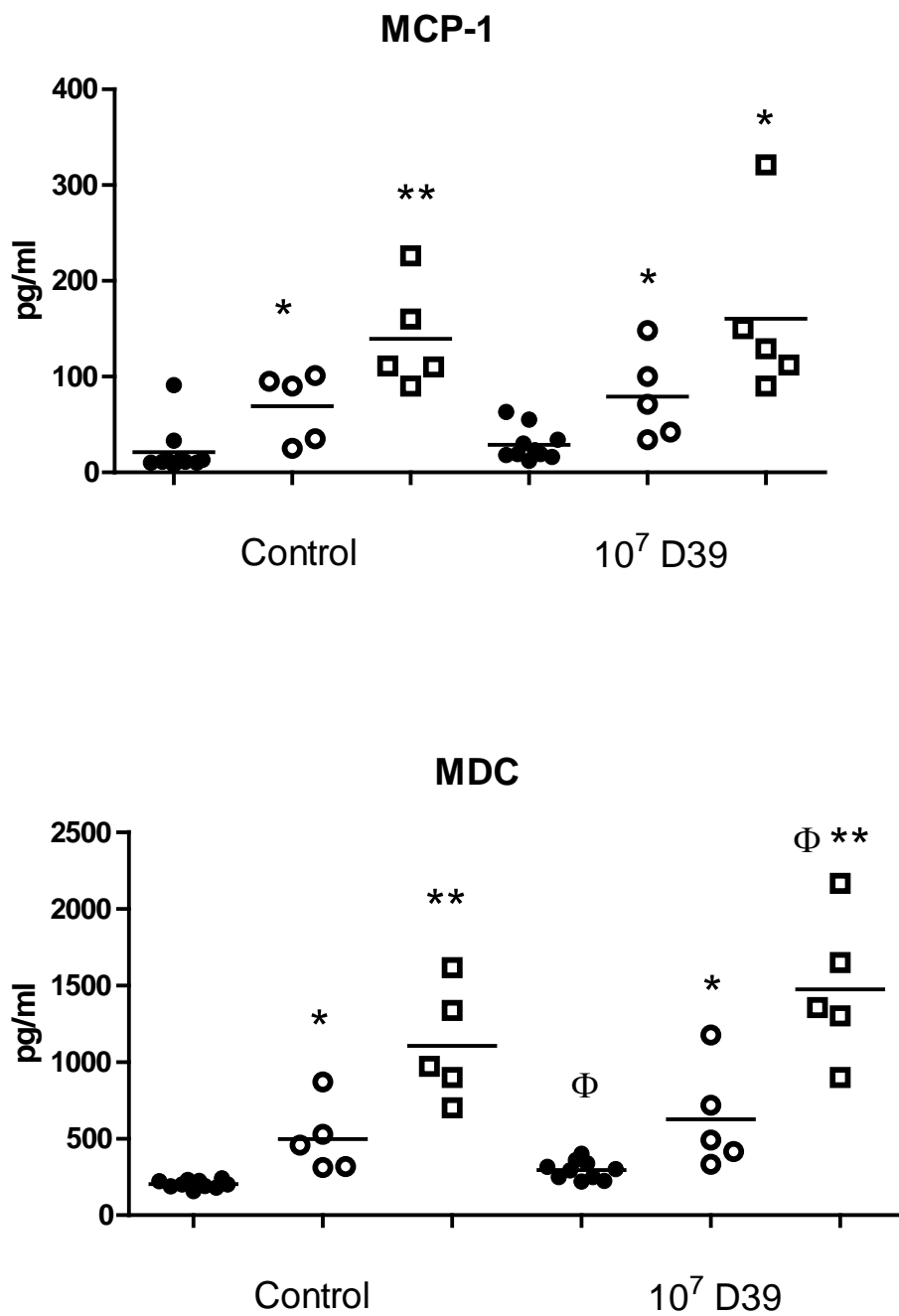
\*Significantly different from the same data in the healthy control ciliated cultures. \*\* Significantly different from the same data in the control and the non static PCD cultures.  $\Phi$  significantly different from respective control.



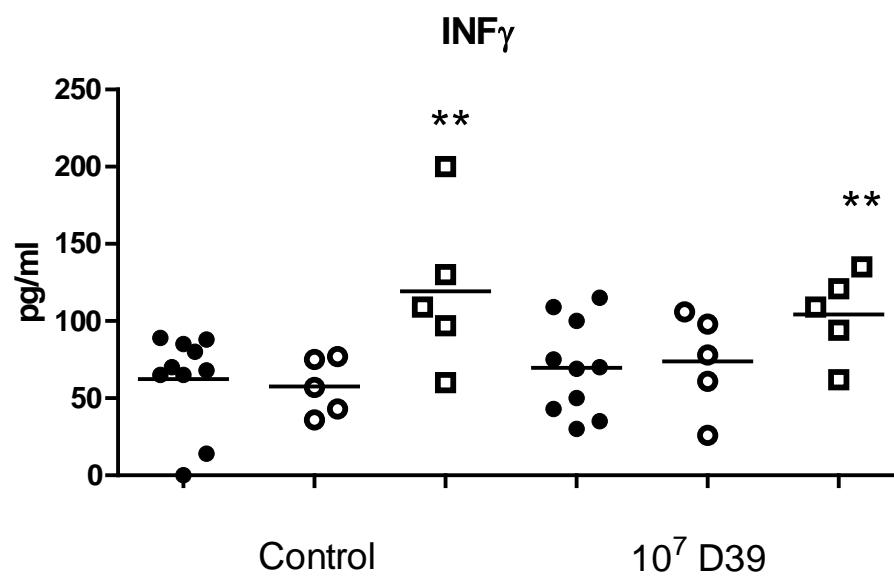
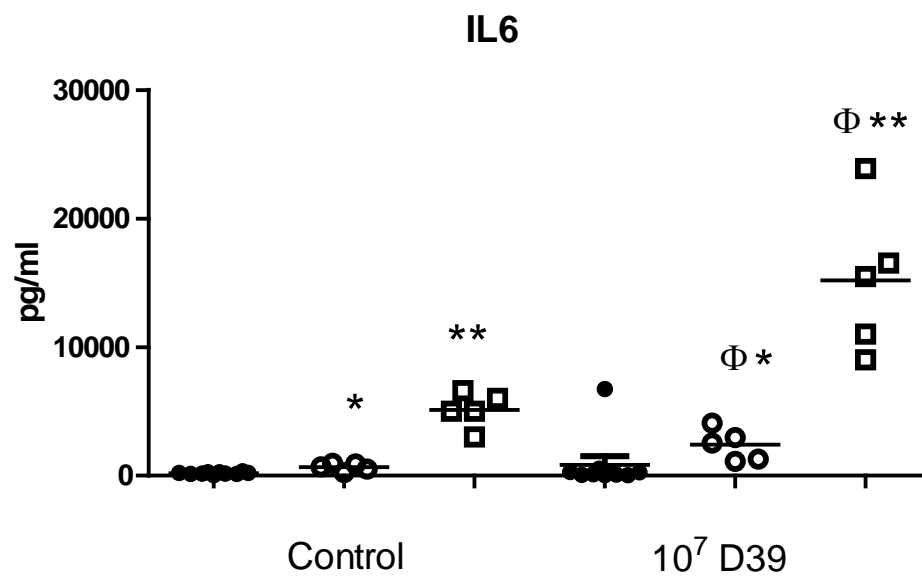
\*Significantly different from the same data in the healthy control ciliated cultures. \*\* Significantly different from the same data in the control and the non static PCD cultures. Φ significantly different from respective control.



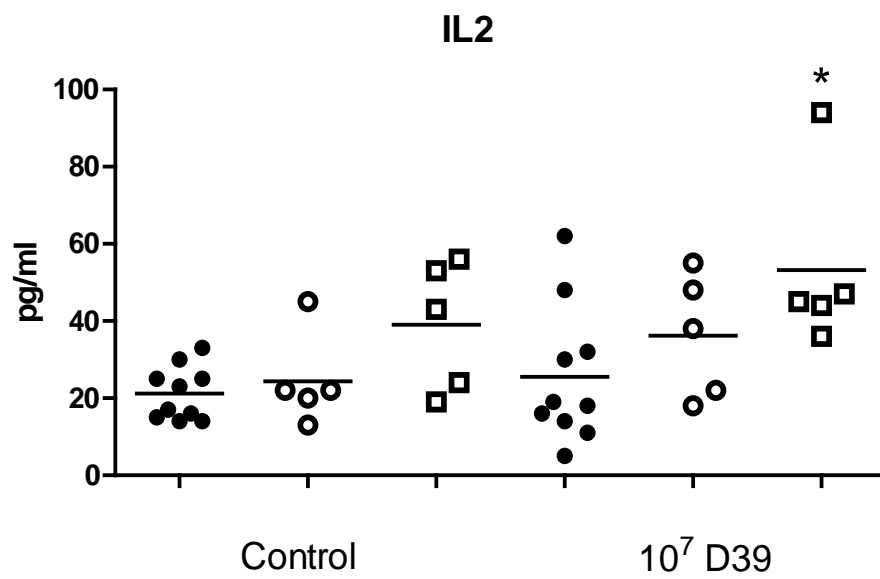
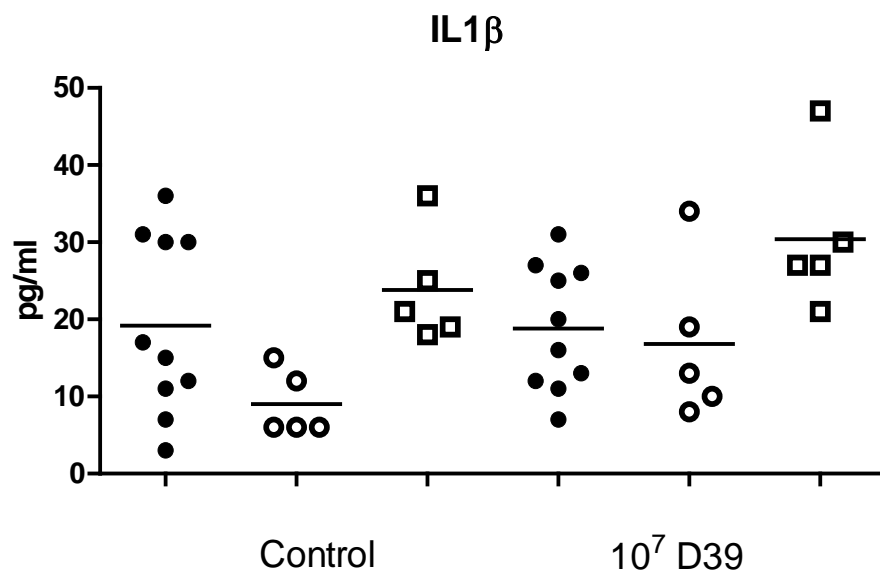
\*Significantly different from the same data in the healthy control ciliated cultures. \*\* Significantly different from the same data in the control and the non static PCD cultures. Φ significantly different from respective control.



\*Significantly different from the same data in the healthy control ciliated cultures. \*\* Significantly different from the same data in the control and the non static PCD cultures. Φ significantly different from respective control.

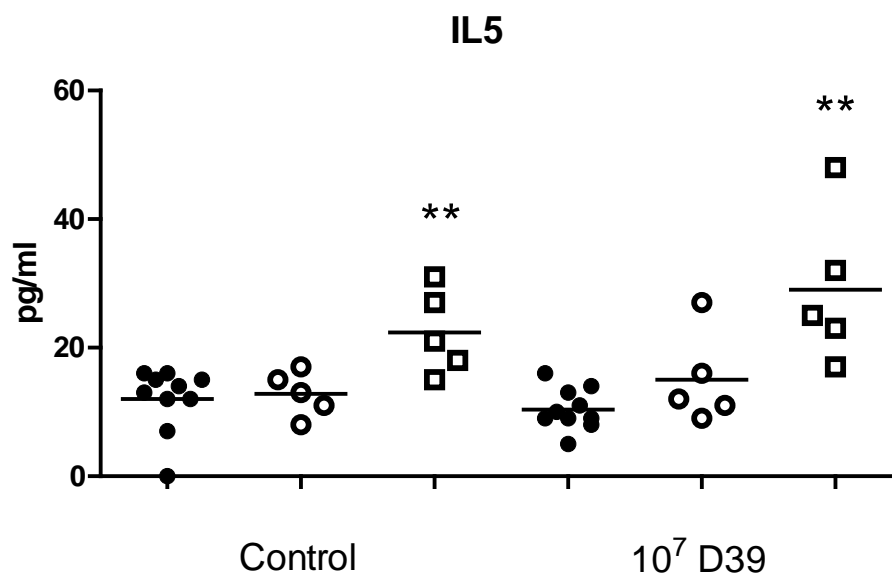
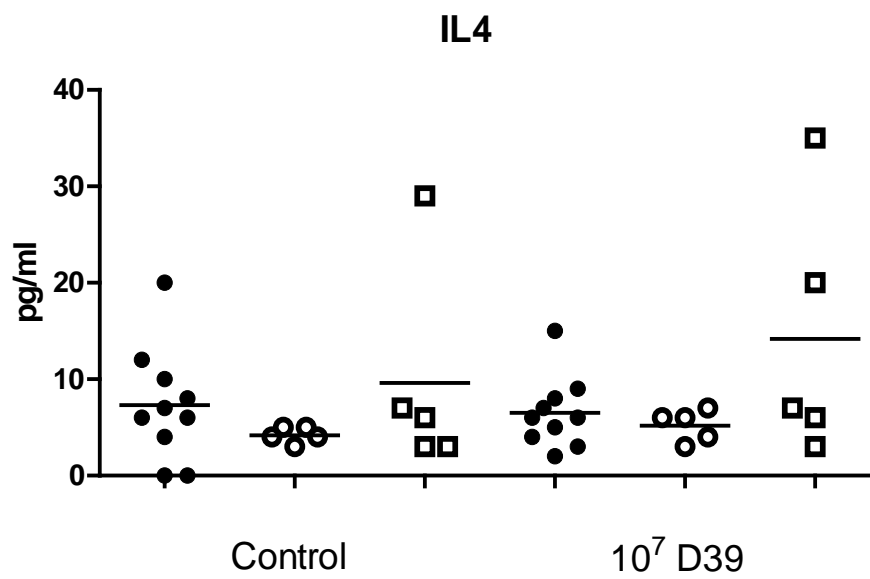


\*Significantly different from the same data in the healthy control ciliated cultures. \*\* Significantly different from the same data in the control and the non static PCD cultures.  $\Phi$  significantly different from respective control.

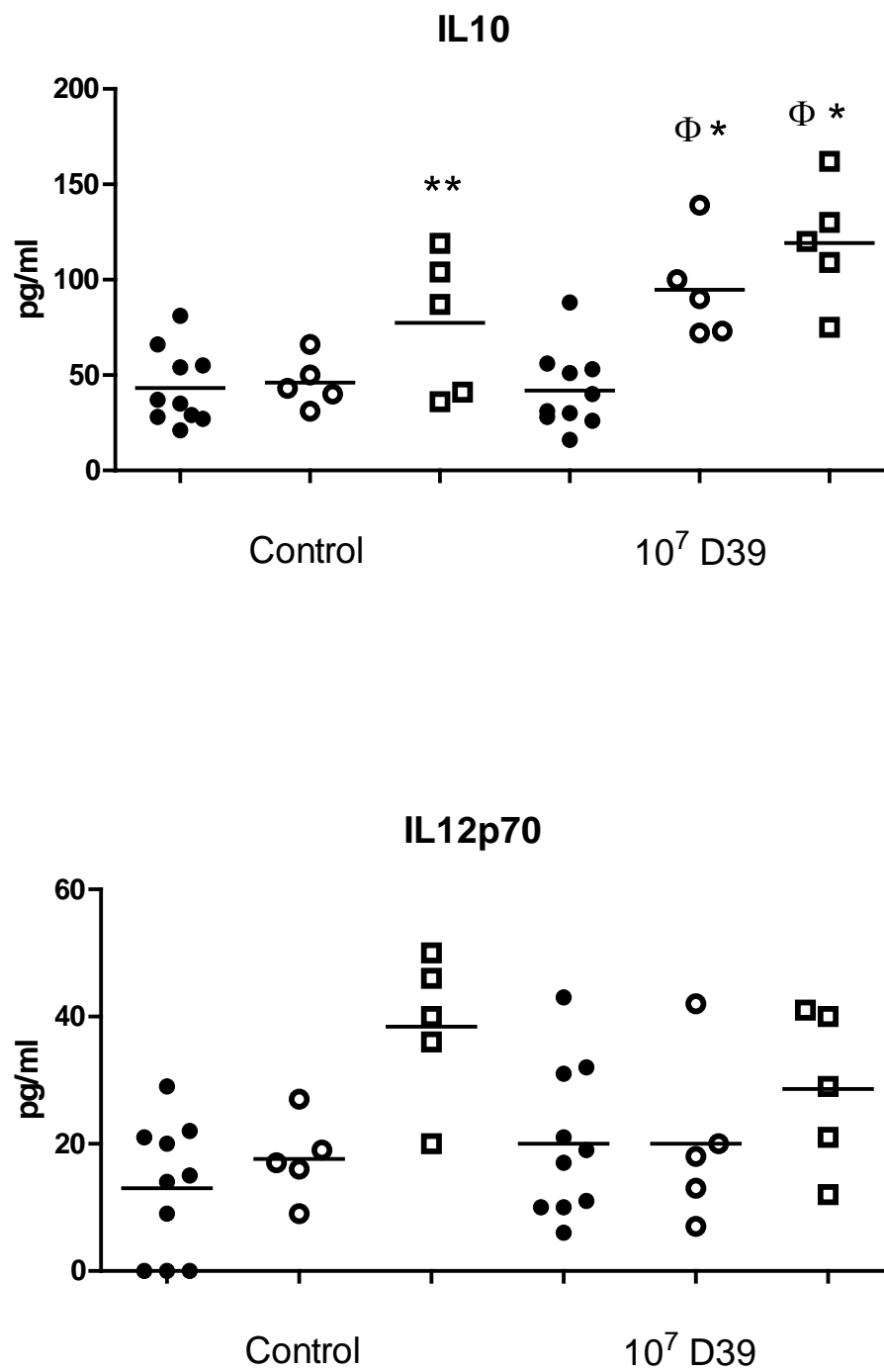


\*Significantly different from the same data in the healthy control ciliated cultures. \*\*

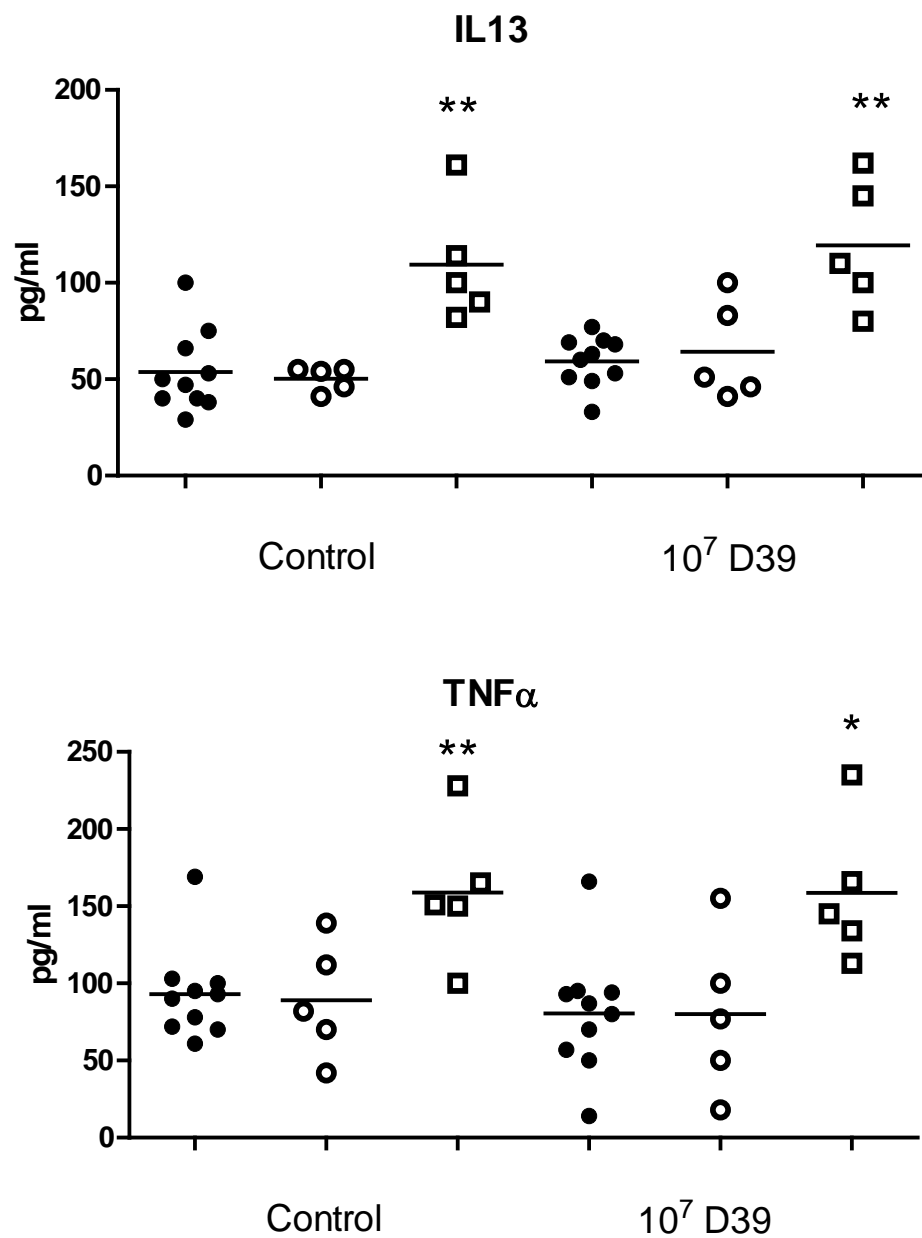
Significantly different from the same data in the control and the non static PCD cultures.  $\Phi$  significantly different from respective control.



\*Significantly different from the same data in the healthy control ciliated cultures. \*\* Significantly different from the same data in the control and the non static PCD cultures.  $\Phi$  significantly different from respective control.



\*Significantly different from the same data in the healthy control ciliated cultures. \*\* Significantly different from the same data in the control and the non static PCD cultures.  $\Phi$  significantly different from respective control.



\*Significantly different from the same data in the healthy control ciliated cultures. \*\* Significantly different from the same data in the control and the non static PCD cultures.  $\Phi$  significantly different from respective control.

**REFERENCE LIST**

- 
- Adriao, A., Vieira, M., Fernandes, I., Barbosa, M., Sol, M., Tenreiro, R.P., Chambel, L., Barata, B., Zilhao, I., Shama, G., Perni, S., Jordan, S.J., Andrew, P.W. & Faleiro, M.L., 2008. Marked intra-strain variation in response of listeria monocytogenes dairy isolates to acid or salt stress and the effect of acid or salt adaptation on adherence to abiotic surfaces. *Int J Food Microbiol*, 123 (1-2), 142-50
- Afzelius, B., 1979. Abnormal cilia. *Br Med J*, 2 (6191), 674
- Afzelius, B.A., 1976. A human syndrome caused by immotile cilia. *Science*, 193 (4250), 317-9
- Afzelius, B.A., 2000. Ciliary structure in health and disease. *Acta Otorhinolaryngol Belg*, 54 (3), 287-91
- Afzelius, B.A., 2004. Cilia-related diseases. *J Pathol*, 204 (4), 470-7
- Afzelius, B.A. & Eliasson, R., 1983. Male and female infertility problems in the immotile-cilia syndrome. *Eur J Respir Dis Suppl*, 127, 144-7
- Afzelius, B.A., Gargani, G. & Romano, C., 1985. Abnormal length of cilia as a possible cause of defective mucociliary clearance. *Eur J Respir Dis*, 66 (3), 173-80
- Al-Shroof, M., Karnik, A.M., Karnik, A.A., Longshore, J., Sliman, N.A. & Khan, F.A., 2001. Ciliary dyskinesia associated with hydrocephalus and mental retardation in a jordanian family. *Mayo Clin Proc*, 76 (12), 1219-24
- Alderton, W.K., Cooper, C.E. & Knowles, R.G., 2001. Nitric oxide synthases: Structure, function and inhibition. *Biochem J*, 357 (Pt 3), 593-615
- Allegrucci, M., Hu, F.Z., Shen, K., Hayes, J., Ehrlich, G.D., Post, J.C. & Sauer, K., 2006. Phenotypic characterization of streptococcus pneumoniae biofilm development. *J Bacteriol*, 188 (7), 2325-35

- 
- Amory-Rivier, C.F., Mohler, J., Bedos, J.P., Azoulay-Dupuis, E., Henin, D., Muffat-Joly, M., Carbon, C. & Moine, P., 2000. Nuclear factor-kappaB activation in mouse lung lavage cells in response to streptococcus pneumoniae pulmonary infection. *Crit Care Med*, 28 (9), 3249-56
- Anderson, R.G. & Hein, C.E., 1977. Distribution of anionic sites on the oviduct ciliary membrane. *J Cell Biol*, 72 (2), 482-92
- Anderton, T.L., Maskell, D.J. & Preston, A., 2004. Ciliostasis is a key early event during colonization of canine tracheal tissue by bordetella bronchiseptica. *Microbiology*, 150 (Pt 9), 2843-55
- Andrade, Y.N., Fernandes, J., Vazquez, E., Fernandez-Fernandez, J.M., Arniges, M., Sanchez, T.M., Villalon, M. & Valverde, M.A., 2005. Trpv4 channel is involved in the coupling of fluid viscosity changes to epithelial ciliary activity. *J Cell Biol*, 168 (6), 869-74
- Andrew, P.W., Mitchell, T.J. & Morgan, P.J., 1997. Relationship of structure to function in pneumolysin. *Microb Drug Resist*, 3 (1), 11-7
- Antonelli, M., Modesti, A., De Angelis, M., Marcolini, P., Lucarelli, N. & Crifo, S., 1981. Immotile cilia syndrome: Radial spokes deficiency in a patient with kartagener's triad. *Acta Paediatr Scand*, 70 (4), 571-3
- Antunes, M.B. & Cohen, N.A., 2007. Mucociliary clearance--a critical upper airway host defense mechanism and methods of assessment. *Curr Opin Allergy Clin Immunol*, 7 (1), 5-10
- Aparicio, O., Geisberg, J.V. & Struhl, K., 2004. Chromatin immunoprecipitation for determining the association of proteins with specific genomic sequences in vivo. *Curr Protoc Cell Biol*, Chapter 17, Unit 17 7

- 
- Arima, T., Shibata, Y. & Yamamoto, T., 1985. Three-dimensional visualization of basal body structures and some cytoskeletal components in the apical zone of tracheal ciliated cells. *J Ultrastruct Res*, 93 (1-2), 61-70
- Armstrong, B.A. & Sword, C.P., 1966. Electron microscopy of listeria monocytogenes-infected mouse spleen. *J Bacteriol*, 91 (3), 1346-55
- Asano, K., Chee, C.B., Gaston, B., Lilly, C.M., Gerard, C., Drazen, J.M. & Stamler, J.S., 1994. Constitutive and inducible nitric oxide synthase gene expression, regulation, and activity in human lung epithelial cells. *Proc Natl Acad Sci U S A*, 91 (21), 10089-93
- Attali, C., Durmort, C., Vernet, T. & Di Guilmi, A.M., 2008. The interaction of streptococcus pneumoniae with plasmin mediates transmigration across endothelial and epithelial monolayers by intercellular junction cleavage. *Infect Immun*, 76 (11), 5350-6
- Austrian, R., 1986. Some aspects of the pneumococcal carrier state. *J Antimicrob Chemother*, 18 Suppl A, 35-45
- Austrian, R., 2000. The enduring pneumococcus. In Tomasz, A. ed. *Streptococcus pneumoniae*. Larchmont, NY: Mary Ann Leibert, Inc.
- Avidor-Reiss, T., Maer, A.M., Koundakjian, E., Polyanovsky, A., Keil, T., Subramaniam, S. & Zuker, C.S., 2004. Decoding cilia function: Defining specialized genes required for compartmentalized cilia biogenesis. *Cell*, 117 (4), 527-39
- Baba, H., Kawamura, I., Kohda, C., Nomura, T., Ito, Y., Kimoto, T., Watanabe, I., Ichiyama, S. & Mitsuyama, M., 2002. Induction of gamma interferon and nitric

- oxide by truncated pneumolysin that lacks pore-forming activity. *Infect Immun*, 70 (1), 107-13
- Badano, J.L., Mitsuma, N., Beales, P.L. & Katsanis, N., 2006. The ciliopathies: An emerging class of human genetic disorders. *Annu Rev Genomics Hum Genet*, 7, 125-48
- Balachandran, P., Hollingshead, S.K., Paton, J.C. & Briles, D.E., 2001. The autolytic enzyme lyta of streptococcus pneumoniae is not responsible for releasing pneumolysin. *J Bacteriol*, 183 (10), 3108-16
- Balakrishnan, I., Crook, P., Morris, R. & Gillespie, S.H., 2000. Early predictors of mortality in pneumococcal bacteraemia. *J Infect*, 40 (3), 256-61
- Balder, R., Krunkosky, T.M., Nguyen, C.Q., Feezel, L. & Lafontaine, E.R., 2009. Hag mediates adherence of moraxella catarrhalis to ciliated human airway cells. *Infect Immun*, 77 (10), 4597-608
- Balfour-Lynn, I.M., Lavery, A. & Dinwiddie, R., 1996. Reduced upper airway nitric oxide in cystic fibrosis. *Arch Dis Child*, 75 (4), 319-22
- Banizs, B., Pike, M.M., Millican, C.L., Ferguson, W.B., Komlosi, P., Sheetz, J., Bell, P.D., Schwiebert, E.M. & Yoder, B.K., 2005. Dysfunctional cilia lead to altered ependyma and choroid plexus function, and result in the formation of hydrocephalus. *Development*, 132 (23), 5329-39
- Bannister, B.A., N. T. Begg and S. H. Gillespie, 1996. *Infectious disease* Oxford: Blackwell Science.
- Barbato, A., Frischer, T., Kuehni, C.E., Snijders, D., Azevedo, I., Baktai, G., Bartoloni, L., Eber, E., Escribano, A., Haarman, E., Hesselmar, B., Hogg, C., Jorissen, M., Lucas, J., Nielsen, K.G., O'callaghan, C., Omran, H., Pohunek, P., Strippoli,

- 
- M.P. & Bush, A., 2009. Primary ciliary dyskinesia: A consensus statement on diagnostic and treatment approaches in children. *Eur Respir J*, 34 (6), 1264-76
- Barnes, P.J., 2009. The cytokine network in chronic obstructive pulmonary disease. *Am J Respir Cell Mol Biol*, 41 (6), 631-8
- Barr, M.M., 2005. Caenorhabditis elegans as a model to study renal development and disease: Sexy cilia. *J Am Soc Nephrol*, 16 (2), 305-12
- Barrera, N.P., Morales, B. & Villalon, M., 2004. Plasma and intracellular membrane inositol 1,4,5-trisphosphate receptors mediate the  $Ca^{2+}$  increase associated with the atp-induced increase in ciliary beat frequency. *Am J Physiol Cell Physiol*, 287 (4), C1114-24
- Barthelson, R., Mobasser, A., Zopf, D. & Simon, P., 1998. Adherence of streptococcus pneumoniae to respiratory epithelial cells is inhibited by sialylated oligosaccharides. *Infect Immun*, 66 (4), 1439-44
- Bartoloni, L., Blouin, J.L., Pan, Y., Gehrig, C., Maiti, A.K., Scamuffa, N., Rossier, C., Jorissen, M., Armengot, M., Meeks, M., Mitchison, H.M., Chung, E.M., Delozier-Blanchet, C.D., Craigen, W.J. & Antonarakis, S.E., 2002. Mutations in the *dnah11* (axonemal heavy chain dynein type 11) gene cause one form of situs inversus totalis and most likely primary ciliary dyskinesia. *Proc Natl Acad Sci U S A*, 99 (16), 10282-6
- Bayles, K.W., 2007. The biological role of death and lysis in biofilm development. *Nat Rev Microbiol*, 5 (9), 721-6
- Belvisi, M.G., Stretton, C.D., Yacoub, M. & Barnes, P.J., 1992. Nitric oxide is the endogenous neurotransmitter of bronchodilator nerves in humans. *Eur J Pharmacol*, 210 (2), 221-2

- 
- Bemis, D.A. & Wilson, S.A., 1985. Influence of potential virulence determinants on bordetella bronchiseptica-induced ciliostasis. *Infect Immun*, 50 (1), 35-42
- Benzing, T. & Walz, G., 2006. Cilium-generated signaling: A cellular gps? *Curr Opin Nephrol Hypertens*, 15 (3), 245-9
- Berry, A.M., Lock, R.A., Hansman, D. & Paton, J.C., 1989a. Contribution of autolysin to virulence of streptococcus pneumoniae. *Infect Immun*, 57 (8), 2324-30
- Berry, A.M., Lock, R.A. & Paton, J.C., 1996. Cloning and characterization of nanb, a second streptococcus pneumoniae neuraminidase gene, and purification of the nanb enzyme from recombinant escherichia coli. *J Bacteriol*, 178 (16), 4854-60
- Berry, A.M., Lock, R.A., Thomas, S.M., Rajan, D.P., Hansman, D. & Paton, J.C., 1994. Cloning and nucleotide sequence of the streptococcus pneumoniae hyaluronidase gene and purification of the enzyme from recombinant escherichia coli. *Infect Immun*, 62 (3), 1101-8
- Berry, A.M. & Paton, J.C., 1996. Sequence heterogeneity of psaa, a 37-kilodalton putative adhesin essential for virulence of streptococcus pneumoniae. *Infect Immun*, 64 (12), 5255-62
- Berry, A.M., Yother, J., Briles, D.E., Hansman, D. & Paton, J.C., 1989b. Reduced virulence of a defined pneumolysin-negative mutant of streptococcus pneumoniae. *Infect Immun*, 57 (7), 2037-42
- Biggart, E., Pritchard, K., Wilson, R. & Bush, A., 2001. Primary ciliary dyskinesia syndrome associated with abnormal ciliary orientation in infants. *Eur Respir J*, 17 (3), 444-8

- 
- Blanchard, B., Vena, M.M., Cavalier, A., Le Lannic, J., Gouranton, J. & Kobisch, M., 1992. Electron microscopic observation of the respiratory tract of spf piglets inoculated with mycoplasma hyopneumoniae. *Vet Microbiol*, 30 (4), 329-41
- Blouin, J.L., Meeks, M., Radhakrishna, U., Sainsbury, A., Gehring, C., Sail, G.D., Bartoloni, L., Dombi, V., O'rawe, A., Walne, A., Chung, E., Afzelius, B.A., Armengot, M., Jorissen, M., Schidlow, D.V., Van Maldergem, L., Walt, H., Gardiner, R.M., Probst, D., Guerne, P.A., Delozier-Blanchet, C.D. & Antonarakis, S.E., 2000. Primary ciliary dyskinesia: A genome-wide linkage analysis reveals extensive locus heterogeneity. *Eur J Hum Genet*, 8 (2), 109-18
- Booth, J.W., Telio, D., Liao, E.H., Mccaw, S.E., Matsuo, T., Grinstein, S. & Gray-Owen, S.D., 2003. Phosphatidylinositol 3-kinases in carcinoembryonic antigen-related cellular adhesion molecule-mediated internalization of neisseria gonorrhoeae. *J Biol Chem*, 278 (16), 14037-45
- Borucki, M.K., Peppin, J.D., White, D., Loge, F. & Call, D.R., 2003. Variation in biofilm formation among strains of listeria monocytogenes. *Appl Environ Microbiol*, 69 (12), 7336-42
- Boucher, 1994a. Human airway ion transport. Part 1. *Am J Respir Crit Care Med.*, 150, 271-281
- Boucher, 1994b. Human airway ion transport. Part 2. *Am J Respir Crit Care Med.*, 150, 581-593.
- Boulnois, G.J., Paton, J.C., Mitchell, T.J. & Andrew, P.W., 1991. Structure and function of pneumolysin, the multifunctional, thiol-activated toxin of streptococcus pneumoniae. *Mol Microbiol*, 5 (11), 2611-6

- 
- Bove, P.F. & Van Der Vliet, A., 2006. Nitric oxide and reactive nitrogen species in airway epithelial signaling and inflammation. *Free Radic Biol Med*, 41 (4), 515-27
- Boyle, E.C. & Finlay, B.B., 2003. Bacterial pathogenesis: Exploiting cellular adherence. *Curr Opin Cell Biol*, 15 (5), 633-9
- Bradbury, K. & Lumsden, C.E., 1979. The chemical composition of myelin in organ cultures of rat cerebellum. *J Neurochem*, 32 (1), 145-54
- Braiman, A. & Priel, Z., 2008. Efficient mucociliary transport relies on efficient regulation of ciliary beating. *Respir Physiol Neurobiol*, 163 (1-3), 202-7
- Braiman, A., Zagoory, O. & Priel, Z., 1998. Pka induces ca<sup>2+</sup> release and enhances ciliary beat frequency in a ca<sup>2+</sup>-dependent and -independent manner. *Am J Physiol*, 275 (3 Pt 1), C790-7
- Braun, J.S., Novak, R., Gao, G., Murray, P.J. & Shenep, J.L., 1999. Pneumolysin, a protein toxin of streptococcus pneumoniae, induces nitric oxide production from macrophages. *Infect Immun*, 67 (8), 3750-6
- Breeuwer, P., Drocourt, J., Rombouts, F.M. & Abee, T., 1996. A novel method for continuous determination of the intracellular ph in bacteria with the internally conjugated fluorescent probe 5 (and 6-)-carboxyfluorescein succinimidyl ester. *Appl Environ Microbiol*, 62 (1), 178-183
- Breeze, R.G. & Wheeldon, E.B., 1977. The cells of the pulmonary airways. *Am Rev Respir Dis*, 116 (4), 705-77
- Briles, D.E., Ades, E., Paton, J.C., Sampson, J.S., Carlone, G.M., Huebner, R.C., Virolainen, A., Swiatlo, E. & Hollingshead, S.K., 2000a. Intranasal immunization of mice with a mixture of the pneumococcal proteins psaa and

- 
- pspa is highly protective against nasopharyngeal carriage of streptococcus pneumoniae. *Infect Immun*, 68 (2), 796-800
- Briles, D.E., Hollingshead, S., Brooks-Walter, A., Nabors, G.S., Ferguson, L., Schilling, M., Gravenstein, S., Braun, P., King, J. & Swift, A., 2000b. The potential to use pspa and other pneumococcal proteins to elicit protection against pneumococcal infection. *Vaccine*, 18 (16), 1707-11
- Brody, S.L., 2004. Genetic regulation of cilia assembly and the relationship to human disease. *Am J Respir Cell Mol Biol*, 30 (4), 435-7
- Brody, S.L., Yan, X.H., Wuerffel, M.K., Song, S.K. & Shapiro, S.D., 2000. Ciliogenesis and left-right axis defects in forkhead factor hfh-4-null mice. *Am J Respir Cell Mol Biol*, 23 (1), 45-51
- Brown, J.S., Gilliland, S.M., Ruiz-Albert, J. & Holden, D.W., 2002. Characterization of pit, a streptococcus pneumoniae iron uptake abc transporter. *Infect Immun*, 70 (8), 4389-98
- Bruni, J.E., Del Bigio, M.R. & Clattenburg, R.E., 1985. Ependyma: Normal and pathological. A review of the literature. *Brain Res*, 356 (1), 1-19
- Budny, B., Chen, W., Omran, H., Fliegauf, M., Tzschach, A., Wisniewska, M., Jensen, L.R., Raynaud, M., Shoichet, S.A., Badura, M., Lenzner, S., Latos-Bielenska, A. & Ropers, H.H., 2006. A novel x-linked recessive mental retardation syndrome comprising macrocephaly and ciliary dysfunction is allelic to oral-facial-digital type i syndrome. *Hum Genet*, 120 (2), 171-8
- Bush, A., Chodhari, R., Collins, N., Copeland, F., Hall, P., Harcourt, J., Hariri, M., Hogg, C., Lucas, J., Mitchison, H.M., O'callaghan, C. & Phillips, G., 2007.

- 
- Primary ciliary dyskinesia: Current state of the art. *Arch Dis Child*, 92 (12), 1136-40
- Bush, A., Cole, P., Hariri, M., Mackay, I., Phillips, G., O'callaghan, C., Wilson, R. & Warner, J.O., 1998. Primary ciliary dyskinesia: Diagnosis and standards of care. *Eur Respir J*, 12 (4), 982-8
- Camara, M., Boulnois, G.J., Andrew, P.W. & Mitchell, T.J., 1994. A neuraminidase from streptococcus pneumoniae has the features of a surface protein. *Infect Immun*, 62 (9), 3688-95
- Canvin, J.R., Marvin, A.P., Sivakumaran, M., Paton, J.C., Boulnois, G.J., Andrew, P.W. & Mitchell, T.J., 1995. The role of pneumolysin and autolysin in the pathology of pneumonia and septicemia in mice infected with a type 2 pneumococcus. *J Infect Dis*, 172 (1), 119-23
- Carson, J.L. & Collier, A.M., 1988. Ciliary defects: Cell biology and clinical perspectives. *Adv Pediatr*, 35, 139-65
- Castleman, V.H., Romio, L., Chodhari, R., Hirst, R.A., De Castro, S.C., Parker, K.A., Ybot-Gonzalez, P., Emes, R.D., Wilson, S.W., Wallis, C., Johnson, C.A., Herrera, R.J., Rutman, A., Dixon, M., Shoemark, A., Bush, A., Hogg, C., Gardiner, R.M., Reish, O., Greene, N.D., O'callaghan, C., Purton, S., Chung, E.M. & Mitchison, H.M., 2009. Mutations in radial spoke head protein genes rsph9 and rsph4a cause primary ciliary dyskinesia with central-microtubular-pair abnormalities. *Am J Hum Genet*, 84 (2), 197-209
- Cathcart, R.S., 3rd & Worthington, W.C., Jr., 1964. Ciliary movement in the rat cerebral ventricles: Clearing action and directions of currents. *J Neuropathol Exp Neurol*, 23, 609-18

- 
- Chakraborty, T., Leimeister-Wachter, M., Domann, E., Hartl, M., Goebel, W.,  
Nichterlein, T. & Notermans, S., 1992. Coordinate regulation of virulence genes  
in *listeria monocytogenes* requires the product of the *prfa* gene. *J Bacteriol*, 174  
(2), 568-74
- Chao, J., Turner, J.A. & Sturgess, J.M., 1982. Genetic heterogeneity of dynein-  
deficiency in cilia from patients with respiratory disease. *Am Rev Respir Dis*,  
126 (2), 302-5
- Chapman, S.J., Khor, C.C., Vannberg, F.O., Frodsham, A., Walley, A., Maskell, N.A.,  
Davies, C.W., Segal, S., Moore, C.E., Gillespie, S.H., Denny, P., Day, N.P.,  
Crook, D.W., Davies, R.J. & Hill, A.V., 2007. Ikappab genetic polymorphisms  
and invasive pneumococcal disease. *Am J Respir Crit Care Med*, 176 (2), 181-7
- Chico-Calero, I., Suarez, M., Gonzalez-Zorn, B., Scotti, M., Slaghuis, J., Goebel, W. &  
Vazquez-Boland, J.A., 2002. Hpt, a bacterial homolog of the microsomal  
glucose- 6-phosphate translocase, mediates rapid intracellular proliferation in  
*listeria*. *Proc Natl Acad Sci U S A*, 99 (1), 431-6
- Chilvers, M.A. & O'callaghan, C., 2000a. Analysis of ciliary beat pattern and beat  
frequency using digital high speed imaging: Comparison with the  
photomultiplier and photodiode methods. *Thorax*, 55 (4), 314-7
- Chilvers, M.A. & O'callaghan, C., 2000b. Local mucociliary defence mechanisms.  
*Paediatr Respir Rev*, 1 (1), 27-34
- Chilvers, M.A., Rutman, A. & O'callaghan, C., 2003a. Ciliary beat pattern is associated  
with specific ultrastructural defects in primary ciliary dyskinesia. *J Allergy Clin  
Immunol*, 112 (3), 518-24

- 
- Chilvers, M.A., Rutman, A. & O'callaghan, C., 2003b. Functional analysis of cilia and ciliated epithelial ultrastructure in healthy children and young adults. *Thorax*, 58 (4), 333-8
- Chodhari, R., Mitchison, H.M. & Meeks, M., 2004. Cilia, primary ciliary dyskinesia and molecular genetics. *Paediatr Respir Rev*, 5 (1), 69-76
- Clausen, J.D., Christiansen, G., Holst, H.U. & Birkelund, S., 1997. Chlamydia trachomatis utilizes the host cell microtubule network during early events of infection. *Mol Microbiol*, 25 (3), 441-9
- Cockeran, R., Durandt, C., Feldman, C., Mitchell, T.J. & Anderson, R., 2002. Pneumolysin activates the synthesis and release of interleukin-8 by human neutrophils in vitro. *J Infect Dis*, 186 (4), 562-5
- Cook, H.T. & Cattell, V., 1996. Role of nitric oxide in immune-mediated diseases. *Clin Sci (Lond)*, 91 (4), 375-84
- Corbelli, R., Bringolf-Isler, B., Amacher, A., Sasse, B., Spycher, M. & Hammer, J., 2004. Nasal nitric oxide measurements to screen children for primary ciliary dyskinesia. *Chest*, 126 (4), 1054-9
- Cordier, A.C., 1975. Ultrastructure of the cilia of thymic cysts in "Nude" Mice. *Anat Rec*, 181 (2), 227-49
- Coren, M.E., Meeks, M., Morrison, I., Buchdahl, R.M. & Bush, A., 2002. Primary ciliary dyskinesia: Age at diagnosis and symptom history. *Acta Paediatr*, 91 (6), 667-9
- Cossart, P. & Lecuit, M., 1998. Interactions of listeria monocytogenes with mammalian cells during entry and actin-based movement: Bacterial factors, cellular ligands and signaling. *Embo J*, 17 (14), 3797-806

- 
- Crain, M.J., Waltman, W.D., 2nd, Turner, J.S., Yother, J., Talkington, D.F., Mcdaniel, L.S., Gray, B.M. & Briles, D.E., 1990. Pneumococcal surface protein a (pspa) is serologically highly variable and is expressed by all clinically important capsular serotypes of streptococcus pneumoniae. *Infect Immun*, 58 (10), 3293-9
- Croen, K.D., 1993. Evidence for antiviral effect of nitric oxide. Inhibition of herpes simplex virus type 1 replication. *J Clin Invest*, 91 (6), 2446-52
- Csoma, Z., Bush, A., Wilson, N.M., Donnelly, L., Balint, B., Barnes, P.J. & Kharitonov, S.A., 2003. Nitric oxide metabolites are not reduced in exhaled breath condensate of patients with primary ciliary dyskinesia. *Chest*, 124 (2), 633-8
- Cucarella, C., Solano, C., Valle, J., Amorena, B., Lasa, I. & Penades, J.R., 2001. Bap, a staphylococcus aureus surface protein involved in biofilm formation. *J Bacteriol*, 183 (9), 2888-96
- Cundell, D.R., Gerard, N.P., Gerard, C., Idanpaan-Heikkila, I. & Tuomanen, E.I., 1995. Streptococcus pneumoniae anchor to activated human cells by the receptor for platelet-activating factor. *Nature*, 377 (6548), 435-8
- De Jongh, R.U. & Rutland, J., 1995. Ciliary defects in healthy subjects, bronchiectasis, and primary ciliary dyskinesia. *Am J Respir Crit Care Med*, 151 (5), 1559-67
- De Rose, V., 2002. Mechanisms and markers of airway inflammation in cystic fibrosis. *Eur Respir J*, 19 (2), 333-40
- De Santi, M.M., Magni, A., Valletta, E.A., Gardi, C. & Lungarella, G., 1990. Hydrocephalus, bronchiectasis, and ciliary aplasia. *Arch Dis Child*, 65 (5), 543-4
- Deboeck, K., Jorissen, M., Wouters, K., Van Der Schueren, B., Eyssen, M., Casteels-Vandaele, M. & Corbeel, L., 1992. Aplasia of respiratory tract cilia. *Pediatr Pulmonol*, 13 (4), 259-65

- 
- Deckert, M., Soltek, S., Geginat, G., Lutjen, S., Montesinos-Rongen, M., Hof, H. & Schluter, D., 2001. Endogenous interleukin-10 is required for prevention of a hyperinflammatory intracerebral immune response in *listeria monocytogenes* meningoencephalitis. *Infect Immun*, 69 (7), 4561-71
- Del Bigio, M.R., 1995. The ependyma: A protective barrier between brain and cerebrospinal fluid. *Glia*, 14 (1), 1-13
- Dentler, W.L., 1981. Microtubule-membrane interactions in cilia and flagella. *Int Rev Cytol*, 72, 1-47
- Dentler, W.L. & Lecluyse, E.L., 1982. Microtubule capping structures at the tips of tracheal cilia: Evidence for their firm attachment during ciliary bend formation and the restriction of microtubule sliding. *Cell Motil*, 2 (6), 549-72
- Di Benedetto, G., Magnus, C.J., Gray, P.T. & Mehta, A., 1991a. Calcium regulation of ciliary beat frequency in human respiratory epithelium in vitro. *J Physiol*, 439, 103-13
- Di Benedetto, G., Manara-Shediac, F.S. & Mehta, A., 1991b. Effect of cyclic amp on ciliary activity of human respiratory epithelium. *Eur Respir J*, 4 (7), 789-95
- Dintilhac, A., Alloing, G., Granadel, C. & Claverys, J.P., 1997. Competence and virulence of streptococcus pneumoniae: Adc and psaa mutants exhibit a requirement for zn and mn resulting from inactivation of putative abc metal permeases. *Mol Microbiol*, 25 (4), 727-39
- Dirksen, E.R. & Satir, P., 1972. Ciliary activity in the mouse oviduct as studied by transmission and scanning electron microscopy. *Tissue Cell*, 4 (3), 389-403
- Domann, E., Wehland, J., Rohde, M., Pistor, S., Hartl, M., Goebel, W., Leimeister-Wachter, M., Wuenscher, M. & Chakraborty, T., 1992. A novel bacterial

- 
- virulence gene in listeria monocytogenes required for host cell microfilament interaction with homology to the proline-rich region of vinculin. *Embo J*, 11 (5), 1981-90
- Downing, K.H. & Sui, H., 2007. Structural insights into microtubule doublet interactions in axonemes. *Curr Opin Struct Biol*, 17 (2), 253-9
- Drevets, D.A. & Elliott, A.M., 1995. Fluorescence labeling of bacteria for studies of intracellular pathogenesis. *J Immunol Methods*, 187 (1), 69-79
- Drevets, D.A., Leenen, P.J. & Greenfield, R.A., 2004. Invasion of the central nervous system by intracellular bacteria. *Clin Microbiol Rev*, 17 (2), 323-47
- Dry, K.L., Manson, F.D., Lennon, A., Bergen, A.A., Van Dorp, D.B. & Wright, A.F., 1999. Identification of a 5' splice site mutation in the rpgr gene in a family with x-linked retinitis pigmentosa (rp3). *Hum Mutat*, 13 (2), 141-5
- Dutcher, S.K., 2003. Elucidation of basal body and centriole functions in chlamydomonas reinhardtii. *Traffic*, 4 (7), 443-51
- Dute, R. & Kung, C., 1978. Ultrastructure of the proximal region of somatic cilia in paramecium tetraurelia. *J Cell Biol*, 78 (2), 451-64
- Edwards, J.A., Groathouse, N.A. & Boitano, S., 2005. Bordetella bronchiseptica adherence to cilia is mediated by multiple adhesin factors and blocked by surfactant protein a. *Infect Immun*, 73 (6), 3618-26
- Eggenschwiler, J.T. & Anderson, K.V., 2007. Cilia and developmental signaling. *Annu Rev Cell Dev Biol*, 23, 345-73
- El-Rachkidy, R.G., Davies, N.W. & Andrew, P.W., 2008. Pneumolysin generates multiple conductance pores in the membrane of nucleated cells. *Biochem Biophys Res Commun*, 368 (3), 786-92

- 
- Eliasson, R., Mossberg, B., Camner, P. & Afzelius, B.A., 1977. The immotile-cilia syndrome. A congenital ciliary abnormality as an etiologic factor in chronic airway infections and male sterility. *N Engl J Med*, 297 (1), 1-6
- Ellerman, A. & Bisgaard, H., 1997. Longitudinal study of lung function in a cohort of primary ciliary dyskinesia. *Eur Respir J*, 10 (10), 2376-9
- Engelbrecht, F., Chun, S.K., Ochs, C., Hess, J., Lottspeich, F., Goebel, W. & Sokolovic, Z., 1996. A new prfa-regulated gene of listeria monocytogenes encoding a small, secreted protein which belongs to the family of internalins. *Mol Microbiol*, 21 (4), 823-37
- Engesaeth, V.G., Warner, J.O. & Bush, A., 1993. New associations of primary ciliary dyskinesia syndrome. *Pediatr Pulmonol*, 16 (1), 9-12
- Fader, R.C., Gondesens, K., Tolley, B., Ritchie, D.G. & Moller, P., 1988. Evidence that in vitro adherence of klebsiella pneumoniae to ciliated hamster tracheal cells is mediated by type 1 fimbriae. *Infect Immun*, 56 (11), 3011-3
- Farber, J.M. & Peterkin, P.I., 1991. Listeria monocytogenes, a food-borne pathogen. *Microbiol Rev*, 55 (3), 476-511
- Feldman, C., Mitchell, T.J., Andrew, P.W., Boulnois, G.J., Read, R.C., Todd, H.C., Cole, P.J. & Wilson, R., 1990. The effect of streptococcus pneumoniae pneumolysin on human respiratory epithelium in vitro. *Microb Pathog*, 9 (4), 275-84
- Feldman, C., Munro, N.C., Jeffery, P.K., Mitchell, T.J., Andrew, P.W., Boulnois, G.J., Guerreiro, D., Rohde, J.A., Todd, H.C., Cole, P.J. & Et Al., 1991. Pneumolysin induces the salient histologic features of pneumococcal infection in the rat lung in vivo. *Am J Respir Cell Mol Biol*, 5 (5), 416-23

- 
- Feldman, C., Read, R., Rutman, A., Jeffery, P.K., Brain, A., Lund, V., Mitchell, T.J., Andrew, P.W., Boulnois, G.J., Todd, H.C. & Et Al., 1992. The interaction of streptococcus pneumoniae with intact human respiratory mucosa in vitro. *Eur Respir J*, 5 (5), 576-83
- Ferkol, T. & Leigh, M., 2006. Primary ciliary dyskinesia and newborn respiratory distress. *Semin Perinatol*, 30 (6), 335-40
- Ferrante, A., Rowan-Kelly, B. & Paton, J.C., 1984. Inhibition of in vitro human lymphocyte response by the pneumococcal toxin pneumolysin. *Infect Immun*, 46 (2), 585-9
- Ferrante, M.I., Giorgio, G., Feather, S.A., Bulfone, A., Wright, V., Ghiani, M., Selicorni, A., Gammara, L., Scolari, F., Woolf, A.S., Sylvie, O., Bernard, L., Malcolm, S., Winter, R., Ballabio, A. & Franco, B., 2001. Identification of the gene for oral-facial-digital type i syndrome. *Am J Hum Genet*, 68 (3), 569-76
- Fiorini, R., Littarru, G.P., Coppa, G.V. & Kantar, A., 2000. Plasma membrane polarity of polymorphonuclear leucocytes from children with primary ciliary dyskinesia. *Eur J Clin Invest*, 30 (6), 519-25
- Fitzgerald, T.J. & Repesh, L.A., 1987. The hyaluronidase associated with treponema pallidum facilitates treponemal dissemination. *Infect Immun*, 55 (5), 1023-8
- Fliegauf, M., Benzing, T. & Omran, H., 2007. When cilia go bad: Cilia defects and ciliopathies. *Nat Rev Mol Cell Biol*, 8 (11), 880-93
- Fliegauf, M., Olbrich, H., Horvath, J., Wildhaber, J.H., Zariwala, M.A., Kennedy, M., Knowles, M.R. & Omran, H., 2005. Mislocalization of dnah5 and dnah9 in respiratory cells from patients with primary ciliary dyskinesia. *Am J Respir Crit Care Med*, 171 (12), 1343-9

- 
- Foliguet, B. & Puchelle, E., 1986. Apical structure of human respiratory cilia. *Bull Eur Physiopathol Respir*, 22 (1), 43-7
- Forteza, R., Lieb, T., Aoki, T., Savani, R.C., Conner, G.E. & Salathe, M., 2001. Hyaluronan serves a novel role in airway mucosal host defense. *Faseb J*, 15 (12), 2179-86
- Freitag, N.E., 2006. From hot dogs to host cells: How the bacterial pathogen listeria monocytogenes regulates virulence gene expression. *Future Microbiol*, 1, 89-101
- Freitag, N.E., Rong, L. & Portnoy, D.A., 1993. Regulation of the prfa transcriptional activator of listeria monocytogenes: Multiple promoter elements contribute to intracellular growth and cell-to-cell spread. *Infect Immun*, 61 (6), 2537-44
- Freitag, N.E., Youngman, P. & Portnoy, D.A., 1992. Transcriptional activation of the listeria monocytogenes hemolysin gene in bacillus subtilis. *J Bacteriol*, 174 (4), 1293-8
- Freshney, R. ed. 1987. *Culture of animal cells: A manual of basic technique*, New York: Liss, Inc.
- Friedland, I.R., Paris, M.M., Hickey, S., Shelton, S., Olsen, K., Paton, J.C. & Mccracken, G.H., 1995. The limited role of pneumolysin in the pathogenesis of pneumococcal meningitis. *J Infect Dis*, 172 (3), 805-9
- Gardner, L.C., O'toole, E., Perrone, C.A., Giddings, T. & Porter, M.E., 1994. Components of a "Dynein regulatory complex" Are located at the junction between the radial spokes and the dynein arms in chlamydomonas flagella. *J Cell Biol*, 127 (5), 1311-25

- 
- Garton, H.J. & Piatt, J.H., Jr., 2004. Hydrocephalus. *Pediatr Clin North Am*, 51 (2), 305-25
- Gaston, B., Drazen, J.M., Loscalzo, J. & Stamler, J.S., 1994. The biology of nitrogen oxides in the airways. *Am J Respir Crit Care Med*, 149 (2 Pt 1), 538-51
- Geary, C.A., Davis, C.W., Paradiso, A.M. & Boucher, R.C., 1995. Role of cnp in human airways: Cgmp-mediated stimulation of ciliary beat frequency. *Am J Physiol*, 268 (6 Pt 1), L1021-8
- Gedde, M.M., Higgins, D.E., Tilney, L.G. & Portnoy, D.A., 2000. Role of listeriolysin o in cell-to-cell spread of listeria monocytogenes. *Infect Immun*, 68 (2), 999-1003
- Geremek, M. & Witt, M., 2004. Primary ciliary dyskinesia: Genes, candidate genes and chromosomal regions. *J Appl Genet*, 45 (3), 347-61
- Gershoni-Baruch, R., Gottfried, E., Pery, M., Sahin, A. & Etzioni, A., 1989. Immotile cilia syndrome including polysplenia, situs inversus, and extrahepatic biliary atresia. *Am J Med Genet*, 33 (3), 390-3
- Gertsberg, I., Hellman, V., Fainshtein, M., Weil, S., Silberberg, S.D., Danilenko, M. & Priel, Z., 2004. Intracellular ca<sup>2+</sup> regulates the phosphorylation and the dephosphorylation of ciliary proteins via the no pathway. *J Gen Physiol*, 124 (5), 527-40
- Gheber, L., Korngreen, A. & Priel, Z., 1998. Effect of viscosity on metachrony in mucus propelling cilia. *Cell Motil Cytoskeleton*, 39 (1), 9-20
- Gheber, L. & Priel, Z., 1989. Synchronization between beating cilia. *Biophys J*, 55 (1), 183-91
- Gibbons, I.R., 1995. Dynein family of motor proteins: Present status and future questions. *Cell Motil Cytoskeleton*, 32 (2), 136-44

- 
- Gilbert, R.J., Heenan, R.K., Timmins, P.A., Gingles, N.A., Mitchell, T.J., Rowe, A.J., Rossjohn, J., Parker, M.W., Andrew, P.W. & Byron, O., 1999. Studies on the structure and mechanism of a bacterial protein toxin by analytical ultracentrifugation and small-angle neutron scattering. *J Mol Biol*, 293 (5), 1145-60
- Gilula, N.B. & Satir, P., 1972. The ciliary necklace. A ciliary membrane specialization. *J Cell Biol*, 53 (2), 494-509
- Girard, P.R. & Kennedy, J.R., 1986. Calcium regulation of ciliary activity in rabbit tracheal epithelial explants and outgrowth. *Eur J Cell Biol*, 40 (2), 203-9
- Glaser, P., Frangeul, L., Buchrieser, C., Rusniok, C., Amend, A., Baquero, F., Berche, P., Bloecker, H., Brandt, P., Chakraborty, T., Charbit, A., Chetouani, F., Couve, E., De Daruvar, A., Dehoux, P., Domann, E., Dominguez-Bernal, G., Duchaud, E., Durant, L., Dussurget, O., Entian, K.D., Fsihi, H., Garcia-Del Portillo, F., Garrido, P., Gautier, L., Goebel, W., Gomez-Lopez, N., Hain, T., Hauf, J., Jackson, D., Jones, L.M., Kaerst, U., Kreft, J., Kuhn, M., Kunst, F., Kurapkat, G., Madueno, E., Maitournam, A., Vicente, J.M., Ng, E., Nedjari, H., Nordsiek, G., Novella, S., De Pablos, B., Perez-Diaz, J.C., Purcell, R., Rimmel, B., Rose, M., Schlueter, T., Simoes, N., Tierrez, A., Vazquez-Boland, J.A., Voss, H., Wehland, J. & Cossart, P., 2001. Comparative genomics of listeria species. *Science*, 294 (5543), 849-52
- Goebel, W. & Kreft, J., 1997. Cytolysins and the intracellular life of bacteria. *Trends Microbiol*, 5 (3), 86-8
- Goldfine, H., Knob, C., Alford, D. & Bentz, J., 1995. Membrane permeabilization by listeria monocytogenes phosphatidylinositol-specific phospholipase c is

- independent of phospholipid hydrolysis and cooperative with listeriolysin o.  
*Proc Natl Acad Sci U S A*, 92 (7), 2979-83
- Goldfine, H., Wadsworth, S.J. & Johnston, N.C., 2000. Activation of host phospholipases c and d in macrophages after infection with listeria monocytogenes. *Infect Immun*, 68 (10), 5735-41
- Gomez, M.I. & Prince, A., 2007. Opportunistic infections in lung disease: Pseudomonas infections in cystic fibrosis. *Curr Opin Pharmacol*, 7 (3), 244-51
- Gosink, K.K., Mann, E.R., Guglielmo, C., Tuomanen, E.I. & Masure, H.R., 2000. Role of novel choline binding proteins in virulence of streptococcus pneumoniae. *Infect Immun*, 68 (10), 5690-5
- Gould, S.J., Howard, S. & Papadaki, L., 1990. The development of ependyma in the human fetal brain: An immunohistological and electron microscopic study. *Brain Res Dev Brain Res*, 55 (2), 255-67
- Grafe, G., Handrik, W. & Geyer, C., 2001. Hydrocephalus internus--first manifestation of chronic meningitis due to listeria monocytogenes. *Eur J Pediatr Surg*, 11 Suppl 1, S46-7
- Gray, M.L. & Killinger, A.H., 1966. Listeria monocytogenes and listeric infections. *Bacteriol Rev*, 30 (2), 309-82
- Gray, T.E., Guzman, K., Davis, C.W., Abdullah, L.H. & Nettesheim, P., 1996. Mucociliary differentiation of serially passaged normal human tracheobronchial epithelial cells. *Am J Respir Cell Mol Biol*, 14 (1), 104-12
- Greene, C.M. & Mcelvaney, N.G., 2005. Toll-like receptor expression and function in airway epithelial cells. *Arch Immunol Ther Exp (Warsz)*, 53 (5), 418-27

- 
- Greenstone, M., Rutman, A., Dewar, A., Mackay, I. & Cole, P.J., 1988. Primary ciliary dyskinesia: Cytological and clinical features. *Q J Med*, 67 (253), 405-23
- Greenstone, M.A., Jones, R.W., Dewar, A., Neville, B.G. & Cole, P.J., 1984. Hydrocephalus and primary ciliary dyskinesia. *Arch Dis Child*, 59 (5), 481-2
- Greenwood, B., 1999. The epidemiology of pneumococcal infection in children in the developing world. *Philos Trans R Soc Lond B Biol Sci*, 354 (1384), 777-85
- Grondona, J.M., Perez-Martin, M., Cifuentes, M., Perez, J., Estivill-Torres, G., Perez-Figares, J.M., Fernandez-Llebrez, P. & Rodriguez, E.M., 1998. Neuraminidase injected into the cerebrospinal fluid impairs the assembly of the glycoproteins secreted by the subcommissural organ preventing the formation of reissner's fiber. *Histochem Cell Biol*, 109 (4), 391-8
- Guichard, C., Harricane, M.C., Lafitte, J.J., Godard, P., Zaegel, M., Tack, V., Lalau, G. & Bouvagnet, P., 2001. Axonemal dynein intermediate-chain gene (dnai1) mutations result in situs inversus and primary ciliary dyskinesia (kartagener syndrome). *Am J Hum Genet*, 68 (4), 1030-5
- Guo, F.H., Comhair, S.A., Zheng, S., Dweik, R.A., Eissa, N.T., Thomassen, M.J., Calhoun, W. & Erzurum, S.C., 2000. Molecular mechanisms of increased nitric oxide (no) in asthma: Evidence for transcriptional and post-translational regulation of no synthesis. *J Immunol*, 164 (11), 5970-80
- Gustafsson, L.E., Leone, A.M., Persson, M.G., Wiklund, N.P. & Moncada, S., 1991. Endogenous nitric oxide is present in the exhaled air of rabbits, guinea pigs and humans. *Biochem Biophys Res Commun*, 181 (2), 852-7
- Hagiwara, H., Ohwada, N., Aoki, T. & Takata, K., 2000. Ciliogenesis and ciliary abnormalities. *Med Electron Microsc*, 33 (3), 109-14

- 
- Haimo, L.T. & Rosenbaum, J.L., 1981. Cilia, flagella, and microtubules. *J Cell Biol*, 91 (3 Pt 2), 125s-130s
- Hall-Stoodley, L. & Stoodley, P., 2009. Evolving concepts in biofilm infections. *Cell Microbiol*, 11 (7), 1034-43
- Hamon, M., Bierne, H. & Cossart, P., 2006. *Listeria monocytogenes*: A multifaceted model. *Nat Rev Microbiol*, 4 (6), 423-34
- Han, C.Y. & Backous, D.D., 2005. Basic principles of cerebrospinal fluid metabolism and intracranial pressure homeostasis. *Otolaryngol Clin North Am*, 38 (4), 569-76
- Harrison, A. & King, S.M., 2000. The molecular anatomy of dynein. *Essays Biochem*, 35, 75-87
- Heesemann, J. & Laufs, R., 1985. Double immunofluorescence microscopic technique for accurate differentiation of extracellularly and intracellularly located bacteria in cell culture. *J Clin Microbiol*, 22 (2), 168-75
- Heineman, H.S., 1973. Quellung test for pneumonia. *N Engl J Med*, 288 (19), 1027
- Henrichsen, J., 1995. Six newly recognized types of streptococcus pneumoniae. *Journal of Clinical Microbiology*, 33 (10), 2759-2762
- Hirst, R.A., Gosai, B., Rutman, A., Andrew, P.W. & O'callaghan, C., 2003. Streptococcus pneumoniae damages the ciliated ependyma of the brain during meningitis. *Infect Immun*, 71 (10), 6095-100
- Hirst, R.A., Gosai, B., Rutman, A., Guerin, C.J., Nicotera, P., Andrew, P.W. & O'callaghan, C., 2008. Streptococcus pneumoniae deficient in pneumolysin or autolysin has reduced virulence in meningitis. *J Infect Dis*, 197 (5), 744-51

- 
- Hirst, R.A., Kadioglu, A., O'callaghan, C. & Andrew, P.W., 2004a. The role of pneumolysin in pneumococcal pneumonia and meningitis. *Clin Exp Immunol*, 138 (2), 195-201
- Hirst, R.A., Mohammed, B.J., Mitchell, T.J., Andrew, P.W. & O'callaghan, C., 2004b. Streptococcus pneumoniae-induced inhibition of rat ependymal cilia is attenuated by antipneumolysin antibody. *Infect Immun*, 72 (11), 6694-8
- Hirst, R.A., Rutman, A., Sikand, K., Andrew, P.W., Mitchell, T.J. & O'callaghan, C., 2000a. Effect of pneumolysin on rat brain ciliary function: Comparison of brain slices with cultured ependymal cells. *Pediatr Res*, 47 (3), 381-4
- Hirst, R.A., Sikand, K.S., Rutman, A., Mitchell, T.J., Andrew, P.W. & O'callaghan, C., 2000b. Relative roles of pneumolysin and hydrogen peroxide from streptococcus pneumoniae in inhibition of ependymal ciliary beat frequency. *Infect Immun*, 68 (3), 1557-62
- Holzmann, D., Ott, P.M. & Felix, H., 2000. Diagnostic approach to primary ciliary dyskinesia: A review. *Eur J Pediatr*, 159 (1-2), 95-8
- Homolya, L., Steinberg, T.H. & Boucher, R.C., 2000. Cell to cell communication in response to mechanical stress via bilateral release of atp and utp in polarized epithelia. *J Cell Biol*, 150 (6), 1349-60
- Hong, D.H., Pawlyk, B., Sokolov, M., Strissel, K.J., Yang, J., Tulloch, B., Wright, A.F., Arshavsky, V.Y. & Li, T., 2003. Rpgr isoforms in photoreceptor connecting cilia and the transitional zone of motile cilia. *Invest Ophthalmol Vis Sci*, 44 (6), 2413-21

- 
- Hong, D.H., Pawlyk, B.S., Adamian, M., Sandberg, M.A. & Li, T., 2005. A single, abbreviated rpgr-orf15 variant reconstitutes rpgr function in vivo. *Invest Ophthalmol Vis Sci*, 46 (2), 435-41
- Hong, K.U., Reynolds, S.D., Watkins, S., Fuchs, E. & Stripp, B.R., 2004. Basal cells are a multipotent progenitor capable of renewing the bronchial epithelium. *Am J Pathol*, 164 (2), 577-88
- Honig, M.G. & Hume, R.I., 1986. Fluorescent carbocyanine dyes allow living neurons of identified origin to be studied in long-term cultures. *J Cell Biol*, 103 (1), 171-87
- Hornef, N., Olbrich, H., Horvath, J., Zariwala, M.A., Fliegauf, M., Loges, N.T., Wildhaber, J., Noone, P.G., Kennedy, M., Antonarakis, S.E., Blouin, J.L., Bartoloni, L., Nusslein, T., Ahrens, P., Griese, M., Kuhl, H., Sudbrak, R., Knowles, M.R., Reinhardt, R. & Omran, H., 2006. Dnah5 mutations are a common cause of primary ciliary dyskinesia with outer dynein arm defects. *Am J Respir Crit Care Med*, 174 (2), 120-6
- Houldsworth, S., Andrew, P.W. & Mitchell, T.J., 1994. Pneumolysin stimulates production of tumor necrosis factor alpha and interleukin-1 beta by human mononuclear phagocytes. *Infect Immun*, 62 (4), 1501-3
- Houtmeyers, E., Gosselink, R., Gayan-Ramirez, G. & Decramer, M., 1999. Regulation of mucociliary clearance in health and disease. *Eur Respir J*, 13 (5), 1177-88
- Hsu, T., Artiushin, S. & Minion, F.C., 1997. Cloning and functional analysis of the p97 swine cilium adhesin gene of mycoplasma hyopneumoniae. *J Bacteriol*, 179 (4), 1317-23

- 
- Hu, L. & Kopecko, D.J., 1999. Campylobacter jejuni 81-176 associates with microtubules and dynein during invasion of human intestinal cells. *Infect Immun*, 67 (8), 4171-82
- Hultgren, S.J., Porter, T.N., Schaeffer, A.J. & Duncan, J.L., 1985. Role of type 1 pili and effects of phase variation on lower urinary tract infections produced by escherichia coli. *Infect Immun*, 50 (2), 370-7
- Humphrey, 1948. Hyaluronidase production by pneumococci. *J. Pathol. Bacteriol.*, 55, 273-275
- Iannaccone, A., Breuer, D.K., Wang, X.F., Kuo, S.F., Normando, E.M., Filippova, E., Baldi, A., Hiriyan, S., Macdonald, C.B., Baldi, F., Cosgrove, D., Morton, C.C., Swaroop, A. & Jablonski, M.M., 2003. Clinical and immunohistochemical evidence for an x linked retinitis pigmentosa syndrome with recurrent infections and hearing loss in association with an rpgr mutation. *J Med Genet*, 40 (11), e118
- Ibanez-Tallon, I., Heintz, N. & Omran, H., 2003. To beat or not to beat: Roles of cilia in development and disease. *Hum Mol Genet*, 12 Spec No 1, R27-35
- Ibanez-Tallon, I., Pagenstecher, A., Fliegauf, M., Olbrich, H., Kispert, A., Ketelsen, U.P., North, A., Heintz, N. & Omran, H., 2004. Dysfunction of axonemal dynein heavy chain mdnah5 inhibits ependymal flow and reveals a novel mechanism for hydrocephalus formation. *Hum Mol Genet*, 13 (18), 2133-41
- Ibricevic, A., Pekosz, A., Walter, M.J., Newby, C., Battaile, J.T., Brown, E.G., Holtzman, M.J. & Brody, S.L., 2006. Influenza virus receptor specificity and cell tropism in mouse and human airway epithelial cells. *J Virol*, 80 (15), 7469-80

- 
- Inayama, Y., Hook, G.E., Brody, A.R., Cameron, G.S., Jetten, A.M., Gilmore, L.B., Gray, T. & Nettesheim, P., 1988. The differentiation potential of tracheal basal cells. *Lab Invest*, 58 (6), 706-17
- Jain, B., Rubinstein, I., Robbins, R.A., Leise, K.L. & Sisson, J.H., 1993. Modulation of airway epithelial cell ciliary beat frequency by nitric oxide. *Biochem Biophys Res Commun*, 191 (1), 83-8
- Jain, B., Rubinstein, I., Robbins, R.A. & Sisson, J.H., 1995. Tnf-alpha and il-1 beta upregulate nitric oxide-dependent ciliary motility in bovine airway epithelium. *Am J Physiol*, 268 (6 Pt 1), L911-7
- Jakiela, B., Brockman-Schneider, R., Amineva, S., Lee, W.M. & Gern, J.E., 2008. Basal cells of differentiated bronchial epithelium are more susceptible to rhinovirus infection. *Am J Respir Cell Mol Biol*, 38 (5), 517-23
- Jedrzejewski, M.J., 2007. Unveiling molecular mechanisms of bacterial surface proteins: *Streptococcus pneumoniae* as a model organism for structural studies. *Cell Mol Life Sci*, 64 (21), 2799-822
- Jeganathan, D., Chodhari, R., Meeks, M., Faeroe, O., Smyth, D., Nielsen, K., Amirav, I., Luder, A.S., Bisgaard, H., Gardiner, R.M., Chung, E.M. & Mitchison, H.M., 2004. Loci for primary ciliary dyskinesia map to chromosome 16p12.1-12.2 and 15q13.1-15.1 in faroe islands and israeli druze genetic isolates. *J Med Genet*, 41 (3), 233-40
- Johanson, C.E., Duncan, J.A., 3rd, Klinge, P.M., Brinker, T., Stopa, E.G. & Silverberg, G.D., 2008. Multiplicity of cerebrospinal fluid functions: New challenges in health and disease. *Cerebrospinal Fluid Res*, 5, 10

- 
- Johansson, C.B., Svensson, M., Wallstedt, L., Janson, A.M. & Frisen, J., 1999. Neural stem cells in the adult human brain. *Exp Cell Res*, 253 (2), 733-6
- Johnson, N.T., Villalon, M., Royce, F.H., Hard, R. & Verdugo, P., 1991. Autoregulation of beat frequency in respiratory ciliated cells. Demonstration by viscous loading. *Am Rev Respir Dis*, 144 (5), 1091-4
- Jones, M.R., Simms, B.T., Lupa, M.M., Kogan, M.S. & Mizgerd, J.P., 2005. Lung nf-kappab activation and neutrophil recruitment require il-1 and tnf receptor signaling during pneumococcal pneumonia. *J Immunol*, 175 (11), 7530-5
- Jordan, S.J., Perni, S., Glenn, S., Fernandes, I., Barbosa, M., Sol, M., Tenreiro, R.P., Chambel, L., Barata, B., Zilhao, I., Aldsworth, T.G., Adriaio, A., Faleiro, M.L., Shama, G. & Andrew, P.W., 2008. *Listeria monocytogenes* biofilm-associated protein (bapl) may contribute to surface attachment of *L. Monocytogenes* but is absent from many field isolates. *Appl Environ Microbiol*, 74 (17), 5451-6
- Jorgensen, O.S., 1988. Neural cell adhesion molecule (ncam) and prealbumin in cerebrospinal fluid from depressed patients. *Acta Psychiatr Scand Suppl*, 345, 29-37
- Jurado, R.L., Farley, M.M., Pereira, E., Harvey, R.C., Schuchat, A., Wenger, J.D. & Stephens, D.S., 1993. Increased risk of meningitis and bacteremia due to *Listeria monocytogenes* in patients with human immunodeficiency virus infection. *Clin Infect Dis*, 17 (2), 224-7
- Kadioglu, A., Gingles, N.A., Grattan, K., Kerr, A., Mitchell, T.J. & Andrew, P.W., 2000. Host cellular immune response to pneumococcal lung infection in mice. *Infect Immun*, 68 (2), 492-501

- 
- Kadioglu, A., Taylor, S., Iannelli, F., Pozzi, G., Mitchell, T.J. & Andrew, P.W., 2002. Upper and lower respiratory tract infection by streptococcus pneumoniae is affected by pneumolysin deficiency and differences in capsule type. *Infect Immun*, 70 (6), 2886-90
- Kadioglu, A., Weiser, J.N., Paton, J.C. & Andrew, P.W., 2008. The role of streptococcus pneumoniae virulence factors in host respiratory colonization and disease. *Nat Rev Microbiol*, 6 (4), 288-301
- Kalin, M., Kanclerski, K., Granstrom, M. & Mollby, R., 1987. Diagnosis of pneumococcal pneumonia by enzyme-linked immunosorbent assay of antibodies to pneumococcal hemolysin (pneumolysin). *J Clin Microbiol*, 25 (2), 226-9
- Kamerling, J.P., 2000a. Pneumococcal polysaccharides: A chemical view. In Tomasz, A. ed. *Streptococcus pneumoniae*.
- Kamerling, J.P. ed. 2000b. *Streptococcus pneumoniae: Molecular biology & mechanisms of disease*, New York: Man Ann Liebert
- Karadag, B., James, A.J., Gultekin, E., Wilson, N.M. & Bush, A., 1999. Nasal and lower airway level of nitric oxide in children with primary ciliary dyskinesia. *Eur Respir J*, 13 (6), 1402-5
- Kawakami, M., Nagira, T., Hayashi, T., Shimamoto, C., Kubota, T., Mori, H., Yoshida, H. & Nakahari, T., 2004. Hypo-osmotic potentiation of acetylcholine-stimulated ciliary beat frequency through atp release in rat tracheal ciliary cells. *Exp Physiol*, 89 (6), 739-51
- Kawamoto, H., Takeno, S. & Yajin, K., 1999. Increased expression of inducible nitric oxide synthase in nasal epithelial cells in patients with allergic rhinitis. *Laryngoscope*, 109 (12), 2015-20

- 
- Kennedy, M.P., Noone, P.G., Carson, J., Molina, P.L., Ghio, A., Zariwala, M.A., Minnix, S.L. & Knowles, M.R., 2007. Calcium stone lithoptysis in primary ciliary dyskinesia. *Respir Med*, 101 (1), 76-83
- Kerem, E., Bistrizter, T., Hanukoglu, A., Hofmann, T., Zhou, Z., Bennett, W., Maclaughlin, E., Barker, P., Nash, M., Quittell, L., Boucher, R. & Knowles, M.R., 1999. Pulmonary epithelial sodium-channel dysfunction and excess airway liquid in pseudohypoaldosteronism. *N Engl J Med*, 341 (3), 156-62
- Kerr, A.R., Wei, X.Q., Andrew, P.W. & Mitchell, T.J., 2004. Nitric oxide exerts distinct effects in local and systemic infections with streptococcus pneumoniae. *Microb Pathog*, 36 (6), 303-10
- Keskes, L., Giroux-Widemann, V., Serres, C., Pignot-Paintrand, I., Jouannet, P. & Feneux, D., 1998. The reactivation of demembrated human spermatozoa lacking outer dynein arms is independent of pH. *Mol Reprod Dev*, 49 (4), 416-25
- Kharitonov, S.A. & Barnes, P.J., 2000. Clinical aspects of exhaled nitric oxide. *Eur Respir J*, 16 (4), 781-92
- Kharitonov, S.A., Cailes, J.B., Black, C.M., Du Bois, R.M. & Barnes, P.J., 1997. Decreased nitric oxide in the exhaled air of patients with systemic sclerosis with pulmonary hypertension. *Thorax*, 52 (12), 1051-5
- Killer, H.E., Jaggi, G.P., Flammer, J., Miller, N.R., Huber, A.R. & Mironov, A., 2007. Cerebrospinal fluid dynamics between the intracranial and the subarachnoid space of the optic nerve. Is it always bidirectional? *Brain*, 130 (Pt 2), 514-20
- Kim, K.C., Mccracken, K., Lee, B.C., Shin, C.Y., Jo, M.J., Lee, C.J. & Ko, K.H., 1997. Airway goblet cell mucin: Its structure and regulation of secretion. *Eur Respir J*, 10 (11), 2644-9

- 
- Kim, S.W., Ihn, K.S., Han, S.H., Seong, S.Y., Kim, I.S. & Choi, M.S., 2001. Microtubule- and dynein-mediated movement of orientia tsutsugamushi to the microtubule organizing center. *Infect Immun*, 69 (1), 494-500
- Knapp, S., Wieland, C.W., Van 'T Veer, C., Takeuchi, O., Akira, S., Florquin, S. & Van Der Poll, T., 2004. Toll-like receptor 2 plays a role in the early inflammatory response to murine pneumococcal pneumonia but does not contribute to antibacterial defense. *J Immunol*, 172 (5), 3132-8
- Knowles, M.R. & Boucher, R.C., 2002. Mucus clearance as a primary innate defense mechanism for mammalian airways. *J Clin Invest*, 109 (5), 571-7
- Kocks, C., Gouin, E., Tabouret, M., Berche, P., Ohayon, H. & Cossart, P., 1992. L. Monocytogenes-induced actin assembly requires the acta gene product, a surface protein. *Cell*, 68 (3), 521-31
- Kocks, C., Hellio, R., Gounon, P., Ohayon, H. & Cossart, P., 1993. Polarized distribution of listeria monocytogenes surface protein acta at the site of directional actin assembly. *J Cell Sci*, 105 ( Pt 3), 699-710
- Koedel, U., Angele, B., Rupprecht, T., Wagner, H., Roggenkamp, A., Pfister, H.W. & Kirschning, C.J., 2003. Toll-like receptor 2 participates in mediation of immune response in experimental pneumococcal meningitis. *J Immunol*, 170 (1), 438-44
- Koh, Y.Y., Sun, Y.H., Min, Y.G., Chi, J.G. & Kim, C.K., 2003. Chemotaxis of blood neutrophils from patients with primary ciliary dyskinesia. *J Korean Med Sci*, 18 (1), 36-41
- Koto, M., Miwa, M., Shimizu, A., Tsuji, K., Okamoto, M. & Adachi, J., 1987a. Inherited hydrocephalus in csk: Wistar-imamichi rats; hyd strain: A new disease model for hydrocephalus. *Jikken Dobutsu*, 36 (2), 157-62

- 
- Koto, M., Miwa, M., Tsuji, K., Okamoto, M. & Adachi, J., 1987b. [change in the electrical impedance caused by cornification of the epithelial cell layer of the vaginal mucosa in the rat]. *Jikken Dobutsu*, 36 (2), 151-6
- Kozminski, K.G., Johnson, K.A., Forscher, P. & Rosenbaum, J.L., 1993. A motility in the eukaryotic flagellum unrelated to flagellar beating. *Proc Natl Acad Sci U S A*, 90 (12), 5519-23
- Krawczynski, M.R., Dmenska, H. & Witt, M., 2004. Apparent x-linked primary ciliary dyskinesia associated with retinitis pigmentosa and a hearing loss. *J Appl Genet*, 45 (1), 107-10
- Kreft, J. & Vazquez-Boland, J.A., 2001. Regulation of virulence genes in listeria. *Int J Med Microbiol*, 291 (2), 145-57
- Krunkosky, T.M., Jordan, J.L., Chambers, E. & Krause, D.C., 2007. Mycoplasma pneumoniae host-pathogen studies in an air-liquid culture of differentiated human airway epithelial cells. *Microb Pathog*, 42 (2-3), 98-103
- Kuhn, C., 3rd & Engleman, W., 1978. The structure of the tips of mammalian respiratory cilia. *Cell Tissue Res*, 186 (3), 491-8
- Kuhn, M., Kathariou, S. & Goebel, W., 1988. Hemolysin supports survival but not entry of the intracellular bacterium listeria monocytogenes. *Infect Immun*, 56 (1), 79-82
- Kultgen, P.L., Byrd, S.K., Ostrowski, L.E. & Milgram, S.L., 2002. Characterization of an a-kinase anchoring protein in human ciliary axonemes. *Mol Biol Cell*, 13 (12), 4156-66
- Lang, B., Song, B., Davidson, W., Mackenzie, A., Smith, N., Mccaig, C.D., Harmar, A.J. & Shen, S., 2006. Expression of the human pac1 receptor leads to dose-

- dependent hydrocephalus-related abnormalities in mice. *J Clin Invest*, 116 (7), 1924-34
- Lansley, A.B., Sanderson, M.J. & Dirksen, E.R., 1992. Control of the beat cycle of respiratory tract cilia by  $ca^{2+}$  and camp. *Am J Physiol*, 263 (2 Pt 1), L232-42
- Lecuit, M., Dramsi, S., Gottardi, C., Fedor-Chaiken, M., Gumbiner, B. & Cossart, P., 1999. A single amino acid in e-cadherin responsible for host specificity towards the human pathogen listeria monocytogenes. *Embo J*, 18 (14), 3956-63
- Lecuit, M., Vandormael-Pournin, S., Lefort, J., Huerre, M., Gounon, P., Dupuy, C., Babinet, C. & Cossart, P., 2001. A transgenic model for listeriosis: Role of internalin in crossing the intestinal barrier. *Science*, 292 (5522), 1722-5
- Lee, C.H., Lee, S.S., Mo, J.H., Kim, I.S., Quan, S.H., Wang, S.Y., Yi, W.J., Rhee, C.S. & Min, Y.G., 2005. Comparison of ciliary wave disorders measured by image analysis and electron microscopy. *Acta Otolaryngol*, 125 (5), 571-6
- Leimeister-Wachter, M., Haffner, C., Domann, E., Goebel, W. & Chakraborty, T., 1990. Identification of a gene that positively regulates expression of listeriolysin, the major virulence factor of listeria monocytogenes. *Proc Natl Acad Sci U S A*, 87 (21), 8336-40
- Lemessurier, K.S., Ogunniyi, A.D. & Paton, J.C., 2006. Differential expression of key pneumococcal virulence genes in vivo. *Microbiology*, 152 (Pt 2), 305-11
- Lesinski, G.B., Smithson, S.L., Srivastava, N., Chen, D., Widera, G. & Westerink, M.A., 2001. A DNA vaccine encoding a peptide mimic of streptococcus pneumoniae serotype 4 capsular polysaccharide induces specific anti-carbohydrate antibodies in balb/c mice. *Vaccine*, 19 (13-14), 1717-26

- 
- Levison, H., Mindorff, C.M., Chao, J., Turner, J.A., Sturgess, J.M. & Stringer, D.A., 1983. Pathophysiology of the ciliary motility syndromes. *Eur J Respir Dis Suppl*, 127, 102-17
- Li, D., Shirakami, G., Zhan, X. & Johns, R.A., 2000. Regulation of ciliary beat frequency by the nitric oxide-cyclic guanosine monophosphate signaling pathway in rat airway epithelial cells. *Am J Respir Cell Mol Biol*, 23 (2), 175-81
- Lieb, T., Forteza, R. & Salathe, M., 2000. Hyaluronic acid in cultured ovine tracheal cells and its effect on ciliary beat frequency in vitro. *J Aerosol Med*, 13 (3), 231-7
- Liedtke, C.M., 1988. Differentiated properties of rabbit tracheal epithelial cells in primary culture. *Am J Physiol*, 255 (6 Pt 1), C760-70
- Lim, W.S., Macfarlane, J.T., Boswell, T.C., Harrison, T.G., Rose, D., Leinonen, M. & Saikku, P., 2001. Study of community acquired pneumonia aetiology (scapa) in adults admitted to hospital: Implications for management guidelines. *Thorax*, 56 (4), 296-301
- Linnan, M.J., Mascola, L., Lou, X.D., Goulet, V., May, S., Salminen, C., Hird, D.W., Yonekura, M.L., Hayes, P., Weaver, R. & Et Al., 1988. Epidemic listeriosis associated with mexican-style cheese. *N Engl J Med*, 319 (13), 823-8
- Loges, N.T., Olbrich, H., Fenske, L., Mussaffi, H., Horvath, J., Fliegau, M., Kuhl, H., Baktai, G., Peterffy, E., Chodhari, R., Chung, E.M., Rutman, A., O'callaghan, C., Blau, H., Tiszlavicz, L., Voelkel, K., Witt, M., Zietkiewicz, E., Neesen, J., Reinhardt, R., Mitchison, H.M. & Omran, H., 2008. Dnai2 mutations cause primary ciliary dyskinesia with defects in the outer dynein arm. *Am J Hum Genet*, 83 (5), 547-58

- 
- Look, D.C., Walter, M.J., Williamson, M.R., Pang, L., You, Y., Sreshta, J.N., Johnson, J.E., Zander, D.S. & Brody, S.L., 2001. Effects of paramyxoviral infection on airway epithelial cell foxj1 expression, ciliogenesis, and mucociliary function. *Am J Pathol*, 159 (6), 2055-69
- Lopez, R., Garcia, E., Garcia, P. & Garcia, J.L., 1997. The pneumococcal cell wall degrading enzymes: A modular design to create new lysins? *Microb Drug Resist*, 3 (2), 199-211
- Loukides, S., Kharitonov, S., Wodehouse, T., Cole, P.J. & Barnes, P.J., 1998. Effect of arginine on mucociliary function in primary ciliary dyskinesia. *Lancet*, 352 (9125), 371-2
- Lundberg, J.O., Weitzberg, E., Nordvall, S.L., Kuylenstierna, R., Lundberg, J.M. & Alving, K., 1994. Primarily nasal origin of exhaled nitric oxide and absence in kartagener's syndrome. *Eur Respir J*, 7 (8), 1501-4
- Lungarella, G., De Santi, M.M., Palatresi, R. & Tosi, P., 1985. Ultrastructural observations on basal apparatus of respiratory cilia in immotile cilia syndrome. *Eur J Respir Dis*, 66 (3), 165-72
- Maccormick, J., Robb, I., Kovesi, T. & Carpenter, B., 2002. Optimal biopsy techniques in the diagnosis of primary ciliary dyskinesia. *J Otolaryngol*, 31 (1), 13-7
- Magee, A.D. & Yother, J., 2001. Requirement of capsule in colonisation by streptococcus pneumoniae. *Infection and Immunity*, 69 (6), 3755-3761
- Malley, R., Henneke, P., Morse, S.C., Cieslewicz, M.J., Lipsitch, M., Thompson, C.M., Kurt-Jones, E., Paton, J.C., Wessels, M.R. & Golenbock, D.T., 2003. Recognition of pneumolysin by toll-like receptor 4 confers resistance to pneumococcal infection. *Proc Natl Acad Sci U S A*, 100 (4), 1966-71

- 
- Manco, S., Herson, F., Yesilkaya, H., Paton, J.C., Andrew, P.W. & Kadioglu, A., 2006. Pneumococcal neuraminidases a and b both have essential roles during infection of the respiratory tract and sepsis. *Infect Immun*, 74 (7), 4014-20
- Mandell, G.L., 1973. Interaction of intraleukocytic bacteria and antibiotics. *J Clin Invest*, 52 (7), 1673-9
- Marcelo, F., He, Y., Yuzwa, S.A., Nieto, L., Jimenez-Barbero, J., Sollogoub, M., Vocadlo, D.J., Davies, G.D. & Bleriot, Y., 2009. Molecular basis for inhibition of gh84 glycoside hydrolases by substituted azepanes: Conformational flexibility enables probing of substrate distortion. *J Am Chem Soc*,
- Marr, A.K., Joseph, B., Mertins, S., Ecke, R., Muller-Altrock, S. & Goebel, W., 2006. Overexpression of prfa leads to growth inhibition of listeria monocytogenes in glucose-containing culture media by interfering with glucose uptake. *J Bacteriol*, 188 (11), 3887-901
- Marra, A., Lawson, S., Asundi, J.S., Brigham, D. & Hromockyj, A.E., 2002. In vivo characterization of the psa genes from streptococcus pneumoniae in multiple models of infection. *Microbiology*, 148 (Pt 5), 1483-91
- Marriott, H.M., Hellewell, P.G., Cross, S.S., Ince, P.G., Whyte, M.K. & Dockrell, D.H., 2006. Decreased alveolar macrophage apoptosis is associated with increased pulmonary inflammation in a murine model of pneumococcal pneumonia. *J Immunol*, 177 (9), 6480-8
- Marsh, E.J., Luo, H. & Wang, H., 2003. A three-tiered approach to differentiate listeria monocytogenes biofilm-forming abilities. *FEMS Microbiol Lett*, 228 (2), 203-10
- Matsui, H., Grubb, B.R., Tarran, R., Randell, S.H., Gatzky, J.T., Davis, C.W. & Boucher, R.C., 1998a. Evidence for periciliary liquid layer depletion, not abnormal ion

- 
- composition, in the pathogenesis of cystic fibrosis airways disease. *Cell*, 95 (7), 1005-15
- Matsui, H., Randell, S.H., Peretti, S.W., Davis, C.W. & Boucher, R.C., 1998b. Coordinated clearance of periciliary liquid and mucus from airway surfaces. *J Clin Invest*, 102 (6), 1125-31
- Mcdaniel, L.S., Scott, G., Kearney, J.F. & Briles, D.E., 1984. Monoclonal antibodies against protease-sensitive pneumococcal antigens can protect mice from fatal infection with streptococcus pneumoniae. *J Exp Med*, 160 (2), 386-97
- Mcgrath, J. & Brueckner, M., 2003. Cilia are at the heart of vertebrate left-right asymmetry. *Curr Opin Genet Dev*, 13 (4), 385-92
- Mclauchlin, J., 1997. The pathogenicity of listeria monocytogenes: A public health perspective. *Reviews in Medical Microbiology*, 8 (1), 1-14
- Mcshane, D., Davies, J.C., Wodehouse, T., Bush, A., Geddes, D. & Alton, E.W., 2004. Normal nasal mucociliary clearance in cf children: Evidence against a cftr-related defect. *Eur Respir J*, 24 (1), 95-100
- Meeks, M. & Bush, A., 2000. Primary ciliary dyskinesia (pcd). *Pediatr Pulmonol*, 29 (4), 307-16
- Mengaud, J., Dramsi, S., Gouin, E., Vazquez-Boland, J.A., Milon, G. & Cossart, P., 1991. Pleiotropic control of listeria monocytogenes virulence factors by a gene that is autoregulated. *Mol Microbiol*, 5 (9), 2273-83
- Mewe, M., Tielker, D., Schonberg, R., Schachner, M., Jaeger, K.E. & Schumacher, U., 2005. Pseudomonas aeruginosa lectins i and ii and their interaction with human airway cilia. *J Laryngol Otol*, 119 (8), 595-9

- 
- Michelet, C., Leib, S.L., Bentue-Ferrer, D. & Tauber, M.G., 1999. Comparative efficacies of antibiotics in a rat model of meningoencephalitis due to listeria monocytogenes. *Antimicrob Agents Chemother*, 43 (7), 1651-6
- Miles, A.A. & Misra, S.S., 1938. The estimation of the bactericidal power of blood. *J. Hyg.*, 38, 732-749
- Milohanic, E., Glaser, P., Coppee, J.Y., Frangeul, L., Vega, Y., Vazquez-Boland, J.A., Kunst, F., Cossart, P. & Buchrieser, C., 2003. Transcriptome analysis of listeria monocytogenes identifies three groups of genes differently regulated by prfa. *Mol Microbiol*, 47 (6), 1613-25
- Mitchell, T.J., 2004. Pneumolysin and other virulence factors. *In* Tuomanen, E.I. ed. *The pneumococcus*. Washington D.C.: ASM Press, 61-73.
- Mitchell, T.J., Walker, J.A., Saunders, F.K., Andrew, P.W. & Boulnois, G.J., 1989. Expression of the pneumolysin gene in escherichia coli: Rapid purification and biological properties. *Biochim Biophys Acta*, 1007 (1), 67-72
- Mnkkonen, K.S., Hirst, R.A., Laitinen, J.T. & O'callaghan, C., 2008. Pacap27 regulates ciliary function in primary cultures of rat brain ependymal cells. *Neuropeptides*, 42 (5-6), 633-40
- Mocharla, R., Mocharla, H. & Hodes, M.E., 1987. A novel, sensitive fluorometric staining technique for the detection of DNA in rna preparations. *Nucleic Acids Res*, 15 (24), 10589
- Mohammed, B.J., Mitchell, T.J., Andrew, P.W., Hirst, R.A. & O'callaghan, C., 1999. The effect of the pneumococcal toxin, pneumolysin on brain ependymal cilia. *Microb Pathog*, 27 (5), 303-9

- 
- Moncada, S. & Higgs, A., 1993. The l-arginine-nitric oxide pathway. *N Engl J Med*, 329 (27), 2002-12
- Monkkonen, K.S., Hakumaki, J.M., Hirst, R.A., Miettinen, R.A., O'callaghan, C., Mannisto, P.T. & Laitinen, J.T., 2007. Intracerebroventricular antisense knockdown of g alpha i2 results in ciliary stasis and ventricular dilatation in the rat. *BMC Neurosci*, 8, 26
- Moore, A., Escudier, E., Roger, G., Tamalet, A., Pelosse, B., Marlin, S., Clement, A., Geremek, M., Delaisi, B., Bridoux, A.M., Coste, A., Witt, M., Duriez, B. & Amselem, S., 2006. Rpgri is mutated in patients with a complex x linked phenotype combining primary ciliary dyskinesia and retinitis pigmentosa. *J Med Genet*, 43 (4), 326-33
- Moreland, J.G. & Bailey, G., 2006. Neutrophil transendothelial migration in vitro to streptococcus pneumoniae is pneumolysin dependent. *Am J Physiol Lung Cell Mol Physiol*, 290 (5), L833-40
- Morrison, K.E., Lake, D., Crook, J., Carlone, G.M., Ades, E., Facklam, R. & Sampson, J.S., 2000. Confirmation of psaa in all 90 serotypes of streptococcus pneumoniae by pcr and potential of this assay for identification and diagnosis. *J Clin Microbiol*, 38 (1), 434-7
- Moscoso, M., Garcia, E. & Lopez, R., 2009. Pneumococcal biofilms. *Int Microbiol*, 12 (2), 77-85
- Mueller, K.J. & Freitag, N.E., 2005. Pleiotropic enhancement of bacterial pathogenesis resulting from the constitutive activation of the listeria monocytogenes regulatory factor prfa. *Infect Immun*, 73 (4), 1917-26

- 
- Munro, N.C., Currie, D.C., Lindsay, K.S., Ryder, T.A., Rutman, A., Dewar, A., Greenstone, M.A., Hendry, W.F. & Cole, P.J., 1994. Fertility in men with primary ciliary dyskinesia presenting with respiratory infection. *Thorax*, 49 (7), 684-7
- Murdoch, C., Read, R.C., Zhang, Q. & Finn, A., 2002. Choline-binding protein a of streptococcus pneumoniae elicits chemokine production and expression of intercellular adhesion molecule 1 (cd54) by human alveolar epithelial cells. *J Infect Dis*, 186 (9), 1253-60
- Murray, E.G.D., R. A. Webb, and M. B. R. Swann., 1926. A disease of rabbit characterised by a large mononuclear leucocytosis, caused by a hitherto undescribed bacillus: *Bacterium monocytogenes* (n. Sp.). *J. Pathol. Bacteriol.*, 29, 407-439
- Mwimbi, X.K., Muimo, R., Green, M.W. & Mehta, A., 2003. Making human nasal cilia beat in the cold: A real time assay for cell signalling. *Cell Signal*, 15 (4), 395-402
- Mygind, N. & Wihl, J.A., 1977. Scanning electron microscopy of a bacterial infection of the human nasal mucosa. *Br J Dis Chest*, 71 (4), 259-67
- Nakajima, M., Kawanami, O., Jin, E., Ghazizadeh, M., Honda, M., Asano, G., Horiba, K. & Ferrans, V.J., 1998. Immunohistochemical and ultrastructural studies of basal cells, clara cells and bronchiolar cuboidal cells in normal human airways. *Pathol Int*, 48 (12), 944-53
- Nakamura, Y. & Sato, K., 1993. Role of disturbance of ependymal ciliary movement in development of hydrocephalus in rats. *Childs Nerv Syst*, 9 (2), 65-71

- 
- Narang, I., Ersu, R., Wilson, N.M. & Bush, A., 2002. Nitric oxide in chronic airway inflammation in children: Diagnostic use and pathophysiological significance. *Thorax*, 57 (7), 586-9
- Narayan, D., Krishnan, S.N., Upender, M., Ravikumar, T.S., Mahoney, M.J., Dolan, T.F., Jr., Teebi, A.S. & Haddad, G.G., 1994. Unusual inheritance of primary ciliary dyskinesia (kartagener's syndrome). *J Med Genet*, 31 (6), 493-6
- Nauli, S.M., Alenghat, F.J., Luo, Y., Williams, E., Vassilev, P., Li, X., Elia, A.E., Lu, W., Brown, E.M., Quinn, S.J., Ingber, D.E. & Zhou, J., 2003. Polycystins 1 and 2 mediate mechanosensation in the primary cilium of kidney cells. *Nat Genet*, 33 (2), 129-37
- Nelson, A.L., Roche, A.M., Gould, J.M., Chim, K., Ratner, A.J. & Weiser, J.N., 2007. Capsule enhances pneumococcal colonization by limiting mucus-mediated clearance. *Infect Immun*, 75 (1), 83-90
- Neustein, H.B., Nickerson, B. & O'neal, M., 1980. Kartagener's syndrome with absence of inner dynein arms of respiratory cilia. *Am Rev Respir Dis*, 122 (6), 979-81
- Nguyen, T., Chin, W.C., O'brien, J.A., Verdugo, P. & Berger, A.J., 2001. Intracellular pathways regulating ciliary beating of rat brain ependymal cells. *J Physiol*, 531 (Pt 1), 131-40
- Nicastro, D., Schwartz, C., Pierson, J., Gaudette, R., Porter, M.E. & Mcintosh, J.R., 2006. The molecular architecture of axonemes revealed by cryoelectron tomography. *Science*, 313 (5789), 944-8
- Niemann, H.H., Schubert, W.D. & Heinz, D.W., 2004. Adhesins and invasins of pathogenic bacteria: A structural view. *Microbes Infect*, 6 (1), 101-12

- 
- Niggemann, B., Muller, A., Nolte, A., Schnoy, N. & Wahn, U., 1992. Abnormal length of cilia--a cause of primary ciliary dyskinesia--a case report. *Eur J Pediatr*, 151 (1), 73-5
- Nishimoto, N. & Kishimoto, T., 2006. Interleukin 6: From bench to bedside. *Nat Clin Pract Rheumatol*, 2 (11), 619-26
- Nogales, E., 1999. A structural view of microtubule dynamics. *Cell Mol Life Sci*, 56 (1-2), 133-42
- Nonaka, S., Tanaka, Y., Okada, Y., Takeda, S., Harada, A., Kanai, Y., Kido, M. & Hirokawa, N., 1998. Randomization of left-right asymmetry due to loss of nodal cilia generating leftward flow of extraembryonic fluid in mice lacking kif3b motor protein. *Cell*, 95 (6), 829-37
- Noone, P.G., Leigh, M.W., Sannuti, A., Minnix, S.L., Carson, J.L., Hazucha, M., Zariwala, M.A. & Knowles, M.R., 2004. Primary ciliary dyskinesia: Diagnostic and phenotypic features. *Am J Respir Crit Care Med*, 169 (4), 459-67
- O'callaghan, C., 2004. Innate pulmonary immunity: Cilia. *Pediatr Pulmonol Suppl*, 26, 72-3
- O'callaghan, C., Chetcuti, P. & Moya, E., 2009. High prevalence of primary ciliary dyskinesia in a british asian population. *Arch Dis Child*, 95 (1), 51-2
- O'callaghan, C., Sikand, K. & Rutman, A., 1999. Respiratory and brain ependymal ciliary function. *Pediatr Res*, 46 (6), 704-7
- Obaro, S.K., 2001. Protein conjugate vaccines--how much is enough? *Trends Microbiol*, 9 (8), 364-5
- Obaro, S.K., Monteil, M.A. & Henderson, D.C., 1996. The pneumococcal problem. *Bmj*, 312 (7045), 1521-5

- 
- Oggioni, M.R., Trappetti, C., Kadioglu, A., Cassone, M., Iannelli, F., Ricci, S., Andrew, P.W. & Pozzi, G., 2006. Switch from planktonic to sessile life: A major event in pneumococcal pathogenesis. *Mol Microbiol*, 61 (5), 1196-210
- Ogunniyi, A.D., Folland, R.L., Briles, D.E., Hollingshead, S.K. & Paton, J.C., 2000. Immunization of mice with combinations of pneumococcal virulence proteins elicits enhanced protection against challenge with streptococcus pneumoniae. *Infect Immun*, 68 (5), 3028-33
- Okada, Y., Takeda, S., Tanaka, Y., Belmonte, J.C. & Hirokawa, N., 2005. Mechanism of nodal flow: A conserved symmetry breaking event in left-right axis determination. *Cell*, 121 (4), 633-44
- Olbrich, H., Haffner, K., Kispert, A., Volkel, A., Volz, A., Sasmaz, G., Reinhardt, R., Hennig, S., Lehrach, H., Konietzko, N., Zariwala, M., Noone, P.G., Knowles, M., Mitchison, H.M., Meeks, M., Chung, E.M., Hildebrandt, F., Sudbrak, R. & Omran, H., 2002. Mutations in *dnah5* cause primary ciliary dyskinesia and randomization of left-right asymmetry. *Nat Genet*, 30 (2), 143-4
- Oliver, J.D., 2005. The viable but nonculturable state in bacteria. *J Microbiol*, 43 Spec No, 93-100
- Omran, H., Kobayashi, D., Olbrich, H., Tsukahara, T., Loges, N.T., Hagiwara, H., Zhang, Q., Leblond, G., O'toole, E., Hara, C., Mizuno, H., Kawano, H., Fliegauf, M., Yagi, T., Koshida, S., Miyawaki, A., Zentgraf, H., Seithe, H., Reinhardt, R., Watanabe, Y., Kamiya, R., Mitchell, D.R. & Takeda, H., 2008. Ktu/pf13 is required for cytoplasmic pre-assembly of axonemal dyneins. *Nature*, 456 (7222), 611-6

- 
- Opitz, B., Puschel, A., Schmeck, B., Hocke, A.C., Rosseau, S., Hammerschmidt, S., Schumann, R.R., Suttorp, N. & Hippenstiel, S., 2004. Nucleotide-binding oligomerization domain proteins are innate immune receptors for internalized streptococcus pneumoniae. *J Biol Chem*, 279 (35), 36426-32
- Orihuela, C.J., Gao, G., Francis, K.P., Yu, J. & Tuomanen, E.I., 2004. Tissue-specific contributions of pneumococcal virulence factors to pathogenesis. *J Infect Dis*, 190 (9), 1661-9
- Ostrowski, L.E., Blackburn, K., Radde, K.M., Moyer, M.B., Schlatzer, D.M., Moseley, A. & Boucher, R.C., 2002. A proteomic analysis of human cilia: Identification of novel components. *Mol Cell Proteomics*, 1 (6), 451-65
- Ozgen, B., Haliloglu, M. & Tuncer, G., 2000. A 7-year-old boy with dextrocardia and dysphagia. *Eur J Pediatr*, 159 (4), 297-8
- Pamer, E.G., 2004. Immune responses to listeria monocytogenes. *Nat Rev Immunol*, 4 (10), 812-23
- Pan, J., You, Y., Huang, T. & Brody, S.L., 2007. Rhoa-mediated apical actin enrichment is required for ciliogenesis and promoted by foxj1. *J Cell Sci*, 120 (Pt 11), 1868-76
- Paraskakis, E., Zihlif, N. & Bush, A., 2007. Nitric oxide production in pcd: Possible evidence for differential nitric oxide synthase function. *Pediatr Pulmonol*, 42 (10), 876-80
- Parker, D., Soong, G., Planet, P., Brower, J., Ratner, A.J. & Prince, A., 2009. The nana neuraminidase of streptococcus pneumoniae is involved in biofilm formation. *Infect Immun*, 77 (9), 3722-30

- 
- Paton, J.C., Andrew, P.W., Boulnois, G.J. & Mitchell, T.J., 1993. Molecular analysis of the pathogenicity of streptococcus pneumoniae: The role of pneumococcal proteins. *Annu Rev Microbiol*, 47, 89-115
- Paton, J.C., Berry, A.M., Lock, R.A., Hansman, D. & Manning, P.A., 1986. Cloning and expression in escherichia coli of the streptococcus pneumoniae gene encoding pneumolysin. *Infect Immun*, 54 (1), 50-5
- Paton, J.C. & Ferrante, A., 1983. Inhibition of human polymorphonuclear leukocyte respiratory burst, bactericidal activity, and migration by pneumolysin. *Infect Immun*, 41 (3), 1212-6
- Pedersen, H. & Mygind, N., 1976. Absence of axonemal arms in nasal mucosa cilia in kartagener's syndrome. *Nature*, 262 (5568), 494-5
- Pedersen, M. & Stafanger, G., 1983. Bronchopulmonary symptoms in primary ciliary dyskinesia. A clinical study of 27 patients. *Eur J Respir Dis Suppl*, 127, 118-28
- Pennarun, G., Escudier, E., Chapelin, C., Bridoux, A.M., Cacheux, V., Roger, G., Clement, A., Goossens, M., Amselem, S. & Duriez, B., 1999. Loss-of-function mutations in a human gene related to chlamydomonas reinhardtii dynein ic78 result in primary ciliary dyskinesia. *Am J Hum Genet*, 65 (6), 1508-19
- Pettigrew, M.M., Fennie, K.P., York, M.P., Daniels, J. & Ghaffar, F., 2006. Variation in the presence of neuraminidase genes among streptococcus pneumoniae isolates with identical sequence types. *Infect Immun*, 74 (6), 3360-5
- Picco, P., Leveratto, L., Cama, A., Vigliarolo, M.A., Levato, G.L., Gattorno, M., Zammarchi, E. & Donati, M.A., 1993. Immotile cilia syndrome associated with hydrocephalus and precocious puberty: A case report. *Eur J Pediatr Surg*, 3 Suppl 1, 20-1

- 
- Picketts, D.J., 2006. Neuropeptide signaling and hydrocephalus: Sco with the flow. *J Clin Invest*, 116 (7), 1828-32
- Pils, S., Schmitter, T., Neske, F. & Hauck, C.R., 2006. Quantification of bacterial invasion into adherent cells by flow cytometry. *J Microbiol Methods*, 65 (2), 301-10
- Poole, A.W., Pula, G., Hers, I., Crosby, D. & Jones, M.L., 2004. Pkc-interacting proteins: From function to pharmacology. *Trends Pharmacol Sci*, 25 (10), 528-35
- Porter, M.E. & Sale, W.S., 2000. The 9 + 2 axoneme anchors multiple inner arm dyneins and a network of kinases and phosphatases that control motility. *J Cell Biol*, 151 (5), F37-42
- Portnoy, D.A., Auerbuch, V. & Glomski, I.J., 2002. The cell biology of listeria monocytogenes infection: The intersection of bacterial pathogenesis and cell-mediated immunity. *J Cell Biol*, 158 (3), 409-14
- Portnoy, D.A., Jacks, P.S. & Hinrichs, D.J., 1988. Role of hemolysin for the intracellular growth of listeria monocytogenes. *J Exp Med*, 167 (4), 1459-71
- Poyart, C., Abachin, E., Razafimanantsoa, I. & Berche, P., 1993. The zinc metalloprotease of listeria monocytogenes is required for maturation of phosphatidylcholine phospholipase c: Direct evidence obtained by gene complementation. *Infect Immun*, 61 (4), 1576-80
- Pracht, D., Elm, C., Gerber, J., Bergmann, S., Rohde, M., Seiler, M., Kim, K.S., Jenkinson, H.F., Nau, R. & Hammerschmidt, S., 2005. Pava of streptococcus pneumoniae modulates adherence, invasion, and meningeal inflammation. *Infect Immun*, 73 (5), 2680-9

- 
- Praetorius, H.A. & Spring, K.R., 2001. Bending the mdck cell primary cilium increases intracellular calcium. *J Membr Biol*, 184 (1), 71-9
- Price, K.E. & Camilli, A., 2009. Pneumolysin localizes to the cell wall of streptococcus pneumoniae. *J Bacteriol*, 191 (7), 2163-8
- Racke, K. & Matthiesen, S., 2004. The airway cholinergic system: Physiology and pharmacology. *Pulm Pharmacol Ther*, 17 (4), 181-98
- Rautiainen, M., Nuutinen, J. & Collan, Y., 1991. Short nasal respiratory cilia and impaired mucociliary function. *Eur Arch Otorhinolaryngol*, 248 (5), 271-4
- Rayner, C.F., Jackson, A.D., Rutman, A., Dewar, A., Mitchell, T.J., Andrew, P.W., Cole, P.J. & Wilson, R., 1995. Interaction of pneumolysin-sufficient and -deficient isogenic variants of streptococcus pneumoniae with human respiratory mucosa. *Infect Immun*, 63 (2), 442-7
- Rayner, C.F., Rutman, A., Dewar, A., Greenstone, M.A., Cole, P.J. & Wilson, R., 1996. Ciliary disorientation alone as a cause of primary ciliary dyskinesia syndrome. *Am J Respir Crit Care Med*, 153 (3), 1123-9
- Remer, K.A., Jungi, T.W., Fatzer, R., Tauber, M.G. & Leib, S.L., 2001. Nitric oxide is protective in listeric meningoencephalitis of rats. *Infect Immun*, 69 (6), 4086-93
- Ren, B., Szalai, A.J., Thomas, O., Hollingshead, S.K. & Briles, D.E., 2003. Both family 1 and family 2 pspa proteins can inhibit complement deposition and confer virulence to a capsular serotype 3 strain of streptococcus pneumoniae. *Infect Immun*, 71 (1), 75-85
- Rhodin, J.A., 1966. The ciliated cell. Ultrastructure and function of the human tracheal mucosa. *Am Rev Respir Dis*, 93 (3), Suppl:1-15

- 
- Richard, S., Nezelof, C., Pfister, A., De Blic, J., Scheinmann, P. & Paupe, J., 1989. Congenital ciliary aplasia in two siblings. A primitive dysregulation of ciliogenesis? *Pathol Res Pract*, 185 (2), 181-3
- Rosenbaum, J.L. & Witman, G.B., 2002. Intraflagellar transport. *Nat Rev Mol Cell Biol*, 3 (11), 813-25
- Rossjohn, J., Gilbert, R.J., Crane, D., Morgan, P.J., Mitchell, T.J., Rowe, A.J., Andrew, P.W., Paton, J.C., Tweten, R.K. & Parker, M.W., 1998. The molecular mechanism of pneumolysin, a virulence factor from streptococcus pneumoniae. *J Mol Biol*, 284 (2), 449-61
- Rossmann, C.M. & Newhouse, M.T., 1988. Primary ciliary dyskinesia: Evaluation and management. *Pediatr Pulmonol*, 5 (1), 36-50
- Roth, Y., Kimhi, Y., Edery, H., Aharonson, E. & Priel, Z., 1985. Ciliary motility in brain ventricular system and trachea of hamsters. *Brain Res*, 330 (2), 291-7
- Rubino, S., Leori, G., Rizzu, P., Erre, G., Colombo, M.M., Uzzau, S., Masala, G. & Cappuccinelli, P., 1993. Typhoid salmonella abortusovis mutants unable to adhere to epithelial cells and with reduced virulence in mice. *Infect Immun*, 61 (5), 1786-92
- Rubins, J.B., Duane, P.G., Clawson, D., Charboneau, D., Young, J. & Niewoehner, D.E., 1993. Toxicity of pneumolysin to pulmonary alveolar epithelial cells. *Infect Immun*, 61 (4), 1352-8
- Rubins, J.B., Mitchell, T.J., Andrew, P.W. & Niewoehner, D.E., 1994. Pneumolysin activates phospholipase A in pulmonary artery endothelial cells. *Infect Immun*, 62 (9), 3829-36

- 
- Rubins, J.B., Paddock, A.H., Charboneau, D., Berry, A.M., Paton, J.C. & Janoff, E.N., 1998. Pneumolysin in pneumococcal adherence and colonization. *Microb Pathog*, 25 (6), 337-42
- Runer, T., Cervin, A., Lindberg, S. & Uddman, R., 1998. Nitric oxide is a regulator of mucociliary activity in the upper respiratory tract. *Otolaryngol Head Neck Surg*, 119 (3), 278-87
- Rutland, J., Griffin, W. & Cole, P., 1981. Nasal brushing and measurement of ciliary beat frequency. An in vitro method for evaluating pharmacologic effects on human cilia. *Chest*, 80 (6 Suppl), 865-7
- Rutman, A., Cullinan, P., Woodhead, M., Cole, P.J. & Wilson, R., 1993. Ciliary disorientation: A possible variant of primary ciliary dyskinesia. *Thorax*, 48 (7), 770-1
- Sadek, C.M., Jimenez, A., Damdimopoulos, A.E., Kieselbach, T., Nord, M., Gustafsson, J.A., Spyrou, G., Davis, E.C., Oko, R., Van Der Hoorn, F.A. & Miranda-Vizuete, A., 2003. Characterization of human thioredoxin-like 2. A novel microtubule-binding thioredoxin expressed predominantly in the cilia of lung airway epithelium and spermatid manchette and axoneme. *J Biol Chem*, 278 (15), 13133-42
- Saeki, H., Kondo, S., Morita, T., Sasagawa, I., Ishizuka, G. & Koizumi, Y., 1984. Immotile cilia syndrome associated with polycystic kidney. *J Urol*, 132 (6), 1165-6
- Salathe, M., 2007. Regulation of mammalian ciliary beating. *Annu Rev Physiol*, 69, 401-22

- 
- Salathe, M. & Bookman, R.J., 1995. Coupling of  $[Ca^{2+}]_i$  and ciliary beating in cultured tracheal epithelial cells. *J Cell Sci*, 108 ( Pt 2), 431-40
- Salathe, M. & Bookman, R.J., 1999. Mode of  $Ca^{2+}$  action on ciliary beat frequency in single ovine airway epithelial cells. *J Physiol*, 520 Pt 3, 851-65
- Salathe, M., Lipson, E.J., Ivonnet, P.I. & Bookman, R.J., 1997. Muscarinic signaling in ciliated tracheal epithelial cells: Dual effects on  $Ca^{2+}$  and ciliary beating. *Am J Physiol*, 272 (2 Pt 1), L301-10
- Salathe, M., Pratt, M.M. & Wanner, A., 1993. Protein kinase c-dependent phosphorylation of a ciliary membrane protein and inhibition of ciliary beating. *J Cell Sci*, 106 ( Pt 4), 1211-20
- Sanderson, M.J., Charles, A.C., Boitano, S. & Dirksen, E.R., 1994. Mechanisms and function of intercellular calcium signaling. *Mol Cell Endocrinol*, 98 (2), 173-87
- Sanderson, M.J., Charles, A.C. & Dirksen, E.R., 1990. Mechanical stimulation and intercellular communication increases intracellular  $Ca^{2+}$  in epithelial cells. *Cell Regul*, 1 (8), 585-96
- Sanderson, M.J. & Dirksen, E.R., 1986. Mechanosensitivity of cultured ciliated cells from the mammalian respiratory tract: Implications for the regulation of mucociliary transport. *Proc Natl Acad Sci U S A*, 83 (19), 7302-6
- Sanderson, M.J. & Dirksen, E.R., 1989. Mechanosensitive and beta-adrenergic control of the ciliary beat frequency of mammalian respiratory tract cells in culture. *Am Rev Respir Dis*, 139 (2), 432-40
- Sanderson, M.J. & Sleigh, M.A., 1981. Ciliary activity of cultured rabbit tracheal epithelium: Beat pattern and metachrony. *J Cell Sci*, 47, 331-47

- 
- Satir, P., 1989. The role of axonemal components in ciliary motility. *Comp Biochem Physiol A*, 94 (2), 351-7
- Satir, P., 1999. The cilium as a biological nanomachine. *Faseb J*, 13 Suppl 2, S235-7
- Satir, P. & Christensen, S.T., 2007. Overview of structure and function of mammalian cilia. *Annu Rev Physiol*, 69, 377-400
- Satir, P. & Sleight, M.A., 1990. The physiology of cilia and mucociliary interactions. *Annu Rev Physiol*, 52, 137-55
- Sawamoto, K., Wichterle, H., Gonzalez-Perez, O., Cholfin, J.A., Yamada, M., Spassky, N., Murcia, N.S., Garcia-Verdugo, J.M., Marin, O., Rubenstein, J.L., Tessier-Lavigne, M., Okano, H. & Alvarez-Buylla, A., 2006. New neurons follow the flow of cerebrospinal fluid in the adult brain. *Science*, 311 (5761), 629-32
- Scheid, P., Kempster, L., Griesenbach, U., Davies, J.C., Dewar, A., Weber, P.P., Colledge, W.H., Evans, M.J., Geddes, D.M. & Alton, E.W., 2001. Inflammation in cystic fibrosis airways: Relationship to increased bacterial adherence. *Eur Respir J*, 17 (1), 27-35
- Schidlow, D.V., 1994. Primary ciliary dyskinesia (the immotile cilia syndrome). *Ann Allergy*, 73 (6), 457-68; quiz 468-70
- Schlech, W.F., 3rd, Lavigne, P.M., Bortolussi, R.A., Allen, A.C., Haldane, E.V., Wort, A.J., Hightower, A.W., Johnson, S.E., King, S.H., Nicholls, E.S. & Broome, C.V., 1983. Epidemic listeriosis--evidence for transmission by food. *N Engl J Med*, 308 (4), 203-6
- Schmeck, B., Huber, S., Moog, K., Zahlten, J., Hocke, A.C., Opitz, B., Hammerschmidt, S., Mitchell, T.J., Kracht, M., Rosseau, S., Suttorp, N. & Hippenstiel, S., 2006. Pneumococci induced tlr- and rac1-dependent nf-kappab-

- 
- recruitment to the il-8 promoter in lung epithelial cells. *Am J Physiol Lung Cell Mol Physiol*, 290 (4), L730-L737
- Schmeck, B., Zahlten, J., Moog, K., Van Laak, V., Huber, S., Hocke, A.C., Opitz, B., Hoffmann, E., Kracht, M., Zerrahn, J., Hammerschmidt, S., Rosseau, S., Suttorp, N. & Hippenstiel, S., 2004. Streptococcus pneumoniae-induced p38 mapk-dependent phosphorylation of rela at the interleukin-8 promoter. *J Biol Chem*, 279 (51), 53241-7
- Scholey, J.M., 2003. Intraflagellar transport. *Annu Rev Cell Dev Biol*, 19, 423-43
- Schwabe, G.C., Hoffmann, K., Loges, N.T., Birker, D., Rossier, C., De Santi, M.M., Olbrich, H., Fliegauf, M., Faily, M., Liebers, U., Collura, M., Gaedicke, G., Mundlos, S., Wahn, U., Blouin, J.L., Niggemann, B., Omran, H., Antonarakis, S.E. & Bartoloni, L., 2008. Primary ciliary dyskinesia associated with normal axoneme ultrastructure is caused by dnah11 mutations. *Hum Mutat*, 29 (2), 289-98
- Schwartz, B., Hexter, D., Broome, C.V., Hightower, A.W., Hirschhorn, R.B., Porter, J.D., Hayes, P.S., Bibb, W.F., Lorber, B. & Faris, D.G., 1989. Investigation of an outbreak of listeriosis: New hypotheses for the etiology of epidemic listeria monocytogenes infections. *J Infect Dis*, 159 (4), 680-5
- Scorti, M., Monzo, H.J., Lacharme-Lora, L., Lewis, D.A. & Vazquez-Boland, J.A., 2007. The prfa virulence regulon. *Microbes Infect*, 9 (10), 1196-207
- Seeliger, D.J.A.H., 1986. "*Genus listeria*".
- Shaper, M., Hollingshead, S.K., Benjamin, W.H., Jr. & Briles, D.E., 2004. Pspa protects streptococcus pneumoniae from killing by apolactoferrin, and antibody to pspa

- 
- enhances killing of pneumococci by apolactoferrin [corrected]. *Infect Immun*, 72 (9), 5031-40
- Shimizu, A. & Koto, M., 1992. Ultrastructure and movement of the ependymal and tracheal cilia in congenitally hydrocephalic wic-hyd rats. *Childs Nerv Syst*, 8 (1), 25-32
- Shoemark, A. & Wilson, R., 2009. Bronchial and peripheral airway nitric oxide in primary ciliary dyskinesia and bronchiectasis. *Respir Med*, 103 (5), 700-6
- Sisson Jh, M.J., Spurzem Jr, Wyatt Ta., 2000. Localization of pka and pkg in bovine bronchial epithelial cells and axonemes. *Am. J. Respir. Crit. Care Med.*, 161, A449
- Sisson, J.H., Papi, A., Beckmann, J.D., Leise, K.L., Wisecarver, J., Brodersen, B.W., Kelling, C.L., Spurzem, J.R. & Rennard, S.I., 1994. Smoke and viral infection cause cilia loss detectable by bronchoalveolar lavage cytology and dynein elisa. *Am J Respir Crit Care Med*, 149 (1), 205-13
- Sleigh, M.A., Blake, J.R. & Liron, N., 1988. The propulsion of mucus by cilia. *Am Rev Respir Dis*, 137 (3), 726-41
- Smith, E.F., 2002. Regulation of flagellar dynein by calcium and a role for an axonemal calmodulin and calmodulin-dependent kinase. *Mol Biol Cell*, 13 (9), 3303-13
- Smith, G.A., Marquis, H., Jones, S., Johnston, N.C., Portnoy, D.A. & Goldfine, H., 1995. The two distinct phospholipases c of listeria monocytogenes have overlapping roles in escape from a vacuole and cell-to-cell spread. *Infect Immun*, 63 (11), 4231-7

- 
- Sodeik, B., Ebersold, M.W. & Helenius, A., 1997. Microtubule-mediated transport of incoming herpes simplex virus 1 capsids to the nucleus. *J Cell Biol*, 136 (5), 1007-21
- Sollid, L.M., Kvale, D., Brandtzaeg, P., Markussen, G. & Thorsby, E., 1987. Interferon-gamma enhances expression of secretory component, the epithelial receptor for polymeric immunoglobulins. *J Immunol*, 138 (12), 4303-6
- Song, X.M., Connor, W., Hokamp, K., Babiuk, L.A. & Potter, A.A., 2008. Streptococcus pneumoniae early response genes to human lung epithelial cells. *BMC Res Notes*, 1, 64
- Soong, G., Muir, A., Gomez, M.I., Waks, J., Reddy, B., Planet, P., Singh, P.K., Kaneko, Y., Wolfgang, M.C., Hsiao, Y.S., Tong, L. & Prince, A., 2006. Bacterial neuraminidase facilitates mucosal infection by participating in biofilm production. *J Clin Invest*, 116 (8), 2297-2305
- Sorkin, S.P., 1968. Reconstruction of centriole formation and ciliogenesis in mammalian lungs. *J. Cell Sci*, 3, 207-230
- Spellerberg, B., Rosenow, C., Sha, W. & Tuomanen, E.I., 1996. Pneumococcal cell wall activates nf-kappa b in human monocytes: Aspects distinct from endotoxin. *Microb Pathog*, 20 (5), 309-17
- Stahlman, M.T., Gray, M.E. & Whitsett, J.A., 1998. Temporal-spatial distribution of hepatocyte nuclear factor-3beta in developing human lung and other foregut derivatives. *J Histochem Cytochem*, 46 (8), 955-62
- Stannard, W. & O'callaghan, C., 2006. Ciliary function and the role of cilia in clearance. *J Aerosol Med*, 19 (1), 110-5

- 
- Stannard, W., Rutman, A., Wallis, C. & O'callaghan, C., 2004. Central microtubular agenesis causing primary ciliary dyskinesia. *Am J Respir Crit Care Med*, 169 (5), 634-7
- Steagall, W.K., Elmer, H.L., Brady, K.G. & Kelley, T.J., 2000. Cystic fibrosis transmembrane conductance regulator-dependent regulation of epithelial inducible nitric oxide synthase expression. *Am J Respir Cell Mol Biol*, 22 (1), 45-50
- Sternberg, G.M., 1981. A fatal form of septicaemia in the rabbit, produced by subcutaneous injection of human saliva. An experimental research. *National Board Health Bulletin*, 2, 781-783
- Stewart, P.S., 2001. Multicellular resistance: Biofilms. *Trends Microbiol*, 9 (5), 204
- Straub, V., Ratjen, F., Amthor, H., Voit, T. & Grasemann, H., 2002. Airway nitric oxide in duchenne muscular dystrophy. *J Pediatr*, 141 (1), 132-4
- Strieter, R.M., Belperio, J.A. & Keane, M.P., 2003. Host innate defenses in the lung: The role of cytokines. *Curr Opin Infect Dis*, 16 (3), 193-8
- Sturgess, J.M., Chao, J. & Turner, J.A., 1980. Transposition of ciliary microtubules: Another cause of impaired ciliary motility. *N Engl J Med*, 303 (6), 318-22
- Sturgess, J.M., Chao, J., Wong, J., Aspin, N. & Turner, J.A., 1979. Cilia with defective radial spokes: A cause of human respiratory disease. *N Engl J Med*, 300 (2), 53-6
- Sturrock, R.R. & Smart, I.H., 1980. A morphological study of the mouse subependymal layer from embryonic life to old age. *J Anat*, 130 (Pt 2), 391-415
- Sui, H. & Downing, K.H., 2006. Molecular architecture of axonemal microtubule doublets revealed by cryo-electron tomography. *Nature*, 442 (7101), 475-8

- 
- Suomalainen, M., Nakano, M.Y., Keller, S., Boucke, K., Stidwill, R.P. & Greber, U.F., 1999. Microtubule-dependent plus- and minus end-directed motilities are competing processes for nuclear targeting of adenovirus. *J Cell Biol*, 144 (4), 657-72
- Sutto, Z., Conner, G.E. & Salathe, M., 2004. Regulation of human airway ciliary beat frequency by intracellular pH. *J Physiol*, 560 (Pt 2), 519-32
- Tappero, J.W., Schuchat, A., Deaver, K.A., Mascola, L. & Wenger, J.D., 1995. Reduction in the incidence of human listeriosis in the united states. Effectiveness of prevention efforts? The listeriosis study group. *JAMA*, 273 (14), 1118-22
- Tarran, R., Grubb, B.R., Gatzky, J.T., Davis, C.W. & Boucher, R.C., 2001. The relative roles of passive surface forces and active ion transport in the modulation of airway surface liquid volume and composition. *J Gen Physiol*, 118 (2), 223-36
- Thai, C.H., Gambling, T.M. & Carson, J.L., 2002. Freeze fracture study of airway epithelium from patients with primary ciliary dyskinesia. *Thorax*, 57 (4), 363-5
- Tilney, L.G., Connelly, P.S. & Portnoy, D.A., 1990. Actin filament nucleation by the bacterial pathogen, *listeria monocytogenes*. *J Cell Biol*, 111 (6 Pt 2), 2979-88
- Tilney, L.G. & Portnoy, D.A., 1989. Actin filaments and the growth, movement, and spread of the intracellular bacterial parasite, *listeria monocytogenes*. *J Cell Biol*, 109 (4 Pt 1), 1597-608
- Tong, H.H., Blue, L.E., James, M.A. & Demaria, T.F., 2000. Evaluation of the virulence of a streptococcus pneumoniae neuraminidase-deficient mutant in nasopharyngeal colonization and development of otitis media in the chinchilla model. *Infect Immun*, 68 (2), 921-4

- 
- Tong, H.H., Li, D., Chen, S., Long, J.P. & Demaria, T.F., 2005. Immunization with recombinant streptococcus pneumoniae neuraminidase nana protects chinchillas against nasopharyngeal colonization. *Infect Immun*, 73 (11), 7775-8
- Tsang, K.W., Leung, R., Fung, P.C., Chan, S.L., Tipoe, G.L., Ooi, G.C. & Lam, W.K., 2002. Exhaled and sputum nitric oxide in bronchiectasis: Correlation with clinical parameters. *Chest*, 121 (1), 88-94
- Tu, A.H., Fulgham, R.L., Mccrory, M.A., Briles, D.E. & Szalai, A.J., 1999. Pneumococcal surface protein a inhibits complement activation by streptococcus pneumoniae. *Infect Immun*, 67 (9), 4720-4
- Tuomanen, E., 1999. Molecular and cellular biology of pneumococcal infection. *Curr Opin Microbiol*, 2 (1), 35-9
- Tuomanen, E., and Masure, R. ed. 2000. *Molecular and cellular biology of pneumococcal infection*, New York: Mary Ann Liebert.
- Tuomanen, E., Towbin, H., Rosenfelder, G., Braun, D., Larson, G., Hansson, G.C. & Hill, R., 1988. Receptor analogs and monoclonal antibodies that inhibit adherence of bordetella pertussis to human ciliated respiratory epithelial cells. *J Exp Med*, 168 (1), 267-77
- Tuomanen, E.I., 1997. The biology of pneumococcal infection. *Pediatr Res*, 42 (3), 253-8
- Tuomanen, E.I. & Masure, H.R., 1997. Molecular and cellular biology of pneumococcal infection. *Microb Drug Resist*, 3 (4), 297-308
- Tuomanen, E.I. & Masure, H.R., 2000. Molecular and cellular biology of pneumococcal infection. In Tomasz, A. ed. *Streptococcus pneumoniae*. Larchmont, NY: Mary Ann Liebert Inc.

- 
- Uzlaner, N. & Priel, Z., 1999. Interplay between the no pathway and elevated  $[Ca^{2+}]_i$  enhances ciliary activity in rabbit trachea. *J Physiol*, 516 ( Pt 1), 179-90
- Valerius, N.H., Knudsen, B.B. & Pedersen, M., 1983. Defective neutrophil motility in patients with primary ciliary dyskinesia. *Eur J Clin Invest*, 13 (6), 489-94
- Van Dorp, D.B., Wright, A.F., Carothers, A.D. & Bleeker-Wagemakers, E.M., 1992. A family with rp3 type of x-linked retinitis pigmentosa: An association with ciliary abnormalities. *Hum Genet*, 88 (3), 331-4
- Vaudaux, P. & Waldvogel, F.A., 1979. Gentamicin antibacterial activity in the presence of human polymorphonuclear leukocytes. *Antimicrob Agents Chemother*, 16 (6), 743-9
- Vazquez-Boland, J.A., Dominguez-Bernal, G., Gonzalez-Zorn, B., Kreft, J. & Goebel, W., 2001a. Pathogenicity islands and virulence evolution in listeria. *Microbes Infect*, 3 (7), 571-84
- Vazquez-Boland, J.A., Kocks, C., Dramsi, S., Ohayon, H., Geoffroy, C., Mengaud, J. & Cossart, P., 1992. Nucleotide sequence of the lecithinase operon of listeria monocytogenes and possible role of lecithinase in cell-to-cell spread. *Infect Immun*, 60 (1), 219-30
- Vazquez-Boland, J.A., Kuhn, M., Berche, P., Chakraborty, T., Dominguez-Bernal, G., Goebel, W., Gonzalez-Zorn, B., Wehland, J. & Kreft, J., 2001b. Listeria pathogenesis and molecular virulence determinants. *Clin Microbiol Rev*, 14 (3), 584-640
- Vent, J., Wyatt, T.A., Smith, D.D., Banerjee, A., Luduena, R.F., Sisson, J.H. & Hallworth, R., 2005. Direct involvement of the isotype-specific c-terminus of beta tubulin in ciliary beating. *J Cell Sci*, 118 (Pt 19), 4333-41

- 
- Verdugo, P., 1980. Ca<sup>2+</sup>-dependent hormonal stimulation of ciliary activity. *Nature*, 283 (5749), 764-5
- Verdugo, P., Raess, B.V. & Villalon, M., 1983a. The role of calmodulin in the regulation of ciliary movement in mammalian epithelial cilia. *J Submicrosc Cytol*, 15 (1), 95-6
- Verdugo, P., Tam, P.Y. & Butler, J., 1983b. Conformational structure of respiratory mucus studied by laser correlation spectroscopy. *Biorheology*, 20 (2), 223-30
- Villalon, M., Hinds, T.R. & Verdugo, P., 1989. Stimulus-response coupling in mammalian ciliated cells. Demonstration of two mechanisms of control for cytosolic [Ca<sup>2+</sup>]. *Biophys J*, 56 (6), 1255-8
- Vogel, G., 2005. News focus: Betting on cilia. *Science*, 310 (5746), 216-8
- Wade, J.T., Struhl, K., Busby, S.J. & Grainger, D.C., 2007. Genomic analysis of protein-DNA interactions in bacteria: Insights into transcription and chromosome organization. *Mol Microbiol*, 65 (1), 21-6
- Wadsworth, S.J. & Goldfine, H., 1999. *Listeria monocytogenes* phospholipase c-dependent calcium signaling modulates bacterial entry into j774 macrophage-like cells. *Infect Immun*, 67 (4), 1770-8
- Wadsworth, S.J. & Goldfine, H., 2002. Mobilization of protein kinase c in macrophages induced by *Listeria monocytogenes* affects its internalization and escape from the phagosome. *Infect Immun*, 70 (8), 4650-60
- Walley, K.R., McDonald, T.E., Higashimoto, Y. & Hayashi, S., 1999. Modulation of proinflammatory cytokines by nitric oxide in murine acute lung injury. *Am J Respir Crit Care Med*, 160 (2), 698-704

- 
- Waltman, W.D., Mcdaniel, L.S., Gray, B.M. & Briles, D.E., 1990. Variation in the molecular weight of pspa (pneumococcal surface protein a) among streptococcus pneumoniae. *Microb Pathog*, 8 (1), 61-9
- Wang, H. & Satir, P., 1998. The 29 kda light chain that regulates axonemal dynein activity binds to cytoplasmic dyneins. *Cell Motil Cytoskeleton*, 39 (1), 1-8
- Wang, Q., Pan, J. & Snell, W.J., 2006. Intraflagellar transport particles participate directly in cilium-generated signaling in chlamydomonas. *Cell*, 125 (3), 549-62
- Wanner, A., Salathe, M. & O'riordan, T.G., 1996. Mucociliary clearance in the airways. *Am J Respir Crit Care Med*, 154 (6 Pt 1), 1868-902
- Warner, F.D., 1976. Ciliary inter-microtubule bridges. *J Cell Sci*, 20 (1), 101-14
- Watkins, D.N., Lewis, R.H., Basclain, K.A., Fisher, P.H., Peroni, D.J., Garlepp, M.J. & Thompson, P.J., 1998. Expression and localization of the inducible isoform of nitric oxide synthase in nasal polyp epithelium. *Clin Exp Allergy*, 28 (2), 211-9
- Weibel, M., Pettmann, B., Artault, J.C., Sensenbrenner, M. & Labourdette, G., 1986. Primary culture of rat ependymal cells in serum-free defined medium. *Brain Res*, 390 (2), 199-209
- Weinberg, J.B., Granger, D.L., Pisetsky, D.S., Seldin, M.F., Misukonis, M.A., Mason, S.N., Pippen, A.M., Ruiz, P., Wood, E.R. & Gilkeson, G.S., 1994. The role of nitric oxide in the pathogenesis of spontaneous murine autoimmune disease: Increased nitric oxide production and nitric oxide synthase expression in mrl-lpr/lpr mice, and reduction of spontaneous glomerulonephritis and arthritis by orally administered ng-monomethyl-l-arginine. *J Exp Med*, 179 (2), 651-60
- Whitelaw, A., Evans, A. & Corrin, B., 1981. Immotile cilia syndrome: A new cause of neonatal respiratory distress. *Arch Dis Child*, 56 (6), 432-5

- 
- Widdicombe, J.H., Coleman, D.L., Finkbeiner, W.E. & Tuet, I.K., 1985. Electrical properties of monolayers cultured from cells of human tracheal mucosa. *J Appl Physiol*, 58 (5), 1729-35
- Wilkerson, C.G., King, S.M. & Witman, G.B., 1994. Molecular analysis of the gamma heavy chain of chlamydomonas flagellar outer-arm dynein. *J Cell Sci*, 107 ( Pt 3), 497-506
- Wilson, P.D., 2004. Polycystic kidney disease: New understanding in the pathogenesis. *Int J Biochem Cell Biol*, 36 (10), 1868-73
- Wirschell, M., Zhao, F., Yang, C., Yang, P., Diener, D., Gaillard, A., Rosenbaum, J.L. & Sale, W.S., 2008. Building a radial spoke: Flagellar radial spoke protein 3 (rsp3) is a dimer. *Cell Motil Cytoskeleton*, 65 (3), 238-48
- Witman, G.B., Plummer, J. & Sander, G., 1978. Chlamydomonas flagellar mutants lacking radial spokes and central tubules. Structure, composition, and function of specific axonemal components. *J Cell Biol*, 76 (3), 729-47
- Wodehouse, T., Kharitonov, S.A., Mackay, I.S., Barnes, P.J., Wilson, R. & Cole, P.J., 2003. Nasal nitric oxide measurements for the screening of primary ciliary dyskinesia. *Eur Respir J*, 21 (1), 43-7
- Wong, L.B., Miller, I.F. & Yeates, D.B., 1990. Stimulation of tracheal ciliary beat frequency by capsaicin. *J Appl Physiol*, 68 (6), 2574-80
- Wong, L.B., Park, C.L. & Yeates, D.B., 1998. Neuropeptide y inhibits ciliary beat frequency in human ciliated cells via npkc, independently of pka. *Am J Physiol*, 275 (2 Pt 1), C440-8
- Woolley, D., 2000. The molecular motors of cilia and eukaryotic flagella. *Essays Biochem*, 35, 103-15

- 
- Woolley, D.M., 1997. Studies on the eel sperm flagellum. I. The structure of the inner dynein arm complex. *J Cell Sci*, 110 ( Pt 1), 85-94
- Wu, H.Y., Virolainen, A., Mathews, B., King, J., Russell, M.W. & Briles, D.E., 1997. Establishment of a streptococcus pneumoniae nasopharyngeal colonization model in adult mice. *Microb Pathog*, 23 (3), 127-37
- Wyatt, T.A., Schmidt, S.C., Rennard, S.I., Tuma, D.J. & Sisson, J.H., 2000. Acetaldehyde-stimulated pkc activity in airway epithelial cells treated with smoke extract from normal and smokeless cigarettes. *Proc Soc Exp Biol Med*, 225 (1), 91-7
- Wyatt, T.A. & Sisson, J.H., 2001. Chronic ethanol downregulates pka activation and ciliary beating in bovine bronchial epithelial cells. *Am J Physiol Lung Cell Mol Physiol*, 281 (3), L575-81
- Wyatt, T.A., Spurzem, J.R., May, K. & Sisson, J.H., 1998. Regulation of ciliary beat frequency by both pka and pkg in bovine airway epithelial cells. *Am J Physiol*, 275 (4 Pt 1), L827-35
- Xu, B.P., Shen, K.L., Hu, Y.H., Feng, X.L., Li, H.M. & Lang, Z.Q., 2008. [clinical characteristics of primary ciliary dyskinesia in children]. *Zhonghua Er Ke Za Zhi*, 46 (8), 618-22
- Yang, P., Diener, D.R., Rosenbaum, J.L. & Sale, W.S., 2001. Localization of calmodulin and dynein light chain lc8 in flagellar radial spokes. *J Cell Biol*, 153 (6), 1315-26
- Yang, P., Diener, D.R., Yang, C., Kohno, T., Pazour, G.J., Dienes, J.M., Agrin, N.S., King, S.M., Sale, W.S., Kamiya, R., Rosenbaum, J.L. & Witman, G.B., 2006.

- 
- Radial spoke proteins of chlamydomonas flagella. *J Cell Sci*, 119 (Pt 6), 1165-74
- Yesilkaya, H., Manco, S., Kadioglu, A., Terra, V.S. & Andrew, P.W., 2008. The ability to utilize mucin affects the regulation of virulence gene expression in streptococcus pneumoniae. *FEMS Microbiol Lett*, 278 (2), 231-5
- Yeung, P.S., Zagorski, N. & Marquis, H., 2005. The metalloprotease of listeria monocytogenes controls cell wall translocation of the broad-range phospholipase c. *J Bacteriol*, 187 (8), 2601-8
- Yokoyama, T., 2004. Motor or sensor: A new aspect of primary cilia function. *Anat Sci Int*, 79 (2), 47-54
- Yother, J. & White, J.M., 1994. Novel surface attachment mechanism of the streptococcus pneumoniae protein pspa. *J Bacteriol*, 176 (10), 2976-85
- You, Y., Huang, T., Richer, E.J., Schmidt, J.E., Zabner, J., Borok, Z. & Brody, S.L., 2004. Role of f-box factor foxj1 in differentiation of ciliated airway epithelial cells. *Am J Physiol Lung Cell Mol Physiol*, 286 (4), L650-7
- Zabner, J., Zeiher, B.G., Friedman, E. & Welsh, M.J., 1996. Adenovirus-mediated gene transfer to ciliated airway epithelia requires prolonged incubation time. *J Virol*, 70 (10), 6994-7003
- Zagoory, O., Braiman, A. & Priel, Z., 2002. The mechanism of ciliary stimulation by acetylcholine: Roles of calcium, pka, and pkg. *J Gen Physiol*, 119 (4), 329-39
- Zahm, J.M., Pierrot, D., Vaquez-Girod, S., Duvivier, C., King, M. & Puchelle, E., 1989. The role of mucus sol phase in clearance by simulated cough. *Biorheology*, 26 (4), 747-52

- 
- Zariwala, M., Noone, P.G., Sannuti, A., Minnix, S., Zhou, Z., Leigh, M.W., Hazucha, M., Carson, J.L. & Knowles, M.R., 2001. Germline mutations in an intermediate chain dynein cause primary ciliary dyskinesia. *Am J Respir Cell Mol Biol*, 25 (5), 577-83
- Zariwala, M.A., Knowles, M.R. & Omran, H., 2007. Genetic defects in ciliary structure and function. *Annu Rev Physiol*, 69, 423-50
- Zariwala, M.A., Leigh, M.W., Ceppia, F., Kennedy, M.P., Noone, P.G., Carson, J.L., Hazucha, M.J., Lori, A., Horvath, J., Olbrich, H., Loges, N.T., Bridoux, A.M., Pennarun, G., Duriez, B., Escudier, E., Mitchison, H.M., Chodhari, R., Chung, E.M., Morgan, L.C., De Iongh, R.U., Rutland, J., Pradal, U., Omran, H., Amselem, S. & Knowles, M.R., 2006. Mutations of *dnai1* in primary ciliary dyskinesia: Evidence of founder effect in a common mutation. *Am J Respir Crit Care Med*, 174 (8), 858-66
- Zhan, X., Li, D. & Johns, R.A., 2003. Expression of endothelial nitric oxide synthase in ciliated epithelia of rats. *J Histochem Cytochem*, 51 (1), 81-7
- Zhang, J.R., Mostov, K.E., Lamm, M.E., Nanno, M., Shimida, S., Ohwaki, M. & Tuomanen, E., 2000. The polymeric immunoglobulin receptor translocates pneumococci across human nasopharyngeal epithelial cells. *Cell*, 102 (6), 827-37
- Zhang, L. & Sanderson, M.J., 2003. The role of cgmp in the regulation of rabbit airway ciliary beat frequency. *J Physiol*, 551 (Pt 3), 765-76
- Zhang, Q., Taulman, P.D. & Yoder, B.K., 2004. Cystic kidney diseases: All roads lead to the cilium. *Physiology (Bethesda)*, 19, 225-30

Zimmermann, K.W., 1898. Beiträge zur kenntniss einiger drüsen und epithelien. *Arch. f. mikr. Anat.*, 52, 552-706

Zito, I., Downes, S.M., Patel, R.J., Cheetham, M.E., Ebenezer, N.D., Jenkins, S.A.,  
Bhattacharya, S.S., Webster, A.R., Holder, G.E., Bird, A.C., Bamiou, D.E. &  
Hardcastle, A.J., 2003. Rprgr mutation associated with retinitis pigmentosa,  
impaired hearing, and sinorespiratory infections. *J Med Genet*, 40 (8), 609-15

---

## **Publications**

Fadaee-Shohada, M.J., Hirst, R.A., Rutman, A., Roberts, I.S., O'callaghan, C. & Andrew, P.W., 2010. The behaviour of both listeria monocytogenes and rat ciliated ependymal cells is altered during their co-culture. *PLoS One*, 5 (5), e10450